NMR STUDIES ON FIVE MEMBERED 1,2,3/1,2,4-TRIAZOLES AND THEIR HYBRID SYSTEMS.

BY

GANESH F. JOGDAND

AUGUST 2016

NMR STUDIES ON FIVE MEMBERED 1,2,3/1,2,4-TRIAZOLES AND THEIR HYBRID SYSTEMS.

THESIS SUBMITTED TO THE

UNIVERSITY OF PUNE

FOR THE DEGREE OF

DOCTOR OF PHILOSOPHY

IN

CHEMISTRY

By

GANESH F. JOGDAND

Central NMR Facility

Physical Chemistry Division

National Chemical Laboratory

Pune - 411008

India

August 2016

CERTIFICATE

Certified that the work incorporated in the thesis entitled **"NMR studies on five membered 1,2,3/1,2,4-triazoles and their hybrid systems"**, submitted by **Mr. Ganesh F. Jogdand** for the Degree of **Doctor of Philosophy** was carried out by the candidate under my supervision at the Central NMR Facility, Physical Chemistry Division, National Chemical Laboratory, Pune, India. Materials obtained from other sources have been duly acknowledged in the thesis.

Date:

Place: Pune

Dr. P. R. Rajamohanan
(Research Guide)
Central NMR Facility
Division of Physical Chemistry
NCL, Pune-8

Dedicated to my family, friends and Teachers.

Acknowledgement

After God, I thank my parents, teachers and well wishers who helped me to complete the reserach work done by me. I am specially thankful to my research Guide **Dr. P. R. Rajamohanan**, who helped and guided me enormously in carrying out NMR studies. I thaks to Dr. Kalkote , Dr. S.P. Chavan for their valuable support and encouragement. I am also thankful to Dr. T. G. Ajithkumar for helping me from time to time. I thank Dr. Uday for his kind help along with **Dr. S. Ganapathy**, **Dr. Sapna Ravindranathan, Sathe** sir and **Phalgune** madam who taught me 2D and analysis and for their encouraging words and support.I very much greatful to Mr. **P.M. Suryavamshi.** I also thak to **K.D. Deshpande, Chapale data, P.K. Mane, Laxman Malge** and **Umesh Kamatkar** who helped me a lot in the time of very much adversery. My special thank you Pravin, Kondiba. I will always remember the help by **Sachin Kate**, Application Engineer, Bruker for his technical help. And finally I thank my family and daughters for keeping patience with me.

Ganesh F. Jogdand

Contents:

PREFACE

Triazoles are synthetic heterocyclic compounds which find applications in various research fields including biological science, material chemistry, medicinal chemistry, and synthetic organic chemistry. Tautomerism, a phenomenon by which the same molecule exists in two or more labile forms, in triazoles has been a subject of considerable interest due to their biological activities and pharmaceutical importance. Both the isomeric forms of triazoles viz. 1,2,3 and 1,2,4 triazoles, exhibit tautomerism. The NH hydrogen of triazoles can be attached to any of the three nitrogen atoms in triazoles. The number and nature of tautomers present depends on many parameters such as temperature, solvent, pH, nature of substituents etc. As many as five tautomeric forms are possible for substituted-1,2,4-triazole thiones. Chemical properties and reactions of these systems depend greatly on the nature of the tautomer. Hence, it is necessary to understand tatutomerism of triazoles in detail. Tautomerism in solution is considered as a dynamic system where different tautomers co-exist in equilibrium under fast exchange. The dynamic nature makes tautomerism a challenging problem in experimental science. Hence, it is essential that the experimental techniques required for the study of tatuomerism should be capable of providing information about the structure of the tautomers as well as their populations under the conditions of measurement. The present thesis entitled "**NMR studies on five membered 1,2,3/1,2,4-triazoles and their hybrid systems**"describes an effort to understand tautomerism in substituted 1,2,4 triazole thiones

and their C,S-disubstituted analogs using Nuclear Magnetic Resonance (NMR) techniques and computational chemistry. Besides, these two techniques have also been employed to get a better understanding of hybrid molecular systems containing both 1,2,3 and 1,2,4 triazole rings. The thesis is divided into five chapters as described below.

CHAPTER I

Introduction.

Chapter 1 provides a general introduction to the triazole ring systems and tautomerism with special emphasize on tautomerism in 1,2,4 triazoles along with a background of information available in the literature. An overview of various experimental techniques employed to study tautomerism is also provided with special emphasis on NMR techniques, which is used extensively in the present work, and theoretical studies. This chapter also give an introduction to various NMR techniques employed in the present work in addition to some of the computational techniques such as DFT, molecular dynamics etc.

CHAPTER II

Tautomerism in substituted-1,2,4-triazole thiones by NMR techniques.

This chapter addresses the issue of tautomerism in substituted 1,2,4 triazole thiones in solution and solid state by NMR spectroscopic techniques. Substituted triazoles can exist in three tautomeric forms as shown below.

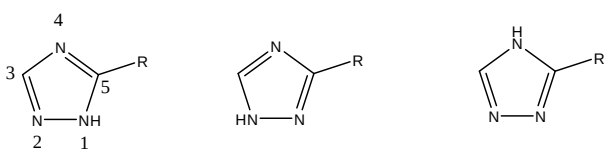

Scheme-1: *Tautomers of substituted 1,2,4 triazole*

The situation becomes more complicated if the substituent is OH, SH or NHR due to the presence of an extra "labile" proton, which can also take part in tautomerism. This will lead to the formation of two additional tautomers with exo cyclic double bonds. The tautomers of the molecules employed in this investigation is shown in Scheme-2

Scheme-2: *Possible tatutomers of the systems investigated.*

This chapter is organized in two sections. Section A describes the approach based on solution state NMR while section B deals with solid state NMR studies.

Section A: Solution state NMR studies of tautomerism in substituted 1,2,4-triazole thiones

In the section A, an approach comprising of 1D as well as 2D experiments based on ^{1}H, ^{13}C and ^{15}N nuclei is used for characterization of tautomers in the solution state. The use of a combination of various 1D/2D NMR experiments in obtaining information about the nature of tautomers in these systems is discussed. All the systems studied show the presence of only one tautomer *viz,* the 1, 4 dihydro thione (1a,scheme-2), which is

characterized by the presence of two low field NH resonances between 13-14 ppm, confirmed by ^{1}H-^{15}N HSQC experiment (Fig .1). Assignment strategies used are shown in scheme-3. Substituent on the triazole ring does not have any influence on the nature of tautomeric form. In all the cases studied the two NH of the 1,2,4-triazole ring behave differently in DMSO solution. H-1 always appears as a sharp signal while the H-4 exhibits broadness due to chemical exchange with residual water present in the solvent. This clearly points to the labile nature of H4 compared H1 and helps in its assignment. Other characteristic features of 1,4 dihydro thione are ^{13}C chemical shift of ~165-168 ppm for C=S carbon, ^{15}N chemical shifts of -95 to -106 ppm for N2, -170 to -180 ppm for N1 and -200 to -210 ppm for N4.

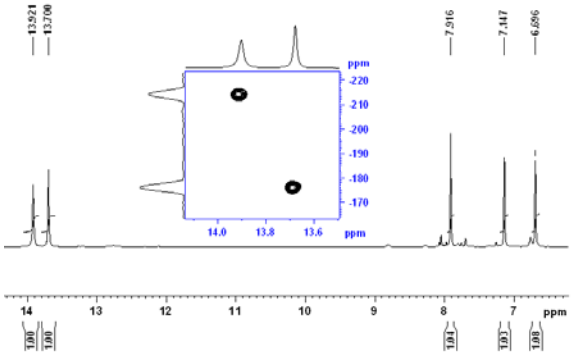

Fig.1: *^{1}H NMR spectrum of compound 1 (R=furyl). ^{1}H-^{15}N HSQC spectrum is shown as inset*

Some of the triazole thiones described above was found to be difficult to characterize, especially to extract chemical shits for all nitrogen atoms by solution state NMR techniques due to exchange of NH protons of triazole ring with trace amounts of water, even though tautomer 1a (*1H,4H* thione) was confirmed unambiguously. The

problem of dynamic equilibrium is absent in the solid state or if present, is extremely slow. Unlike X-ray crystallography, solid state NMR can conveniently be employed for structural characterization in samples in the powder form, which can be amorphous or microcrystalline. Section B of this chapter describes the use of ^{1}H MAS, ^{13}C CP-MAS and ^{15}N-CP MAS for the characterization of the triazole systems studied in the previous section and some other similar compounds.

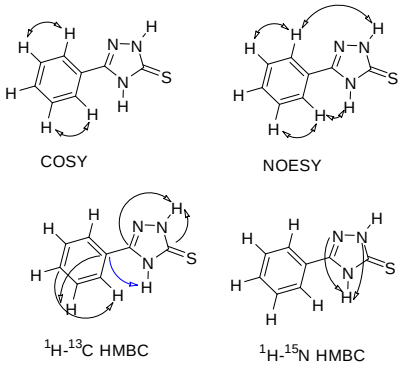

Scheme-3: *Important homonuclear and heteronuclear correlations observed for a typical case.*

Section B: **Solid state NMR studies on tautomerism in substituted 1,2,4-triazole thiones**

^{1}H MAS spectrum of the compound is recorded at a spinning speed of 40 Khz with a relaxation delay of 100 - 500 seconds. From the features of ^{1}H MAS spectrum (Fig-2) and comparison with the ^{1}H NMR spectrum in solution state, it is clear that the tautomer present in the solid state also has two protons directly bonded with similar type of hetero atoms (nitrogen) of the triazole ring. Presence of the same tautomer is also supported by the ^{13}C and ^{15}N CP-MAS spectra. (Fig.3)

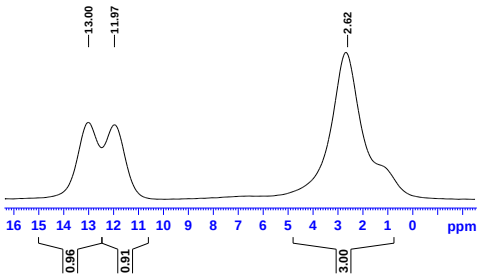

Fig.2: *[1]H MAS of the compound 2 (methyl thione) at 40 Khz spinning speed (700 MHz,).*

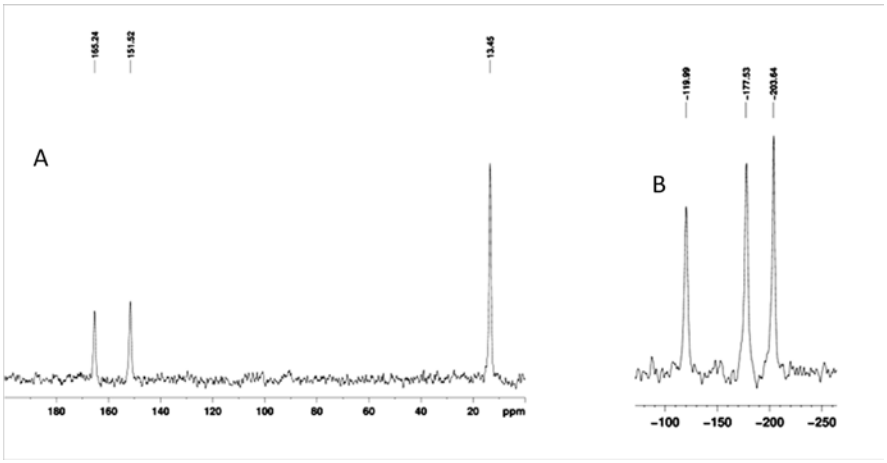

Fig.3: *[13]C CP-MAS (left) and [15]N CP-MAS (right) spectra of the compound 2 (methyl thione) at 8 Khz spinning speed.*

The ^{13}C spectra indicated that a chemical shift at ~165 ppm for triazole ring carbon for C5 is an unambiguous evidence for the presence of *1H, 4H* thione tautomer in solid state, though ^{13}C nuclei are not directly involved in tautomerism. Chemical shift of other ring carbon (C3), as expected, varies with substituent. The ^{15}N spectrum showed three distinct signals and the chemical shifts observed in the solid state are very close to the chemical shifts in the solution state, especially for N1 and N4. All these observations confirm the presence of only one tautomer, 1,4 dihydro tautomer, 1a in solution as well as solid state.

CHAPTER III:

Tautomerism in disubstituted sulfanyl 1,2,4-triazoles in solution and solid state.

The *S*-substituted derivatives of 1,2,4 triazole thiones are well known intermediates for synthesis of various important classes of compounds. These systems also exhibit tautomerism. The number of tautomers reduce to three as the sulphur atom is substituted. The three possible tautomers are shown below (scheme-4) which differs in occupation of the labile proton. Approaches based on NMR spectroscopy have been employed to study tautomerism in solid and solution state for some *S*-propargyl and *S*-allyl derivatives of substituted 1,2,4 triazoles thiones (disubstitued sulfanyl 1,2,4 triazoles) in this chapter. This chapter is also divided into two sections. Section A comprises studies based on solution state NMR and section B describes solid state NMR investigations. Various systems studied are as shown in scheme 4 along with the possible tautomers.

Scheme 4: *Possible tatutomers of the systems investigated.*

Section A: **Solution state NMR studies on tautomerism in *C,S* disubstituted sulfanyl 1,2,4-triazole derivatives.**

Three tautomers are possible for *S*-substituted triazoles studied here, as shown in scheme-4. Some of the *S*-substituted 1,2, 4 triazoles are reported to be existing in equilibrium between tautomers 3a and 3b. The 3c type of tautomer is unstable due to the presence of two C=N groups attached to two adjacent nitrogen atoms of the five membered ring ("α-diaza effect"). Even theoretical calculations showed very little difference in the free energies of 3a and 3b. Tautomerism in this type of compounds is more ambiguous than in the case of thiones discussed in the previous chapter. Hence, detailed investigations of these systems have been carried out to get more insight into the tautomers and their dynamic nature. ^{1}H NMR spectrum in DMSO shows changes in the spectral pattern with time. For example, NH peak splits in to two with time and accompanying changes are also seen for other resonances (Fig.4)

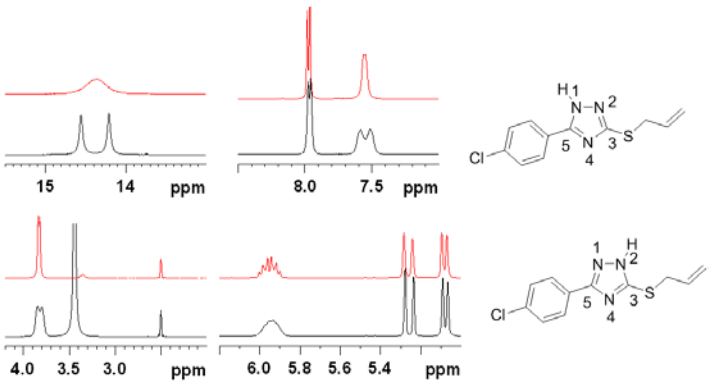

Fig.4: *^{1}H NMR spectrum of a disubstituted 1,2,4 triazole sulfanyl compound. Spectrum shown in red colour is of a freshly prepared sample and the one in black is recorded after two months of aging.*

Most of the samples investigated show the existence of two types of spcies in a dynamic equilibrium which is attributed to *N1-H/N2-H* tautomer (3a/3b). The NH region of ^{1}H spectrum shows two peaks in different proportions while the ^{13}C spectra are very broad (Fig.5). Broadening of ^{13}C signals are mainly noticed for the triazole ring carbons (165-150 ppm). These observations clearly demonstrate the existence of a dynamic situation involving the two tautomers in DMSO solution. The ^{1}H and ^{13}C NMR spectra of a representative case are shown in Fig.6 for furyl, *S*-propargyl system where multiplicity of the signals are clearly seen in the ^{1}H as well as ^{13}C spectrum.

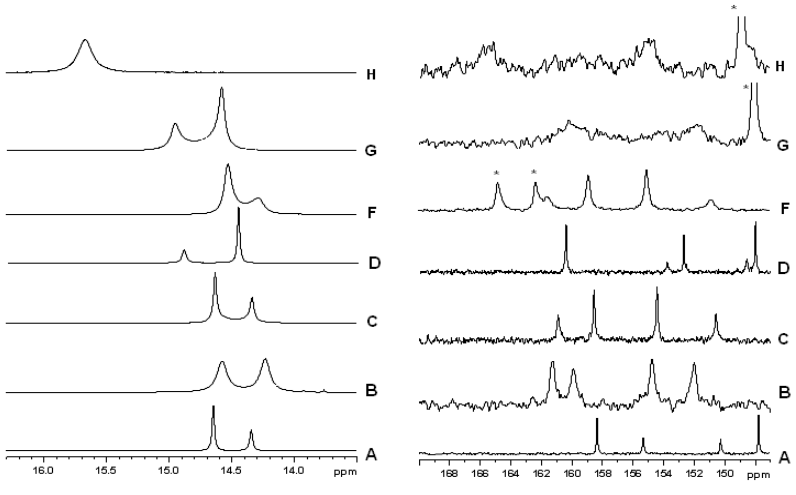

Fig.5: *^{1}H (left) and ^{13}C (right) NMR spectra of some of the disubstituted sulfanyl 1,2,4 triazoles (Scheme 4) in DMSO d_6. Only the NH region is shown in the ^{1}H spectrum while ^{13}C spectra depict the region of triazole ring carbons. Signals marked with * belong to carbons of substituents.*

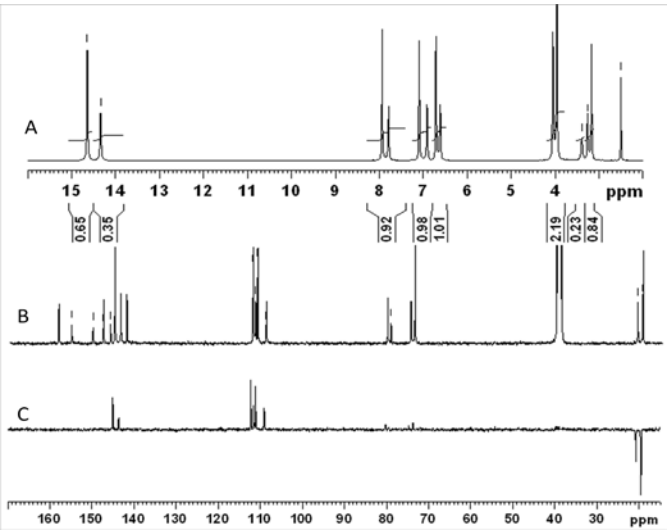

Fig.6: *^{1}H (A) and ^{13}C (B) and DEPT135 (C) NMR spectra of 5-furyl, S-propargyl sulfanyl 1,2,4 triazol*e

NOESY spectrum shows positive and negative cross peaks (Fig.7). Strong positive cross peaks are seen between signals of the major and minor tautomer and clearly demonstrate the presence of exchange equilibrium between the two tautomeric species. The negative cross peaks in the NOESY spectrum are due to actual nOe contacts. But, the most intriguing observation is the negative cross peak seen between the major and the minor peaks (Fig.7).

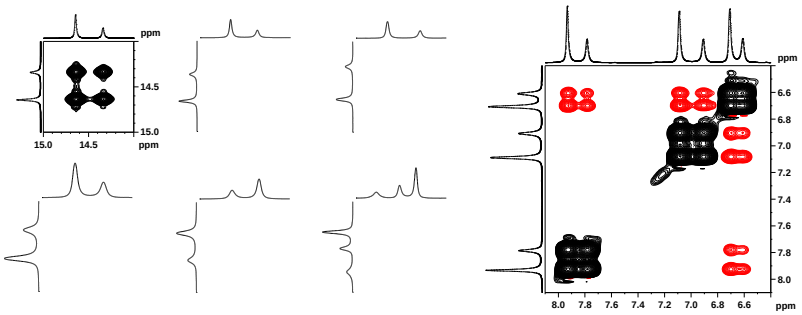

Fig.7: *Expanded NOESY NMR of 5-furyl, S-propargyl sulfanyl 1,2,4 triazole. The diagonal and exchange peaks have same phase and are represented by black contours. Red contours represent negative nOe cross peaks.*

The NOESY data indeed suggests that both the major and minor form not only undergo chemical exchange but they also are within nOe distance of 5Å. Such situation can arise only if a dimeric structure involving both these environments together with exchange is envisaged. It is likely that the two environments correspond to the two tautomers (3a,3b) with NH proton on either N1 or N2 and the NH proton hops between N1 and N2. The

two triazole molecules may be close enough in space to show inter molecular nOe during this process and the life time of the transition state may also be long enough to manifest nOe contacts. Further, the negative cross peak also suggest that the molecular system as such still experiences dynamics corresponding to short correlation times. These observations do not rule out the possibility of the presence of *N4H* tautomer, however it is expected to be less stable on the basis of theoretical calculations, . Hence, this possibility has not been considered. Moreover, the close nature of ^{15}N chemical shifts observed (-174.6,-168.6ppm) for the two forms also favours a situation where in the chemical shifts are not much disturbed. Taking all these into consideration the following dynamic model involving two tautomers is proposed (Scheme 5). All the systems studied exist in a dynamic equilibrium involving the two tautomeric species in DMSO solution. The population of these tauomers varies with the system. In some of the cases studied, the dynamics seems to slow down with time. Variable temperature NMR measurements shows that the dynamic is very slow on the NMR time scale and the equilibrium is reversible in nature.

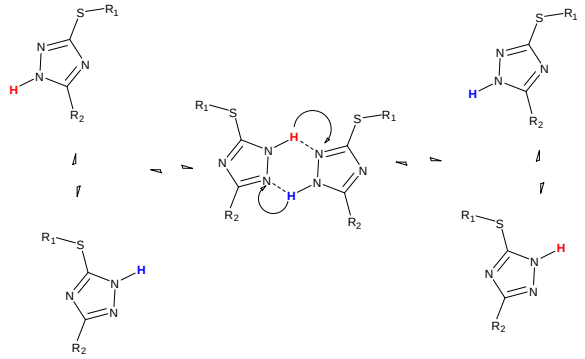

Scheme 5: *The proposed dynamic equilibrium of two tatuomers*

^{13}C NMR chemical shifts of the triazole ring carbons (C3 and C5) and C1'of the substituent is sensitive to the nature of tautomers present and carry the signature of the tautomer present. Triazole ring carbons adjacent to the ring NH is always found to be shielded. The NH proton of *N2-H*(3a) tautomer is more deshielded than that of *N1-H* (3b) form.

Section B: Solid state NMR studies on tautomerism in *C,S* disubstituted sulfanyl-1,2,4-triazole derivatives:

The dynamic nature of the tautomeric species in solution and related problems in their characterization has been discussed in the previous section. Solid state NMR technique is very handy in such situations for characterization. Of course, it will reflect the nature of tautomer present in solid state which may or may not differ from that present in solution. A number of disubstitued sulfanyl 1,2,4 systems have been investigated by ^{13}C CP-MAS, ^{15}N CP-MAS and ^{1}H MAS and the results are discussed in this section.

^{1}H chemical shift of proton donors like NH group is very sensitive to the nature of hydrogen bond with other acceptors. They experience down field shift in presence of acceptors and the magnitude of the shift is a measure of the strength of the hydrogen bond. The ^{1}H chemical shift of NH proton in the solid state span a range of ~4.5 ppm (13 to 17.5 ppm) compared to ~1.2 ppm (13.7 to 14.9 ppm) in DMSO solution. In the solid state, intermolecular interaction is the source of hydrogen bond acceptors. It is interesting to note that the ^{1}H chemical shift of the donor NH group is relatively shielded in the molecules which showed the presence of more than one tatuomer in solution suggesting weaker inter molecular interactions in solid state.

Comparison of ^{15}N CP-MAS spectra and chemical shifts in the solid state provides some interesting insights. The number of signals obtained for triazole ring nitrogen atoms corresponds to the number of different molecular environments present in

the solid state. Most of the molecules studied show only three well separated signals corresponding to N1 (-160 to -171 ppm), N2 (-82 to -109 ppm) and N4 (-138 to -153 ppm) nitrogen atoms thereby indicating the existence of only one type of tautomer in the solid state. But, two of the systems studied (*p*-fluoro-phenyl, *S*-propargyl and *p*-nitro phenyl, *S*-propargyl cases), clearly showed six well separated resonances for the three triazole nitrogen atoms in the ring (Fig.8) and demonstrated the co-existence of two types of different molecular environments. Whereas, the nitro group in the *para* nitro case (compound 3a, scheme 4) showed only one signal. The above observations indicate that the extra signals observed for the three nitrogen atoms of the 1,2,4-triazole ring are from two different tautomeric species (tautomorphs) present in the system, which is same as observed in the solution state, rather than due to phenomena such as polymorphism or solavtomorphism. Besides, comparison of ^{15}N chemical shift data provides information about the differences in the solid state structural features in the systems investigated, which also has implication in their solution state behavior. Two of the systems investigated, viz, the *para* fluoro phenyl *S*-propargyl and *para* nitro phenyl *S*-propargyl sulfanyl 1,2,4 triazoles (compound 2, and 3a,scheme 4) definitely behave differently from others. The magnitudes of difference seen in the ^{13}C CP-MAS spectra are not significant as that in the case of ^{15}N spectra.

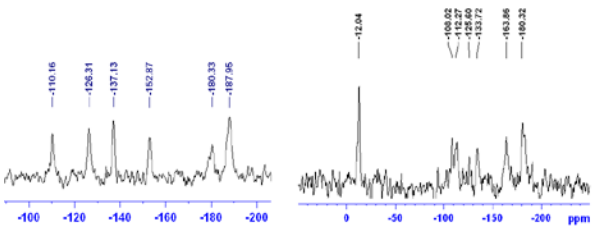

Fig.8: *^{15}N CP-MAS spectra of p-fluoro-phenyl, S-propargyl (left) and p-nitro phenyl, S-propargyl (right).The signal at -12.04 ppm is that of the nitro group.*

CHAPTER IV

NMR studies on the mixed hybrid derivatives of 1,2,4 and 1,2,3-triazoles.

The aim of the work carried out in this part of the thesis is to characterize hybrid molecular systems that contains 1,2,3-triazole and 1,2,4-triazole moieties in the same molecule and study of some of their molecular properties using multi nuclear magnetic resonance approach. Self assembling behavior of these systems is also examined in addition to their ability to bind halide ions. Many hybrid triazoles, which contain triazole moiety and another pharmacophore in the same molecule, are known for their biological activity, especially to overcome the problem drug resistance. Hybrid triazoles are also known to be molecular systems of considerable interest due to their potential applications. This chapter is divided into two parts. Part A deals with structural characterization of hybrid triazoles and Part B describes their self assembling nature and interaction with halogen.

Part A: NMR characterization of the hybrid derivatives of 1,2,4 and 1,2,3-triazoles

A number of hybrid triazoles shown below (Scheme.6) have been completely characterized by various NMR spectroscopic techniques. Assignment of ^{1}H, ^{13}C and ^{15}N chemical shifts in these systems are not very straight forward. The present investigation describes the use of homonuclear and heteronuclear 2D NMR experiments to achieve unambiguous assignments of all the protons, carbons and nitrogens in the systems studied.

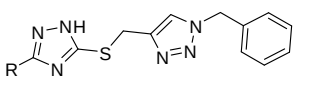

R= 1) H, 2) CH_3, 3) t-Bu

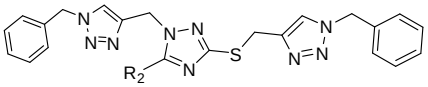

Where R_2= 9) H, 10) CH_3, 11) t-Bu, 12) P-C_6H_4-OMe

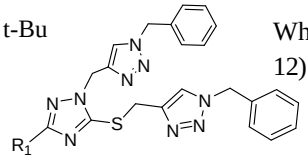

R_1 = 4) H, 5) CH_3, 6) t-Bu, 7) p-C_6H_4-Cl, 8) p-C_6H_4-OMe.

Scheme 6: *Structure of hybrid triazoles investigated*

A combination of COSY, NOESY, ^{1}H-^{13}C HMBC and ^{1}H-^{15}N HMBC spectral analysis is employed for complete assignments of resonances. ^{1}H-^{15}N HMBC is very handy in achieving unambiguous assignments. As an example, ^{1}H-^{15}N HMBC spectrum of one of the systems studied and a schematic representation of important homo and hetero nuclear correlations observed are shown in Fig. 9.

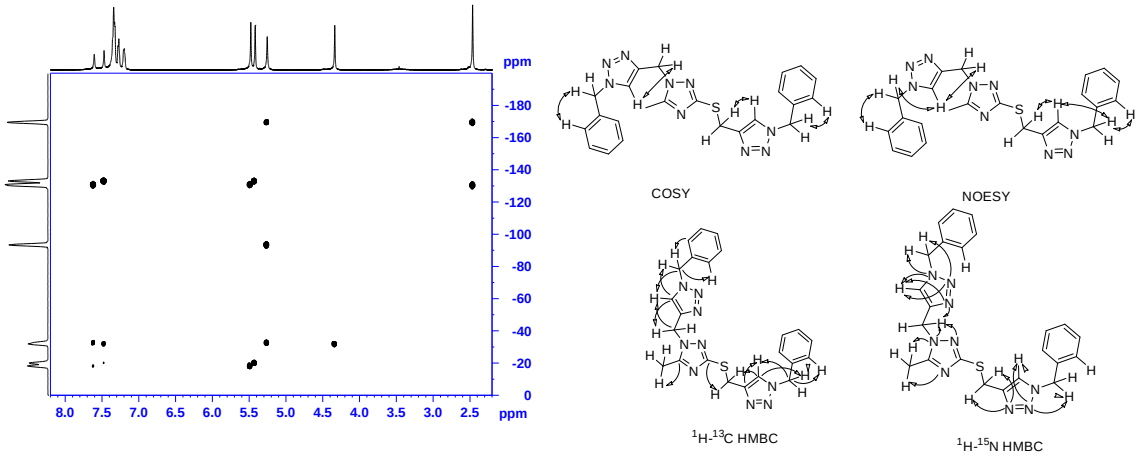

Fig.9: *^{1}H-^{15}N HMBC spectrum (left) and schematic representations of the important homo and hetero nuclear correlations used for assignments.*

In general, COSY cross peaks arising from long range scalar coupling are found to be very useful for assignments of various methylene bridges in these hybrid molecules. ^{1}H- ^{15}N HMBC along with the ^{1}H-^{13}C HMBC spectra are very useful for unambiguous assignments. Unexpected long range NOESY cross peaks were observed for some of the compounds which is further investigated in detail. An example of such an observation of cross peaks is in Fig.10 for one of the systems studied.

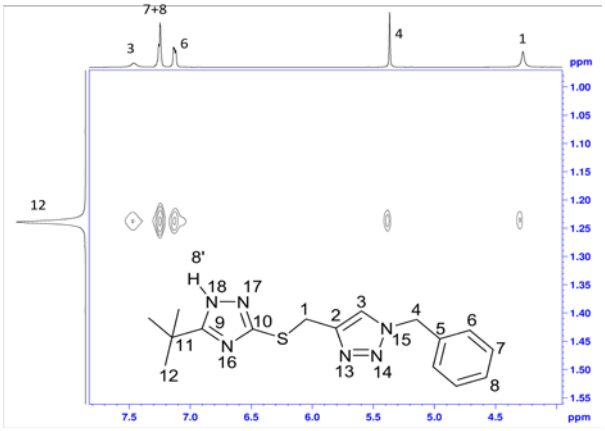

Fig.10: *NOESY spectrum of compound 1 (Scheme-6) showing nOe contacts of t-butyl group*

The t-Bu group substituent at C-9 of the 1,2,4-triazole ring, exhibits NOESY cross peaks with H-1, H-3, H-4, H-6, and H-7 protons which are located almost on the opposite side of the t-Bu substituent. The crystal structure of the compound shows that the groups which show NOESY cross peaks are not oriented spatially close to each other. Hence, the nOe pattern obtained is either from the intermolecular interactions (self assembling) or from a solution state structure which is different from the solid state structure. Organic molecules, which posses the property of self-aggregation can show such intermolecular nOe's and self-aggregation is a known phenomenon in triazole derivatives. This triggered the study of self-assembly (intermolecular interactions) in these triazoles.

Part B: Studies on self-assembly of flexible triazoles and non-covalent bidentate contacts with halide anions.

In this part of the thesis, self-assembling nature of some of the triazole systems studied in the previous section has been examined through the effect of temperature and concentration on ^{1}H NMR chemical shift and also by following the changes in diffusion coefficients with concentration. Considerable change in the magnitude of the NH chemical shift with temperature ($\Delta\delta/\Delta T$=-38.6ppb/K) indicates that the NH is involved in some type of intermolecular interactions in one the systems studied (Fig.11). The triazole H-3 proton of this compound exhibits weak upfield shift of $\Delta\delta$ = 0.04 ppm ($\Delta\delta/\Delta T$=-0.53 ppb/K) and indiactes very weak intermolecular interactions involving the triazole CH.

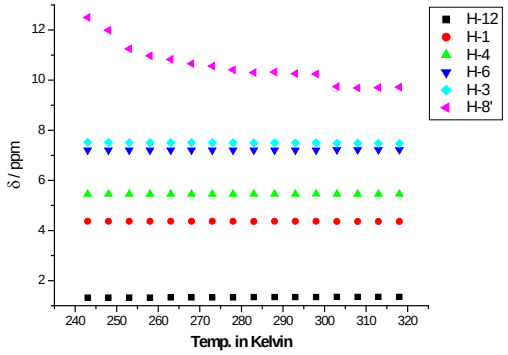

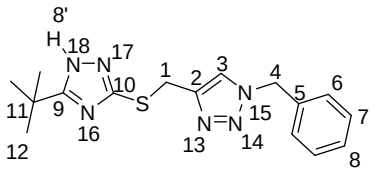

Fig.11: *Plot of ^{1}H chemical shift verses temperature for the molecule shown*

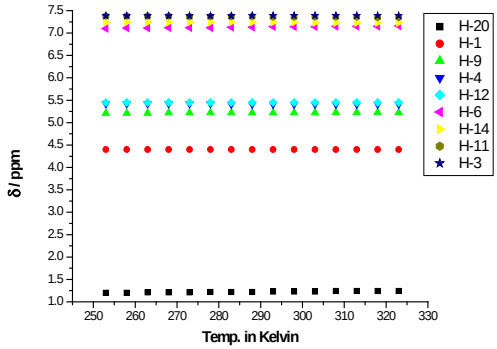

Fig.12: *Plot of ^{1}H chemical shift verses temperature for the molecule shown*

Compound without NH groups showed only minor negative temperature coefficients for triazole protons (Fig.12). The 1,2,3 triazole CH proton, H-11, shows

slight upfield shift of $\Delta\delta$ = 0.022 ppm with a temperature coefficient of -0.31 ppb/K while H3, shows minor deshielding effect with increase in temperature (temperature coefficient +0.057 ppb/K). These studies favour the presence of very weak intermolecular interactions involving triazole C-H. Nevertheless, these measurements definitely rules out the possibilities of any strong pi-pi stack interactions which would have resulted in an appreciable up field shift of protons on cooling. Dilution experiments were also performed to get more insight into self-assembly phenomenon in these compounds and the results support the conclusions from variable temperature measurements since the changes in chemical shifts observed are found to be negligible.

NMR self diffusion coefficient measurements were carried out on solutions of 100, 10 and 5 mM concentrations. A 10 fold increase in concentration from 10mM to 100mM does not change the diffusion coefficients to any greater extent, though the molecules in 5mM solution diffuse faster which is attributed to changes in viscosity or very weak association. All these observations show that intermolecular interactions, even if present, do not lead to any molecular self assembly or bigger aggregates. Probably weak aggregates of small order are formed under the experimental conditions which cannot result in the intermolecular nOe's observed for these molecular systems. Therefore, the NOESY cross peaks obtained for these compounds is likely to be of intra molecular origin. In order to verify this, Molecular Dynamics (MD) simulation studies have been performed to obtain 3D structures.

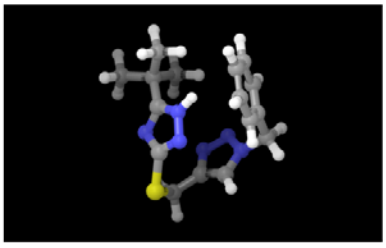

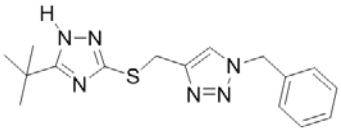

Fig.13: *Optimized structure of the molecule shown obtained from MD study*

The optimized structure for a typical case (Fig.13) shows that the hybrid triazole molecules do not have a liner structure and hybrid triazoles containing at least one 1,4 disubstituted 1,2,3 triazole moiety, show a bent structure similar to a turn in oligo peptides. In such molecular conformations, protons of tertiary butyl group come closer to protons present in groups away from it and develop dipolar interactions resulting in the observed nOes.

Binding studies of the triazole CH with the halide anions:

Triazole molecules are known to interact with halide ions and this part of the thesis discusses the study of halide ion binding capability of some of the triazoles that have been investigated for structural characterization. There are many reports on binding of halogen ions to rigid macrocyclic triazoles through aromatic CH proton. Open or flexible aryl triazoles are also known to bind halide anion through complexation induced conformational changes, where suitably located aromatic protons also take part in the binding processes with the halide anion. The triazole molecules studied here are more flexible in nature compared to the structurally constrained macro cyclic cases and they also have aromatic rings as well as triazole C-H which can take part in binding with the halide ions. Triazole derivatives studied here also show antitubercular activity by selectively killing dormant pathogenic *tuberculi bacilli*. Binding of the triazole CH with halide anion generally results in downfield shift of triazole C-H proton. The anion binding properties of these compounds were monitored by ^{1}H NMR titration in $CDCl_3$, which is known to be a poor solvent to induce halogen binding. This helps to reduce the

assistance of solvent and thus provide a realistic picture of the affinity of triazole-halide interactions.

Results of this study show only minor alteration of chemical shift of the 1,2,3-triazole C-H protons and the other protons thereby suggesting weak interactions with halide anions. This study demonstrates that hybrid triazoles are interesting unsupported triazoles systems that can form weak intermolecular interactions with halide anions and also supports the formation of weak halogen bonds by triazoles through C-H bonds. It is observed that except fluoride anion, all the other halide anions show some interactions with the t-Bu substituent in the compounds studied. Molecular dynamics simulations show that the 1,2,3-triazole ring protons take part in the binding of the halide anion along with the NH of the 1,2,4-triazole ring as shown in the Fig.14 where t-Bu group is also orientated towards the halide anion.

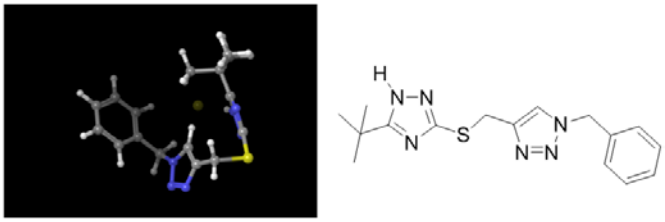

Fig.14: *Optimized structure of the molecule shown (left) obtained from MD study in presence of bromide ion.*

CHAPTER V

Theoretical calculations of geometry optimized strictures and NMR shielding constants of substituted triazole thiones, *C,S* disubstituted 1,2,4-triazole sulfanyl compounds and hybrid of 1,2,3 and 1,2,4-triazoles by Density Functional Theory.

The substituted triazole thiones studied in Chapter II exclusively exist as 1,4 dihydro tautomer in solids as well as in DMSO solutions. The sulfanyl derivatives of triazole thiones investigated in Chapter III is found to be present in a dynamic equilibrium in solution while solid state NMR studies indicated co existence of two tautomers, at least in two cases. These observations prompted a study some of these systems by theoretical calculations whichcan provide information about the relative stability of different tautomers, their spatial geometry and other molecular properties. Besides, such an approach will also allow calculation of NMR chemical shift for each tautomer and a comparison of this with experimentally determined values will be useful in identifying the nature of tauomer/s observed in solution and solid state. The observed NMR chemical shift in solution is a population weighted average of the chemical shifts of the exchanging forms, while the chemical shift can be computed for each of the different tautomeric species involved in the dynamic equilibrium. Hence, theoretical calculation of chemical shifts is very useful in understanding the nature of dynamic events. Besides, it is also possible to find out stable conformers and tautomers in the systems by comparing the experimental chemical shifts with theoretically calculated chemical shifts.

Some of the systems discussed in Chapters II,III and IV were studied computationally by Density Functional Theory to get minimum energy geometry optimized structures which is further used for calculation of shielding constants to extract ^{1}H, ^{13}C and ^{15}N theoretical chemical shifts. This chapter is divided into two parts, Part A deals with theoretical studies of thiones and sulfanyl derivatives of 1,2,4 triazoles while part B is devoted to hybrid triazoles. “Jaguar” software, an *ab initio* calculation software available as a module in “Schrodinger” package at the M06-2X/6-31G**++ level is

employed in this work for theoretical calculations which has continuum solvation models to account for solvent effects.

Part A: Geometry optimized structure and calculation of the NMR shielding constants of mono substituted 1,2,4-triazole thione and *C,S*-disubstituted sulfanyl-1,2,4-triazole derivatives by Density Functional Theory

In part A of this chapter, minimum energy tautomeric structures of various substituted 1,2,4 triazole thiones discussed in Chapter II and their sulfanyl derivatives discussed in Chapter III are calculated. These structures are further compared with the structure predicted from NMR studies. ^{1}H, ^{13}C and ^{15}N chemical shifts of all the tautomers are obtained from theoretically calculated shielding constants and compared with the experimentally measured values to obtain information on the nature of tautomers present in the solution and solid state. The geometry optimized structure obtained from DFT calculations showed that for all the substituted 1,2,4 triazole thiones investigated, the 1,4 dihydro tautomer (1a, Scheme-2) has the minimum energy which is same as the one envisaged from NMR studies described in Chapter II. The observed chemical shift correlated well with the calculated chemical shift of the minimum energy 1,4 dihydro tautomer (Fig.15). The 1,2 dihydro tautomer (1b, Scheme-2) is the least stable.

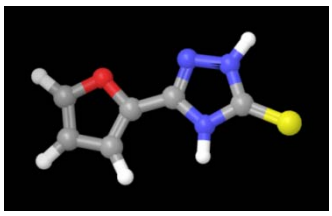

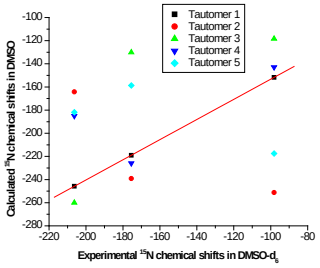

Fig.15: *Geometry optimized minimum energy structure of the most stable tautomer of furyl thione (left) and Correlation between the experimentally observed and the calculated ^{15}N chemical shifts for the H-thione 1,2,4-triazole in which tautomer1 corresponds to the 1,4 dihydro thione.*

In the case of disubstituted 1,2,4-triazole sufanyl derivatives, geometry optimization (Fig.16) energy for the tautoemer-3b (*N2-H* form,Scheme-4) is least (more negative) therefore it is the most stable tautomer among all the three tauotmers. The difference in energy between the 3a (*N1-H* form, Scheme-4) and 3b (*N2-H* form, Scheme-4) is less compared with the 3c (*N4-H* form, Scheme-4) therefore in most cases, in the solution state, an equilibrium between the tautomeric forms 3a and 3b can be expected with the 3b being the major one. This is in line with the observations made in Chapter III. The computed ^{1}H,^{13}C and ^{15}N chemical shifts of the tautomers showed that the ^{13}C and ^{15}N chemical shifts are very sensitive to the structure of the tautomer. For example, the traizole ring carbon chemical shifts are very different for *N1-H* and *N2-H* forms (3a and 3b, respectively in Scheme-4) of tautomers. Importance of triazole ring carbon (C3 and C5) chemical shifts in the determination of the nature of the tautomer as seen in solution state NMR studies is also validated by the calculated chemical shifts. This is in accordance with the ^{13}C chemical shifts of the triazole ring carbons observed for the two species in DMSO solution as represented in Scheme.7 which depicts a comparison of the calculated and experimental chemical shifts for a representative case.

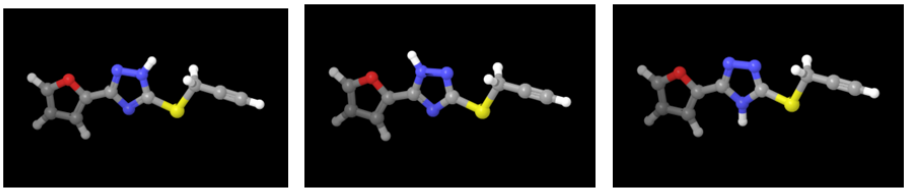

Fig.16: *Geometry optimized structures obtained for tautomers of furyl sulfanyl 1,2,4 triazole corresponding to the 3a (left),3b(middle) and 3c(right) forms.*

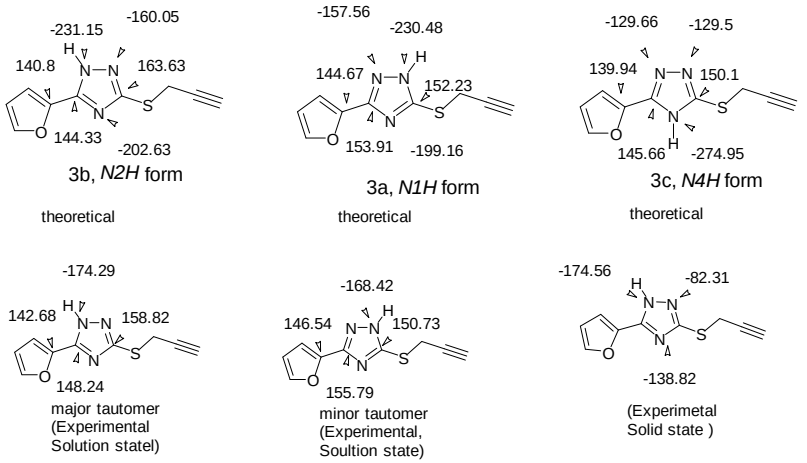

Scheme 7: *Comparison of the predicted and experimental ^{13}C and ^{15}N chemical shifts of furyl substituted sulfanyl 1,2,4-triazole.*

Part B: Geometry optimized structures and calculation of the NMR shielding constants of hybrid triazoles by Density Functional Theory

This section summarizes the results of the theoretical calculation of minimum energy structures of the hybrid triazole molecules characterized in Chapter IV and comparison of the calculated ^{1}H,^{13}C and^{15}N chemical shifts with the measured values. The minimum energy conformation of the hybrid triazoles are compared with the

structural features predicted from the solution state NMR studies. The optimized structures of these hybrid triazoles, containing at least one 1,4 disubstituted 1,2,3 triazole ring, always show a bent structure (Fig.17) with a geometry similar to a β turn. These observations are in line with the nOe contacts observed for t-butyl substituent with protons on the other side of triazole ring as discussed in Chapter IV. The correlation graphs obtained for the calculated and experimental ^{1}H, ^{13}C and ^{15}N chemical shifts exhibit linear dependency (Fig.18).The best correlation graph is obtained for ^{13}C followed by ^{15}N.

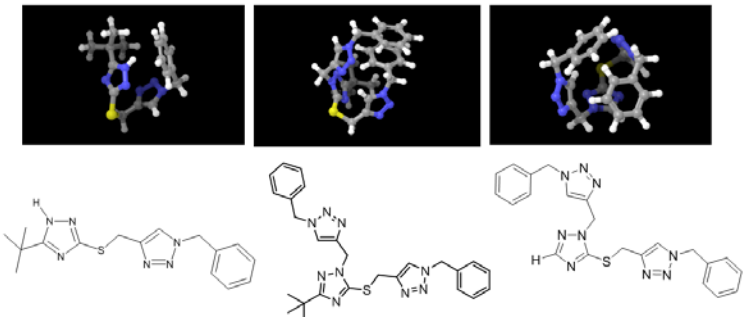

Fig.17: *Geometry optimized conformations of hybrid triazoles. Corresponding structures are given below the calculated structures.*

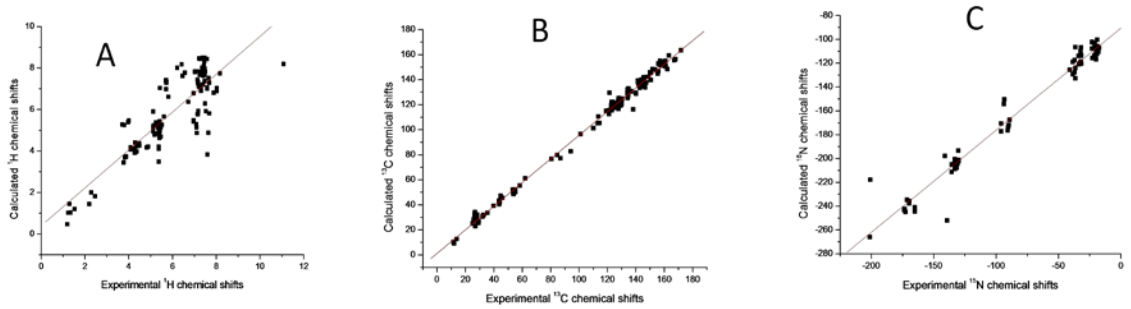

Fig.18: *Graph showing comparison of the experimental and theoretical ^{1}H (A), ^{13}C (B) and ^{15}N (C) chemical shits for hybrid triazole derivatives.*

In conclusion the studies undertaken in this thesis clearly bring out the power of NMR spectroscopic techniques and computational chemistry in understanding the nature of tautomers present in solution and solid state. The NMR investigation and theoretical calculations showed that all the substituted triazole thiones studied exist in only one tautomeric form, out of the five possibilities, with the proton on the N1 and N4 nitrogen (1a, Scheme-2). In the case of *C, S* disubstitued sulfanyl 1,2,4 triazoles, theoretical calculations predicts very close energy separation between two of the minimum energy structures of tautomers *viz*, the *N1-H* and *N2-H* forms (3a and 3b, respectively,Scheme-4), the stability of the latter being more. The solution state NMR investigations unambiguously demonstrate the presence of a slow dynamic equilibrium involving these two tautomeric forms. Besides, the thesis also demonstrate how NMR spectroscopy and computational chemistry can be effectively used in the study of hybrid triazole systems containing both 1,2,3 and 1,2,4 triazole moieties in the same molecule

.

Table of Contents

The two downfield protons at 11.97 and 13.00 ppm, showing integration around one each, corresponds to NH protons of the 1,2,4-triazole ring while the most upfield signal at 2.62 ppm corresponds to three protons of the methyl group. From the features of this ^{1}H MAS spectrum and its analogy with the ^{1}H NMR spectrum in solution state, it is clear that the tautomer present in solid state has two protons directly bonded with hetero atoms (nitrogen) of the triazole ring. This is possible only if the tautomeric form 2a or 2b is present. Forms 2c, 2d or 2e are not likely to be present since these forms bear only one proton directly bonded with nitrogen of the triazole ring. ^{1}H MAS spectral analysis does not prove conclusively about whether the tautomeric form 2a or 2b is present in the solid state. Therefore, studies based on the carbon

CHAPTER I

Introduction

1.1 Introduction to the heterocyclic systems:

Heterocyclic compounds form the largest class of organic compounds and are of immense importance in the area of chemical and biological sciences. The majority of pharmaceuticals and biologically active agrochemicals are heterocyclic in nature. Heterocyclic compounds have contributed to the development of society from a biological and industrial point of view. Most of the heterocyclic compounds are nitrogen containing compounds. Heterocycles with other hetero atoms such as oxygen [1] phosphorus [2] and selenium [3] are important as well. Many naturally occurring alkaloids [4-7] such as papaverine, quinine, emetine, theophylline, atropine, codeine, reserpine and morphine are heterocyclic in nature. The synthetic drugs used such as diazepam, chlorpromazine, isoniazid, azidothymidine, barbiturates, captopril and methotrexate are heterocycles. A large number of synthetic heterocyclic compounds find a variety of applications such as fungicides, herbicides, anticorrosive agents, photostabilizers, agrochemicals, dyestuff, copolymers, photographic developers, fluorescent whiteners, sensitizers, booster agent, antioxidant in rubber and flavouring agent etc.. [8-18] Heterocyclic compounds are part and parcel of many biological processes such as energy metabolism, neurotransmission, genetic coding etc. The versatile reactivity of the heterocycles is linked to their electronic distributions in the molecules.[19] The ability of heterocycles to produce stable complexes with metal ions has great biochemical significance. Pyrimidine (cytosine, thymine and uracil) and purine (adenine and guanine) derivatives which are monocyclic and bicyclic heterocycles

with two or four nitrogen atoms, are key components of the deoxyribonucleic acid (DNA) molecules and participate directly in the encoding of genetic information. They also pass information to the related ribonucleic acid (RNA) molecules which control the sequence of the amino acids in protein synthesis. [20-21] Vitamins in the B group (thiamine, folic acid, riboflavin, cyanocobalamine) are nitrogen-containing heterocycles [22] and function either as coenzymes or their precursors. Other vitamins such as ascorbic acid (vitamin C) [23] and α-tocopherol (vitamin E) are oxygen heterocycles [24]. The essential amino acid proline, histidine and tryptophan [25], photosynthesizing pigment chlorophyll; the oxygen transporting pigment haemoglobin [26], the hormones kinetin, heteroauxin, cytokinins [27], neurotransmitter serotonin, histamine respectively are also heterocyclic compounds. Nature utilizes pyrrole and pyridine as the basis of most essential biological systems mainly because the introduction of a heteroatom into a cyclic compound imparts new properties. Heterocycles are chemically more flexible and adaptable to the demands of biochemical systems.

1.1.1 Five membered heterocycles: Five membered heterocylic molecules contain nitrogen, oxygen or sulphur in the ring. These molecular systems can be saturated, unsaturated or with more than one heteroatom in the ring. These systems have important applications in the area of chemical and biological sciences. Some of the five membered hetrocyclic molecules like pyrrole, furan, thiophene, oxazole, thiazole, pyrazole, isoxazole, isothiazole, triazoles etc. (Scheme.1.1) are classified as aromatics. The introductory part on heterocylic systems will be restricted to the ring system of the present investigation *viz*., triazoles.

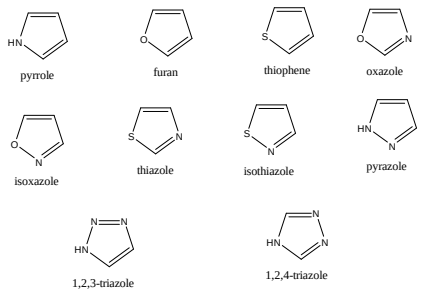

Scheme.1.1: Some *five membered heterocyclic ring systems*

1.1.2 Triazoles: Triazoles are heterocyclic systems with two carbon atoms and three nitrogen atoms. They can exist in two isomeric forms, namely1,2,3 and 1,2,4-triazoles depending on the arrangements of nitrogens and carbons in the heterocyclic system. Both these systems are aromatic in nature. In 1,2,3-triazoles the three nitrogen atoms are arranged in a continuous manner while in 1,2,4 triazole they are intervened by a carbon atom. The numbers in these compounds indicates the position of nitrogen atoms in the ring. Both the isomers are aromatic in character and hence posses a planar ring structure. The heterocycles containing 1,2,3-triazole rings find widespread applications in therapeutics, antifungal compounds, pharmaceuticals etc.[28-31] A few examples are fluconazole, isavuconazole, voriconazole, ravuconazole, itraconazole and posaconazole. Chlorophenylpiperazine derivatives etoperidone, nefazodone and trazodone are effective pshychoactive compounds based on the 1,2,4-triazole system. The antidiabetic drug sitagliptin possess the 1,2,4-triazole ring. There are very few reports in which both the 1,2,3 and the 1,2,4-triazole rings are present in the same molecule.[32,33a]

When a proton is bonded to the electronegative nitrogen atoms of triazoles the electron present in the N-H bond is more polarized towards the nitrogen atom which renders an acidic character to the proton. Hence it can break away easily and can also accept lone pair of electrons from the other nitrogen present in the ring giving rise to formation of a different form called tautomer.

1.2 Tautomerism: The term “tautomerism” is derived from the Greek words, *tauto* means same, and *meros* means part which together means the “same part”. [33b] It is associated with the phenomenon by which the same molecule exists in two or more labile forms. Tautomerism is a type of isomerization in certain type of chemical compounds wherein an atom or a group, G, of a molecule, attached to another atom D, is transferred to a third atom A of the same molecule. Here, the atoms D and A are considered as donor and acceptor atoms.

G-D-X=A D=X-A-G

G, which may be an atom or group transferred during rearrangement from D (donor) to A (acceptor). The migration of G also involves simultaneous movement of π electrons.

According to the IUPAC recommendations, tautomerism is defined as an equilibrium.[34a]

G-D-X=A ⇌ D=X-A-G

The molecules involved in tautomerism are called tautomers. Tautomers are different from isomers. Different tautomers are likely to co-exist in equilibrium and depending on the conditions they can interchange their nature. In other words, they are dynamic in their existence. The acceptor atoms and donor atoms can be carbon, nitrogen, oxygen, sulphur etc. and are linked through bonds involving π electrons. The group G, which is being transferred, is either proton or any other group of atoms. If the transferred group is proton, the tautomerism involved is called as protropy or prototropic tautomerism. If G consists of a group of atoms, the tautomerism, involving relocation of a substituent other than H, can in general be considered as non-prototropic tautomerism. Examples of this type of tautomerisms are : acylotropism (transfer of acyl group), methylotropism (transfer of a methyl group) and aroylotropism (transfer of an aryl group), and elementotropism (transfer of halogens or metals) etc. Another type of tautomerism commonly encountered is valence tautomerism**.** This involves the reorganization of bonding electrons rather than atoms or group of atoms and results in changes in molecular geometry. A classical example is the tautomerism between 1,3,5-cyclo-octatriene and bicyclo[4.2.0]octa-2,4-diene, and bullvalene as shown in the Scheme.1.2.

Scheme.1.2: *Valence tautomerism in1,3,5-cyclo-octatriene and bullvalene.*

Prototropy, the most widely studied type of tautomerism, is of prime importance to chemical and biological sciences. Knowledge of tautomers is very essential in understanding reaction mechanisms in organic chemistry and in biological process such as protein-substrate interactions and chemistry of nucleic acids. In prototropy the transfer of protons is also usually accompanied by redistribution of the π electrons in the system. Hence, different tautomers may differ in their nature of functional group, π electron distribution etc, which determines their physicochemical properties. The hydrogen bonding patterns in prototropic tautomers differ considerably and thus play a crucial role in their structural features and properties. In general, the nature of tautomers present depends on many parameters such as temperature, solvent, pH, nature of substituents, aromaticity, hydrogen bonding, presence of lone pairs etc.[34b]

The most common, popular and widely studied tautomerism is the keto-enol tautomerism involving a carbonyl group in organic compounds. For example the aromatic compounds such as naphthalene-1,4-diol can be present in the enol (form A) as well as keto form (form B) under different conditions as shown in the Scheme.1.3. When the diol form of this compound is heated then the keto form can be formed. The keto form is non-aromatic in nature but still it is kinetically stable. Both the forms are interconvertible under the different conditions.

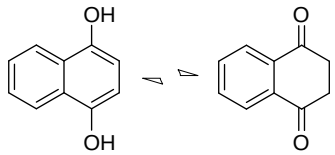

Scheme.1.3: *Different tautomeric forms of the naphthalene-1,4-diol in which form A is the enol form and the form B is the keto form.*

This kind of tautomerism is called keto enol tautomerism because the compounds involved in the tautomerism have the functional groups such as keto and enol before and after the transfer of proton or *vice versa*. On the similar grounds there are other types of

tautomerism depending upon the kind of the functional groups involved before and after the transfer of the proton in the system some of which are discussed below.

1.2.1 Imine-amine tautomerism: A typical example of imine –amine taumerism is 1,3-indandione skeleton as shown in the Scheme.1.4**.** This compound can be present in two imino-enamine forms A and B and another imino-imino form C. [35]

Scheme.1.4: *1,3-indandione skeleton showing imino-enamine forms A and B while C represents the imino-imino form.*

1.2.2 Lactam-Lactim tautomerism: A lactam is a cyclic amide while Lactim is a cyclic carboximidic acid compound characterized by an endocyclic carbon-nitrogen double bond.[36] Lactam and lactim can be converted into each other by tautomerism. The compound 7-OH(SH,NH2)-1,2,4-triazolo[1,5-a]pyrimidines is present in the lactim form A when X=NH while in the lactam form B and C when X=O, S in the solution state as shown in the Scheme.1.5.

Scheme.1.5: *Lactam-Lactim tautomerism in pyrimidines.*

1.2.3 Nitroso (N-Oxide)-Oxime tautomerism: Nitroso refers to a functional group in organic chemistry which has the NO group attached to an organic moiety whereas the oximes are the compounds containing the imine functional group with the hydroxy group bonded directly with the nitrogen of the imine. The compound 2-Nitro-1-nitrosoethylbenzene (nitroso form A) can be converted into its tautomer 2-isonitroso-1-

nitro-phenylethane (oxime form B) in acetone solvent at 25^0C as shown in the Scheme.1.6 [37]

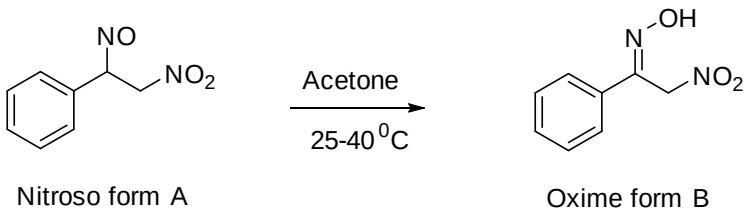

Scheme.1.6: *Conversion of nitroso form A to the oxime form B in 2-Nitro-1-nitrosoethylbenzene.*

1.2.4 Azo-hydrazone tautomerism: In azo compounds two nitrogen atoms are bonded to each other through double bond. Shifting of the double bond between two nitrogens towards one of the nitrogens results in formation of the hydrazone compounds. The compound 1-phenylazo-2-hydroxynaphthol can be present in the azo as well as hydrazone form B as shown in the Scheme.1.7. [38]

Scheme.1.7**:** *Azo form A and the hydrazone form B of 1-phenylazo-2-hydroxynaphthol.*

Ring chain tautomerism [39-48] of cyclic and open sugars is also a well known system exhibiting prototropic tautomerism. Here, the proton shift leads to a structural change from an acyclic to cyclic form. (eg. glucose, fructose etc.) The ring chain tautomerism in D-glucose is as shown in the Scheme.1.8.

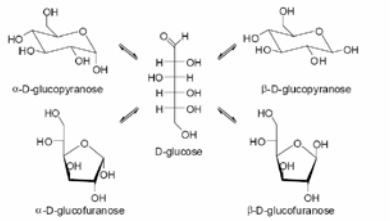

Scheme.1.8: *Ring chain tautomerism in D-glucose.*

1.2.5 Tetrazole-azide tautomerism: In this case one of the tautomeric forms contains a tetrazole moiety and the other contains an azide moiety. An example for this type of tautomerism is shown in Scheme.1.9.

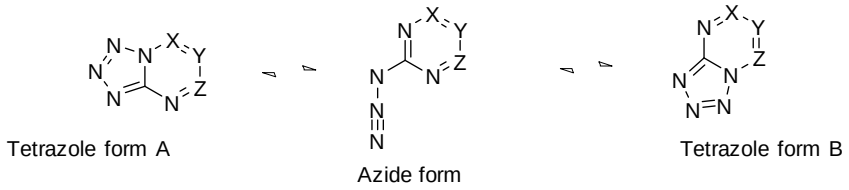

Scheme.1.9: *Azido-tetrazole tautomerism in a series of azido-1,2,3-triazines and azidopyrimidines.*

Another type of prototropic tautomerism is the annular tautomerism of heterocyclic systems where the proton/s shifts between two or more positions of hetero atoms. A few well known examples of this type of tautomerism are; 1-*H* and 3-*H* forms of imidazole, 1-*H*,2-*H*,4-H forms of 1,2,4 triazoles. Substituted imidazole can be present in different tautomeric forms as A and B (Scheme.1.10).

Scheme.1.10**:** *Different tautomeric forms in imidazole.*

Many of the biologically important molecules such as histidine, arginine, cytosine, thymine, uracil, adenine, guanine, histamine and porphyrin etc. also exhibit prototropy as shown in the Scheme.1.11. The different tautomeric forms of porphin and porphyrin are shown in the Scheme.1.12.

Among heterocycles, sulfur and nitrogen containing heterocyclic compounds have been of great interest due to their widespread application as antibacterial, antiviral, CNS active agents etc. They are also used as corrosion inhibitors due to their ability to form

complexes with metal ions. Tautomerism is one of the factors that determine the properties of these systems. Tautomerism is of prime importance in many chemical and biological processes. Hence a proper understanding of tautomeric behavior of systems is essential to support the correct mechanisms in many chemical and biological reactions. [49] Tautomerism is an equilibrium process involving intra or intermolecular rearrangements. It is a common phenomenon encountered in many molecular systems of interest including nucleic acids, drugs, and many other biologically active molecules. The structure and properties of nucleic acids depend greatly on the prototrophy in purines and pyrimidine nucleobases. Base pairing is possible only between the proper tautomers. Specific hydrogen bonds between proper tautomeric forms of the complementary bases control the processes like DNA replication, transcription and stabilization of secondary and tertiary structures of the nucleic acids [50, 51]. The

significance of a particular type of tautomer is very evident from the structure model proposed by Watson and Crick. The presence of non specific or improper

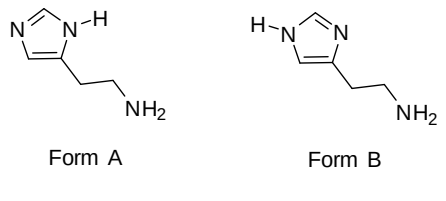

Histamine tautomeric forms A and B

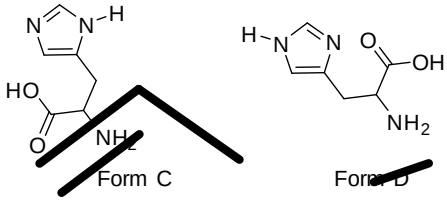

Tautomeric forms of histidine forms C and D

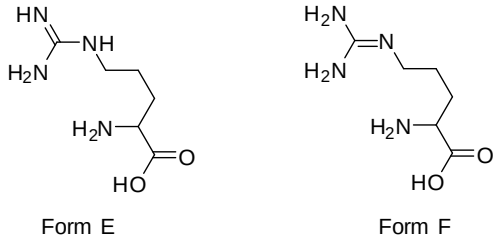

Tautomeric forms in arginine forms E and F

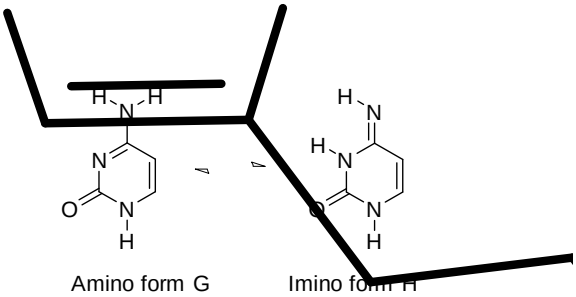

tautomers in cytosine form G and H

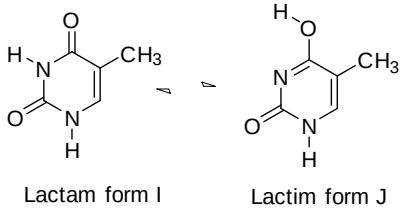

tautomers of thymine I and J

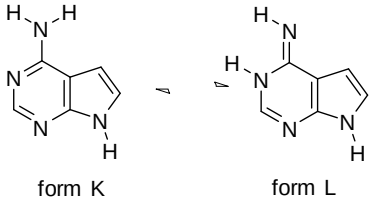

tautomeric forms in adenine K and L

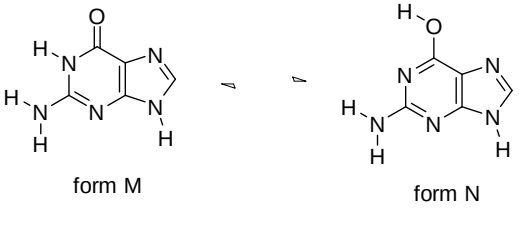

tautomeric forms in guanine M and N

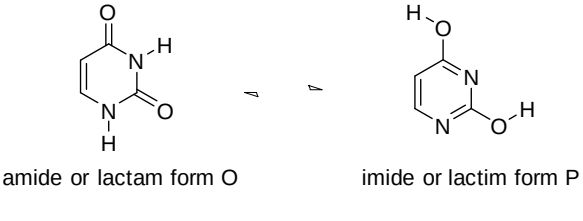

tautomeric forms of uracil form O and P

Scheme.1.11**:** *Tautomerism in some biologically important molecules*

tautomers may result in mismatch and hence mutations.

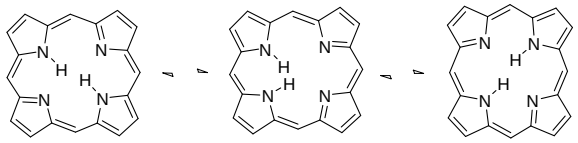

Different tautomeric forms of the simplest porphyrin called porphin A, B and C.

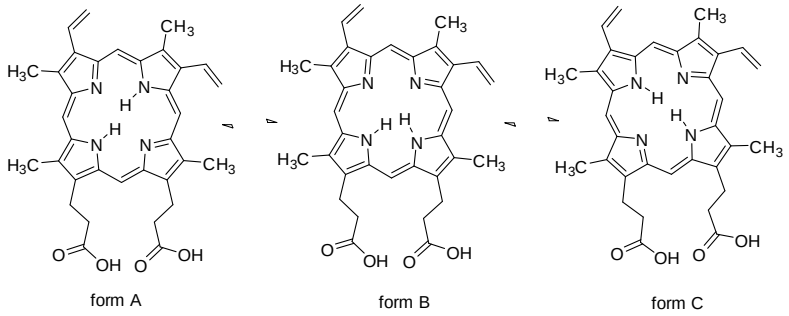

Different tautomeric forms in porphyrin A, B and C.

Scheme.1.12**:** *Tautomerism in porphin and porphyrin.*

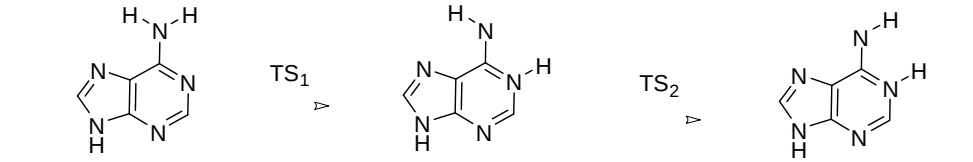

Scheme.1.13**:** *Tautomerization processes of A → A1 in adenine systems.*

Experimental and theoretical studies have shown that the presence of less stable tautomer of pyrimidines and purines leads to mutations resulting from mispairing. [52] Adenine in Watson–Crick base p airs exists in canonical form (A). Besides, it can also form higher energy imino tautomers A1 and A2, relative stability being A>A2>A1. (Scheme.1.13) It is now understood that presence of the imino form A2 induces lethal mutation of adenine in nucleobase mispairings. Thus a fundamental understanding of the phenomenon of tautomerism is important which is evident from many conflicting reports in literature for similar molecular systems. For example the main tautomer guanine was not recognized for a long time. [53-57]

1.3 Tautomerism in 1,2,4-triazoles: Tautomerism in triazoles has been a subject of considerable interest due to their biological activities and pharmaceutical importance. Hence, triazole tautomerism has been a subject of many studies. Both the isomeric forms *viz*. 1,2,3 and 1,2,4 triazoles exhibit tautomerism as shown in Scheme.1.14.

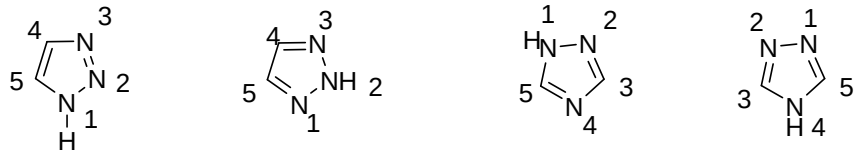

A B

Scheme.1.14: *Tautomers of 1,2,3-triazole (A) and 1,2,4-triazoles (B*).

The NH hydrogen can be attached to any of the three nitrogens in 1,2,3 triazole and thus can be present in three different tautomeric forms *viz*., *N1-H,N2-H* and *N3-H* in *C*-substituted cases as shown in Scheme.1.15. In unsubstituted cases, (R=H), *N1-H* form is identical to *N3-H* form.

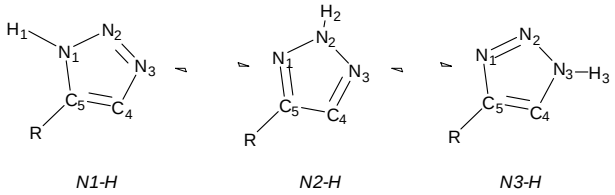

N1-H *N2-H* *N3-H*

Scheme.1.15: *Different tautomeric forms possible in substituted 1,2,3-triazoles.*

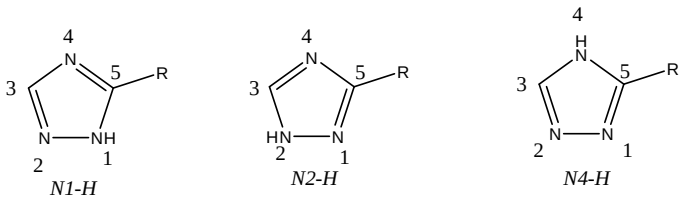

N1-H *N2-H* *N4-H*

Scheme.1.16: *Different tautomeric forms possible in substituted 1,2,4-triazoles.*

1,2,4 triazoles can also exist in three different tautomeric forms (*1-H, 2-H, 4-H*). [58] But, only two of them are possible (*1-H, 4-H*) in unsubstituted 1,2,4 triazoles due to symmetry in the system. All the three tautomers are possible, in principle, in *C*-substituted triazoles. In all these heteroaromatic systems, the proton transfer is associated with migration of π-electrons. It is difficult to say anything about which of the tautomer exists under a given condition. The property and the reactions depend greatly on the

nature of tautomer. Hence, it is necessary to understand tatutomerism in detail for systems exhibiting it.

1.4 Study of tautomerism: Tautomerism in solution is considered as dynamic where different tautomers co-exist in equilibrium under fast exchange conditions.[59] The dynamic nature makes tautomerism a challenging problem in experimental science. Hence, it is essential that the experimental techniques required for the study of tautomerism should be capable of providing information about the structure of tautomers as well as their population under the conditions of measurement. Tautomerism is difficult to study because of its dependency on solvents, concentration, temperature, pH, pressure, nature of substituent and the dynamic nature. Polarity of solvents plays an important role in determining the nature of tautomeric species in solution.

Aprotic solvents can also change charge distribution of molecules and affect the tautomerism. Even though a few of the important factors which affect tautomeism are mentioned above, many other internal and external factors such as acid-base properties of the tautomeric sites, functionalities, aromaticity, intra- and intermolecular interactions, hydration, protonation, and metal binding etc., can affect tautomerization and also result in formation of non-canonical forms with higher energy. Catalytic action of water has been implied in a variety of biologically important proton-transfer reactions. It is also known that water could disturb the tautomeric equilibrium.[60]

The electronic structures and photophysical properties change significantly in tautomers. Tautomerism accompanied by migration of double bonds, atoms or groups modify the electron density distribution, acid-base properties, polarity etc, which can be correlated with changes in π-electron delocalization. These changes may result in (i) increased stability, (ii) modified bond lengths intermediate between those typical for single and double bonds.

1.4.1 Mechanistic insight into the prototropic tautomerism: It is well known that different tautomeric forms exhibit different reactivities [61,62] and direct the

reactions to form regio isomers. For example, in mercapto-azoles the two tautomeric forms show different reactivities, metal complexation behaviour and substitution reactions [63]. Molecules of amphoteric nature exhibit tautomerism in neutral pH conditions wherein the acidic center loses a proton which is gained by a basic center of the same or the tautomeric molecule and *vice versa*. Lima *et al*. theoretically proved that the water plays an important role in transferring proton in 2-Mercaptopyrimidine in converting from Pym-SH to its tautomer Pym-NH [64] as shown in the Scheme.1.17.

Scheme.1.17: *Conversion of tautomeric form Pym-SH to Pym-NH in 2-mercaptopyrimidine.*

Kakkar *et al.* theoretically proposed a dissociative mechanism, similar to acid base equilibrium for the transfer of the proton in case of the alloxan [65] as shown in the Scheme1.18

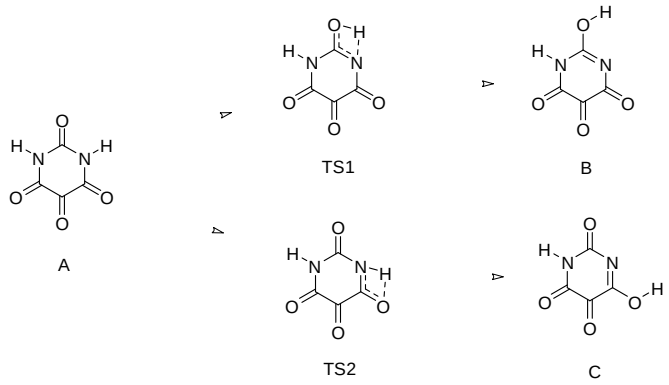

Mechanism of the transfer of the proton in the conversion of the tautomeric forms in alloxan

Scheme.1.18**:** *Dissociative mechanism of proton transfer in the conversion of one tautomeric form to another in alloxan.*

The transfer of proton may be intra molecular or intermolecular. The intra molecular proton transfer is a preferred path for isolated molecules (in vapor phase at a very low pressure or at high dilutions in aprotic solvents). Intermolecular proton transfer takes place for aggregated molecules. Such a situation can arise if the molecules exist in

dimeric, trimeric, or polymeric states or in a concentrated solution in an aprotic solvent, or in crystals. The molecular aggregates are formed either by identical tautomeric molecules or by different tautomers and are stabilized by hydrogen bonds. Polar protic solvents (e.g., H_2O or ROH) can also take part in the process of tautomerization by forming a complex with the tautomers. The nature of such complexes (cyclic or linear) is governed by the conformation and configuration of the tautomers. The proton transfer process in tautomerization is usually accompanied by the formation of a cation or an anion as an intermediate.

1.5 Methods to study tautomerism: The phenomenon of tautomerism has been investigated by many analytical techniques. Spectroscopic techniques such as UV-Vis, IR, NMR, Raman spectroscopy, theoretical calculations etc. are widely used in the study of tautomers in addition to mass spectrometry, time-resolved optical techniques, fluorescence etc.[34b] X- ray crystallography provides unequivocal evidence on the tautomer/s present in crystals. The advent of faster, efficient and accurate computational techniques has lead to numerous theoretical studies on tautomers in recent past.

A few of the important techniques are:

1) UV-Vis absorption spectroscopy
2) IR spectroscopy
3) Mass spectrometry
4) X-ray spectroscopy
5) NMR spectroscopy
6) Theoretical/Computational

1.2.1 UV-Vis absorption spectroscopy: This techniques is useful only if the different tautomers posses differences in (i) extent of the conjugation, (ii) planarity of the substituent group, (iii) aggregation, (iv) complexing properties or (v) extent of the π-π stacking. These factors result in the shifting of λ_{max} to different extent in different tautomers. The number of absorption peaks obtained may give an idea about the number

of the possible tautomers present. For example, the tautomer which has greater extent of conjugation has higher λ_{max}.

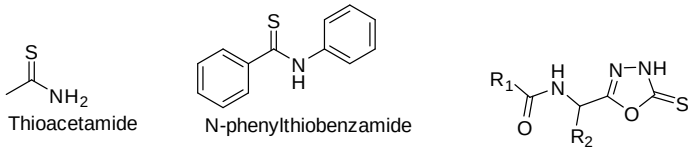

Scheme.1.19*: A few representative tautomers studied by UV and IR.*

It is observed that compared to thioacetamide (A), *N*-phenylthiobenzamide (B) (Scheme.1.19), for which the thioamide structure was confirmed, exhibit longer UV wavelength absorption than the *S*-methyl derivatives of their thiol forms. [66] It is likely that the conclusions based on UV spectroscopic method itself may not be sufficient to deduce the nature of tautomer. However, it is difficult to use this technique if the difference in the absorption is less for various tautomers.

1.5.2 IR spectroscopy in tautomerism: IR spectroscopy is one of the most powerful techniques frequently used for investigation of tautomeric species and relies on the changes in the nature of functional groups.[67]. For instance in thione-thiol tautomerism, the presence of an absorption in the region 1290–1349 cm^{-1} is characteristic of the C=S group [68], while the S-H stretching around 2500–2600 cm^{-1} is characteristic for the comp. C type of compounds shown in Scheme.1.19.

1.5.3 Mass Spectrosmetry in tautomerism: Mass spectrometry can also be used to study the tautomerism since different tautomers may have the different fragmentation pattern. It has the advantage that external factors like solvents, intermolecular interactions etc., which can also govern the nature of tautomers, can be completely excluded as systems are studied in gas phase.[69] However, oxidizable compounds may not be appropriate to study by the mass spectrometry. Studying tautomerism in the natural conditions is not feasible by means of mass spectrometry since under the conditions of measurements, the solute may not be able to maintain the solution/solid state environment.

1.5.4 X-ray spectroscopy in tautomerism: Single-crystal X-ray diffraction has been proved to be the most powerful tool to characterize various tautomers in solid state. Diffraction data are collected from a single crystal and structure is solved and refined, if necessary. On the basis of which the bond length, bond angle, torsion angles bond order etc can clearly be established.[70,71] It has been reported that the crystal structures of C (Scheme.1.19) correspond to the thione form but they showed thiol–thione tautomerism in solution.[72] Gorczyca *et al.* found by single crystal X-ray that the compound 4-ethyl-5-(2-thienyl)-2,4-dihydro-3*H*-1,2,4-triazole-3-thione is present in the thione form [73] as shown in Scheme.1.20 (A). 3-Amino-5-nitro-1,2,4-2*H*-triazole crystallizes in the *2H*-ANTA form as given in Scheme.1.20 (B). [74, 75]

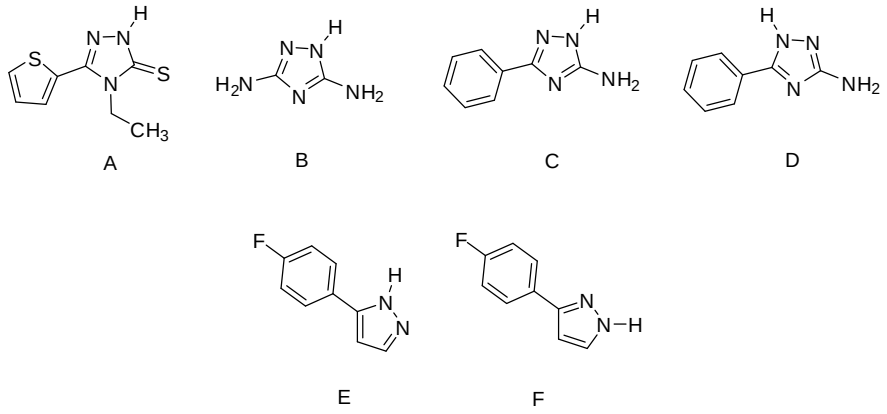

Scheme.1.20**:** *A few representative tautomers studied by X-ray spectroscopy.*

The major limitation of X-ray spectroscopy is that the H atoms cannot be seen directly and are positioned by using the available data for the molecular structure. The X-ray spectroscopy is best suitable in the cases where the compound forms the single tautomer in the system. The extension of crystal structural information on the tautomers to solutions should be done with certain caution since the possibility of dynamic equilibrium in solution exists. Co-existence of tautomers as aggregates can also be present in crystals (topomers). Dolzhenko, *et al.* [76] found that two tautomeric forms of the same compound like 5-amino-3-phenyl-1,2,4-triazole and 3-amino-5-phenyl-1,2,4-triazole (Scheme.1.20 C and D) exist together in the same crystal under the same conditions. Similarly Yamuna *et al.* found that two tautomers 3-(4-fluorophenyl)-1*H*-

pyrazole and 5-(4-fluorophenyl)-1*H*-pyrazole present in the same crystal as shown in Scheme.1.20 E and F. In this case the second tautomer arises from the exchange of the single proton between the two nitrogen atoms placed at the two different positions in the molecule. [77]

Formation of good quality crystals is essential. Weak diffractions from poorly formed crystals hamper the quality of data. Techniques such as Raman spectroscopy, electronic absorption spectroscopy have also been employed (even though less frequently) to study the phenomenon of tautomerism.

1.5.5 NMR Spectroscopy: NMR spectroscopy is the most suitable technique available to study tautomerism since it can be used in both solution and solid state. Solution state NMR is more widely used than solid state. It is possible to monitor various NMR active nuclei such as ^{1}H, ^{13}C, ^{15}N etc. present in a tautomeric systems. NMR techniques also provide information on the dynamics and population of various tautomers present. A simple ^{1}H NMR spectrum itself can give a lot of information about tautomers present in the system. NMR is one of the best techniques to study imine-amine tautomerism, lactam-lactim tautomerism, nitroso (N-oxide)-oxime tautomerism, azo-hydrazone tautomerism, tetrazole-azide tautomerism. NMR can also be used to study the aspects of the thiol-thione tautomerism.[34b] Studying the thiol-thione tautomerism by NMR could be easy mainly because if the thiol form is present in the system then the proton signal corresponding to the SH can be found in the region 3-6 ppm while if the thione form is present then the carbon signal corresponding to the C=S can be found in the region 160-175 ppm.[78]

The structure of the compound A **(**Scheme.1.21**)** is confirmed by its ^{1}H NMR spectrum (DMSO-d_6), which showed two signals at low field. The lower one (δ 13-12 ppm), exchangeable with deuterium oxide, corresponds to the NH proton and the other one (δ 10-9 ppm) is attributed to the N=CH- group proton which supported the thione form present in the system. [79]

Scheme.1.21**:** *Two examples of thiol-thione tautomerim studied by NMR technique.*

Siwek *et al.* reported the ^{1}H NMR spectrum of (B**,** Scheme.1.21) with a sharp singlet at 14.21–14.58 ppm typical for the proton linked to N1, indicating the presence thione tautomer.[80] Belmar *et al.* identified the tautomeric equilibrium for the compounds shown in Scheme.1.22 on the basis of the NMR data. The ^{13}C data of this compound in DMSO-d_6, showed number of signals that agrees with the existence of more than one species in solution. The signals for the chain bonded to N1 are duplicated (59.9 and 58.6 ppm) for the CH_2OH and (47.7 and 46.1 ppm) for the CH_2N. [81]

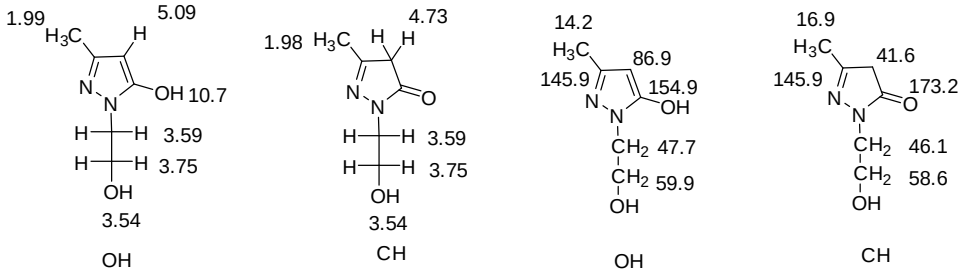

Scheme.1.22**:** *^{1}H and ^{13}C NMR chemical shifts of OH and CH tautomers in DMSO-d6.*

^{15}N NMR spectroscopy can be very much suitable to study the tautomerism in azoles.[82] It can be used to study the tautomerism in 1,2,4-triazole-thione where the signals can be assigned on the basis of the type of the hybridization state of the nitrogen atom.[83] It should be noted that if the equilibrium between the two tautomers is too fast on the NMR scale, then the observed chemical shifts is always population weighted average

$$\delta_{obs} = x_{\alpha}\delta_{\alpha}+x_{\beta}\delta_{\beta}$$

where, x_α and x_β are mole fractions of tautomers, $x_\alpha + x_\beta = 1$, and δ_α and δ_β are intrinsic NMR parameters. In general, x_α, x_β, δ_α, and δ_β cannot be obtained from a signal value of δ_{obs}, and thus a proper correlation between NMR observables and tautomers is hard to establish.

Among the various methods used to characterize tautomers, X-ray crystallography and NMR spectroscopy are the most widely used techniques. X-ray crystallography is limited to systems that can form good quality crystals. While NMR spectroscopy has clear advantage that the measurements can be carried out in solution, under conditions of interest as well as in solid state, which need not require any crystalline form. NMR spectroscopy not only provides structural information but also gives information about inter molecular as well as intra molecular dynamics, if present. However, NMR spectroscopy provides indirect structural information that needs to be correlated to three dimensional structures with very careful data analysis followed by computation techniques for structural simulation.

1.6 NMR spectroscopy: Over view:

Nuclear Magnetic Resonance spectroscopy, is a technique that exploits the magnetic properties of certain atomic nuclei. This technique can provide detailed information about the structure and dynamics of molecules. NMR spectroscopy is applicable to any systems that contains nuclei with a non zero spin quantum number I (I>0). The interaction of nuclear spin with an external magnetic field leads to formation of (2nI+1) energy levels and transition between these energy levels are achieved in presence of radio frequency waves which ultimately give rise to NMR signals. These signals are further modified by the intrinsic molecular properties such as electronic distribution, bond orders, bond angles, etc. and thus transform NMR into a versatile analytical technique. This is very much evident from the application of this technique in the area of physical, chemical, biological and material sciences to study small molecules, macromolecules (biological and synthetic) and materials. The important parameters monitored to get structural and dynamics information are: (i) chemical shift, (ii) scalar coupling constants and (iii) relaxation. The first two are related to the structure of

molecule while relaxation behavior provides information on dynamics and three dimensional structures of molecules. The dipolar and quadrupole (for systems with I>1/2) interactions, which dominate in solid state, are effectively used along with chemical shift for characterization of solids.

The development of this technique is an indispensible tool in many areas since its demonstration in 1945 by Bloch *et al.* and Purcell *et al*. is assisted by the simultaneous advancement of technologies in the area of electronics, magnets and computation etc. Introduction of pulsed NMR, 2D NMR, multi-dimensional NMR, high field magnets, cryogenically cooled probes, development of novel pulse sequences etc. gave major boost and wider application. The advancement in solid state includes, cross-polarization, magic angle spinning, multiple quantum techniques etc.

1.7 Overview of 1D/2D NMR techniques: A simple 1D NMR experiment (Fig.1.1) consists of a preparation and detection period. Preparation is a RF pulse applied along an axis orthogonal to the magnetic field (z-axis). The RF pulse creates transverse magnetization which decays through transverse relaxation during detection. The extent of creation of the transverse magnetization or the flip angle is governed by the length of the pulse. The spin system is then allowed to reach the equilibrium by giving an appropriate delay, which depends on the spin lattice relaxation time, prior to the application of next pulse. This process is repeated 'n' times to improve signal to noise ratio. The optimum sensitivity is obtained by pulsing at Ernst angle according to the equation

$$\cos(\theta_E) = e^{-(d_1+a_t)/T_1}$$

where θ_E is the flip angle or nutation angle, d_1 is the inter pulse delay, a_t is the acquisition time and T_1 is the longitudinal relaxation time.

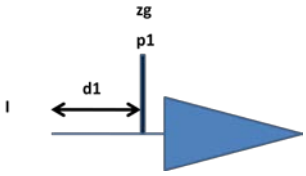

Fig.1.1**:** *Basic 1D NMR pulse sequence*.

Carbon-13 NMR spectroscopy is less sensitive due to its poor natural abundance (1.1%) and lower gyro magnetic ratio (6.728284×10^7 rad T^{-1} s^{-1}) which is ~ 1/4 that of ^1H. The presence of spin-spin coupling (typically from 100 to 250 Hz) between carbon-13 nucleus and hydrogen atoms bonded to it, further hampers the sensitivity. This can be circumvented by ^1H decoupling either during detection or during the entire duration of the experiment (Fig.1.2). The latter type of decoupling leads to additional enhancement in sensitivity due to nuclear Overhauser enhancement (nOe) but, render the measurement more qualitative in nature. The observation of ^{15}N spectra by this manner is not advisable due to negative gyromagentic ratio of ^{15}N nucleus which generates negative nOe and might lead to cancellation of some of the signals.

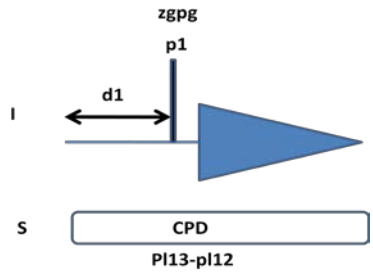

Fig.1.2: *Basic 1D ^{13}C NMR pulse sequence with decoupling*.

The normal ^1H decoupled ^{13}C spectrum is usually collected in combination with DEPT (**D**istortionless **E**nhancement by **P**olarization **T**ransfer) experiment (Fig.1.3) for differentiation of various types of carbons. The DEPT experiment is a pulse technique based on polarization transfer which also increases sensitivity. The selection of various types of carbons is achieved by varying the angle θ of the 'sorting' pulse (θ=45, 90 or 135). The wide range of $^1J_{C\text{-}H}$ (120-250 Hz) may, at times, hamper the selectivity of various types of carbons especially when *sp*, sp^2 and sp^3 types of C-H carbons are present in system under investigation.

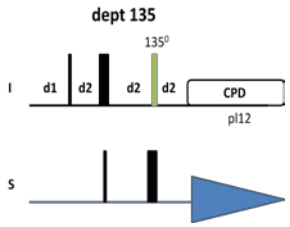

Fig.1.3**:** *Basic 1D ^{13}C DEPT135 NMR pulse sequence with decoupling.*

1.8 Two dimensional spectroscopy: The major difference between one and two-dimensional NMR methods is the insertion of a variable evolution time, t_1 between the preparation and detection period in two dimensional techniques. Such an approach permits to correlate pairs of spins which are dipolar or scalar coupled. The NMR signal is collected as a function of two time variables t_1 (evolution) and t_2 (detection) which is Fourier transformed with respect to both the time variables to yield a spectrum which is a function of two variable frequencies.

The four sequential steps involved in a 2D experiment are preparation, evolution, mixing and detection.[84] The introduction of a mixing period, prior to detection in essential for a 2D experiment. Mixing period is usually a pulse, combination pulses or delays which allow the interacting spins to mutually transfer information that results in their correlations. During the evolution period the spin systems evolves with various interactions and impart phase character (phase encoding). While in 'mixing' the phase encoded spins pass the phase information to its partners. Information passed through scalar couplings results in correlations between coupled partners while information passed through dipolar couplings results in spins connected through nOe. These interactions can be between the same type of spins, homonuclear (eg. ^{1}H-^{1}H) or heteronuclear (eg ^{1}H-^{13}C).

1.8.1 Correlation spectroscopy (COSY): It is a homonuclear chemical shift correlation experiment based on the transfer of magnetization between J-coupled spins and thus, traces out homonuclear spin systems that are directly involved in J couplings. The standard COSY experiment consists of a 90 degree preparation pulse, variable evolution time and a mixing pulse which can be 90 degree or less. The pulse sequence for the COSY experiment is as shown in the Fig.1.4.

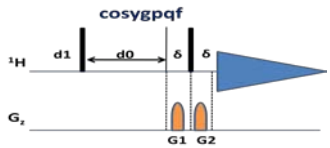

Fig.1.4**:** *The pulse sequence for COSY experiment.*

There are many variations of COSY experiments (DQFCOSY, long range COSY, etc.) which are commonly used. Total Correlation Spectroscopy (TOCSY) is a very useful technique (Fig1.5) which shows correlations between the entire spin systems.

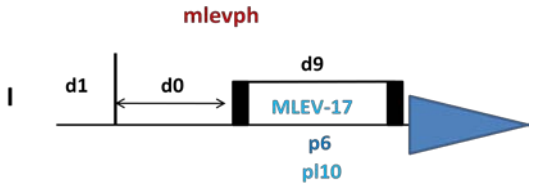

Fig.1.5**:** *The pulse sequence for TOCSY experiment.*

1.8.2 Through-space correlation methods:

NOESY: A 2D technique that establishes correlations between nuclei which are spatially close to each other (within about 5 Å) is nuclear Overhauser Effect spectroscopy (NOESY). Thus, the cross peaks of a NOESY spectrum indicates which protons are close to each other in space. The basic NOESY sequence consists of three $\pi/2$ pulses (Fig1.6). The first pulse creates transverse spin magnetization. The second pulse after the evolution time produces longitudinal magnetization corresponding to the transverse magnetization component. Any cross relaxation between nuclear spins during the mixing period τ_m establishes the connectivity. The third $\pi/2$ pulse further creates transverse magnetization which is detected.

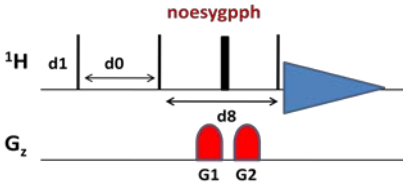

Fig.1.6**:** *The pulse sequence for NOESY experiment.*

NOESY is widely used for 3D structural determination of small as well as biological macromolecules. The correlation time of the system being studied has profound effect on sign of the cross peaks. The cross peaks are weak and negative for small molecules while are positive and large for macromolecules. For medium size

molecules there is a cross over point ($\omega_0\tau_c$=1.12) and the nOes are either weak or absent as shown in the Fig.1.7.

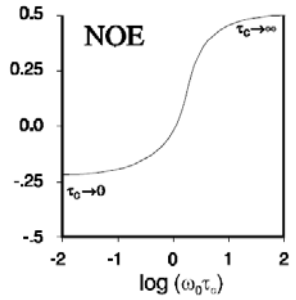

Fig.1.7: *Correlation time dependency of nOe.*

These types of molecules are studied by ROESY (Rotating frame Overhauser Effect spectroscopy) for the establishment of nOe contacts. The ROESY spectrum shows negative cross peaks irrespective of the correlation time involved. Systems undergoing chemical exchange also show cross peaks in NOESY as well as ROESY. These cross peaks are positive and are usually strong. ROESY is similar to NOESY, except that in ROESY instead of observing cross relaxation from an initial state of *z*-magnetization, the equilibrium magnetization is rotated onto the *x* axis and then spin-locked (Fig.1.8). During the spin lock mixing time the magnetization transfer occurs between the spin locked pairs.

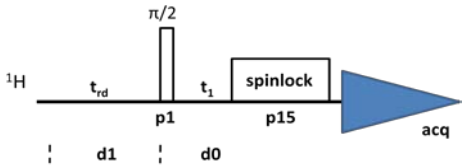

Fig.1.8**:** *The pulse sequence for ROESY experiment.*

1.8.3 Heteronuclear Correlations: Heteronuclear correlation spectroscopy in general correlates the X-nucleus with their scalar coupled partners. The most common spin pairs for organic chemist are ^{1}H-^{13}C and ^{1}H-^{15}N. Correlations can be established between the protons that are directly bonded to the heteroatom or those connected by multiple bonds. Experiments that correlate directly bonded hetero nuclear spin pairs are known as HETCOR when the nucleus of detection is ‘X’ nucleus. Experiments which record the proton instead of X nucleus are called "inverse" or indirect experiments.

HMQC and HSQC are the ^{1}H detected version of HETCOR. The experiment in which the observed correlations are spins connected by more than single bond are known as COLOC (Correlation through long range) for X-detection or HMQC (Heteronuclear Multiple-Quantum Correlation) and HMBC (Heteronuclear Multiple Bond Correlation) for ^{1}H detected version.

The one-bond coupling between a carbon-13 and the proton directly attached to it is relatively constant (125-150 Hz), and much larger than any of the long-range carbon-13 proton couplings (1-8 Hz). By utilizing this large difference in the coupling constants the experiments can be devised which can map either directly attached protons or long range coupled protons. Carbon-13 has a natural abundance of only ~1%, thus 99% of the molecules in the sample contain NMR inactive C-12. Hence, in the ^{1}H spectrum, the signals from ^{13}C (^{13}C satellites) are mixed with stronger signals from protons attached to C-12, which is unwanted in inverse mode of detection of X nuclei signals. These unwanted signals are suppressed by coherence selection in inverse experiments, which is currently achieved by the use of gradients (Gradient accelerated spectroscopy, GRASP).

1.8.4 Heteronuclear Single Quantum Coherence spectroscopy (1H-13C HSQC): This experiment provides correlation between the carbon and its attached protons. ^{1}H-^{13}C experiment correlates the chemical shift of proton with the chemical shift of the directly bonded carbon. On the F2 axis is a proton spectrum and on the F-1 axis is a carbon. This experiment utilizes the one-bond couplings between carbon and proton (J=120-150 Hz). The 2D HSQC spectral data collection is much faster than a single 1D carbon spectrum since it is proton-detected. HSQC works by transferring magnetization from the *I* nucleus (^{1}H) to the *S* nucleus (X) using the INEPT (Insensitive nuclei enhanced by polarization transfer) pulse sequence. The magnetization then evolves and is transferred back to the *I* nucleus (^{1}H) via a retro-INEPT step for observation (Fig1.9). An extra spin echo step can then optionally be used to decouple the signal, simplifying the spectrum by collapsing multiplets to a single peak. The ^{1}H signal is detected in terms of chemical shift of X Nuclei (^{15}N, ^{13}C etc) are recorded in the indirect dimension resulting in a 2D spectrum with ^{1}H chemical shift on one axis and X nucleus on the other.

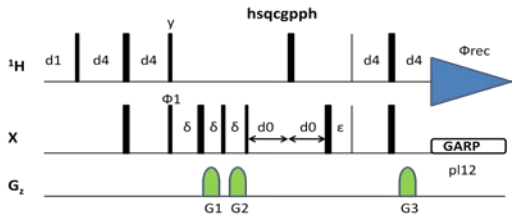

Fig.1.9**:** *The pulse sequence for the ^{1}H-^{13}C HSQC experiment.*

1.8.5 Heteronuclear Multiple Bond Correlation (1H-13C HMBC): This experiment utilizes multiple-bond couplings over two or three bonds (J= 2-15Hz). Cross peaks are between protons and carbons or other hetero nucleus that are multiple (usually two or three) bonds away. The multiple-bond coupling constants cover wide range of couplings and cannot capture all the correlations as in a single HMBC or HMQC experiment. The increase in the range of coupling constants reduces the sensitivity in addition to the signal loss due to relaxation. The basic HMBC pulse sequence introduces artifacts from one-bond couplings. Modified pulse sequences which suppresses these artifacts and that can cover wider range of long range couplings are now available. HMBC provides the information about the chemical shift of hetero atoms that are about 2-3 bonds away from the proton. Hence, the quaternary carbon atoms can also be detected.[85]

The HMBC pulse sequence is shown in Fig. 1.10. The first ^{13}C 90° pulse, which is applied $1/(2\ ^{1}J_{XH})$ after the first ^{1}H 90° pulse, serves as a low-pass J filter to suppress one-bond correlations in the 2D spectrum by creating ^{1}H-^{13}C heteronuclear single quantum coherence which is removed. After the delay; the second ^{13}C 90° pulse is applied along with a delay corresponding to $1/(2\ ^{n}J_{XH})$ to create desired heteronuclear multiple-quantum coherence for long-range ^{1}H-^{13}C J-couplings. Gradient is used to select the desired pathway and to suppress artifacts.

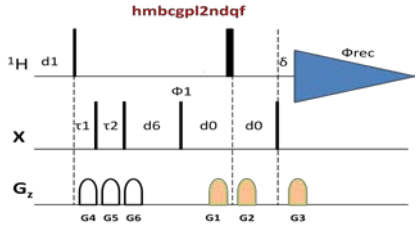

Fig.1.10**:** *The pulse sequence for the ^{1}H-^{13}C HMBC experiment.*

1.8.6 15N NMR spectroscopy: The ^{1}H-^{15}N correlations are very useful for structural identification of nitrogen containing synthetic molecules and natural products. ^{1}H-^{15}N long-range correlations provide a wealth of structural information.[86] ^{15}N NMR spectroscopy is a powerful tool for the characterization of nitrogen containing compounds due to the sensitivity of ^{15}N chemical shifts to structural and electronic effects which result in a broad chemical shift range covering ~ 900 ppm.[87-89] ^{15}N chemical shifts are very sensitive to the nature of solvents, concentration, conformation, non bonding interactions [90] (e.g., H-bonds), pH and temperature etc. Owing to the low natural abundance (0.37%) and the very poor receptivity of ^{15}N (lower gyromagnetic ratio), the signal to noise ratio is poor in comparison with ^{1}H (3.85×10^{-6}, and 1/3 with that of the ^{13}C) , thus the direct observation of the ^{15}N is difficult.[53] But, the ^{1}H detected pulse programs such as HSQC [91], HMQC [92,93] and HMBC [94,95a] can be employed to improve the detection capability. The pulse sequence for the ^{1}H-^{15}N HSQC experiment is same as that of ^{1}H-^{13}C HSQC.

1.8.7 ^{1}H-^{15}N HSQC:

The HSQC experiment can be performed at natural abundance using appropriate polarization transfer delay corresponding to $^{1}J_{N\text{-}H}$ (90-100Hz) and the cross peaks obtained correspond to N-H pairs. It is one of the experiments commonly used to characterize the nature of proteins in structural biology. But for protein NMR all the nitrogen atoms are isotopically labeled. The detection nitrogen by HSQC become difficult if the proton resonances are broadened by chemical exchange processes such as tautomerism, exchange with trace amount of water in the solvent used etc.

1.8.8 ^{1}H-^{15}N HMBC:

Like the ^{13}C case the long-range ^{1}H-^{15}N coupling constants often span a very wide range of values in the same molecule which makes it difficult to detect all the correlations in a single experiment. The pulse sequences such as IMPEACH [95b] have been developed to

overcome this difficulty. ^{4}J couplings are often larger than ^{3}J and ^{2}J couplings so there will be cross peaks connecting atoms that are more bonds apart. The coupling values range from 3 to 15 Hz . Usually the pyridine type nitrogen atoms exhibit larger two and three bond couplings with proton than the pyrrole type. [96]

1.9 Solid-state nuclear magnetic resonance:

In solid-phase, such as crystals, microcrystalline powders, amorphous compounds the dipolar coupling, chemical shift anisotropy, quadrupolar interaction (for I>1/2 spins) become dominant which modifies the Zeeman interaction of the spin with an external magnetic field. In solid state, these interactions are not averaged unlike in solution state and thus would lead to a significant broadening of the resonances. A variety of techniques have been introduced to overcome this and to get a spectra comparable to solution state, especially for spin ½ nuclei such as ^{13}C, ^{15}N, ^{29}Si, ^{31}P etc. For such systems, two important techniques employed in high-resolution solid-state NMR spectroscopy are the Magic Angle Spinning (MAS) and Cross-polarization (CP). For MAS, the samples packed in a rotor are placed at 54.736 deg with respect to the magnetic field and spun at speeds ranging from 5 to 100 kHz, which is determined by the size of rotor (7mm, 4mm, 2.5 mm, 1.3 mm, 1mm etc), probe and the nucleus of interest. The anisotropic interactions leading to broadening of the resonances can thus be averaged.

Cross polarization is a pulse technique employed for sensitivity enhancement, especially for rare spins like ^{13}C, ^{15}N, ^{29}Si etc under specific condition known as Hartmann-Hahn match condition. This is usually used in combination with high power dipolar decoupling during detection to kill the dipolar interaction of ^{1}H with the hetero atoms. The CP-MAS techniques provide sensitivity enhancement in two ways: (i) by polarization transfer from abundant spins (CP) and (ii) by averaging of anisotropic interactions such as CSA (MAS). Besides, application of CP allows to pulse at the rate of T_1 of abundant spin (^{1}H) which is usually less than that of the detected X nucleus. The pulse sequence is as shown in the Fig.1.11

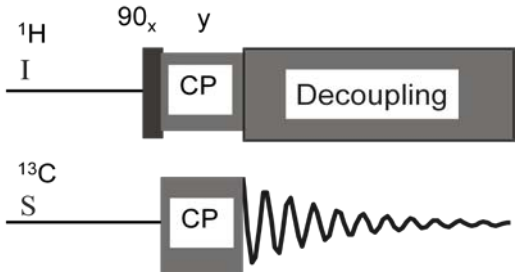

Fig.1.11. *The CP-MAS pulse sequence.*

1.9.1 ^{1}H MAS:

^{1}H NMR in solid state in general is not practical due to strong homonuclear dipolar couplings which broaden the signals considerably (50-100 kHz). Hence,averaging of this homogeneous interaction requires spinning at speeds greater than the magnitude of dipolar couplings or multiple pulse experiments or a combination of MAS and multiple pulse experiments. ^{1}H based solid state NMR experiments are becoming more popular with the advent of high speed MAS units that can spin up to 60-110 kHz which employs rotors with smaller diameter (1.3-1mm).

1.10 Theoretical studies:

Computational chemistry has developed into an area of great potential and application. It employs efficient computer programs to calculate structure and properties of molecules and hence is also used as a complementary technique to verify experimental observations. Computational techniques are extensively used for modeling of biologically important molecular interactions and these “in silico” approaches are indispensable tool in the modern drug discovery programs. The computer simulation approach is not only effective in drug design but also helps to explore their mechanism of action. These methods can also be employed to address both static and dynamic behaviors in the systems of interest. Many of the physical and chemical properties can now be accurately predicted and pave ways to better understanding of reaction mechanisms.

The computational approaches used in theoretical chemistry are based on quantum chemistry or non-quantum chemical calculations. The latter method is based on solutions of analytical expressions to get information on molecular properties. The quantum chemical approach uses *ab initio* or semi-empirical or molecular mechanics to study molecular properties. The *ab initio* methods are based on solution of Schrodinger equation while semi empirical methods use a combination of quantum physics and experimental inputs. Molecular mechanics employs classical physics to explain the behavior of molecules.

Two of the most widely used methods for *ab initio* calculations are based on Hartree−Fock (HF) theory and density functional theory (DFT).HF is an extension of molecular orbital theory and uses mean field approximation where electron-electron repulsions are not considered in the calculations and the accuracy depends on the size of the basis set. The basis function commonly employed are STO (Slater Type Orbitals) or GTO (Gaussian Type Orbitals). The basis function employed are usually mentioned in the calculation for example, as STO-3G, 6-311++G**, 6-31G(3df, 3pd) etc.

The DFT approach uses the electronic density as the fundamental variable for calculations. DFT calculations are suitable for medium to large sized molecules. Other methods based on quantum mechanics include Quantum Monte Carlo (QMC), Generalized Valence Bond (GVB), Many-Body Perturbation Theory (MBPT) etc. The advantage of *ab initio* calculations is its convergence to exact solution though it may take enormous computational time.

Semi-empirical quantum chemistry methods are based on H-F and in addition use parameters from empirical data. The semi-empirical methods are less demanding from the computational point of view but the results can be erratic in nature. Molecular Mechanics (MM) is ideal for bigger molecules where quantum mechanical based calculations have some limitations. MM uses molecular force field for calculating energy associated with molecules based on classical equations and hence does not require elaborate calculations of wave functions to describe properties of molecules. Molecular Dynamics (MD) method is used for describing time depended behavior like rotational

and Brownian motions of molecules. MD simulations are versatile and commonly employed to calculate molecular diffusion and solvation effects.

Basis Sets is a finite set of atom centered functions required to approximately define the molecular orbital (MO) of a system in a quantum mechanical based calculation. It consists of many atomic orbitals differing in local angular momentum and is a mathematical way of description of the molecular systems of interest. The accuracy of calculation depends on the size of basis set. Larger basis set provides better results at the cost of computation time. Choice of an appropriate basis set is important for calculation of molecular parameters which are in turn employed for calculation of experimental parameters, for example NMR chemical shifts, which requires very precise description of several regions of space. Ideally the number of basis functions should be increased to a point at which the molecular property of interest does not change significantly on adding additional basis functions. NMR is one of experimental methods where various parameters depend on the environment of the atom of interest in a molecule. Hence the quantum chemical calculations will be of great help for proper interpretation of the observed NMR parameters. It is interesting to note that the magnetic resonance properties are inherently quantum mechanical in nature. The calculated NMR parameters are very useful in understanding molecular systems which are dynamic in nature like the case of tautomers. The chemical shift of atoms in each tautomer can be theoretically calculated and can be compared with the values observed, which is a population weighted average value. Theoretical calculations also predict the thermodynamic and other properties of various tautomers which can be helpful in understanding their relative stabilities.

A few of the NMR related parameters which can be calculated theoretically are shielding constants, electric field gradients, spin-spin couplings, paramagnetic couplings etc. Chemical shifts are obtained from the shielding constant. It is possible to calculate these parameters for all the atoms present in the molecule. Chemical shifts are very sensitive to molecular structure therefore chemical shift alone can be sufficient to predict secondary structure of proteins.[110]

1.11 Calculations of the NMR Parameters:

1.11.1 Shielding constant: Chemical shifts are very useful to find out the molecular structure and to know the nuclear magnetic environment in a molecule. The chemical shift in turn arises from the magnetic shielding effect of the electrons present around the nucleus.[97,98] When the external field is applied, it induces electronic current in the nuclei which is nothing but the magnetic shielding.[99] The magnetic shielding constant being a second derivative of the molecular energy with respect to the applied field, it can be calculated theoretically as the second derivative of electronic energy with respect to the external magnetic field and the nuclear magnetic moment of the nuclei to be probed. The electronic environment around the different nuclei in the molecule is different therefore the shielding constants for such nuclei are also expected to be characteristic of particular nuclei. The nuclear shielding constants are the local properties because it depends on the electronic environment very close to the nucleus. The chemical shielding constants can described in terms of the linear response function without taking into account the diamagnetic contribution.[100] In order to know the nuclear shielding constants, it is essential to know the unperturbed density matrix and the corresponding perturbed density matrices.[101]

Gauss and Werner [101] developed the algorithm for calculating shielding constants. This algorithm is implemented in the JAGUAR software package which is used to calculate the NMR shielding constants in the present dissertation.[102] In order to calculate the shielding constants for particular nuclei the reference compound is used and the shielding constants of both the reference and the nuclei of interest are calculated with the same basis set as discussed in Chapter V. The chemical shifts for the different nuclei can be calculated from the shielding constants because both depends on the electron density surrounding the nuclei and can be inter converted using a using a linear fit with the experimental data.[103, 104]

1.11.2 Electric Field Gradients: The computation of electric field gradient tensors is less demanding than either shielding or J coupling tensors as it requires only knowledge of the ground-state charge density and is useful for quadrupolar nuclei.

1.11.3 Paramagnetic Coupling: Paramagnetic couplings can also be calculated theoretically. It is of relevance only if the molecular system of interest contains a paramagnetic center such as an unpaired electron.

1.11.4 J Couplings: Several quantum chemistry packages have the ability to compute J coupling tensors in molecular systems.[105]

Various software packages are available for computational chemistry applications. We have employed SCHRODINGER (Jaguar version 7.9) software package in this dissertation. The details of which are as follows

Product: Jaguar

Version: 79025

Platform: Linux-x86_64

OS: LINUX 2.6.32-279.el6.x86_64

Processor: Intel(R) Xeon(R) CPU E5606 @ 2.13GHz (2128 MHz)

"Jaguar" is an *ab initio* calculation software commercially available as a module in Schrodinger package and used for calculation of molecular properties such as dipole moment, electron density, electrostatic potential, polarizability, solvation, prediction of spectral parameters such as IR, NMR, UV etc.[106]

Jaguar gives high quality optimized structures by using the density functional theory (DFT) and local second-order Møller–Plesset perturbation theory which makes these calculations very accurate. Calculations done on the Jaguar are not only highly precise but also quite fast since it uses the pseudospectral approximation methods. Jaguar basis sets usually use the Gaussian-type atomic orbitals. The basis set 6-31 G** is good enough to do the calculations for the nuclei from hydrogen to argon. For the calculations of the accurate shielding constants which can be converted into the chemical shifts, the PS gauge-including atomic orbitals algorithm [107] is used. These NMR shielding constants

are obtained with the inclusion of solvent effects [108, 109] and are converted into the chemical shifts and compared with the experimental chemical shifts in this dissertation.

References:

[1]. Liu, R. S. *Pure Appl. Chem*. **2001**, *73*, 265.

[2]. Reddy, G. P. V.; Kiran, Y. B.; Reddy S. C.; Reddy, D. C. *Chem. Pharm. Bull*. **2004**, *52*, 307.

[3]. Hafez, A. *Eur. J. Med. Chem*. **2008**, *43*, 1971.

[4]. Chin, Y. W.; Balunas, M. J.; Chai, H. B.; Kinghorn, A. D. *Drug Discovery From Natural Sources*. **2006**, *8*, 239.

[5]. Koehn, F. E.; Carter, G.T. *Nat. Rev. Drug Discov*. **2005**, *4*, 206.

[6].Cordell, G. A.; Quinn-Beattie, M. L.; Farnsworth, N. R. *Phytother Res*, **2001**, *15*, 183.

[7]. Hughes, E. H.; Shanks, J. V. *Metabolic. Metab. Eng*. **2002**, *4*, 41.

[8].(a) Fan, W. Q.; Katritzky, A. R. *In Comprehensive Heterocyclic Chemistry*, **1996.** *(b)* Katritzky, A. R.; Rees, C. W.; Scriven, C. W. V. Eds., *Oxford, Elsevier*, 4:1.

[9]. Dehne, H. *In Methoden der Organischen Chemie (Houben-Weyl), Schaumann, E. Ed*.; *Stuttgart, Thieme*. **1994**, *8*, 305.

[10]. Eicher, T.; Hauptmann, S. *The Chemistry of Heterocycles: Structure, Reactions, Syntheses and Applications. Wiley-VCH, 2nd ed*. **2003**, 371.

[11].(a)Tisler, M.; Stanovnik, B.; Katritzky, A. R.; Rees, C. W. *Eds; Elsevier: Amsterdam,***1984** (b) Coates, W. J. *In Comprehensive Heterocyclic Chemistry II,* **1996**. Katritzky, A. R.; Rees, C. W.; Scriven, E. F. *Eds; Pergamon Press:Oxford*, 6: 1. (c) Stanovnik, B. *Methods of Organic Chemistry (Houben-Weyl)*, **1997**. Schaumann, E.; Georg, E. D. *Thieme Verlag: Stuttgart, E*, **1997**, 557.

[12]. Mittal, A. *Synthetic Sci. Pharm*, **2009**, *77*, 497.

[13]. Nagalakshmi, G. *Indian J. Pharm. Sci*, **2008**, *70*, 49.

[14]. Joule, J. A.; Mills, K. *Heterocyclic Chemistry, 4thEd., Blackwell Publishing*, **2000** pp: 369.

[15]. Nekrasov, D. D. *Chemistry of Heterocyclic Compound*s, **2001**, *37*, 263.

[16]. Sperry, J. B.; Wright, D. L. *Current Opinion in Drug Discovery and Development*, **2005**, *8*, 723.

[17]. Polshettiwar, V.; Varma, R. S. *Pure Appl. Chem*, **2008**, *80*, 777.

[18]. Katritzky, A.R. *Chemistry of Heterocylic Compounds*, **1992**, *28*, 241.

[19]. Norman, S. R. *Drug Development Res*, **2008**, *69*, 15.

[20]. Dahm, R. *Human Genetics*, **2008**, *122*, 565.

[21]. Watson, J. D.; Crick, F. H. *Nature*, **1953**, *171*, 737.

[22] *Food and Nutrition Board., ed* **1998**. Chapter 9 Vitamin B12. Dietary Reference Intakes for Thiamin, Riboflavin, Niacin, Vitamin B6 , Folate, Vitamin B12 , Pantothenic Acid, Biotin and Choline. Washington, D.C. *National Academy Press.* pp: 346.

[23]. Davies, M. B.; Austin, J.; Partridge, D. A. *The Royal Society of Chemistry*, pp: 48.

[24]. Evans, H. M.; Emerson, O. H.; Emerson, G. A. *J. Biological Chemistry*, *113*, 319.

[25]. Furst, P.; Stehle, P. J. Nutrition, **2004**, *134*, 1558.

[26]. Perutz, M. F. *symposia in Biol*, **1960**, *13*, 165.

[27]. Brian, P. W. *Biological Sci*. **1978**, *200*, 231.

[28]. Balkis, M. M.; Leidich, S. D.; Mukherjee, P. K.; Ghannoum, M. A. *An Overview. Drugs*, **2002**, *62*, 1025.

[29]. Shorvon, S. D.; Fish, D. R.; Perucca, E.; Edwin Dodson, W. *The Treatment of Epilepsy (2nd Ed), Published by Blackwell*. **2004**, 472.

[30]. Brodie, M. J.; Rosenfeld, W. E.; Vazquez, B.; Sachdeo, R.; Perdomo, C.; Mann, A.; Arroyo, S. *Epilepsia* **2009**, *50*, 1899.

[31]. Hoke, J. F.; Cunningham, F.; James, M. K.; Muir, K. T.; Hoffman, W. E. *J. Pharmacol. Exp. Ther*. **1997**, *281*, 226.

[32].Sarkar,D.; Deshpande, S. R.; Maybhate, S. P.; Likhite, A. P.; Sarkar, S.; Khan, A.; Chaudhry, P. M.; Chavan, S. R. *International publication number WO 2011/111077 A1 and PCT/IN2011/000172.*

[33a]. Xia, Y.; Fan, Z.; Yao, J.; Liao, Q.; Li, W.; Qu, F.; Peng, L. *Bioorg. Med. Chem. Lett.* **2006**, *16*, 2693., b B.Mcmurry J., Oragnic Chemistry, ninth edition, Cengage learning, **2016**, chapter 22, 728.

[34]. *A. Glossary of Terms Used in Physical Organic Chemistry; IUPAC Recommendations*, **1994**; http://goldbook.iupac.org/T06252.html. [34b]. *book tautomerism methods and theories by Liudmil Antonov*, **2014**, chapter 1 page 5-19.

[35] Mukano, Y.; Momochi, M.; Takanashi, Y.; Suzuki, M.; Wakabayashi, H.; Teramae, H.; Kobayashi, K. *Tetrahedron*, **2010**, *66*, 605.

[36]. Holzer, W.; Eller, G. A.; Schonberger, S. *Heterocycles*, *75*, 77.

[37]. Shaabani,A.; Ameri, M.; Bijanzadeh, H. R. *J. Chem. Research*, **1998**, 572.

[38]. Lee, H. Y.; Song, X.; Park, H.; Baik, M. H.; Lee, D. *J. Am. Chem. Soc*. **2010**, *132*, 12133.

[39]. Sergey, L.; Deev, Z. O.; Shenkarev, T. S.; Shestakova, O. N.; Chupakhin, V. L.; Rusinov.; Alexander, S.; Arseniev. *J. Org. Chem*. **2010**, *75*, 8487.

[40]. Goodman, M. M.; Atwood, J. L.; Carlin, R.; Hunter, W.; Paudler, W. W. *J. Org. Chem*. **1976**, *41*, 2860.

[41]. Goodman, M. M.; Paudler, W. W. *J. Org. Chem*. **1977**, *42*, 1866.

[42]. Messmer, A.; Hajos, G.; Benko, P.; Pallos, L. *J. Heterocycl. Chem*. **1973**, *10*, 575.

[43]. Messmer, A.; Hajos, G.; Tamas, J.; Neszmelyi, A. *J. Org. Chem*. **1979**, *44*, 1823.

[44]. Karczmarzyk, Z.; Mojzych, M.; Rykowski, A. *J. Mol. Stuct*. **2007**, *829*.

[45]. Mojzych, M.; Karczmarzyk, Z.; Rykowski, A. J. *Chem. Crystallogr*. **2005**, *35*, 151.

[46]. Stevens, M. F. G. *J. Chem. Soc., Perkin Trans. 1* **1972**, 1221.

[47]. Castillon, S.; Melendez, E.; Pascual, C.; Vilarrasa, J. *J. Org. Chem*. **1982**, *47*, 3886.

[48]. Castillon, S.; Vilarrasa, J. *J. Org. Chem*. **1982**, *47*, 3168.

[49]. Gold, V. *Pure Appl. Chem.* **1979**, *51*, 1725.

[50]. Saenger, W. Cantor, C. R., In *Principles of Nucleic Acid Structure*, Ed., *Springer-Verlag: New York*, **1984**.

[51]. Watson, J. D.; Crick, F. H. C. *Nature* **1953**, *171*, 964.

[52]. Hongqi, Ai.; Jinpeng, C.; Chong, Z. *J. Phys. Chem. B* **2012**, *116*, 13624.

[53]. Guille, K.; Clegg, W. *Acta Crystallogr. Sect. C* **2006**, *62*, O515.

[54]. Lopes, R. P.; Marques, M. P. M.; Valero, R.; Tomkinson, J.; de Carvalho, L. A. E. *Spectrosc. Int. J.* **2012**, *27*, 273.

[55]. Lo¨wdin, P. O. *Adv. Quantum Chem.* **1965**, *2*, 213.

[56]. Goodman, M. F. *Nature* **1995**, *378*, 237.

[57]. Topal, M. D.; Fresco, J. R. *Nature* **1976**, *263*, 285.

[58]. Elguero, J.; Marzin, C.; Katritzky, A. R.; Linda, P. *Advances in Heterocyclic Chemistry, Supplement 1*; *Academic Press: New York*, **1976**.

[59]. Lachman, A. *J. Am. Chem. Soc.* 1901, **23**, 902–923. Lowry, T. *Proc. Chem. Soc.* **1914,** *30*, 105.

[60]. Kwiatkowski, J. S. *Theoretica chimica acta*, 1976, 42, Issue 1, 83.

[61]. Sych, E. D.; Moreiko, O. V.; *Khim. Geterotsikl. Soedin.* **1973**. 1186.

[62]. Maiyazawa, T.; Yazufuku, K. *Jpn. Patent 88-284173*; *Chem. Abstr*, **1989**, 110, 231609.

[63]. Siwek, A.; Wujec, M.; Wawrzycka-Gorczyca, I.; Dobosz, M.; Paneth, P. *Heteroa Chem* **2008**, *19*, 337.

[64] Carolina, M. P.; Coutinho, L. K.; Canuto, S.; Rocha, W. R. *J. Phys. Chem. A* **2006,** *110*, 7253.

[65]. Kakkar, R.; Sarma, B. K.; Katoch, V. *Proc. Indian Acad. Sci.* (*Chem. Sci.*), **2001**, *113*, 297.

[66]. (a) Bliznyuk, A. A.; Schaefer, H. F., III; Amster, I. J. *J. Am. Chem. Soc.* **1993**, *115*, 5149. (b) Day, R. M.; Thalhauser, C. J.; Sudmeier, J. L.; Vincent, M. P.; Torchilin, E. V.; Sanford, D. G.; Bachovchin, C. W.; Bachovchin, W. W. *Protein Sci.* **2003**, *12*, 794. (c) Huda´ky, P.; Perczel, A. *J. Phys. Chem. A* **2004**, *108*, 6195.

[67]. Iqbal, R.; Rama, N. H.; Yunus, U.; Saeed, A.; Zamani, K. *J Chem Soc Pak* **1997**, *19*, 145.

[68]. Siwek, A,; Stefanska, J.; Wawrzycka-Gorczyca, I.; Wujec, M. *Heteroatom Chemistry*, **2010**, *21*, 131.

[69]. Maquestiau, A.; van Haverbeke, Y.; Williame, M.; Begtrup, M. *Bull. Soc. chim. belges*, **1976**, *85*, 795.

[70]. Buzykin, B. I.; Mironova, E. V.; Gubaidullin, A. T.; Litvinov, I. A.; Nabiullin, V. N. *Russian Journal of General Chemistry*, **2008**, *78*, 634.

[71]. Fun, H. K.; Quah, C. K.; Nithinchandra.; Kalluraya, B. *Acta Cryst.* **2011**, *E67*, 02413.

[72]. Feng, C. T.; Wang, L. D.; Liu, Y. J.; Li, S. H. *Med Chem Res*. **2012**, *21*:315.

[73]. Wawrzycka-Gorczyca, I.; SiwekII, A. Crystallogr. **2011**, *226*, 861.

[74]. Lee, K. Y.; Storm, C. B.; Hiskey, M. A.; Coburn, M. D. *J. Energ. Mater*. **1991**, 9, 415.

[75]. Lee, K.-Y.; Coburn, M. D.; Hiskey, M. A. *Los Alamos National Laboratory Report, LA-12582-MS,***1993**.

[76]. Dolzhenko, A. V.; Tan, G. K.; Koh, L. L.; Dolzhenko, A. V.; Chui, W. K. *Acta Crystallogr., Sect. E,* **2009**, *65*, 0126. CCDC 717328.20.

[77]. Yamuna, T. S.; Kaur, M.; Jasinski, J. P.; Anderson, B. J.; Yathirajan, H. S. *Acta Cryst.* **2014**, *E70*, 0949.

[78]. Agata, S.; Monika W.; Dobosz, M.; Paneth, P. *Heteroatom Chemistry*. **2008**, *19*, 713.

[79]. Jingde, W.; Xinyong, L.; Xianchao, C.; Yuan, C.; Defeng, W.; Zhong, L.; Wenfang, X.; Christophe, P.;, Myriam, W.; Erik, D.; Clerc Q. *Molecules* **2007**, *12*, 2003.

[80]. Agata, S., Monika, W. Tomasz, P.; Edyta, K.; Ewa, J. W.; Anna C. *Heteroatom Chemistry*. **2010**, 256.

[81]. Julio, B.; Jose, Q.; Claudio, A.; Jimenez, P. Gallifa, D.; Jorge, P.; Catalina, R. P. *New J. Chem.* **2013**, *37*, 2002.

[82]. Kolehmainen, E.; Borys, O. S.´*mialowski International Reviews in Physical Chemistry* **2012**, *31*, 567.

[83]. Schulze, K; Richter, C. H.; Klatt, K.; Ludwig, R. Z. *Chem*. **1988**, *28*, 288.

[84]. Lucio, F.; Adonis, L. P.; Tali, S. *J. Am. Chem. Scoc*., **2003**, *10*, 109.

[85]. Sandra, L.; Till, P.; Kühn, B.; Biospin, A.G; Fällanden, *Introduction to 1- and 2-dimensional NMR*, **2005**, *1*.

[86]. Martin, G. E.; Hadden, C. E. *J. Nat. Prod.* **2000**; *63*: 543.

[87]. a) Berger, S.; Braun, S.; Kalinowski, H. O.; *NMR-Spektroskopie von Nichtmetallen, Band 2, 15N-NMR-Spektroskopie*, *Georg Thieme, Stuttgart*, **1992**; b) Witanowski, M.; Stefaniak, L. Webb, G. A. *Annu. Rep. NMR Spectrosc.*, **1972**, *5A*, 395. c) Witanowski, M.; Stefaniak, L.; Webb, G. A. *Annu. Rep. NMR Spectrosc.*, **1977**, *7*, 117; d) Witanowski ,M.; Stefaniak, L.; Webb, G. A.; *Annu. Rep. NMR Spectrosc.*, **1981**, *11B*, 1; e) Witanowski, M. L.; Stefaniak.;

Webb, G. A. *Annu. Rep. NMR Spectrosc.*, **1986**, *18*, 1; f) Witanowski, M.; Stefaniak, L.; Webb, G. A. *Annu. Rep. NMR Spectrosc.*, **1993**, *25*, 1; g) Witanowski, M.; Webb, G. A. *Nitrogen NMR, Plenum Press, London*, **1973**.

[88]. Philipsborn, V. W.; Müller, R.; *Angew. Chem.*, **1986**, *98*, 381. Philipsborn, V, W.; Müller, R. *Angew. Chem., Int. Ed. Engl.*, **1986**, *25*, 383.

[89]. Buchanan, G. W.; *Tetrahedron*, **1989**, *45*, 581.

[90]. Laxer, A.; Dan, T.; Major, H.; Gottlieb, E.; Fischer, B. *J. Org. Chem.* **2001,** *66,* 5463.

[91]. Bodenhausen, G.; Ruben, D. J.; *Chem. Phys. Lett*.**1980**, *69*, 185.

[92]. Mueller, L. *J. Am. Chem. Soc*. **1979**, 101, 4481.

[93]. Bax, A.; Griffey, R. H.; Hawkins, B. L. *Magn. Reson*. **1983**, *55*, 301.

[94]. Bax , A.; Summers, M. F. *J. Am. Chem. Soc*. **1986**, *108,* 2093.

[95]. a) Willker, W.; Leibfritz, D.; Kerssebaum, R.; Bermel, W. *Magn. Reson. Chem*. **1993**, *31*, 287. b) Josep, S.; Gary, E.; Martin, J. F. *Concepts in Magnetic Resonance Part A 43*, **2015**, 177.

[96]. a series of examples of ^{15}N HMBC connectivities: Kline M.; Cheatham, S., Magn *Reson. Chem*., **2003**, *41*, 307.

[97].Mehring, M.*; High Resolution NMR in Solids, second edn., Spring-Verlag, New York*, **1983**.

[98]. Webb, G. A.; *Annual Report on NMR Spectroscopy, Academic Press, New York*, **1989**.

[99]. Christian, B.; Christel, G.; Florence, B.; Cristina, C.; Frédérique, P.; Thierry, T.; Azaïs, S. E.; John, A.; Griffin, M.; Jonathan, R. Yates, F. M.; Chris, J. P. *Chem. Rev*. **2012**, *112*, 5733.

[100]. Trygve, H.; Sonia, C.; Poul, J.; Kasper, K.; Jeppe, O.; Kenneth, R. *Chem. Rev*. **2012**, *112*, 543.

[101]. Jurgen, G.; Hans-J. W. *Chem. Phys*.**, 2000**, *2*, 2083.

[102] Schrodinger, L. L.; Jaguar. B. *Portland, OR*, **1991**.

[103]. Jain, R.; Bally, T.;Rablen, P. R. *J. Org. Chem.* **2009**, *74*, 4017.

[104]. Giesen, D. J.; Zumbulyadis, N. *Phys. Chem. Chem. Phys.* **2002**, *22*, 5498.

[105]. Joyce, S. A.; Yates, J. R.; Pickard, C. J.; Mauri, F. *J. Chem. Phys*. **2007**, *127*, 204107.

[106]. Jaguar, B.; Harder, A. D.; Hughes. E..; Greenwood, T. F.; Braden J. R.; Philipp, D. A.; Rinaldo, D. M.; Halls, D.; Zhang, M. D.; Friesner, J.; *Int . R.A., J. Quantum Chem.* 2013, *113*, 2110.

[107]. Cao, Y.; Beachy, M. D.; Braden, D. A.; Morrill, L.; Ringnalda, M. N.; Friesner, R. A. *J. Chem. Phys.* **2005**, *122*, 224116.

[108]. Tomasi, S.; Mennucci, B.; Cammi, R.; *Chem. Rev***. 2005**, *105*, 2999.

[109]. Cramer, C. J.; Truhlar, D. J. *Chem. Rev.* **1999**, *99*, 2161.

[110] *Wishart D.S, Prog. in Nucl. Magn. Res. Spect.*. ***2011***, *58****,*** *62*

CHAPTER II

Tautomerism in substituted-1,2,4-triazole thiones by NMR techniques.

2.1 Objectives of the study:

Tautomerism in triazoles is an important topic due to the presence of this moiety in many biologically and pharmaceutically important molecules. As many as five tautomeric forms are possible for substituted-1,2,4-triazole thiones. Tautomerism plays an important role in determining their properties and reactivities. However, the structure and nature of tautomers present under a particular condition is governed by many factors such as substituent, solvent, temperature etc. Determination of the precise details of tautomers existing in solution and solid state is an involved process. This issue is addressed here in detail for a few substituted 1,2,4 triazole thiones by NMR spectroscopic techniques. NMR techniques were employed for determination of the structure of tautomer/s in solution and solid state. These studies provided a good insight into the effect of substituents on tautomerism and stability of tautomers.

2.2 Introduction:

Characterization of tautomer forms in traizoles has been a subject of continuing interest. Triazoles can exist in two isomeric forms *viz*. 1,2,3 and 1,2,4 triazoles depending on arrangements of nitrogen and carbon atoms in the heterocyclic system. Both 1,2,3- and 1,2,4-triazole, exhibit tautomerism. The NH hydrogen can be attached to any of the three nitrogen atoms in triazoles and thus can present as three different tautomers *viz*, *N1-H*, *N2-H* and *N3-H* forms for 1,2,3 triazoles and *N1-H*, *N2-H* and *N4-H* for 1,2,4 triazoles in *C*-substituted triazoles (Scheme.2.1). While only two forms are possible in unsubstituted cases.

Scheme.2.1: *Tautomerism in substituted triazoles*

All these tautomers are heteroaromatic systems and the proton transfer is associated with migration of π electrons. Theoretical calculations are employed to estimate the extent of declocalization in these tautomers.[1-3] Accordingly, *2H*-1,2,3-triazole exhibits slightly better delocalization than the *1H*-tautomer. While in the case of 1,2,4 triazole, the *1H* tautomer showed higher delocalization than the *4H*. These theoretical calculations holds good in gas phase, where inter molecular effects are not important and will change in solution and solid state. For 1,2,3 triazoles, *1H* form is more stable in solution while in solid state both *1H* and *2H* forms are equally present.[4-7] Unsubstituted 1,2,4-Triazole exists only as the *1H*-tautomer [8-10]. The situation in *C*-substituted triazoles is very different and depending on the nature of substituents different tatuomeric forms are observed.[11, 12] Important system in the present context is *C*-substituted 1,2,4-triazole compounds with groups such as OH, SH and NHR. Such substituents will further complicate the issue of tautomerism due to the presence of additional “labile” proton, which can also take part in tautomerism. This will lead to formation of two additional tautomers D and E as shown in Scheme.2.2 with exocyclic double bonds. The system of present investigation is the case where X=S.

Scheme.2.2: *Various tautomers of disubstituted triazoles*.

2.3 Tautomerism in mercapto/thione substituted 1,2,4 triazoles.

Mercapto- or thione-substituted 1,2,4-triazole ring systems are not only important in synthetic organic chemistry as structural moiety but also reported to show many biological activities such antibacterial,[13] antifungal,[14,15] antitubercular, anti-mycobacterial, anticancer, hypoglycemic etc. Tautomerism of mercapto/thione 1,2,4 triazole frame work plays a crucial role in determining biological activities of compounds containing them. Though tautomerism in 1,2,4 triazole thiones has been a subject of several studies, it still catches attention due to its intriguing nature. At the same time, scarcity of detailed investigations and inconsistency of conclusions on thiol-thione tautomerism in triazoles has prompted us to carry out this study. In this study, tautomerism in a series of triazole thiones, with various substituents in triazole ring, are studied mainly with the help of NMR spectroscopic techniques. Most of the triazole derivatives studied in this chapter show antitubercular activity by selectively killing dormant pathogenic *tuberculi bacilli.*

There are many conflicting reports in literature on the tautomerism in 1,2,4 triazole thione derivatives. The five possible tautomeric forms A–E, as shown in the Scheme.2.3, are considered in the literature [16-20] for *N*,*S*-unsubstituted sulfanyl-1,2,4-triazoles,

Scheme.2.3: *Various tautomeric forms of N,S-unsubstituted sulfanyl 1,2,4 triazoles. When R= Methyl, the tautomers are named as follows: A) 5-methyl-1H-1,2,4-triazole-3-thiol; B) 3-methyl-1H-1,2,4-triazole-5-thiol; C) 5-methyl-4H-1,2,4-triazole-3-thiol; D) 5-methyl-1,2-dihydro-3H-1,2,4-triazole-3-thione and E: 5-methyl-2,4-dihydro-3H-1,2,4-triazole-3-thione.*

Buzykin *et al.* [21], preferred tautomer A for Sulfanyl-1,2,4-triazoles. However, the 4*H*-3-*SH* tautomer (form C) [22] and 1*H*-5-*SH* tautomer (form B) [23] have also been reported as the dominant species in solution. In many of the reports, [24, 25] structures of *N*,*S*-unsubstituted sulfanyl-1,2,4-triazoles are presented as thione tautomers D and E. [25] In some of the cases, 2,4-dihydro-3*H*-1,2,4-triazole-3-thione tautomer E is preferred over 1*H*,2*H*,3-thione tautomer D.[25] Most of the crystal structures reported are also in 2,4-dihydro-3*H*-1,2,4-triazole-3-thione form. In some of the other reports thione tautomer is favoured in solid state and in neutral solution.[26, 27] The thiol form is usually considered as the reactive species in alkylation reactions. Abbe reported that the thiatriazole derivative (compound. 1, Scheme.2.4) exists in the tautomeric form shown.[28]

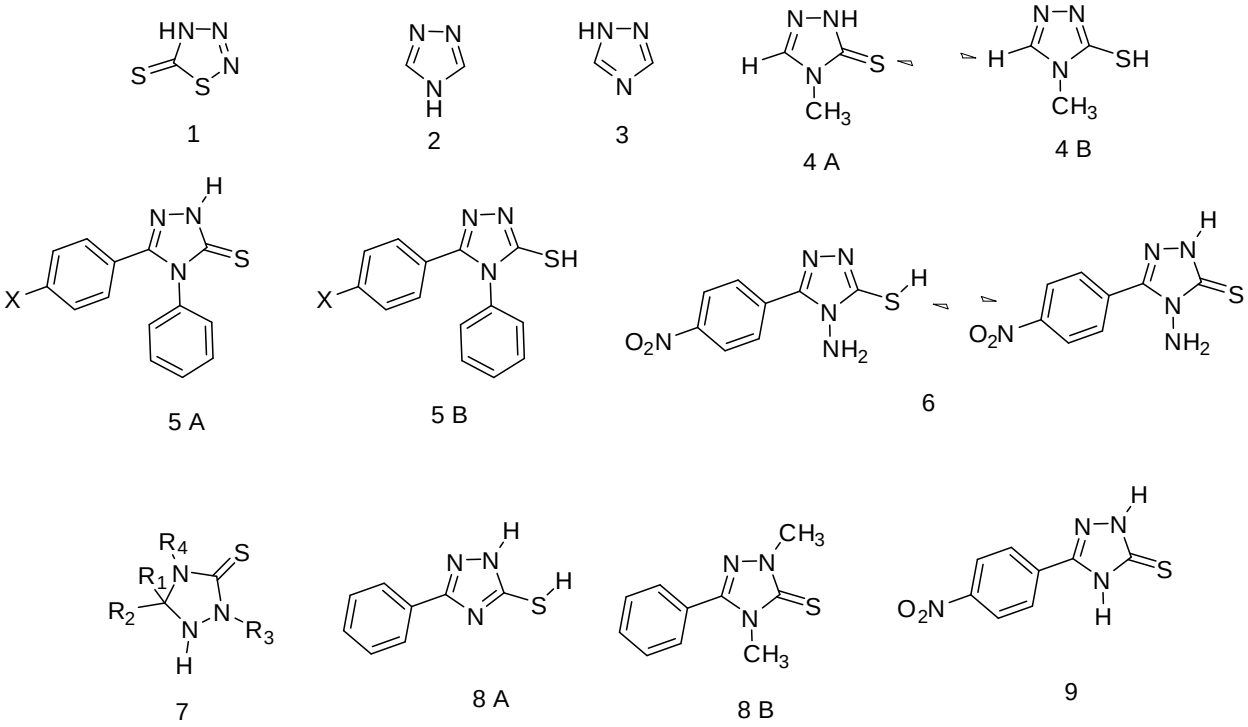

Scheme.2.4: *Various tautomeric forms reported for compounds 1 to 9 in literature.*

Small structural variations can have a significant effect on tautomeric equilibrium. For example, in unsubstituted 1,2,4-triazoles it is found that two tautomers namely 4*H*-1,2,4-and 1*H*-1,2,4-triazole (compounds 2 and 3 respectively, Scheme.2.4) differing in location of hydrogen atom and double bonds within ring are present [29-31]. While when substituent like methyl group is present at N-4, theoretical calculations [32] indicate that thione form S_{NH} (compound. 4A, Scheme.2.4) is more stable than S_{SH} (compound. 4B, Scheme.2.4) by about 10 kcal/mol. These calculations are in agreement with the experimental observation that thione form is predominantly observed in crystals. For 4,5-diphenyl-2,4-dihydro-3*H*-1,2,4-triazole-3-thione (compound 5) both the thione (5A) [33, 34] and thiol (5B) [35]forms have been reported by various investigators.

In the literature various methods such as HPLC (compound 6), Mass spectrometry (compound.7), UV (comp.8,16), single crystal (compounds. 10-15,17, 22, 23), NMR (compounds. 16, 18, 24, 25, 26), IR (compounds. 18, 20, 21), Hammet constant (compound. 19) are reported to study tautomeism in triazole thiones. The systems studied are shown in the Scheme.2.4- 2.6.[36-58]

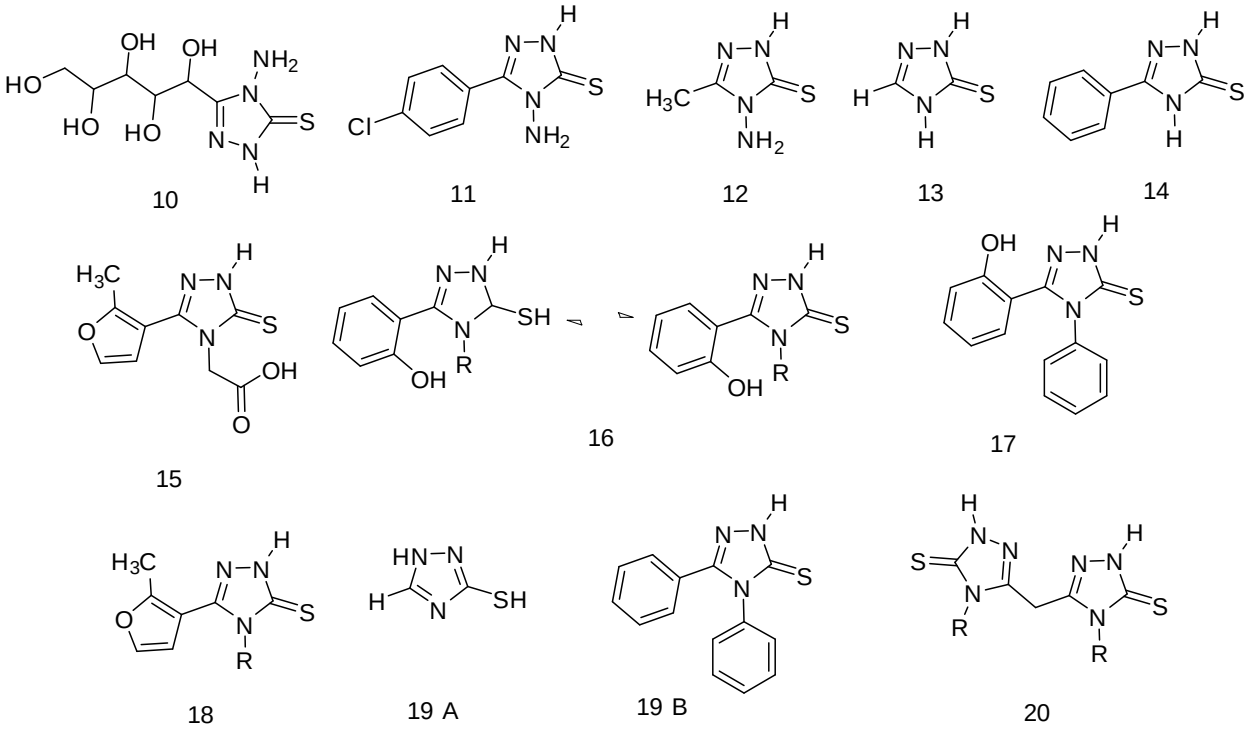

Scheme.2.5: *Reported tautomeric forms for various compounds 10 to 20 in literature.*

Scheme.2.6: *Reported tautomeric forms for various compounds 21 to 26 in literature.*

2.4 Experimental:

2.4.1 Syntheses:

All the triazole thiols were prepared by following the reported [59, 60] procedure.

2.4.2 NMR techniques:

All the solution state NMR measurements were carried out on a Bruker AV 400 (resonating at 400.13, 100.62, and 40.55 MHz for ^{1}H, ^{13}C and ^{15}N nuclei, respectively), AV500 (500.13, 125.75, 50.67 MHz for ^{1}H, ^{13}C and ^{15}N nuclei, respectively), AV 700 (resonating at 700.13, 176.04, 70.94 MHz for ^{1}H, ^{13}C and ^{15}N nuclei, respectively). Solid state NMR measurements were performed on Bruker AV 300 (resonating at 300.13, 75.46, 30.41 MHz for ^{1}H, ^{13}C and ^{15}N nuclei, respectively), JEOL ECX 400 (resonating at 400.13, 100.61, 40.56 MHz for ^{1}H, ^{13}C and ^{15}N nuclei, respectively). The samples were dissolved in DMSO-*d*6 in a standard 5 mm NMR tube and ^{1}H, COSY, NOESY, ^{13}C, ^{13}C DEPT, ^{1}H-^{13}C HSQC, ^{1}H-^{13}C HMBC, ^{1}H-^{15}N HSQC and ^{1}H-^{15}N HMBC experiments were performed on 5 mm broad band observe (BBO) gradient probe at ambient temperature ($\sim 28^{0}C$). Gradient spectroscopic techniques were employed for all the 2D experiments. In general, 256 experiments (*t*1 increments) of 8 to 24 scans were used for COSY and NOESY measurements. The COSY and the ^{1}H-^{13}C HMBC spectra were collected in a magnitude mode while a phase sensitive (States-Time Proportionate Phase Increment (TPPI)) mode was used for HSQC and NOESY measurements. A mixing time of 1 s was employed for NOESY experiment. The number of scans used for each *t*1 increment for other 2D experiments were 8 to 80 for ^{1}H-^{13}C HSQC, ^{1}H-^{15}N HSQC, ^{1}H-^{13}C HMBC, and ^{1}H-^{15}N HMBC. ^{1}H-^{13}C HMBC collected with polarization transfer delay corresponding to long-range coupling constant of 7 Hz whereas the corresponding ^{1}H-^{15}N HMBC measurements were conducted for delays corresponding to long-range couplings of 10 or 4 Hz. The HMBC spectra were acquired without proton decoupling during detection. The 90^{0} pulse lengths were calibrated for ^{1}H, ^{13}C, and ^{15}N were around 13-17.3, 10, and 14 μs, respectively. Appropriate window functions, viz. sine squared bell with no phase shift for all magnitude modes and phase shifted (ssb = 2) sine-squared bell for phase sensitive mode were used for data processing. In general a 1 K×1 K data matrix size was used for the 2-D experiments. ^{1}H chemical shifts were referred to the

residual solvent peak (δ = 2.50 ppm for DMSO-d_6) and for ^{13}C the central signals of the solvent multiplet is used for referencing (δ = 39.95 ppm for DMSO-d_6). ^{15}N chemical shifts were referred to an external sample of nitromethane (δ = 0 ppm). ^{1}H, ^{13}C and ^{15}N chemical shifts (δ in ppm) were measured with an approximate accuracy of 0.01, 0.05 and 0.1 ppm, respectively.

2.4.3 ^{13}C CP-MAS experiment:

The Hartman Hahn match condition for ^{1}H-^{13}C cross polarization experiments was determined by using adamantane. The samples were packed in a 4 mm rotor and spun at 8 kHz for measurements on 300/400 MHz spectrometers. Proton T_1 measurements were conducted by means of saturation recovery pulse sequence for optimizing the relaxation delay of CP-MAS experiment. A delay of five times of proton T_1 is employed for CP-MAS experiments. Acquisition parameters employed are: contact time 1 to 3 msec, acquisition time 40 msec, and relaxation delay and number of scans employed varied from sample to sample. ^{13}C chemical shifts are referred to CH_2 carbon of adamantane at 38.5 ppm (external reference). A standard Bruker 4mm CP-MAS probe is used for measurements.

2.4.4 ^{15}N CP-MAS experiment:

A sample of glycine or NH_4Cl is used for finding out Hartman Hahn match condition for ^{1}H-^{15}N cross polarization and the CP-MAS spectra is acquired with the following parameters: contact time 1-2.5 ms, relaxation delay between 2 sec to 100 sec, acquisition time 42 msec, number of scans 300-800, spinning speed 8 kHz. An estimation of ^{1}H spin lattice relaxation time is done prior to the CP-MAS experiment for optimization of recycle delay between the pulses. The chemical shift is referred to the nitrogen of glycine at -347.6 ppm with respect to nitromethane.

2.4.5 ^{1}H MAS experiment:

Either a 2.5 mm MAS probe (300 MHz) or a 1.3 mm MAS probe (700 MHz) is used for ^{1}H MAS experiments. The 2.5 mm probe is capable to achieve a spinning speed up to 35 kHz while the maximum spinning speed of 67 kHz is possible with the 1.3 mm probe. Adamantane signal at 1.87ppm is used as an external reference. Other parameters used for ^{1}H MAS on 700 MHz spectrometer are: 1.77 μs ^{1}H 90^{0} pulses; relaxation delay of 10-200 s; 446 ppm spectral width and 16 scans.

This Chapter is divided into two parts. Part A deals with the solution state NMR studies while Part B discusses the approach based on solid state NMR

Results and Discussion:

2.5 Part A: Tautomerism in the substituted-1,2,4-triazole-thiones studied by solution state NMR techniques.

The compounds investigated by 1 and 2 dimensional NMR spectroscopic techniques and their different tautomeric structures are given in Scheme.2A.1. The atom numbering pattern shown in this scheme will be followed throughout this thesis for uniformity.

Chemical shifts are inconclusive to distinguish all the tautomers present in solution. Previous studies indicate [59, 61] that among different tautomers, 2a and 2b (thione form) should show chemical shifts around 165 ppm for C=S carbon, while in tautomers 2c, 2d and 2e, the same carbon is expected to appear at higher field. This thumb rule can be used to some extent to distinguish between thione form 2a, 2b and thiol forms 2c, 2d, 2e. ^{15}N chemical shifts are useful in a way to distinguish the tautomers because 'pyridine' type (sp^2) nitrogen signals are usually deshielded compared to 'pyrrole' type (sp^3) one.

Scheme.2A.1: *Substituted triazole thiones investigated by solution state NMR and possible tautomers of them with the atom numbering employed in the present investigation.*

In the present investigation, an approach comprising of 1D as well as 2D experiments based on the ^{1}H, ^{13}C and ^{15}N nuclei is used for characterization of tautomers. How a combination of various 1D/2D NMR experiments is useful to draw the conclusion about the nature of tautomer in systems studied is discussed below.

^{1}H NMR: ^{1}H NMR is the simplest experiment which is very much useful to study tautomerism in substituted-1,2,4-triazole-thiones 1-6 in solution. Thiol group (SH) of the tautomers (1c-1e) is expected to show chemical shift around 3-4 ppm.[62] Since the studies are carried out in DMSO-d_6 the residual water from the solvent appear in this region and hence hamper the observation of the presence of SH protons, if any . Out of the two thione forms 2b is expected to show J coupling between the NH protons. Moreover, species of the type (2b) is reported to be less stable.[61]

^{13}C NMR: In principle ^{13}C spectroscopy should be able to distinguish between thione and thiol forms.[63] Presence of a signal at ~ 165 ppm for C=S group is characteristic of thione tautomers. However, ^{13}C chemical shifts are not only affected by tautomerism but also by substituents and hence one should be careful in drawing conclusions about existence of tautomers on the basis of ^{13}C chemical shifts alone. Besides, the carbons present in these ring systems are not directly involved in tautomerism.

^{15}N NMR: Nitrogen atoms in 1,2,4-triazoles are directly involved in prototropy and are, therefore, more sensitive as a probe. ^{15}N NMR is expected to provide considerable information especially when the difference in chemical shifts of nitrogen atoms between sp^2 and sp^3 hybridization is taken into account. ^{15}N-^{1}H HSQC and ^{15}N-^{1}H HMBC experiments are expected to give a fair idea about the presence of a particular tautomer in the compounds studied here.[64] HSQC correlation of proton resonances to nitrogen nuclei is like a litmus test for thione tautomer 2a or 2b. NMR spectral analysis for various compounds studied is discussed below.

2.5.1 Compound 1: (5-(furan-2-yl)-2,4-dihydro-3H-1,2,4-triazole-3-thione):

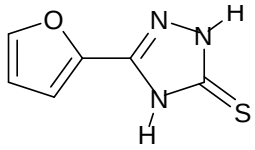

^{1}H NMR spectrum of compound 1 shows (Fig.2A.1) five distinct proton peaks indicating that five different protons are present in the system. Out of these five peaks two singlets appear at 13.66 ppm and 13.9 ppm. These chemical shifts are in accordance with the chemical shifts reported for NH protons in similar systems.[59] Based on this one can exclude the possibility of the presence of thiol tautomers 2c, 2d or 2e and consider presence of one of the thione tautomers, 2a or 2b or both. The ^{1}H NMR of compound also shows three signals (resonating at 7.89, 6.68 and 7.14 ppm) corresponding to three furyl ring protons. Among these protons the most deshielded proton is from H4′. The proton present on C2′ carbon (H2′) is expected to show as doublet by vicinal coupling with neighbouring proton (H3′) and appear at 7.14 ppm while H3 appear as a doublet of doublet at 6.68 ppm. However, the data is not sufficient for the assignments of NH protons.

Tautomeric forms 2a and 2b can in principle be distinguished from the ^{1}H spectrum as form 2b is likely to appear as two doublets since the two NH protons of

triazole ring are chemically inequivalent while in the form 2a, the NH protons can have only a weak 'W' coupling which may be difficult to resolve and hence show as two singlets. The ^{1}H spectrum of compound 1 shows only two broad singlets at 13.66 ppm and 13.90 ppm and suggests the presence of form 2a. The low field signal is broader than the high field one.

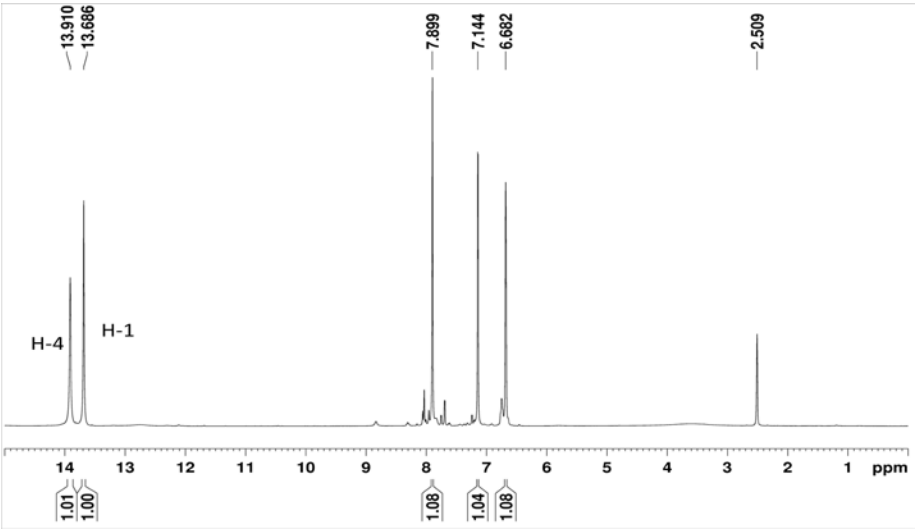

Fig.2A.1: *^{1}H NMR of the compound 1 (400 MHz, DMSO-d_6, 298 K)*

The inherent broadness of NH signals due to quadrupolar nature of the abundant nitrogen nucleus (^{14}N) and broadening due to chemical exchange with water can mask their vicinal scalar couplings. In fact a COSY spectrum of this (Fig.2A.2A) indeed show a weak cross peak between the two NH protons which may arise from a weak 'W' type of coupling between the NH protons in 2a or due a weak vicinal coupling in 2b. The coupling constant is less than the line width (~ 8Hz) of the NH proton at 13.66 ppm. Not much is known about $^{3}J_{HNNH}$ and the available data indicates that it varies from 2-8Hz.[47] Hence detailed investigations are required to confirm the structure of tautomeric species.

NOESY spectrum is very useful in identifying protons which comes spatially closer and eventually to determine three dimensional structure of the molecule. Therefore, NOESY experiment can help in the assignment of NH protons. One of the

protons of furyl ring resonating at 7.14 ppm (H2′) shows strong nOe cross peak with NH proton at 13.90 ppm (Fig.2A.2B) and a weak cross peak with the other NH at 13.66 ppm. This clearly indicates that NH proton at 13.90 is closer to furyl ring than the one at 13.66 which is consistent with thione form 2a. Hence, the signal at 13.90 is assigned to *N4H* of tautomer 2a, considering poor stability of tautomer 2b. The two NH protons resonating at 13.66 and 13.90 ppm also show exchange cross peaks (positive cross peak) with each other Fig.2A.3A.

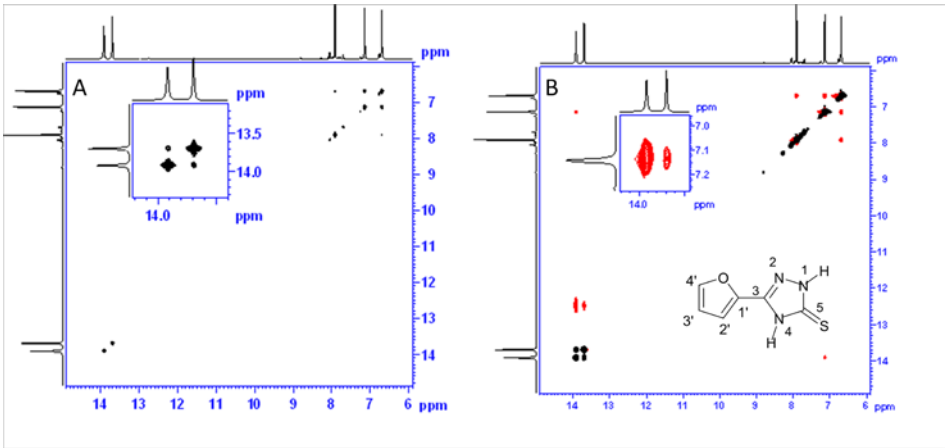

Fig.2A.2: *A) COSY of compound 1. Expansion of NH region is shown as inset. B) NOESY spectrum. Inset shows the cross peaks of NH protons with H2′ proton of furyl moiety. (400 MHz, DMSO-d_6, 298 K)*

The strong exchange cross peaks hinder observation of any nOe cross peak (negative cross peak), if any, in these systems. It is unlikely that the origin of exchange is due to exchange between NH protons of different tautomers. Both the NH protons can individually exchange with water protons. Hence the origin of strong positive cross peak between two NH protons is due to presence of a three site exchange net work involving two NH protons and water protons. That is, for example, proton on N1 nitrogen reside part of its time on water molecule which also spent part of its life time on the other NH *i.e.* in other words, exchange between two NH protons takes place through residual water present in DMSO-d_6, the solvent employed for measurement. This is further supported by the exchange cross peaks (Fig.2A.3B) seen between residual water and NH protons. In Fig.2A.3B, the chemical shift of water peak in the F1 dimension is a bit misleading due to spectral aliasing or folding resulting from the use of reduced spectral width for data

collection for better resolution. Proton signals in molecule 1 appear at 6 to 15 ppm range whereas residual water peak resonates at ~3.4 ppm. It is interesting to note that NH peak at 13.90 ppm shows stronger exchange cross peak with residual water than the other one. This is consistent with the observed larger broadening of this signal (~10 Hz) compared to the other (~7Hz). This in turn implies that N4-*H* is more "active" or "polarized" than N1-*H* in these systems under investigation. Other nOe peaks observed for the furyl ring protons are consistent with their assignments.

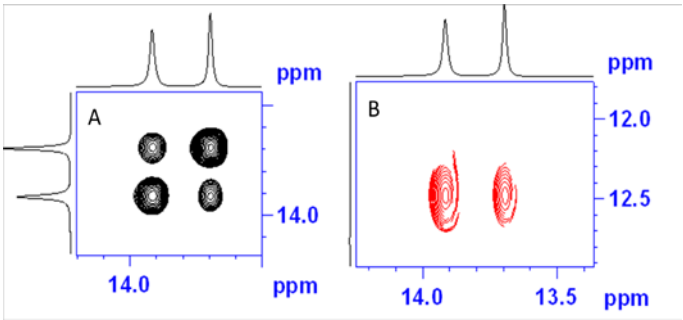

Fig.2A.3: *Expanded NOESY spectrum of the compound **1**. A) NH-NH correlations and B) Exchange cross peak with folded water peak. (500 MHz, DMSO-d_6, 298 K).*

^{13}C NMR of compound 1 shows six distinct peaks for the six chemically different carbons. The quaternary and CH carbons are differentiated by comparing the 1D ^{13}C DEPT and ^{13}C NMR spectrum as shown in Fig.2A.4. Absence of tautomeric forms 2c, 2d, and 2e and presence of either 2a or 2b is supported by the ^{13}C spectrum due to presence of the peak around 166.5 ppm corresponding to thione carbon. However, ^{13}C NMR spectrum does not give any information to differentiate between tautomeric forms 2a and 2b. ^{1}H-^{13}C HSQC spectrum helps to assign carbons attached to CH protons resonating at 112.03, 111.89 and 145.37 ppm. Protons resonating at 13.69 and 13.90 ppm do not show cross peak with the any of the carbon signals indicating that these are not directly attached to any of the carbon atoms, this helps to identify these protons as those directly attached to hetero atoms.

Both carbons of triazole ring (C3, C5) resonating at 143.10 and 166.5 ppm shows ^{1}H-^{13}C- HMBC correlations with both NH protons. The cross peak with NH proton resonating at 13.69 ppm are stronger than those with other NH proton resonating at 13.90 ppm (inset, Fig.2A.4C). This may be due to differences in the two and three bond ($J_{H\text{-}N\text{-}C}$,

$J_{H\text{-}N\text{-}N\text{-}C}$) scalar couplings involved. Faster exchange of NH at 13.90 ppm with residual water may also contribute to the weaker cross peaks involving it. However, this information does not help to identify the presence of a particular tautomer. It is also interesting to note that the carbon of the triazole ring resonating at 143.10 ppm shows a weak correlation with the H4′ proton of the furyl ring which also help in unambiguous assignment of it. The ^{1}H-^{13}C HMBC experiment was optimized for a long range coupling of 7Hz. The carbon at 166.5 did not show any cross peak with furyl ring protons. Apart from these, long range ^{1}H-^{13}C HMBC peaks among various furyl ring protons and carbons are also observed (Fig.2A.4C) and used for confirmation of their assignments.

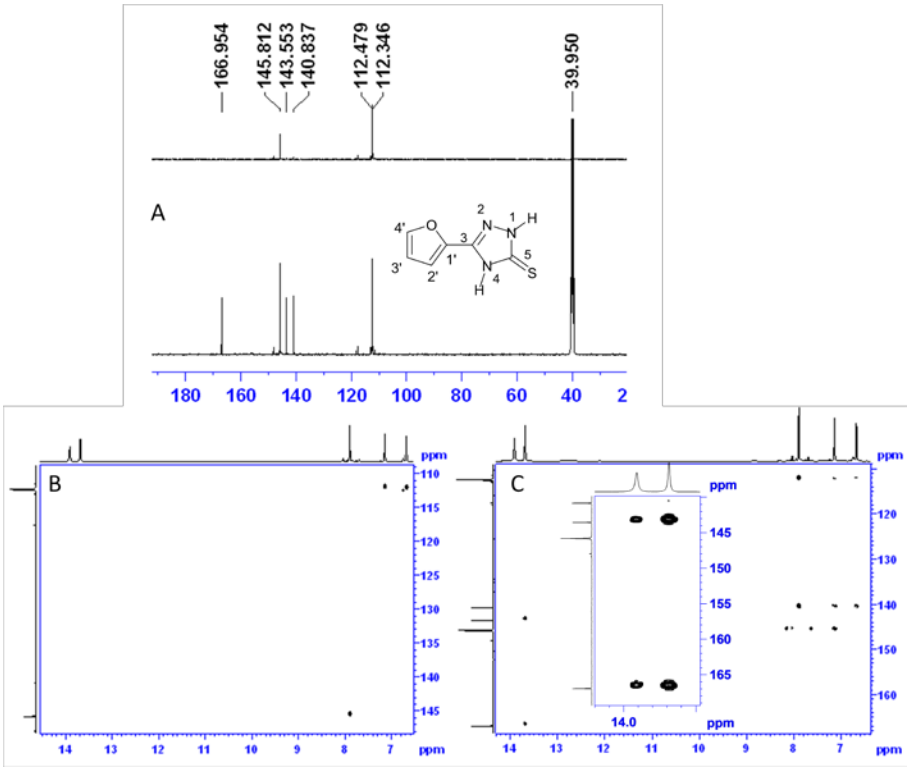

Fig.2A.4: *A) Comparison of 100 MHz ^{13}C DEPT (upper) and ^{13}C spectra (lower) of compound 1 along with B) ^{1}H-^{13}C HSQC and C) HMBC spectra (DMSO-d_6, 298 K)*

^{1}H-^{15}N HSQC gives information about protons and nitrogen which are bonded to each other through one bond coupling. This gives the most valuable information about the nature of tautomers. ^{1}H -^{15}N HSQC spectrum shown in Fig.2A.5A shows that proton resonating at 13.66 ppm shows correlation with a nitrogen resonating at -176.1 ppm (with respect to nitromethane) while proton resonating at 13.90 ppm correlates with nitrogen

signal at -214.0 ppm. This observation is sufficient to rule out the presence of any thiol form (2c-d). ^{1}H-^{15}N HSQC experiment provides chemical shifts for two *sp*^{3} hybridized (pyrrole type) nitrogen atoms assigned to N1 and N4. The chemical shifts observed for N1 and N4 are in agreement with previously reported data. [59] However, chemical shift for the last nitrogen (N2) cannot be obtained from this experiment as it does not have any proton attached to it. Overall, ^{1}H -^{15}N HSQC spectrum shows the two cross peaks which indicate either 2a or 2b form is present.

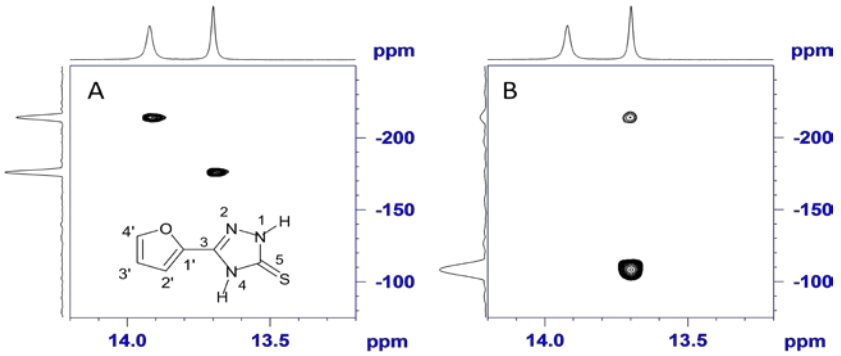

Fig.2A.5: *^{1}H-^{15}N HSQC (A) and HMBC (B) spectra of the compound **1** (DMSO-d$_6$, 298 K).*

In ^{1}H-^{15}N HMBC experiment, correlations between nitrogen and proton separated by two or three chemical bonds are obtained which help to identify the structure of molecule. ^{1}H-^{15}N HMBC spectrum (Fig.2A.5B) shows that the shielded NH proton (N1-H) resonating at 13.66 ppm shows correlations with nitrogen resonating at -109.3 ppm and -214.0 ppm. The cross peak to nitrogen at -109.3 ppm is stronger than the other. The deshielded NH attached to N4 did not show any HMBC correlation which is likely to be due to faster decay of it during the polarization delay time. For ^{1}H-^{15}N HMBC a polarization transfer delay corresponding to a coupling constant of 12Hz has been employed. These data helps to identify chemical shifts for all three nitrogen atoms which are in agreement with tautomer 2a. [59] The NMR observations are summarized in Scheme.2A.2.

M. Koparır *et al*. [65] also studied the compound 1 and proposed that there is large scale thione-thiol tautomerism. On the basis of the derivatization also they have proposed the thiol tautomeric form under the reaction conditions. But, the present

investigation does not show the existence of any thiol form in DMSO. It is likely that the thiol form may be present as short lived reactive form under reaction conditions.

Scheme.2A.2: *Pictorial representation of important homonuclear and heteronuclear correlations observed for compound 1.*

2.5.2 Compound 2: 5-phenyl-2,4-dihydro-3H-1,2,4-triazole-3-thione:

Metal complexes of the compound 2 are known to show antimicrobial activity.[66] ^{1}H NMR spectrum (Fig.2A.6) of the phenyl thione compound shows two peaks in aromatic region at 7.91 and 7.48 ppm corresponding to protons of phenyl ring. The downfield signal resonating at 7.91 ppm corresponds to two *ortho* protons of the phenyl ring (H2′) while remaining three protons are corresponding to the *meta (*H3′*)* and *para* (H4′) hydrogens. The ^{1}H spectrum also shows two signals at 13.88 and 13.72 ppm corresponding to one proton each. The downfield signal at 13.88 ppm is quite broader compared to the upfield signal 13.72 ppm, as in the previous cases, indicating that it is

more labile due to faster exchanges with residual water. From the features of the ^{1}H spectrum and the resemblances with previous case, tautomer form 2a or 2b is envisaged.

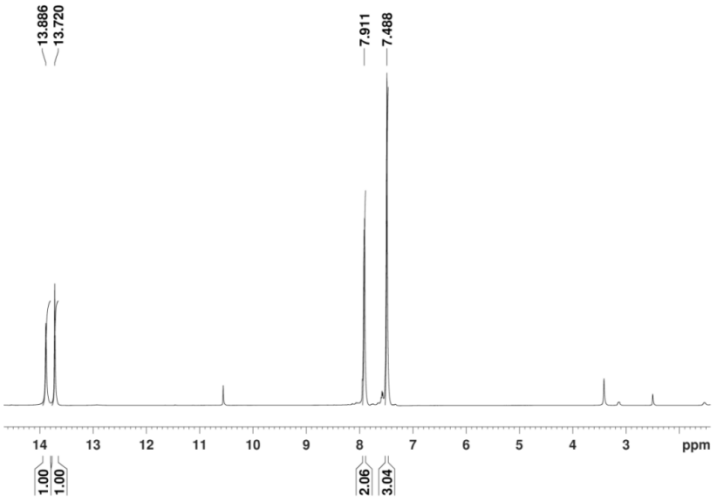

Fig.2A.6: *^{1}H NMR of the compound 2 (400 MHz, DMSO-d_6, 298 K).*

In the present case COSY spectrum can be used to distinguish between the 2a and 2b tautomeric forms. If the form 2b is present then the two vicinal protons bonded with the nitrogens should show COSY correlations. However, these correlations are not seen in the COSY spectrum of compound 2, indicating the absence of the tautomeric form 2b and therefore the 2a tautomeric form might be present.

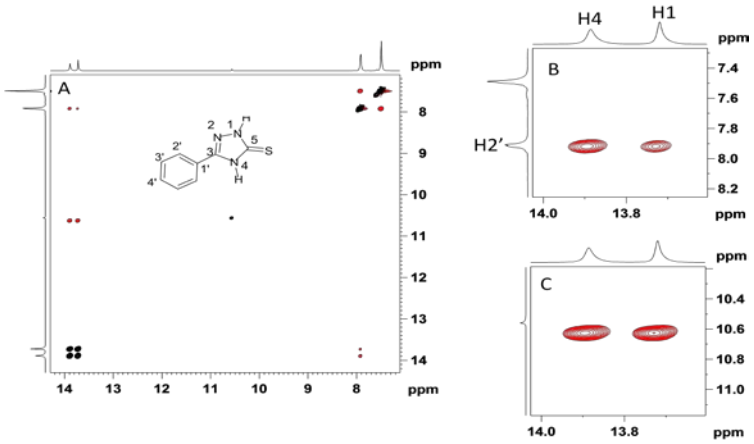

Fig.2A.7: *A) NOESY spectrum of compound 2. B and C are the expanded plots of cross peaks of NH signals with aromatic protons and water, respectively. The F1 chemical shift of water peak is misleading due to spectral aliasing. (400 MHz, DMSO-d_6 at 298 K)*

In NOESY spectrum (Fig.2A.7) both NH protons showed cross peaks of varying intensity with H2'protons of the phenyl ring. This indicates that NH protons are at different distance from the substituent and suggests the existence of tautomer 2a or 2b. As in the previous case, positive cross peaks are observed between both the NH protons and residual water molecule which appear as aliased cross peaks in the spectrum (Fig.2A. 7C) in addition to the nOe cross peaks of NH with aromatic proton H2′ (Fig.2A.7B)

^{1}H-^{13}C HSQC and HMBC experiments have been used for assignments of various carbon atoms. C3 carbon atom of triazole ring could be identified from its HMBC correlation with H2'aromatic protons and appears at 150.19 ppm (Fig.2A.8B). Other triazole ring carbon C5 resonates at 167 ppm. Both these carbons show cross peaks with the shielded N1-H (Fig.2A.8A). Cross peaks with N4-H could not be seen due to loss of signal during polarization transfer delay, which further supports faster dynamics associated with it. The remaining four signals resonating at 130.6, 129.1, 125.6 and 125.4 ppm corresponds to C4',C3',C2'and C1' carbons of the phenyl group.

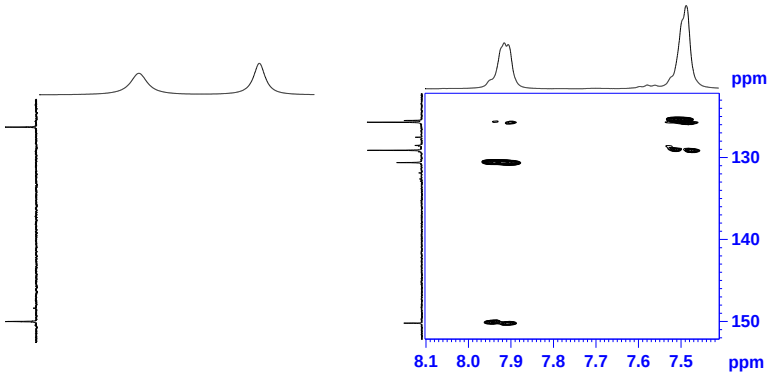

Fig.2A.8: *^{1}H-^{13}C HMBC spectrum of compound **2** highlighting correlations of triazole ring carbons C3 and C5 A) with NH protons and B) with phenyl ring protons. (DMSO, 298 K).*

In ^{15}N-^{1}H HSQC spectrum (Fig.2A.9A), ^{1}H signal at 13.72 ppm show correlation to nitrogen resonating at -175.1 ppm while the other low field proton at 13.89 ppm

correlated to nitrogen resonating at -212.4 ppm and confirm presence of two NH protons in the molecule. These nitrogen chemical shits can be used to distinguish tautomeric forms 2a and 2b. In form 2b, both NH nitrogen atoms (N1 and N2) are expected to show chemical shifts around -175 ppm taking into account the similar nature of them. While for tautomeric form 2a, chemical shifts of two NH's are expected to be considerably different which is also observed as shown in the Fig.2A.9A. The chemical shifts difference of 37.3 ppm observed with the most shielded signal, (N4) confirms the presence of form 2a in DMSO solution. The ^{1}H-^{15}N HMBC spectrum help to determine chemical shift of the remaining nitrogen atom in the molecule. One of NH protons (*N1H*, at 13.72 ppm) shows cross peaks with nitrogen atoms resonating at -212.4 ppm and -106.13 ppm. (Fig.2A.9B) and in turn confirms the presence of the tautomeric form 2a. This conclusion is in agreement with the results found by the Buzykin who reported the thione hydrate form in the solid state by using single crystal data.[44] Various correlations used for structural characterization are depicted in Scheme.2A.3.

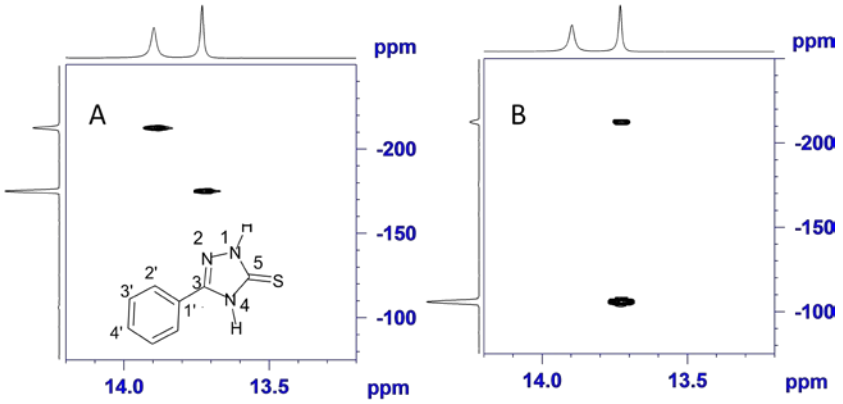

Fig.2A.9: *^{1}H-^{15}N HSQC (A) and HMBC (B) spectra of compound **2** (DMSO-d_6, 298 K)*

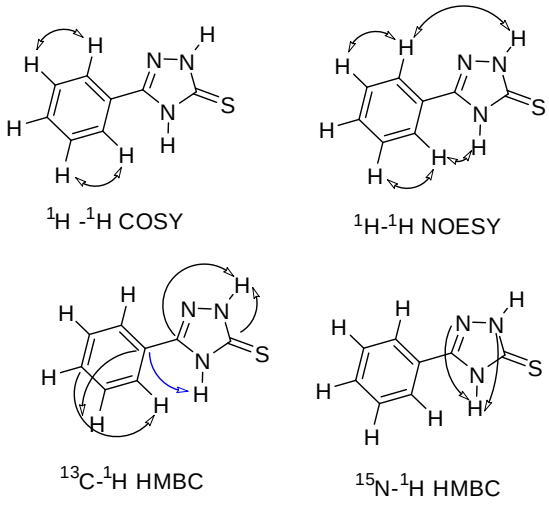

Scheme.2A.3: *Pictorial representation of important homomucear and heteronuclear correlations observed for compound 2.*

2.5.3 Compound 3 :(5-(4-fluorophenyl)-2,4-dihydro-3H-1,2,4-triazole-3-thione):

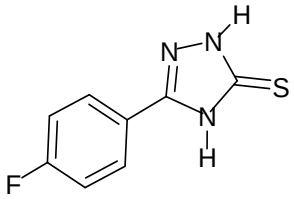

^{1}H NMR spectrum of compound 3 is shown in Fig.2A.10. Two signals are observed at 13.86 and 13.70 ppm corresponding to NH protons. The deshielded signal is found to be broader than in the previous cases (compound 1 and 2) and indicates faster exchange with residual water. Taking into account the spectral features of compounds already studied, this broad signal can be assigned to the H-4 proton. In the present compound the fluorine is present at the *para* position of the phenyl ring and shows two and three bond J couplings with the aromatic protons. This itself can be used for assigning them considering the fact that $^{3}J_{F\text{-}H}$ (~8-9Hz) is greater than $^{4}J_{F\text{-}H}$(~3-4 Hz). Signal at 7.37 ppm is assigned to protons *ortho* to fluorine (H3′) and the downfield signal is of protons *meta* to fluorine (H2’)

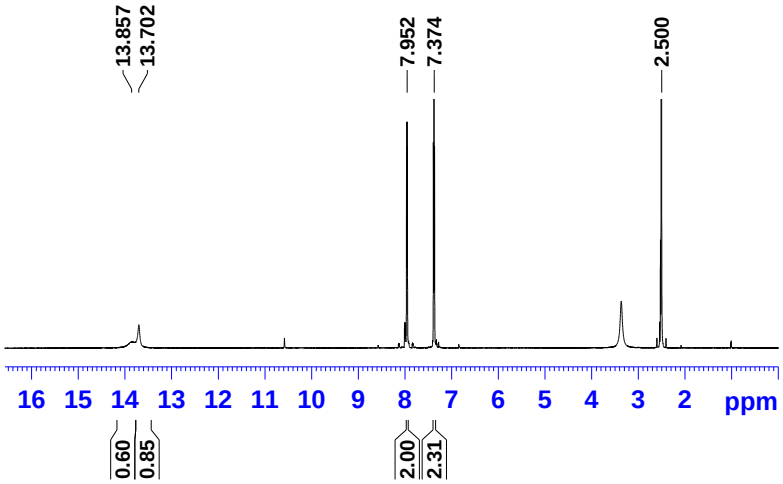

Fig.2A.10: *^{1}H NMR spectrum of compound 3 (700 MHz, DMSO-d_6, 298 K).*

Noticeable features that come out of NOESY spectrum are cross peaks of NH protons with H2' protons of aromatic ring (Fig.2A.11A,) the strong exchange cross peaks between the NH protons (Fig.2A.11B) and NH-H_2O (Fig.2A.11C) resonances. This again substantiates the role of water in broadening one of the NH protons and also in determining the nature of cross peaks between the NH protons.

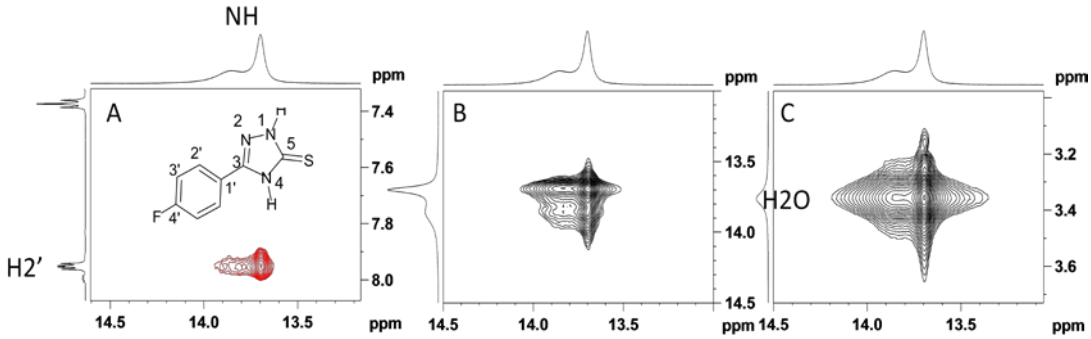

Fig.2A.11: *Expanded NOESY spectrum of the compound **3** showing A) nOe between NH protons and H2', B) exchange between NH protons and C) exchange between NH protons and residual water. (700 MHz, DMSO-d_6 at 298 K)*

Introduction of F atom on phenyl ring also introduce splitting in ^{13}C spectrum (Fig.2A.12A) due to $^{n}J_{C\text{-}F}$ which itself is useful for assignment. The carbon directly bonded to F atom (C4') appears as a doublet in the region 162-165 ppm with $^{1}J_{C\text{-}F}$ of ~250 Hz. The carbons *ortho* to F atom (C3′) also show a doublet feature separated by $^{2}J_{C\text{-}F}$ of ~22 Hz while a $^{3}J_{C\text{-}F}$ of ~8.9 Hz is noticed for the carbons *meta* to fluorine atom (C2'). Complete assignment of all the carbons could be made on the basis of this as wells as ^{1}H-^{13}C HSQC and ^{1}H-^{13}C HMBC spectra. In the ^{1}H-^{13}C HMBC spectrum (Fig.2A.12B) both the carbons of 1,2,4-triazole (C3, C5) did not shown any correlations with NH protons due to the exchange dynamics of the protons bonded with nitrogen. The quaternary carbon of 1,2,4-triazole ring (C3) resonating at 149.47 ppm could be identified by its correlation with the H2' protons resonating at 7.9 ppm. The carbon signal at 167.45 ppm assigned to C=S carbon and indicates that the compound is present in the

form 2a or 2b. Carbon at 122.17ppm is C1' and C2', C3'carbons appear at ~128 and 116 ppm, respectively.

^{1}H-^{15}N HSQC spectrum (Fig.2A.13) displayed only one correlation arising from the sharper NH proton at 13.70 ppm to a nitrogen with a chemical shift of -174.63 assigned to N1. Faster decay of the other NH proton due to exchange dynamics prevents observation of its coupled partner (N4) by HSQC. Cross peak could not be obtained in ^{1}H-^{15}N HMBC experiment due to same reason and hence chemical shift information of the other nitrogen atoms of triazole ring could not be obtained. The various correlations observed in the NMR experiments are summarized in Scheme.2A.4

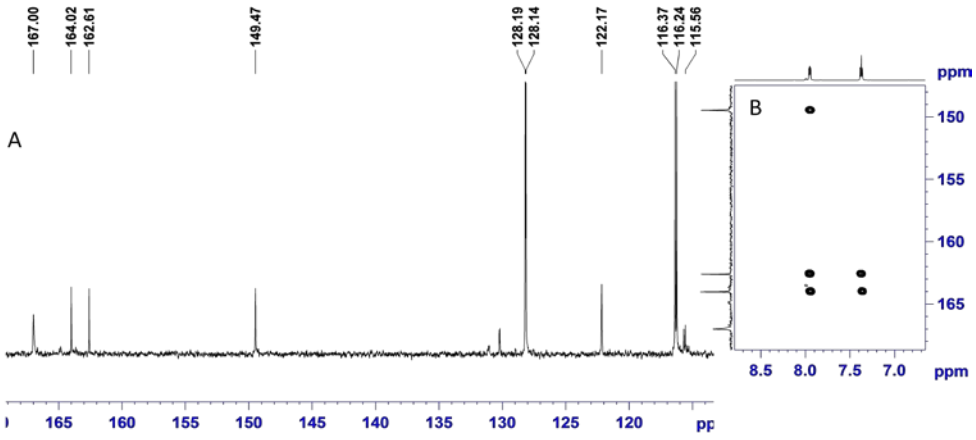

Fig.2A.12: *A) ^{13}C spectrum of the compound 3 (175 MHz, DMSO-d_6, 298 K) and B) important ^{1}H-^{13}C HMBC correlations of aromatic protons used for structural characterization.*

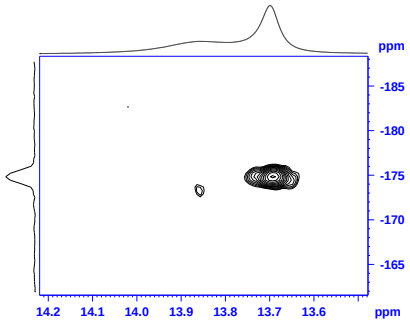

Fig.2A.13*: ^{1}H-^{15}N HSQC spectrum of compound 3 (DMSO-d_6, 298 K).*

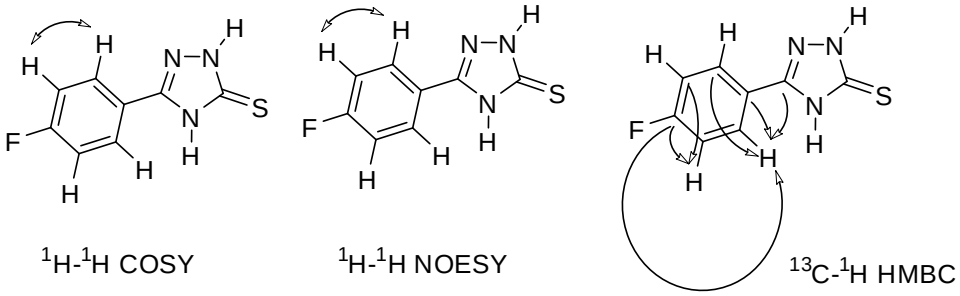

Scheme.2A.4: *Pictorial representation of important homonuclear and heteronuclear correlations observed for compound 3.*

2.5.4 Compound 4: (5-(2-methyl-3-nitrophenyl)-2,4-dihydro-3H-1,2,4-triazole-3-thione):

^{1}H NMR spectrum of compound 4 (Fig.2A.14) shows aromatic peaks in the region from 7-9 ppm, triazole NH peaks at 13.85 ppm and 13.77 ppm in addition to the methyl proton at 2.44 ppm. The NH signal at 13.85 is very sharp while the other one is very broad. In comparison with the previous cases, the broader NH is assigned to H4 of triazole ring. Assignments of other protons are straight forward and can also be easily obtained from the COSY, NOESY, ^{1}H-^{13}C HSQC and ^{1}H-^{13}C HMBC data.

The most upfield phenyl proton, resonating at 7.59 ppm, shows nOe with other two aromatic protons resonating at 7.86 and 8.01 ppm as shown in Fig. 2A.15E indicating that all the three protons of the aromatic ring are spatially close to each other. Aromatic proton resonating at 7.86 ppm and methyl protons at 2.44 ppm both show nOe cross peak with the NH proton of 1,2,4-triazole ring resonating at 13.85 ppm (Fig.2A.15 A,C), indicating their spatial proximity. This cross peak is much weaker compared the one seen between the vicinal aromatic proton (2.48Å) and suggest that the inter proton distances

are much longer than 2.48Å. The expected cross peak of H-4 with the phenyl ring proton could not be seen due to its broad nature arising from a faster decay.

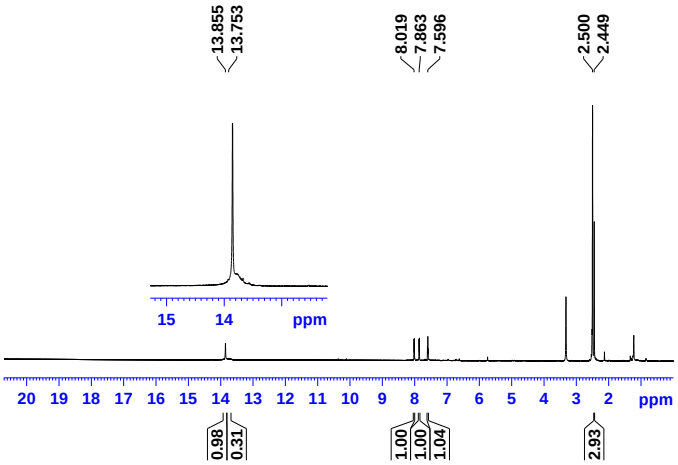

Fig.2A.14: *^{1}H NMR of compound 4 (700 MHz, DMSO-d_6, 298 K).*

Both the NH protons of 1,2,4-triazole ring show a positive cross peak with residual water resonating at 3.32 ppm due to chemical exchange (Fig.2A.15B). nOe contact between H6′ and water molecules has also been noticed (Fig.2A.15D) and show the proximity of water molecules to triazole ring and phenyl ring protons.

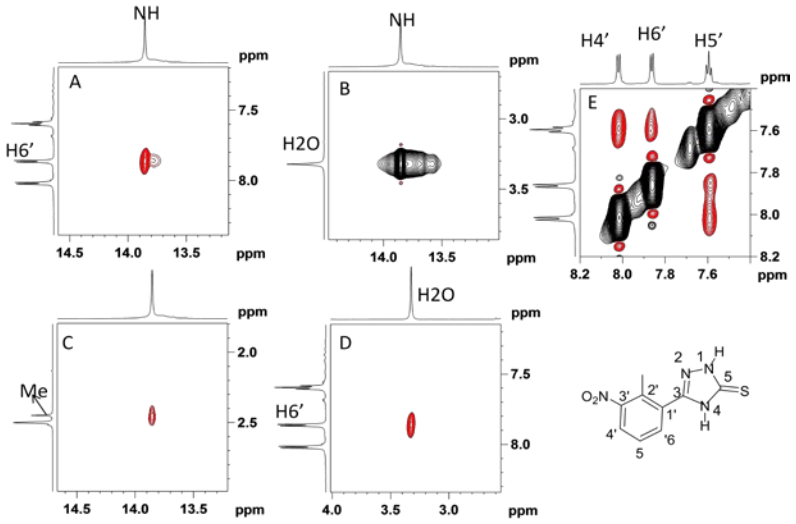

Fig.2A.15**:** *Expanded NOESY spectrum of the compound 4 showing A) nOe between NH protons and H6′, B) exchange between NH protons and residual water, C) nOe between NH proton and methyl group, D) nOe between water protons and H6′ and E) nOe between aromatic protons. (700 MHz, DMSO-d_6 at 298 K)*

^{13}C spectrum showed characteristic signal of the C=S carbon (C5) resonating at 166.72 ppm which also exhibit cross peak with NH in HMBC spectrum (Fig.2A.16A). The other carbon of the triazole ring appears at 148.89 ppm and shows HMBC correlation with NH and H6'protons. Aromatic carbon chemical shifts are 130.58 (C1'), 151.35 (C2'), 127.91 (C3'), 125.54 (C4'), 127.43 (C5') and 133.53 (C6'). Only the narrow NH peak at 13.85 ppm gave ^{1}H-^{15}N HSQC cross peak with nitrogen at -173.12 ppm, a value which is well in agreement with that expected for N1. This in turn confirms that the broad NH peak indeed belongs to H-4. Correlations with this broad peak could not be observed due to its faster decay. HMBC correlation for the sharp NH peak could also be obtained to identify N2 chemical shift at -96.76 ppm. Besides it also allowed to pick up the chemical shift (-4.56 ppm) of NO_2 group nitrogen through correlation with H4′ proton. Important homonuclear and heteronuclear correlations are shown in Scheme.2A.5.

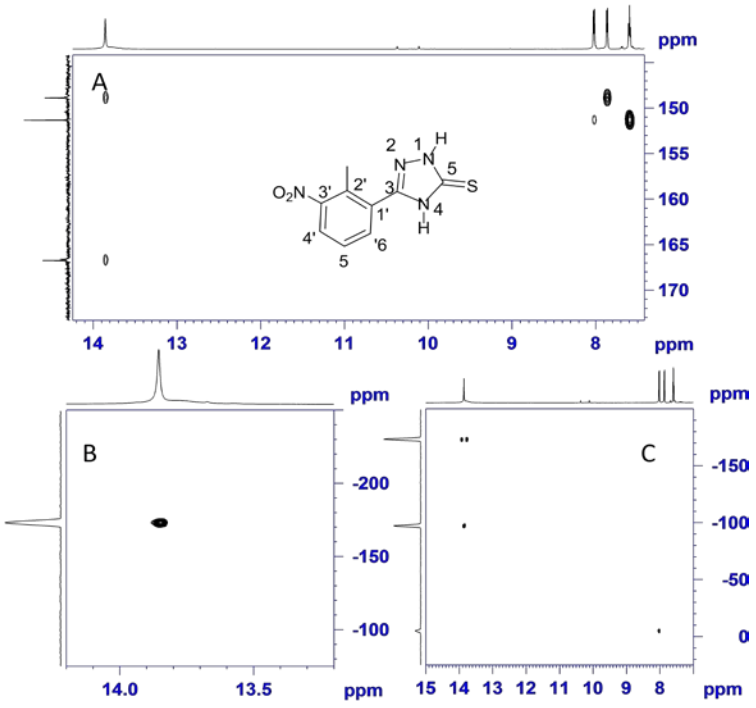

Fig.2A.16: *Important ^{1}H-^{13}C HMBC correlations (A), ^{1}H-^{15}N HSQC (B) and HMBC (C) spectra of compound 4.*

Scheme.2A.5: *Pictorial representation of important homomucear and heteronuclear correlations observed for compound 4.*

2.5.5 Compound 5: (5-(3-methyl-4-nitrophenyl)-2,4-dihydro-3H-1,2,4-triazole-3-thione):

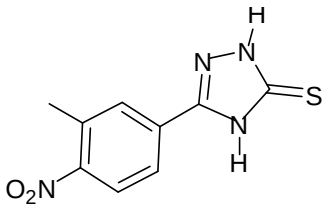

^{1}H spectrum of 3-methyl-4-nitrophenyl derivative (Fig.2A.17) also showed characteristic two NH peaks at 13.90 ppm and 14.03 ppm. As in many of the previous cases, the downfield NH is found to be broader than the other due to the exchange with residual water in the deuterated solvent used (DMSO-d_6). Two protons of the aromatic ring resonating at 8.01 ppm (H2') and 7.93 ppm (H6') show nOe with both NH protons (Fig.2A.18A). In this case also, both NH protons show positive cross peak with each other (Fig.2A.18D) as well as with water (Fig.2A.18B) indicating the chemical exchange between them. In addition, water also showed nOe cross peaks with H2'and H6' protons indicating interaction of water with triazole nitrogen and phenyl ring protons.

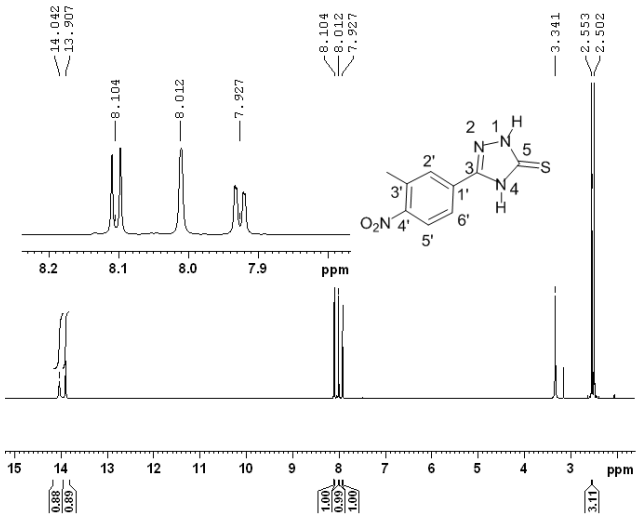

Fig.2A.17: *^{1}H NMR of the compound 5 (700 MHz, DMSO-d_6, 298 K).*

Assignments of all the carbons, especially that belongs to the triazole ring (correlation with NH protons and H2', H6'), are made with the help of ^{1}H-^{13}C HSQC and HMBC (Fig.2A.19A,B). Other assignments are as follows: C=S carbon (C5) chemical shift is 167.58 ppm (shows correlation with NH signal); C3 carbon appears at 148.56 ppm (correaltion with NH protons, H2'and H6'protons); C1' at 129.43 (correlation with H5'); C2'at 129.72 ppm (HSQC), C3'at 133.79 ppm (correlation with methyl protons and H5'); C4'at 149.5 (correlation with methyl and aromatic protons), C5'at 125.41ppm (HSQC) and C6' at 122.34 ppm (HSQC).

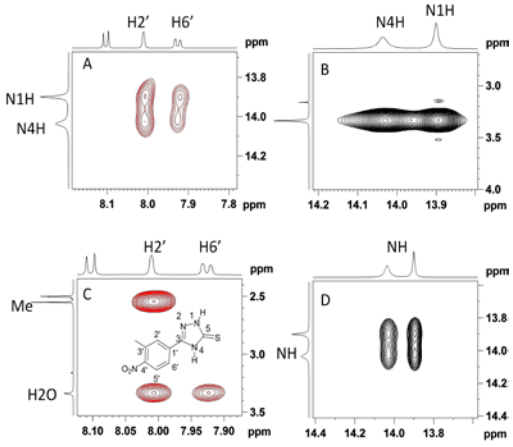

Fig.2A.18: *Expanded NOESY spectrum of the compound 5 showing A) nOe between NH protons and H2' and H6'; B) exchange between NH protons and residual water; C) nOe*

between NH proton and methyl and residual water; D) exchange peak between NH protons. (700 MHz, DMSO-d_6 at 298 K)

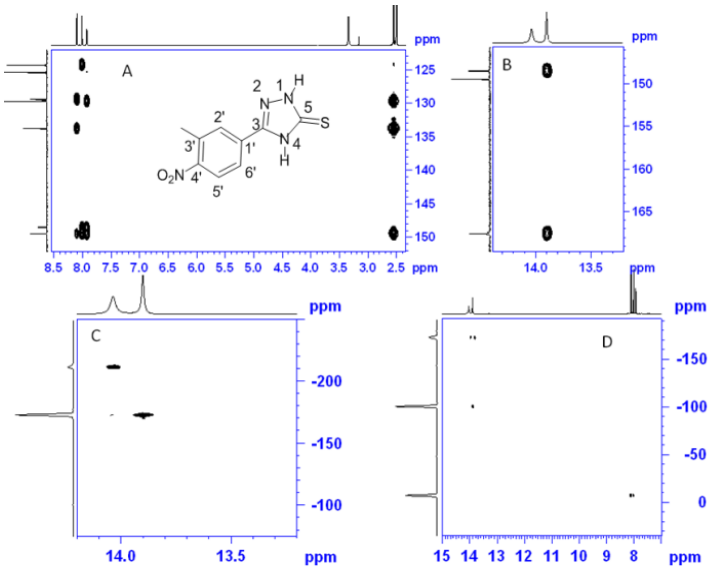

Fig.2A.19: *Important ^{1}H-^{13}C HMBC correlation (A, B), ^{1}H-^{15}N HSQC (C) and HMBC (D) spectra of compound 5.*

^{1}H-^{15}N HSQC (Fig.2A.19C) and HMBC (Fig.2A.19D) are employed to get chemical shift of nitrogen atoms in the triazole ring. ^{1}H-^{15}N HSQC (Fig.2A.19C) provided unequivocal evidence for the presence of thione form. Comparison of this data with the other compounds investigated clearly support tautomer of type 2a as the only species present in solution. Scheme.2A.6 summarizes the important NMR correlations employed for structural characterization.

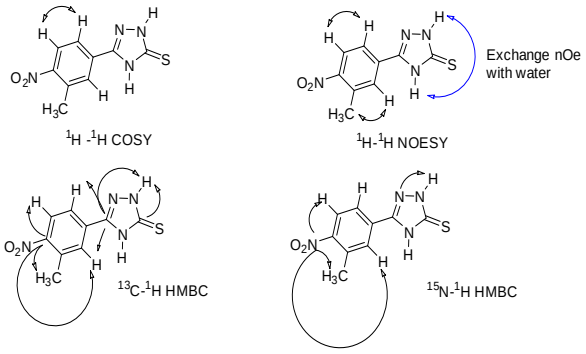

Scheme.2A.6*: Pictorial representation of important homonuclear and heteronuclear correlations observed for compound 5.*

^{1}H , ^{13}C and ^{15}N chemical shifts of triazole thiones investigated are complied in Tables 2A.1, -2A.3. Comparison of ^{1}H NMR chemical shifts of triazole NH protons investigated indicates that in most of the cases, N4H is more deshielded than N1H. The N4H always found broader than N1H proton mainly due to exchange with trace amount of water present in the solvent. This also suggests N4H is more labile or reactive than N1H. ^{13}C NMR data can be used for unambiguous identification of thione form. A chemical shift of 166-165 ppm for C5 carbon is typical of thione form. ^{15}N chemical shifts are also characteristic. Characteristic ^{15}N chemical shift features of 2a tautomer (1,4 dihydro form) are: -170 to -177 ppm for N1, -95 to -110 ppm for N2 and -210 to -215 ppm for N4 in DMSO-d_6.

Table 2A.1: *Comparison of ^{1}H chemical shifts of triazole NH.*

Comp. no.	δ_{H-1} ppm	δ_{H-4} ppm
1	13.66	13.9
2	13.72	13.88
3	13.70	13.86
4	13.85	13.77
5	13.90	14.03

Table 2A.2: *Comparison of ^{13}C chemical shifts of triazole ring carbon atoms.*

Comp. no.	δ_{C-5} ppm	δ_{C-3} ppm
1	166.5	143.6
2	167.44	150.64
3	167.45	149.47
4	166.72	148.89
5	167.58	148.52

Table 2A.3: *Comparison of ^{15}N chemical shifts of triazole ring nitrogen atoms.*

Comp. no.	δ_{N-1} ppm	δ_{N-2} ppm	δ_{N-4} ppm

1	-176.1	-109.3	-214.0
2	-174.90	-105.88	-212.30
3	-174.63	-	-
4	-173.12	-96.76	-
5	-172.61	-100.29	-211.25

2.6 Conclusions:

A combination of ^{1}H, ^{13}C and ^{15}N, 1-D and 2-D NMR studies provide unambiguous characterization of the tautomer present in triazole thiones in solution state. All the systems studied showed only one tautomer *viz*, the 1, 4 dihydro thione, which is characterized by the presence of two downfield NH resonances between 13-14 ppm. Substituent on triazole ring does not have any influence on the nature of tautomeric form. These results are in agreements with the literature reports. [59, 61] In all the cases studied, two NH of the 1,2,4-triazole ring behave differently. H-1 always shows up as a sharp signal while the H-4 exhibit broadness due to chemical exchange with residual water present in the solvent. This clearly points to the labile nature of H4. This also helps in the assignment of it. Other characteristic features of the 1,4 dihydro thione are ^{13}C chemical shift of ~165-168 ppm for C=S carbon, ^{15}N chemical shifts of -95 to -110 (for N2), -170 to -177 for N1 and -210 to -215 for N4.

2.7 Part B: Solid State NMR studies of the substituted-1,2,4-triazole-5-thiones.

The dynamics of tautomers in solution do not allow molecules to be studied in detail at times. Usually, the problem of dynamic equilibrium will be absent in solid state or if present, will be extremely slow. Hence, it would be interesting to study the molecular states in solid state, which shall also give information about the correlation

between solution and solid state conformations of the molecules. Solid state NMR has emerged as a powerful tool to study the structure of molecule since the advent of techniques such as magic angle spinning (MAS) and cross polarization (CP). Unlike X-ray crystallography, solid state NMR can conveniently be employed for structural characterization of samples in powder form, which can be amorphous or microcrystalline in nature. Features observed in solid state NMR of microcrystalline samples have a one to one correspondence with the unit cell information present in X-ray crystallography.

Some of the triazole thiones described in the previous section were found to be difficult to characterize, especially in extracting the chemical shits for all the nitrogens using solution state NMR techniques. This is mainly due to the exchange dynamics of NH protons of the triazole ring with the trace amount of water even though tautomer 2a (*1H,4H* thione) was confirmed unambiguously. Still, it is of interest to know the structural details of them in solid state as well. 1,2,4-triazole thiones contains NMR active nuclei in the form of ^{13}C, ^{15}N, ^{1}H, ^{14}N and ^{33}S. Out of these, the first two, viz. ^{13}C and ^{15}N, though less abundant, are widely used for structural characterization of heterocyclic compounds by solid state NMR. Solid state NMR of ^{1}H nucleus is not very popular due to its inherent broadening resulting from stronger homonuclear dipolar interactions. These “homogeneous” interactions can be averaged either by multiple pulse techniques combined with MAS or with high speed MAS (35 kHz or more). Quadrupolar nature of ^{14}N nucleus (I=1) prevents the routine use of it, though it has high abundance. ^{33}S is quadrupolar (I=3/2) as well as less abundant (0.75%) and hence difficult to study. This section of the chapter describes ^{13}C and ^{15}N solid state NMR studies on triazole systems studied in the previous section and a few more similar compounds. Besides, the observations of ^{1}H high speed MAS (~30-40 kHz) studies of these systems will also be discussed. The aim of this study is to find out the nature of tautomer in solid state and also to have a comparison of it with solution state NMR.

Though ^{13}C nuclei are not directly involved in the process tautomerism; the presence of particular form can be identified from the characteristic chemical shifts, as

discussed in the previous section. However, ^{13}C analysis alone does not give complete information on the tautomeric form present. ^{15}N nucleus provides a better handle since the nitrogen atoms in triazole ring are directly involved in the process of tautomerism. ^{15}N has large chemical shift range and hence the overlap between the nitrogen atoms is less common. Therefore, the changes in ^{15}N chemical shifts, due to change in the status of tautomer, are expected to be considerable compared to ^{13}C nucleus. The above factors make ^{15}N NMR spectroscopy as one of the best methods available to study tautomerism in the present compounds.[64] However, ^{15}N NMR at natural abundance (0.37%) has limitation of poor sensitivity ($3.85*10^{-6}$ in comparison with proton). But, sensitivity can be improved considerably by employment of ^{1}H-^{15}N Cross Polarization (CP) technique in combination with magic angle spinning (MAS). Nevertheless, identification of tautomers present in the smaller percentages can still be difficult at natural abundance.

Various compounds studied by solid state NMR are presented in Scheme. 2B.1

Scheme. 2B.1**:** *Substituted triazole thiones investigated by solid state NMR and their possible tautomers with the atom numbering employed in the present investigation.*

Even though the thione form 2a (*1H,4H* type) was confirmed in the solution state, the compounds are studied by solid state NMR to get more insight into the

aspects of tautomerism in solids. In solution state, extraction of ^{15}N chemicals shifts became difficult due to the presence of the residual moisture which can exchange with NH protons, resulting in the loss of NH signals, if the exchange rate is faster than the NMR time scale. Such complications do not exist in solid state NMR. Therefore, in principle, extraction of chemical shifts for all the ring nitrogen atoms should be possible. But, one of the major problems observed in ^{13}C and ^{15}N CP-MAS experiments of some of these compounds is the long proton spin lattice relaxation times which was found to be in the range 10-125 sec resulting in longer experimental durations.

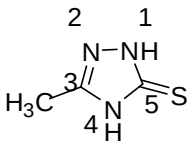

2.7.1 Compound 1: (5-methyl-2,4-dihydro-3H-1,2,4-triazole-3-thione):

^{1}H MAS spectrum of the compound is recorded at the spinning speed of 40 kHz with relaxation delay of 500 seconds which was approximately 5 times the estimated spin lattice relaxation time of the slowest relaxing nuclei. Three distinct signals in the ^{1}H NMR spectrum (Fig.2B.1) of the compound are seen for the three different type of protons.

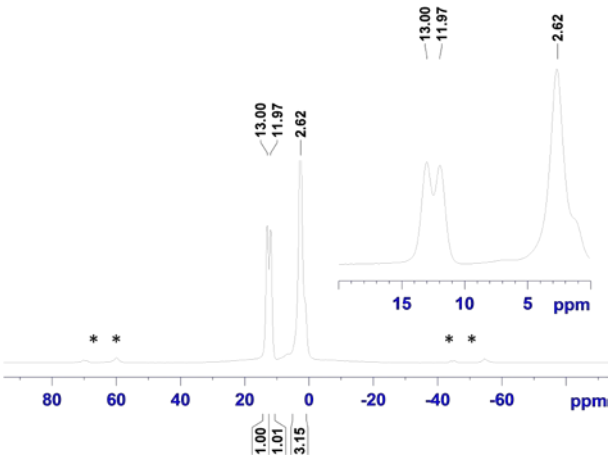

Fig.2B.1**:** *^{1}H MAS spectrum of compound 1 (methyl thione) at 40 kHz spinning speed (700 MHz, 298 K). Spinning side bands are marked with *. Inset shows the expanded spectrum.*

The two downfield protons at 11.97 and 13.00 ppm, showing integration around one each, corresponds to NH protons of the 1,2,4-triazole ring while the most upfield signal at 2.62 ppm corresponds to three protons of the methyl group. From the features of this ^{1}H MAS spectrum and its analogy with the ^{1}H NMR spectrum in solution state, it is clear that the tautomer present in solid state has two protons directly bonded with hetero atoms (nitrogen) of the triazole ring. This is possible only if the tautomeric form 2a or 2b is present. Forms 2c, 2d or 2e are not likely to be present since these forms bear only one proton directly bonded with nitrogen of the triazole ring. ^{1}H MAS spectral analysis does not prove conclusively about whether the tautomeric form 2a or 2b is present in the solid state. Therefore, studies based on the carbon and nitrogen nuclei are explored in order to identify which of the tautomeric form 2a or 2b is present in the system.

^{1}H-^{15}N CP-MAS NMR is expected to give details of the tautomer as ^{15}N is directly involved in this phenomenon. Nitrogen chemical shift itself should carry the signature of tautomer. ^{1}H-^{15}N CP-MAS spectrum of compound 1 is shown in Fig.2B.2 which shows only three nitrogen signals at -120, -177 and -203 ppm indicating the presence of only one type of tautomer. The solution state NMR of this compound recorded in DMSO-d_6 also showed the

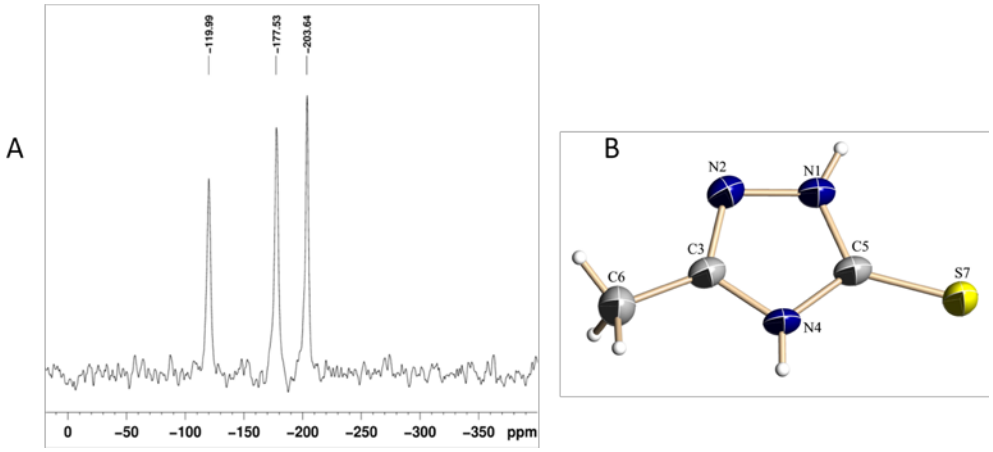

Fig.2B.2: *A) ^{15}N CPMAS spectrum of compound 1 (30.0 MHz, 298 K). B) : Single crystal X-ray of the compound 1*

presence of three nitrogen signals at -104.7, -176.6 and -204 which is similar to that observed in solid state and thus attributed to the *1H,4H* tautomer. Major solvation effect is seen for the N2, which is deshielded by ~ 15 ppm in DMSO. The crystal structure of this compound, obtained in the methanol solvent as shown in Fig.2B.2B, is also in agreement with the 1,4 dihydro tautomer.

Fig.2B.3 shows a comparison of ^{13}C CPMAS spectrum of compound 1 with its solution state spectrum taken in DMSO-d_6. The ^{13}C CP-MAS spectrum shows three carbons signals at 165.24, 151.52 and 13.45 ppm which are pretty close to the values obtained in DMSO. Chemical shifts of the triazole carbons (C5 and C3) were found to be very similar to that in solution state which appeared at 166.3 and 149.3 ppm respectively.[59] Thus the solvation effects are not significant for ^{13}C nucleus.

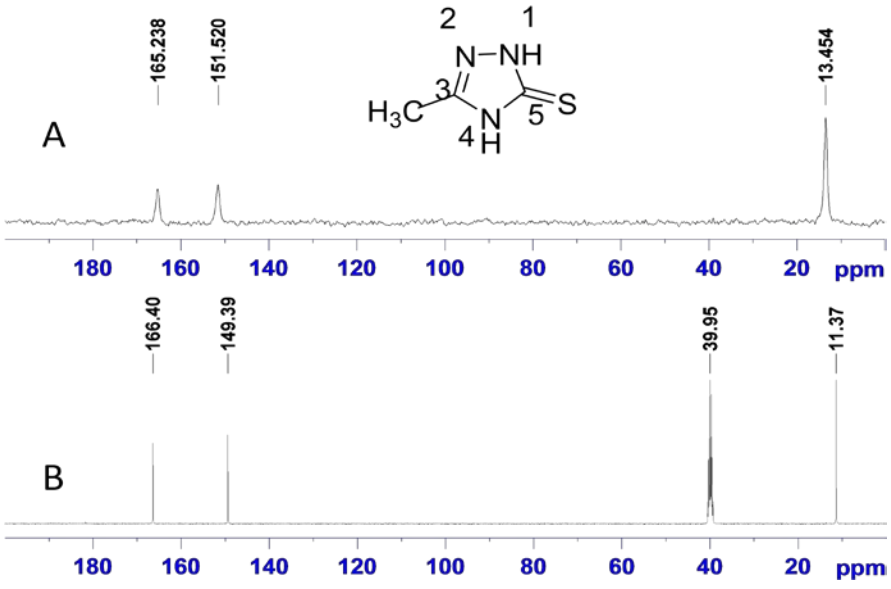

Fig.2B.3**:** *Comparison of ^{13}C spectra of compound 1. A) CP-MAS spectrum (176 MHz, 298 K, 40 kHz) and B) in DMSO solution (100 MHz at 298K).*

2.7.2 Compound 2: (2,4-dihydro-3H-1,2,4-triazole-3-thione):

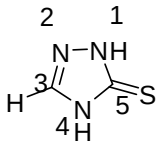

^{1}H MAS spectrum of the compound 2 (H-thione) show three protons split into two different groups as shown in Fig.2B.4 The protons resonating at 13.37 and 12.13 ppm are from the NH protons of the 1,2,4-triazole ring while the protons resonating at 8.42 ppm is bonded to the triazole ring carbon C3. The ^{1}H chemical shifts observed in DMSO solution are 13.47 and 13.26 ppm for the NH protons and 8.22 ppm for the proton directly bonded with the carbon of the triazole ring. This good agreement seen in solution and solid state implies the presence of same 1,4 dihydro tautomer.

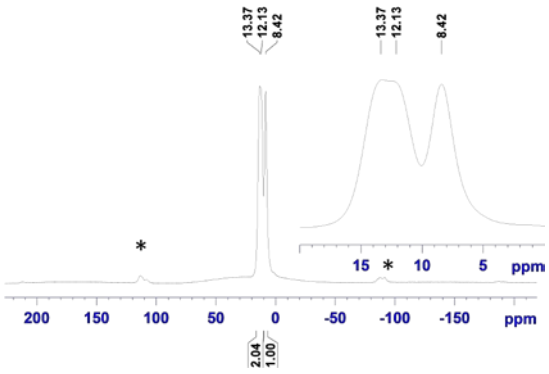

Fig.2B.4: *^{1}H MAS spectrum of compound 2 (H-thione) at 30 kHz spinning speed (300 MHz, 298 K). Spinning side bands are marked with *. Inset shows the expanded spectrum.*

The reported ^{13}C and ^{15}N NMR chemical shifts for compound 2 established the presence of thione form 2a as the only tautomer.[59, 61] The ^{13}C chemical shifts in solution state reported are 140.89 and 165.88 ppm, respectively, for the C-3 and C-5 carbons which are close to the values determined in the solid state (142.83 and 163.73 ppm, respectively). A comparison of the solution and solid state ^{13}C spectra is given in Fig.2B.5A,B and indicates the presence of the same 1,4 dihydro tautomer.

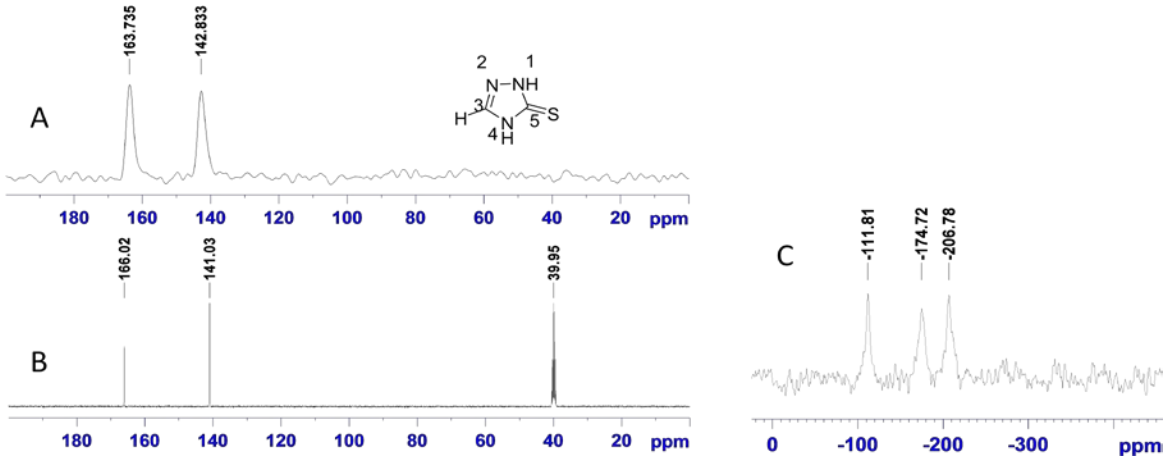

Fig.2B.5**:** *Comparison of ^{13}C spectra of compound 2. A) CP-MAS spectrum (75 MHz, 298 K, 8 kHz) and B) in DMSO solution (100 MHz at 298K). C) ^{15}N CP-MAS NMR spectrum. (30 MHz,10kHz)*

The ^{15}N chemical shifts of compound 2 in DMSO are at −75.5, −98.2 and −206.3 ppm respectively for the N1, N2 and N4 whereas the chemical shifts for these nitrogen atoms in the solid state are found to be -174.72, -111.81 and - 206.78 ppm

respectively (Fig.2B.5C). The non protonated nitrogen, N2 is found to be more affected by solvent DMSO-d_6. In the solid state it is shielded by ~ 13 ppm while N1 and N2 are practically unaffected and confirms the presence of same tautomer 2a both in solid and solution states.

2.7.3 Compound 3: (5-(t-butyl)-2,4-dihydro-3H-1,2,4-triazole-3-thione):

Proton MAS NMR spectrum (Fig.2B.6A) of compound 3 shows two downfield protons resonating at 13.83 and 12.74 ppm assigned to NH protons while the t-butyl group protons appear at 0.99 ppm. Comparison of ^{1}H chemical shifts patterns in solution and solid state suggests the existence of tatuomeric form 2a in both the states. The signal at 4.28 ppm is likely to be from moisture.

^{13}C CPMAS spectrum shows four well resolved signals for the four different carbon atoms of the molecule as shown in Fig.2B.6B and indicates the existence of only one tautomeric form of the type 2a. The triazole ring carbons show the chemical shifts of 162.12 and 164.71 ppm for C-3 and C-5 carbons respectively. These ^{13}C chemical shifts are in agreement with those observed in DMSO-d_6.

All the three nitrogen atoms in the ring are well resolved in the ^{15}N CP-MAS spectrum (Fig.2B.6C) with chemical shifts of -208.26, -178.66 ppm from the pseudo-sp^3 hybridized (pyrrole type) nitrogen atoms N4 and N1 respectively in addition to the pseudo-sp^2 hybridized (pyridine type) nitrogen at -113.09 ppm. The observed chemical shifts are in accordance with the *N1H, N4H* tautomer 2a. In solution state NMR the observed ^{15}N chemical shits are -179.5, -107.7 and -210.4 ppm, respectively for N1, N2 and N4 nitrogen atoms. Here, shielding effect of N2 in solid state is less pronounced (~ 5.3 ppm) compared to compounds 1 and 2.

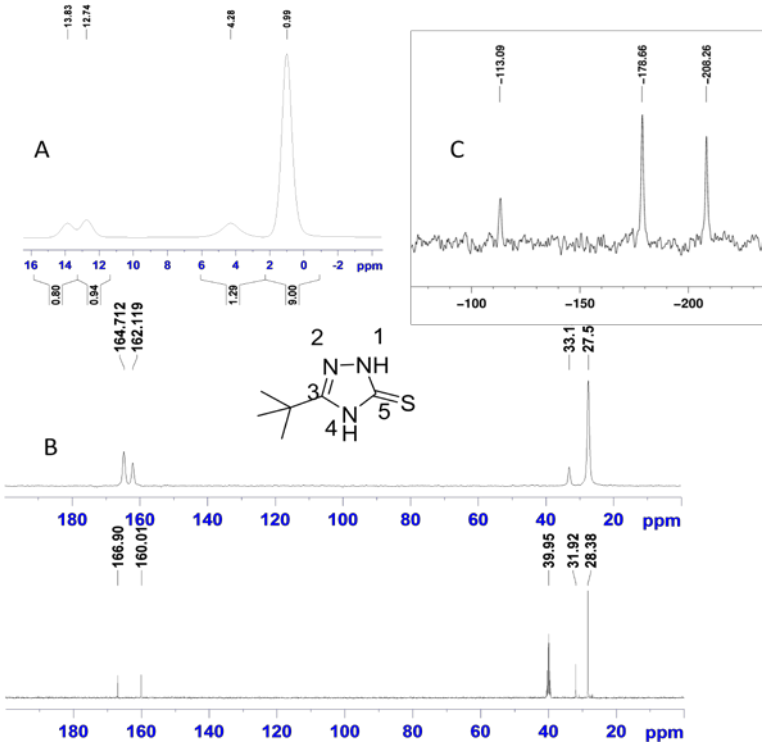

Fig.2B.6: *Solid state NMR spectra of compound 3. A) ^{1}H MAS (700 MHz, spinning speed, ν_r= 40 kHz), B)^{13}C CP-MAS (176 MHz, ν_r= 40 kHz); C) ^{15}N CP-MAS (70.0 MHz, ν_r= 30 kHz). Solution state ^{13}C spectrum (100 MHz) in DMSO is also shown in B (lower trace) for comparison.*

2.7.4 Compound 4:(5-phenyl-2,4-dihydro-3H-1,2,4-triazole-3-thione):

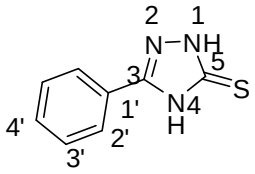

Solid state NMR spectra of compound 4 are shown in Fig.2B.7. Two downfield signals at 13.54 and 12.57 ppm, assignable to NH protons, are well resolved in the ^{1}H MAS spectrum (Fig.2B.7A) while the five protons of the phenyl ring appear in the region 6 to 8 ppm. The solution state ^{13}C NMR spectrum of this compound has been explained earlier in section A. The triazole ring carbons viz. C-5 and C-3 carbons, resonate at the chemical shifts of 150.64 and 167.44 ppm, respectively in solution state. The solid state chemical shifts for the carbons are found to be 149.62 and 163.43 ppm, respectively. In this case C-3 carbon is up field by ~ 4 ppm in the solid state compared to the solution state (Fig.2B.7 B).

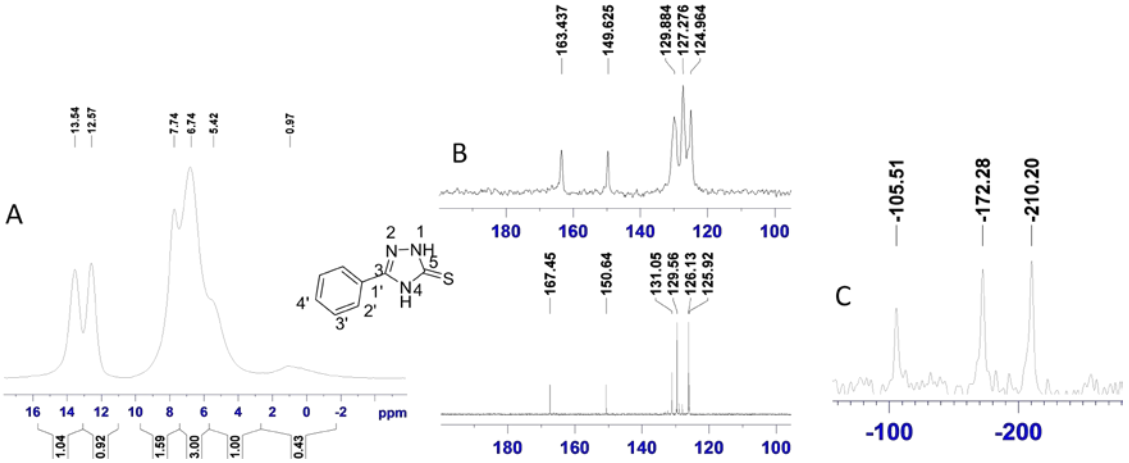

Fig.2B.7: *Solid state NMR spectra of compound 4. A) ^{1}H MAS (700 MHz, spinning speed, ν_r= 40 kHz), B) ^{13}C CP-MAS (176 MHz, ν_r= 40 kHz); C) ^{15}N CP-MAS (30.0 MHz, ν_r= 8 kHz). Solution state ^{13}C spectrum (100 MHz) in DMSO is also shown in B (lower trace) for comparison.*

^{15}N chemical shifts (Fig.2B.7C) for N1, N2 and N3 are -172.28, -105.51 and -210.20 ppm respectively. The corresponding chemical shifts in solution state are -174.90, -105.88 and -212.30 ppm. Here, N2 in solid state is slightly deshielded compared to the one in solution. The similarity of the solid state chemical shifts indicates that the structure of the compound is 2a (*1H,4H* tautomer form) as in the solution state.

2.7.5 Compound 5: (5-(4-chlorophenyl)-2, 4-dihydro-3H-1,2,4-triazole-3-thione):

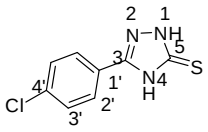

The NH protons of compound 5 appear as an asymmetric signal with a peak maximum at 13.7 ppm (Fig.2B.8A). The asymmetric nature suggests the presence of more than one environment. This compound is known to exist in the thione form 2a in solution.[59,61] The observed chemical shifts of C5 and C3 in solid state (163.96 and 149.57 ppm, respectively, Fig.2B.8B) are comparable with those in solution state (167.61 ppm and 149.74, respectively). The ^{15}N CP-MAS spectrum (Fig.2B.8C) indicated chemical shifts of -173.09 (N1), -107.10 (N2) and -210.99 ppm (N4) which are close to the values reported for *1H,4H* thione form in solution (-174.7, -104.3 and -212.5 ppm, respectively for N1, N2 and N4).

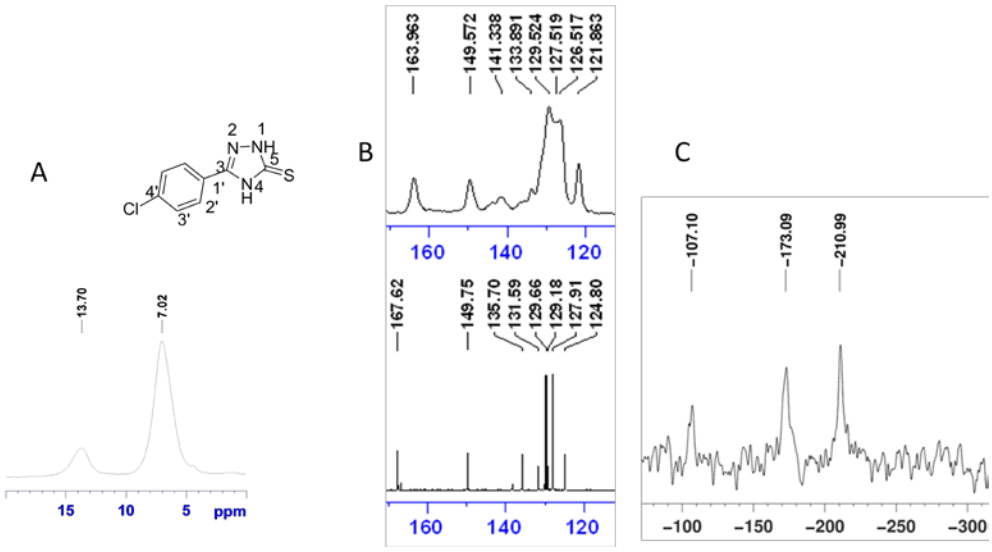

Fig.2B.8: *Solid state NMR spectra of compound 5. A) ^{1}H MAS (700 MHz, spinning speed, ν_r = 40 kHz), B) ^{13}C CP-MAS (75MHz, ν_r= 8 kHz) ; C) ^{15}N CP-MAS (300 MHz, ν_r= 8 kHz). Solution state ^{13}C spectrum (100 MHz) in DMSO is also shown in B (lower trace) for comparison.*

2.7.6 Compound 6: (5-(4-methoxyphenyl)-2,4-dihydro-3H-1,2,4-triazole-3-thione):

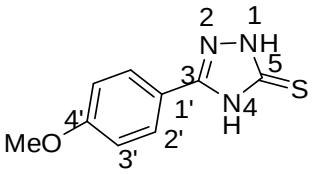

All the types of protons (NH 13.51 ppm, aromatic at ~6.7 and OMe at ~3.8 ppm) are visible in the ^{1}H MAS spectrum (Fig.2B.9A) of compound 6 (*p*-methoxy phenyl thione), though they are not very sharp. As in the case of *p*-Cl derivative (compound 5), the NH protons of compound 6 appear at the same chemical shift even though in solution state they are separated (13.71 and 13.58 ppm). Tautomer 2a (*1H,4H* tautomer) was proposed for this compound as well on the basis of solution state NMR studies.[59] The solid state ^{13}C (Fig.2B.9B) and ^{15}N (Fig.2B.9C) CP-MAS spectra are also in agreement with this.

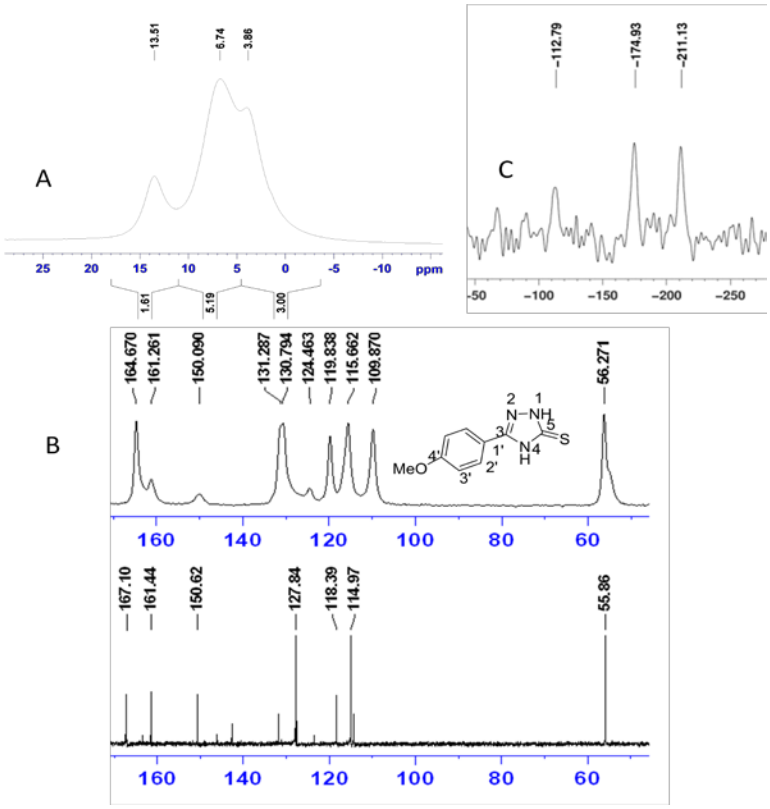

Fig.2B.9: *Solid state NMR spectra of compound 5. A) ^{1}H MAS (300 MHz, spinning speed, ν_r = 30 kHz), B) ^{13}C CP-MAS (176MHz, ν_r= 8 kHz); C) ^{15}N CP-MAS (70 MHz, ν_r = 30 kHz). Solution state ^{13}C spectrum (100 MHz) in DMSO is also shown in B (lower trace) for comparison.*

The reported ^{13}C chemical shifts of this compound for the C3 and C5 are 150.58 and 167.06 ppm in solution state whereas the chemical shifts in the solid state are found to be 150.09 and 161.26 respectively. The ^{15}N CP-MAS spectrum showed three peaks at -174.93, -112.79 and -211.13 ppm for N1, N2 and N4 nitrogens

respectively of the triazole ring, which is in agreement with those observed in solution state (-175.8, -108.9 and -213.4 ppm respectively), except for the effect of solvation in the latter case which is reflected as deshielding of N2.

2.7.7 Compound 7: (5-(4-fluorophenyl)-2,4-dihydro-3H-1,2,4-triazole-3-thione):

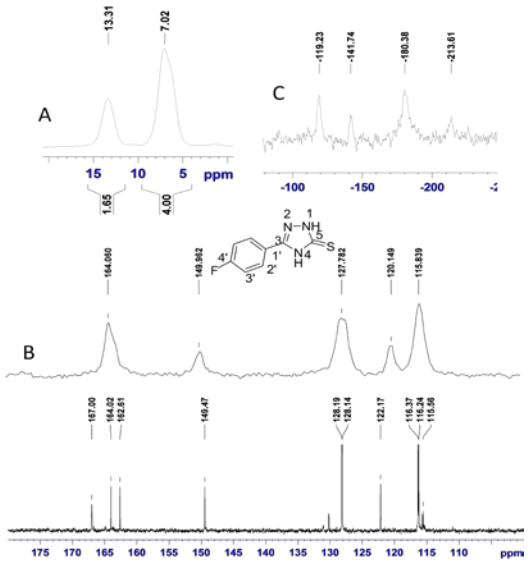

Fig.2B.10: *Solid state NMR spectra of compound 7. A) ^{1}H MAS (700 MHz, spinning speed, ν_r = 40 kHz), B) ^{13}C CP-MAS (176 MHz, ν_r = 8 kHz); C) ^{15}N CP-MAS (40 MHz, ν_r = 8 kHz). Solution state ^{13}C spectrum (176 MHz) in DMSO is also shown in B (lower trace) for comparison. The signal at -141.7 ppm in the ^{15}N spectrum is unidentified and is likely to be from some impurity.*

^{1}H MAS spectrum (Fig.2B.10A) of *p*-F-phenyl thione (compound 7) is very similar to that observed for the previous aromatic derivatives. Both the NH proton appeared at 13.31 ppm while the remaining aromatic protons resonate at 7.02 ppm. It is observed that the ^{13}C signals are broader in the CP-MAS spectrum collected at moderate spinning speed of 8 kHz (Fig.2B.10B) due to residual ^{19}F-^{13}C dipolar

coupling present in the system. In ^{13}C CP-MAS spectrum only the ^{1}H-^{13}C dipolar interactions are killed by high power decoupling of protons.

In the spectrum recorded at lower field and lower spinning speed (8 kHz) more residual ^{19}F-^{13}C dipolar interactions are observed. Fig.2B.11 shows a comparison of ^{13}C CPMAS spectra recorded at two different spinning speeds at two different magnetic fields. Maximum change is seen for the carbons to which the fluorine atom is attached (150-165 ppm). The broadening observed even at high spinning speed (~350 Hz for the most deshielded carbon) is more than the large one bond ^{19}F-^{13}C J- coupling (~250 Hz). The chemical shift of this carbon (~164ppm) is very close to that of the triazole ring C5 (161.26 ppm) carbon. The solution and solid state ^{13}C NMR spectra are compared in Fig.2B.10B and they are found to be very similar.

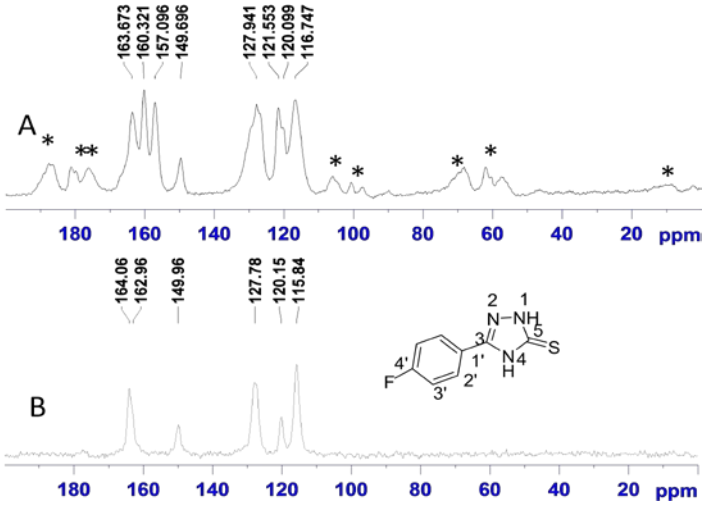

Fig.2B.11: *^{13}C CPMAS spectra of compound 7. A) at 100 MHz, 8kHz and B) at 176 MHz, 40 kHz.*

Chemical shifts of -180.38, -119.23 and -213.61 ppm are observed in the ^{15}N CP-MAS spectrum (Fig.2B.10C) respectively for N1, N2 and N4 nitrogen atoms. The observed chemical shifts favored tautomer 2a. In solution state NMR only the chemical shift of N1 could be obtained (-174.8 ppm).The signal observed at -141.74 ppm seems to be from an unidentified impurity.

2.7.8 Compound 8: 5-(furan-2-yl)-2,4-dihydro-3H-1,2,4-triazole-3-thione:

Solid state NMR spectra of compound 8 are shown in Fig.2B.12. Three protons of the furyl ring appear in the region 6-10 ppm and two NH protons of the triazole ring at ~13 ppm. A weak signal at 16.7 ppm is also noticed which is likely to be from impurity.

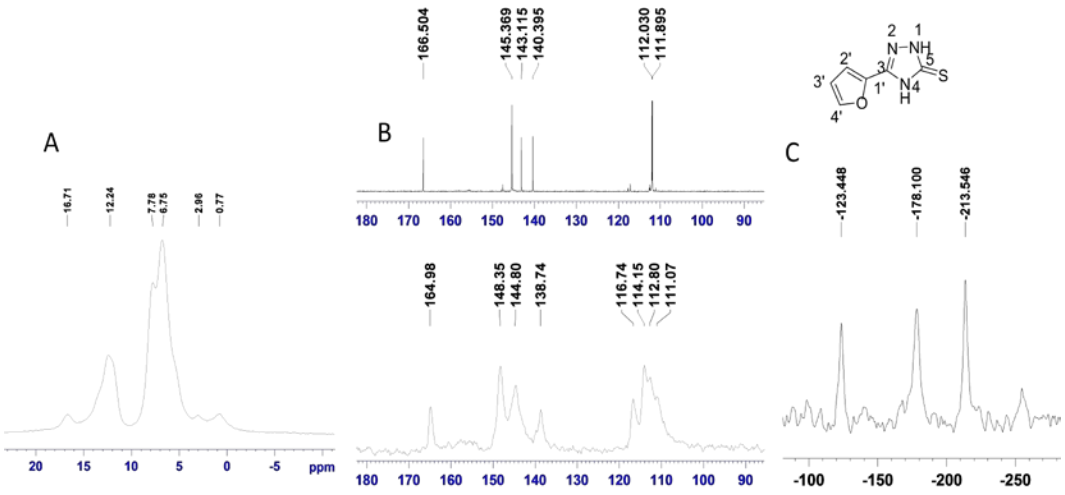

Fig.2B.12: *Solid state NMR spectra of compound 8. A) ^{1}H MAS (700 MHz, spinning speed, ν_r = 40 kHz), B)^{13}C CP-MAS (176MHz, ν_r = 8 kHz); C) ^{15}N CP-MAS (40 MHz, ν_r = 8 kHz). Solution state ^{13}C spectrum (176 MHz) in DMSO is also shown in B (upper trace) for comparison. The signal at -141.7 ppm in the ^{15}N spectrum is unidentified and is likely to be coming from some impurity.*

In compound 8, the carbon resonating at 164.98 ppm corresponds to C5 thione carbon while C-3 resonates at 148.35 ppm in the ^{13}C CP-MAS spectrum (Fig.2B.12B). The other spectral features are found to be very similar to the spectrum in DMSO

except for the broadening noticed for furyl ring carbons (C2, C3') in the 105-120 ppm region due to overlap of signals. The observed features are in line with the presence of 1,4 dihydro tautomer 2a. This is further confirmed by the ^{15}N CP-MAS data which shows signals from N4 and N1 respectively at -213.54 and -178.10 ppm. The sp^2 hybridized N2 nitrogen resonates at -123.44 ppm. The chemical shifts observed in DMSO are -176.1,-109.3 and -214.0 respectively for N1, N2 and N4. This conclusion also matches with thione form reported by Ozturk et al for N-substituted derivatives of compound 8 from single crystal X-ray data.[67]

Thus, all the systems studied show the presence of only one tautomer 2a (1,4-dihydro form) in solid state which is identical to that observed in DMSO solution.

A comparison of the ^{15}N chemical shifts observed in solution and solid state for all the compounds is given in Table 2B.1. A glimpse at the data shows that the chemical shift of N2 is mostly affected on dissolving sample in DMSO. In most of the cases studied N2 experiences shielding in solid state. A possible reason for this is the inter molecular hydrogen bond patterns that are known to alter ^{15}N chemical shifts considerably in solid state. Chemical shifts of a donor NH nitrogen undergo deshieling while that of an acceptor nitrogen, like *sp2* nitrogen, experience shielding effects. Hence, the observed shielding in solid state must be arising from the possibility of N2 forming inter molecular hydrogen bond with proton attached to N1 or N4 nitrogen of other molecules. These type of inter molecular interactions are not present in solution and thus result in deshielding of N2 in solution state. Chemical shifts of N1 and N4, which are good hydrogen bond donors, did not show any appreciable changes in solution and solid state. This is because in solution the solvent used (DMSO) is a good hydrogen bond acceptor and forms hydrogen bonds with N1 and N4 hydrogen atoms. In other words both N1 and N4 have similar hydrogen bonding environments in solids and solutions. In solid state the acceptor is N2 from another molecule while in solution the solvent molecule, DMSO, act as acceptors. Hence their chemical shifts are not perturbed to any great extent.

A comparison of the ^{13}C chemical shifts of the triazole ring carbons of all the compounds is shown in Table 2B.2. Marginal shielding of the thione carbon C5 and

minor deshielding of C3 carbons are noticed in solids. This also likely to be the resultsof inter molecular interactions in solid state.

Table 2B.1: *Comparison of ^{15}N chemical shifts observed in solid and solution state* of all the compounds characterized in this study.

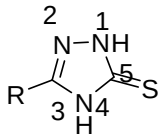

Comp. No R =	δ_{N-2} solid (solution)	δ_{N-1} solid (solution)	δ_{N-4} solid (solution)	$\Delta\delta_{N-2}$ δ solid-δsolution	$\Delta\delta_{N-1}$ δsolid-δsolution	$\Delta\delta_{N-4}$ δsolid-δsolution
1, R= CH_3	-120.00	-177.53	-203.64	-15.30	-0.93	+0.36
	(-104.7)	(-176.6)	(-204)			
2, R= H	-111.81	-174.72	-206.78	-13.61	+0.78	-0.48
	(-98.2)	(-175.5)	(-206.3)			
3, R= t-Bu	-113.09	-178.66	-208.26	-5.39	+0.84	+2.14
	(-107.7)	(-179.5)	(-210.4)			
4, R= Ph	-105.51	-172.28	-210.20	+0.37	+2.62	+2.10
	(-105.88)	(-174.90)	(-212.30)			
5, R= 4-Cl-Ph	-107.10	-173.09	-210.99	-2.8	+1.61	+1.51
	(-104.3)	(-174.7)	(-212.5)			
6, R= 4-OMe-Ph	-112.79	-174.93	-211.13	-3.89	+0.87	+2.27
	(-108.9)	(-175.8)	(-213.4)			

7, R= 4-F-Ph	-119.23	-180.38	-213.61	-	-5.75	-
	-	(-174.63)	-			
8, R= Furyl	-123.44	-178.10	-213.54	-14.14	-2.0	+0.46
	(-109.3)	(-176.1)	(-214.0)			

Table 2B.2: *Comparison of* ^{13}C *chemical shifts observed in solid and solution state* of all the compounds characterized in this study.

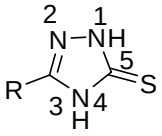

Comp. No R=	δ_{C-5}ppm solid (solution)	δ_{C-3} ppm solid (solution)	ΔδC-5 δsolid- δ solution	Δδ C-3 δsolid- δ solution
1, R= CH_3	165.24	151.52	-1.06	+2.22
	(166.3)	(149.3)		
2, R= H	163.73	142.83	-2.15	+1.94
	(165.88)	(140.89)		
3, R= t-Bu	164.71	162.12	-2.17	+2.17
	(166.88)	(159.95)		
4, R= Ph	163.43	149.62	-4.01	-1.02
	(167.44)	(150.64)		
5, R= 4-Cl-Ph	163.96	149.57	-3.65	-0.17
	(167.61)	(149.74)		
6, R= 4-OMe-Ph	161.26	150.09	-5.80	+-0.49
	(167.06)	(150.58)		
7, R= 4-F-Ph	164.06	149.96	-3.39	+0.49
	(167.45)	(149.47)		

8, R= Furyl	164.98	144.80	-1.52	+1.20
	(166.5)	(143.6)		

2.8 Conclusions: All the substituted triazole thione systems investigated are found to exist in a single tautomeric form 2a, the 1,4 dihydro form and clearly demonstrate that the substituent on triazole ring does not have any bearing on the type of the tautomer present in the solution as well as in the solid state.

References:

[1]. Kruszewski, J.; Krygowski, T. M. *Tetrahedron Lett.* **1972**, 3839.

[2]. Krygowski, T. M. *J. Chem. Inf. Comput. Sci.* **1993**, *33*, 70

[3]. Krygowski, T. M.; Cyran´ ski, M. *Tetrahedron* **1996**, *52*,1713.

[4]. Begtrup, M.; Nielsen, C. J.; Nygaard, L.; Samdal, S.; Sogren, C. E.; Sorensen, G. O. *Acta Chem. Scand. A* **1988**, *42*, 500.

[5]. Catala´n, J.; Sa´nchez-Cabezudo, M.; de Paz, J. L. G.; Elguero, J.; Taft, R. W.; Anvia, F. *J. Comput. Chem.* **1989**, *10*, 426.

[6]. Abboud, J.-L. M.; Foces-Foces, C.; Notario, R.; Trifonov, R. E.; Volovodenko, A. P.; Ostrovskii, V. A.; Alkorta, I.; Elguero, J. *Eur. J. Org. Chem.* **2001**, 3013.

[7]. Murdock, S. E.; Lynden-Bell, R. M.; Kohandoff, J.; Margulis, C. J.; Sexton, G. J. *Phys. Chem. Chem. Phys.* **2002**, *4*, 5288.

[8]. Rauhut, G. *Phys. Chem. Chem. Phys.* **2003**, *5*, 791.

[9]. Claramunt, R. M.; Lo´pez, C.; Garcia, M. A.; Otero, M. D.; Torres,M. R.; Pinilla, E.; Alarco´n, S. H.; Alkorta, I.; Elguero, J. *New J.Chem.* **2001**, *25*, 1061.

[10]. P. Goldstein, J.Ladell and G. Abowitz *Acta Cryst.* (1969). B25, 135.

[11]. Abboud, J.-L. M.; Cabildo, P.; Canada, T.; Catalan, J.; Claramunt, R. M.; de Paz, J. L. G.; Elguero, J.; Homan, H.; Notario, R.; Toiron, C.; Yranzo, G. I. *J. Org. Chem.* **1992**, *57*, 3938.

[12]. Oziminski, W. P.; Dobrowolski, J. Cz.; Mazurek, A. P. *J. Mol. Struct.* **2003**, *651-653*, 697.

[13] [1] (a) Husain, M. I.; Amir, M. J *Indian Chem Soc* **1986**, *63*, 317;
(b) Chiu, S.H. L.; Huskey, S.E. W. *Drug Metabol Dispos* **1998**, *26*, 838;
(c) Sahin, G.; Palaska, E.; Kelicen, P.; Demirdamar, R.; Altmok, G. *Arzneim Forsch* **2001**, *51*, 478;
(d) Al-Soud, Y. A.; Al-Dweri, M. N.; Al-Masoudi, N. A. *Il Farmaco* **2004**, 59, 775;
(e) Mekuskiene, G.; Gaidelis, P.; Vainilavicius, P. *Pharmazie* **1998**, *53*, 94;
(f) Papakonstantinou-Garoufalias, S. S.; Tani, E.; Todoulou, O.; Papadaki-Valiraki, A.; Filippatos, E.; De Clercq, E.; Kourounakis, P. N. *J Pharm Pharmacol* **1998**, *50*, 117;
(g) Bashir, Y.; Kann, M.; Stradling, J. R. *Pulm Pharmacol* **1990**, *3*, 151;
(h) Dogan, H. N.; Rollas, S.; Erdeniz, H. Il *Farmaco* **1998**, *53*, 462;
(i) Mohd, A.; Kumar, S. *Eur J Med Chem* **2004**, *39*, 535;
(j) Palaska, E.; Sahin, G.; Kelicen, P.; Durlu, N. T.; Altinok, G. *Il Farmaco* .**2002**, *57*, 101.
[14]. Kalyoncuoğlu, N.; Rollas, S.; Sür-Altiner, D.; Yegenoğlu, Y.; Anğ, Ö. *Pharmazie* .**1992**, *47*, 796.
[15]. Rollas, S.; Kalyoncuoğlu, N.; Sür-Altiner, D.; Yegenoğlu, Y. *Pharmazie.* **1993**, *48*, 308.

[16] Kubota, S.; and Uda, M. *Chem. Pharm. Bull*. **1973**, *21*, 6, 1342.

[17] Elhajji, A.; Ouijja, N.; Idrissi, M.S.;and Garrigou-Lagrange, C. *Spectrochim. Acta, Part A,* **1997**, *53*, 5, 699.

[18] Krishnakumar, V.; and Xavier, R.J.; *Spectrochim. Acta, Part A,* **2004**, *60*, 3, 709.
[19] Shklyarenko, A.A.; Nasledov, D.G.; and Yakovlev, V.V., *Zh. Org. Khim.*, **2005**,*41*, 4, 636.
[20] Mosselhi, M.A.N.;Abdallah, M.A.; Riyadh, S.M.; Harhash, A.E.;and Shawali, A.S., *J. Prakt. Chem.–Chem.-Ztg*., **1998**, *340*, 2,160.

[21] Buzykin,B.I.; Mironova,E.V.; Gubaidullin,A.T.; LitvinovI.A.; and V. N. Nabiullin *Russian Journal of General Chemistry*, **2008**,*78*, 4,634.

[22] Kurzer, F., *J. Chem. Soc. C*, **1970**, *13*, 1805.

[23] Hoggarth, E., *J. Chem. Soc.*, **1949** , *5*, 1160.

[24] Blacman, A.J.; and Polya, J.B., *J. Chem. Soc. C*, **1971**, *5*, 1016.

[25] Kane, J.M.; Dudley, M.W; Sorensen, S.M.;and Miller, F.P. *J. Med. Chem.*, **1988**,*31*, 6, 1253.

[26]. Raper, E. S. *Coord Chem Rev* **1996**, *153*, 199;

[27] (a) Raper, E. S. *Coord Chem Rev* **1994**, *129*, 91; (b) Creighton, J. R.; Gardiner, D. J.; Gorvin, A.C.; Gutteridge, C.; Jackson, A. R. W.; Raper, E. S.; Sherwood, P. M. A. *Inorg Chim Acta* .**1985**, *103*, 195; (c) Oughtred, R. E.; Raper, E. S.; Nowell, I. W. *Acta Crystallogr, Sect C*: *Cryst Struct Commun* **1985**, *41*, 758; (d) Atkinson, E. R.; Gardiner, D. J.; Jackson, A. R. W.; Raper, E. S. *Inorg Chim Acta* **1985**, *98*, 35; (e) Turan-Zitouni, G.; Kaplancikli, Z. A.; Erol, K.; Kilic¸, F. S. *Il Farmaco* **1999**, *54*, 218; (f) Roy, G.; Mugesh, G. *J Am Chem Soc* **2005**, *127*, 15207; (g) Roy, G.; Das, D.; Mugesh, G. *Inorg Chim Acta* **2007**, *360*, 303; (h) Coyanis, E. M.; Della Vedova, C. O.; Haas, A.; Winter, M. *J Fluorine Chem* **2002**, *117*, 185.

[28]. Abbe,G.L, Toppet,S., Willcox ,A., andMathys, G., *J. Heterocyclic Chem.*, **1977,** *14*, 1417.

[29]. CoxJ.R.,Woodcock S., Hillier I.H., Vincent M.A., *J. Phys. Chem.* **1990**, *94* 5499.

[30] Ramondo.; Bencivenni L.; Portalone G., *A. Domenicano, Struct. Chem.* **1994**, *5*, 1.

[31] ClaramuntR. C.; Elguero J.; KatritzkyA. R. *Adv. Heterocycl. Chem.* **2000**, *77*, 1.

[32]. .Landry V.K.; Minoura M.; Pang K.; Buccella D.; Kelly BV, Parkin G. *J. Am. Chem. Soc.* **2006**, *128:* 12490.

[33]. a) Rollas S.; Kalyoncuoglu N; Altiner D. S.; Yegenoglu Y. *Pharmazie* **1993**,*48*,308; b) Sumanand S. P.; Bahel S. C. *J. Indian Chem. SOC.* **1980**, *57*, 420 ; c) Svanholm U. *Acta Chim. Scand.* **1972**, *26*,459; d) Blackman A. J.; Polya J. B. *J. Chem. SOC. C* **1971**, 1016.

[34]. Blackman A. J.; PolyaJ. B. *J. Chem. SOC.* **1971**, 1016.

[35]. a) Muhi-Eldeen Z.; Al-Obaidi K.; Nair M.; RocheV. F.*Eur. J. Med. Chem*. **1992**,*27*,101; b) Mishra R. K.,R; Tewari K.; Srivastava S. K.; Bahl S.C. *ibid*.**1991**, *68*, 110; c) Tandom .; Barthwal J. B.; Bhalla T. M.,;Bhargava K.P.*Indian J. Chem*. **1981**, *20B*, 1017; d) Singh G.; Yadav L. D. S.; , Bhattacharya B. K. *I. Indian Chem. SOC.* **1979**, *56*, 1013.

[36].Varynskyi B. A.; Scherback M. A.; Kaplaushenko A. G.; and Yurchenko I. A. *Journal of Chemical and Pharmaceutical Research*. **2014**, *6*,1342.

[37]. Zelenin K. N.; Kuznetsova O. B.; Alekseyev V. V. *Tetrahedron.* **1993**, *49*, 1257.

[38]. Kubota S.; and Uda M. *chem. Pharm. Bull*. **1973**, *21*, 1342.

[39]. HogsTarth E. *f .Chem. Soe*.**1949**, 1918.

[40]. Fun H. K.; Quah C. K.; Nithinchandra and Kalluraya B. *Acta. Cryst.* **2011**, *E67*, 02413.

[41]. Zhang L.; Zhang A.; Lei L.; Zou K.,*Acta Cryst* .**2004**, *E60*, 0613.

[42] Sarala G.; Sridhar M.A.; Shashidhara P. *Mol. Cryst. Liq. Cryst.* **2006**, *457*, 215.

[43].Sarala G.; Sridhar M. A.; Shashidhara P. *Mol. Cryst. Liq. Cryst.* **2006**, *457*, 215.

[44]. Buzykin B. I,; Mironova E. V;,Gubaidullin A. T.; Litvinov A. I.; and Nabiullin V. N. *Russian Journal of General Chemistry.* **2008**, *78*, 634.

[45]. Siwek, M.; Wujec, I. ;Wawrzycka-Gorczyca, M.; Dobosz.; and P. Paneth, *Heteroatom Chem*. **2008**, 19, 337.

[46]. Ahmet Cansiz.;Ahmet Centin.;Pelin Kutulay.; and Metin Koparir. *Asian Journal of Chemistry*. 2009,21, 617.

[47]. Kapkan, L et al. Theor. Exp. Chem **1989**,25, 338.

[48]: Siwek A.;Wujec M.; Stefańska J.; Paneth P. *Phosphorus, Sulfur, and Silicon* **2009**, *184*, 3149.

[49]. Siwek A.,Wujec M.; Wawrzycka-Gorczyca I.; Dobosz M.; and Paneth P. *Heteroatom*

Chem. **2008**, *19***,** 337.

[50]. Mosselhi, M.A.N.; Abdallah, M.A.; Riyadh, S.M.; Harhash, A.E.; and Shawali, A.S. *J. Prakt. Chem.–Chem.-Ztg.*, **1998,** *340*, 160.

[51]. Peng-Fei Xu.; Xiao-Wen Su.; Lin-Mei Zhang.; and Zi-Yi Zhang . *J. Chem. Research (S)*,**1999**, 170.

[52]. Iqbal R.; Rama NH.; Yunus U.; Saeed .; Zamani K. *J Chem Soc Pak* **1997**,*19*,145.

[53]. Siwek A.; Wujec M.; Wawrzycka-Gorczyca I.; Dobosz M.; and Paneth M. *Heteroatom Chem.* **2008**,*19*, 337.

[54] Siwek A.; Stefanska A.; Wawrzycka-Gorczyca I.; and Wujec M. *Heteroatom Chemistry* **2010**, *21*, 131.

[55].Isaacs N. W.; and Kennard C. H. L.Chemical Comunication.**1970**, *631*.

[56] Siwek, A.; Wujec, M.; Wawrzycka-Gorczyca, I.; Dobosz, M.; Paneth, P. *Heteroatom Chem* **2008**, *19*, 337.

[57]. Siwek A.; Wujec M.; Dobosz M.; and Paneth P. *Heteroatom Chemistry* **2008**, *19*, 713.

[58]. Vasile-Niclae Bercean.; Creanga .A.A.;Badeal.V.; Calin Deleanu.*; Carol Csunderlik Rev*. (*Bucharest)*, **2011**,*62*, 1, 47.

[59]. Chaudhary.; Chavan S. R.; Kavitha M.; Maybhate S. P.; Deshpande S. R.; Likhite A. P.; and Rajamohanan P .R. *Magn. Reson. Chem.* **2008**, *46*, 1168.

[60]. Sarkar D.; Deshpande S. R.; Maybhate S. P.; Likhite A. P.; Sarkar S.; Khan A.; Chaudhry P. M.; Chavan S. R. *International publication numbe*r WO 2011/111077 A1 and PCT/IN2011/000172.

[61]. Phalgune U. D.; Vanka K.; and Rajamohanan P. R.; *Magn. Reson. Chem*. **2013**, *51*, 767.

[62] Gökce H.; Öztürk N.; Ceylan U.; Alpaslan Y. B. *Gökhan Alpasln Spectrochimica Acta Part* : *Molecular and Biomolecular Spectroscopy* **2016** ,*163*,170.

[63]. El Sayed H.; El Ashry.; El Sayed H.; El Tamany, Mohy El Din Abd El Fattah.; Ahmed T.A. Boraei.; Heba M.; Abd El-Nabi .*European Journal of Medicinal Chemistry* .**2013**,*66* ,106.

[64]. Kolehmainen.E. and Os´mialowski.B. *International Reviews in Physical Chemistry* **2012**, *31*, 4, 567.

[65]. Koparır M.; Çetin A; and*. Cansız* A.*; Molecules* **2005**, *10*, 475.

[66]. Muhi-Eldeen Z.; K Al-Obaidi.; M Nadir. Roche, vf. *Eur. J. Med. Chem*. **1992**, *27*, 101.

[67].Ozturk S.; Akkurt, M.; Cansiz, A.; Koparir, M.; Sekerci, M.; Heinemann, F.W. *Acta Cryst* **2004**, E60, O425.

CHAPTER III

Tautomerism in disubstituted sulfanyl 1,2,4-triazoles in solution and solid state

3.1 Introduction:

Many of the 1,2,4-triazole derivatives show antibacterial activities [1] and also act as GLS1 inhibitors. They are useful for treatment of cancer and immunological and neurological disorders.[2,3] Sulfanyl derivatives of triazoles posses wide variety of applications such as herbicides, fungicides, plant growth regulators, dyes, and medical agents.[4-6]. They find applications in treatment of psychological imbalance [7], in agriculture [8, 9], as metal chelating agents [10, 11], in antitubercular drugs [12, 13], antimicrobial [14], antiphlogistic [15], antiarthritic [16], antimycotic [17], anti-HIV [18], and inhibitors of matrix metalloprotease [19] etc. These systems also exhibit tautomerism. Compared to their parent compounds (1,2,4 triazole thiones), the number of tautomers reduces to three when the sulphur atom is substituted (Scheme.3.1). Various methods such as spectroscopic techniques, crystallography and theoretical calculations have been used to study the phenomenon of tautomerism in these types of compounds as in the case of triazole thiones.

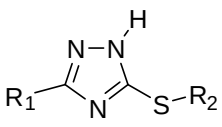

N1-H

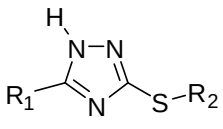

N2-H

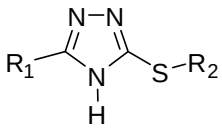

N4-H

Scheme.3.1 : Tautomers of substituted sulfanyl 1,2,4 traizoles.

Kalman *et al.* reported X-ray structures of a few disubstituted sulfanyl derivatives of 1,2,4 triazoles, (compound 1, Scheme.3.2) and found that the nature of tautomer depend on the nature of substituent.[20] Siedle *et al*. reported X-ray structure of a symmetrically substituted tautomer of the 1,2,4-triazole (compound 2 in Scheme.3.2).[21] Chaudhary *et al*. reported the possibility of coexistence of *N1-H* and *N2-H* tautomers in equilibrium in the solution state by NMR spectroscopic techniques.[22] Phalgune *et al.* calculated the theoretical chemical shifts for the different tautomers and compared it with the experimental chemical shifts and found that the free energy difference between *N1-H* and *N2-H* tautomers is very less.[23] Buzykin *et al.*, on the basis of single crystal X-ray spectroscopy, found that 3-butylsulfanyl-5-methyl-1,2,4-triazole (compound 4, Scheme.3.2) is present in the 1*H*-tautomeric form in solid state. He also found that 3-butylsulfanyl-5-phenyl-1,2,4-triazole (compound 5, Scheme.3.2) crystallizes in the 1*H*-tautomeric form and two different tautomers are present in the same crystal.[24]

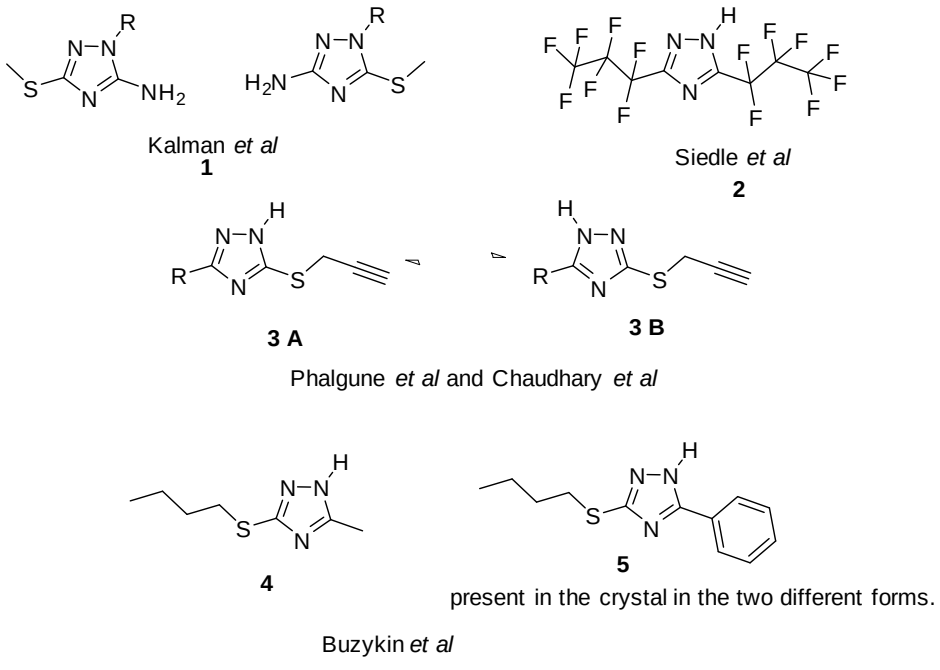

Scheme.3.2: *Some of the reported tautomers of sulfanyl 1,2,4 triazoles.*

Even with the advancement in the analytical techniques, characterization of tautomers in 1,2,4-triazole derivatives in solution state poses difficulty due to inherent problem of dynamics associated with it.[25-31] Many authors claimed the presence of *N1-H* or *N2-H* tautomer [22, 23] while few other reports suggested the existence *N4-H* tautomeric form also.[32, 33].

X-ray spectroscopy is one of the best methods available to study tautomerism in sulfanyl 1,2,4-triazoles and has been extensively used to study single crystals of triazoles derivatives. Buzykin *et al.* [34] investigated many sulfanyl 1,2,4-triazoles by single crystal X-ray [35-51] and proposed that the nature of the tautomer present depends on the electron withdrawing and donating nature of the substituents. According to them the proton always prefer the nitrogen atom which is either relatively far from the electron withdrawing group or close to the electron donating substituent of the 1,2,4-triazole ring. The electron withdrawing or donating nature of the substituents can be found in terms of the Taft constants which are available in the literature for large number of substituents and can also be calculated for any substituent from the known values of the other substituent.[52, 53]

3.2 Nomenclature:

The IUPAC nomenclature of methyl substituted sulfanyl triazole with numbering is given in Scheme.3.3. It is noticed that the numbering scheme is different for the tautomers 3a/3c and 3b and, therefore, the numbering becomes more cumbersome when the *C* and *S* atoms in the triazole rings are substituted. Thus, three names, as shown in Scheme.3.3, are possible for the *C*,*S*-dimethyl derivative of triazole thione tautomers.

Scheme.3.3: *IUPAC nomenclature of dimethyl substituted sulfanyl triazole with numbering.*

NMR spectroscopy is one of the best methods available to study tautomerism in solution and solid state. Therefore, approaches based on NMR spectroscopic techniques have been employed to study tautomerism in solid and solution state for a few disubstitued sulfanyl 1,2,4 triazoles as shown in the Scheme.3A.1. In this study, for clarity, we will be following the numbering of atoms as shown in Scheme.3A.1. This approach keeps the same numbering for a particular atom present in the different tautomers. This is very useful when a comparison of chemical shifts of various nuclei from different tautomers is made for identification of a particular tautomer present in the system. The problem of tautomerism in various *S* and *C* disubstituted 1,2,4-triazoles are addressed here with the help of solution and solid state ^{1}H,^{13}C and ^{15}N NMR studies. This chapter is divided in to two sections depending on the mode of investigation. Section A describes solution state NMR studies while section B is devoted to solid state NMR studies.

3.3 Experimental:

NMR experimental conditions are same as described in Chapter II and therefore it is not repeated here.

3.4 Part A: Tautomerism in disubstituted sulfanyl 1,2,4-triazole derivatives in solution state

Scheme.3A.1: *Tautomers of C, S-disubstituted derivatives of 1,2,4-triazoles*.

Three tautomers, as shown in Scheme.3A.1, are possible for the *S* and *C*-disubstituted triazoles studied here. In previous reports it was observed that *S*-substituted 1,2,4-triazoles exists in equilibrium between tautomer 3a (*N1-H*) and 3b (*N2-H*) forms since the 3c (*N4-H* form) type of tautomer is unstable.[22,23] Tautomer 3c is not favoured due to the presence of two C=N groups attached to two adjacent nitrogen atoms of the five membered ring ("α-diaza effect").[54] Some of the crystal data showed the presence of 3b type of tautomer.[34] Even theoretical calculations showed very less difference in the free energies of 3a and 3b [22] tautomers (Chapter V). In general, the nature of the tautomer present in these types of compounds is more ambiguous than in the case of corresponding thiones, discussed in Chapter II. Hence, in the present work a detailed investigation on these systems is carried out to obtain more insight into the tautomeric processes and their dynamic nature. Six sulfanyl derivatives of 1,2,4 triazole have been investigated in DMSO-d_6 and the results of these studies are given below.

3.4.1 Compound 1a: *p*-Nitrophenyl,*SO*$_2$-propargyl 1,2,4 triazole.

Proton NMR spectrum (Fig.3A.1) of compound 3a (*p* NO_2Ph, *SO*$_2$-propargyl) showed only one downfield signal resonating at 15.67 ppm corresponding to the NH of the 1,2,4-triazole ring indicating that only one tautomeric form is present in this system. However, the ^{1}H spectrum is found to be unexpectedly broad given the size of the molecule. The

methylene protons attached to the sulfone group resonate at 4.32 ppm as an AB quartet. Aromatic protons of the nitro phenyl moiety appear in the region 8.2-8.5 ppm.

NOSEY spectrum shown in Fig.3A.2A shows both positive and negative cross peaks. Strong positive cross peak is noticed between the NH and trace amounts of water present in the solvent (at 3.37 ppm). Negative cross peaks originating from nOe contacts provide structural details. The NH signal shows negative cross peak with shielded aromatic protons (8.28 ppm, 2'H, Fig.3A.2B), which also confirms its assignment as those *meta* to the NO_2 group. This in turn means that the NH proton is close to the

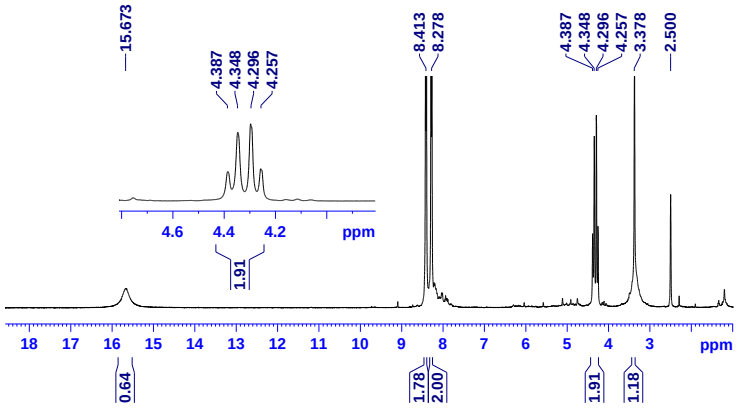

Fig.3A.1: *^{1}H NMR spectrum of compound 1a. (400 MHz, DMSO-d_6, 298 K)*

aromatic ring attached to C3 carbon of triazole ring and suggests the presence of tautomeric form 3b (Scheme.3A.1). A negative cross peak of the same 2'H aromatic protons is also noticed either with water molecule or with propargyl CH proton, which could not be differentiated due to chemical shift overlap at 3.38 ppm (Fig.3.2C). It is also interesting to note that the NH proton does not show detectable cross peak with the sulfone CH_2 group (4.25 -4.38 ppm) which is attached to C5 of triazole ring.

^{13}C NMR spectrum of this compound is found to be very broad, especially the signals associated with carbons on the triazole ring (C-3, C-5) and one of the quaternary carbons (C-1') of the aromatic ring. Fig.3A.3 shows a comparison of the ^{1}H decoupled ^{13}C spectrum and DEPT 135 spectrum. It is interesting to note that the CH carbon of the propargyl group (79.39 ppm) does not appear properly in the DEPT spectrum.

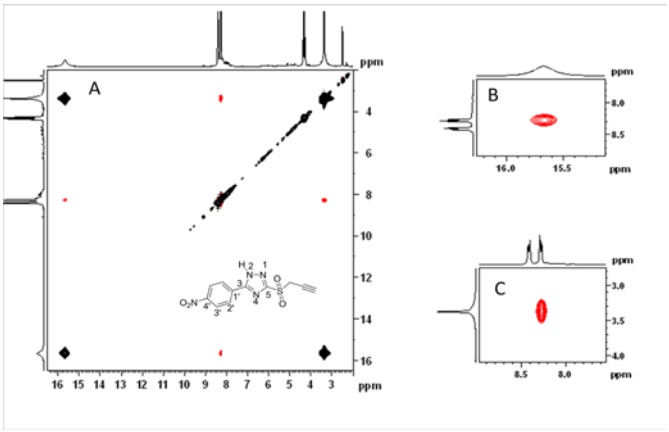

Fig.3A.2: *NOESY spectrum (400 MHz, DMSO-d_6, 298 K) of compound 1a. (400 MHz, DMSO-d_6, 298 K): A) Full NOESY spectrum. B) nOe cross peak of NH with 2'H proton c) nOe of 2' with the signal at 3.78 ppm (possibly from moisture). Negative and positive cross peaks are differentiated by red and black colour, respectively.*

This is due to the fact that the $^{1}J_{CH}$ of this carbon is ~250 Hz while the polarization transfer delay of 1/2J employed during the experiment corresponds to $^{1}J_{CH}$ of 150 Hz. Similarly, the quaternary carbon of the propargyl group does not vanish completely in the DEPT spectrum since the $^{2}J_{CH}$ for *sp* carbon is ~50 Hz. Assignments of some of the carbons were achieved from the analysis of ^{1}H-^{13}C HSQC and HMBC spectra shown in Fig.3A.4. Both carbons of the propargyl group show cross peaks in the HSQC spectrum though one of them is quaternary in nature due to non ideal polarization transfer delay time employed as in the DEPT experiment. ^{1}H-^{13}C HMBC experiment could not show expected correlations for the triazole ring carbons, though the signals from the *para* nitro moiety could be assigned. This is due to loss of signals during the polarization transfer delay (1/2J, J=7 Hz) employed as a result of some dynamic events present in the system.

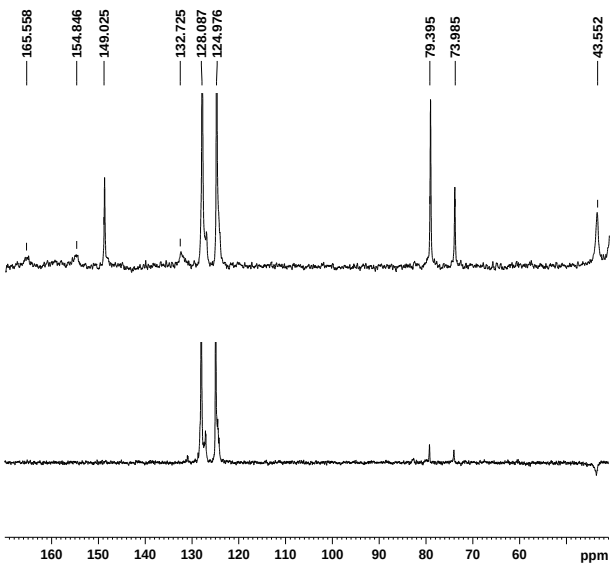

Fig.3A.3: *Comparison of the ^{13}C DEPT (lower) and ^{1}H decoupled ^{13}C spectra (upper) of compound 1a (100 MHz, DMSO-d_6, 298 K).*

Hence, the assignments of triazole ring carbons are tentative. The assignments are presented in Table 3A.1. The most striking feature of the ^{13}C NMR spectrum is the broadness associated with the triazole carbons (C3, C5) and the aromatic quaternary carbon (C1') to which the triazole moiety is attached. This definitely suggests some kind of slow dynamics associated with triazole ring. The most likely possibility is the dynamics between the two tautomeric forms 3a and 3b (Scheme.3A.1) where the NH proton hops between N1 and N2. The result of this exchange is reflected as broadness in the ^{1}H and ^{13}C NMR spectra, the latter seems to be more affected. This is further supported by the fact that the ^{1}H-^{15}N HSQC fails to show any cross peak due loss of signals during polarization transfer delay. In this case one has to consider the dynamics of NH proton with water molecules which can also contribute to the poor HSQC response.

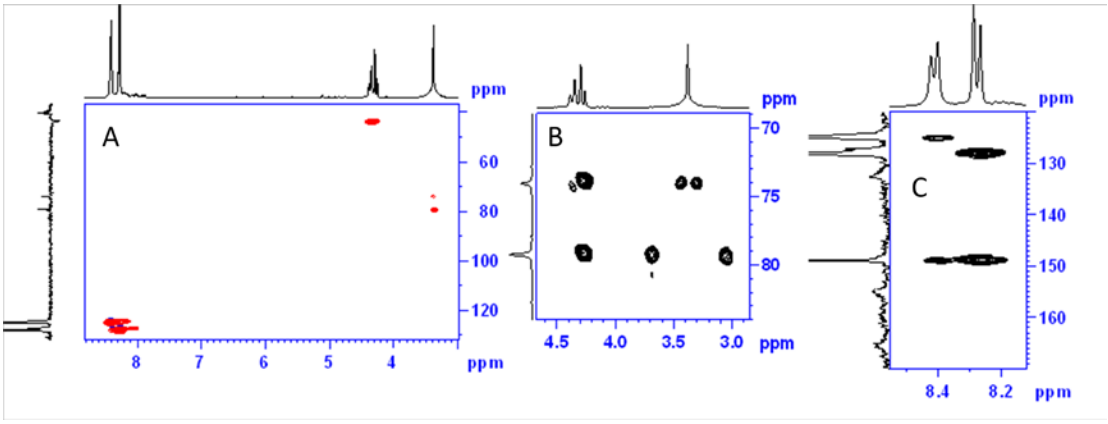

Fig.3A.4: *^{1}H-^{13}C HSQC (A) and HMBC (B,C) correlations of sample 1a. Only expanded HMBC spectrum showing correlations of propargyl groups (B) and aromatic protons (C) are shown.*

Table 3A.1: *Chemical shift Assignments of compound 1a.*

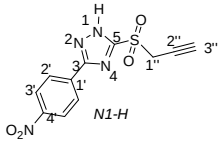

Atom	Chemical Shift (ppm)	Atom	Chemical Shift (ppm)
1	-	1’	δ_C 132.14
2	δ_H 15.67	2’	δ_C 127.61
3	δ_C 154.44	3’	δ_C 124.53
4	-	4’	δ_C 148.52
5	δ_C 165.09	1’’	δ_H 4.32 δ_C 43.15
		2’’	δ_C 73.59
		3’’	δ_H 3.38 δ_C 79.39

3.4.2 Compound 1b: p-Nitrophenyl, S-propargyl 1,2,4 triazole

Proton and the ^{13}C NMR spectra of *p*-nitrophenyl *S*-propargyl sulfanyl triazole compound (Fig.3A.5 and 6) show that their features are very similar to that of compound 1a except for the chemical shift change of propargyl CH_2 protons and carbon, which are more shielded in the present case. Triazole carbon signals (C3, C5) are broad and indicate dynamics involving them.

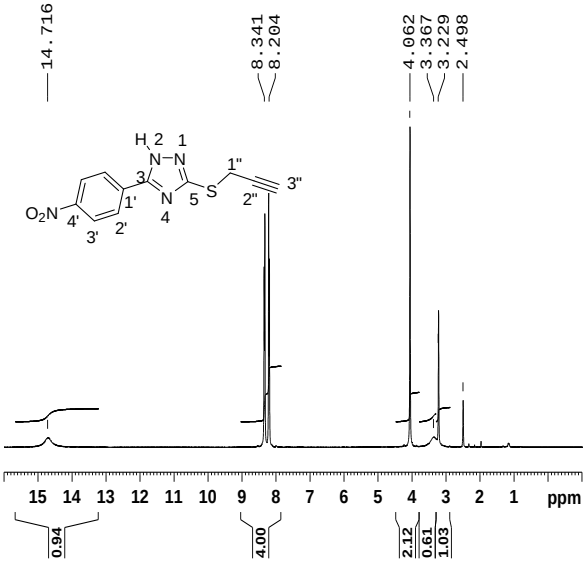

Fig.3A.5: *^{1}H NMR spectrum of compound 1b (400 MHz, DMSO-d_6, 298 K).*

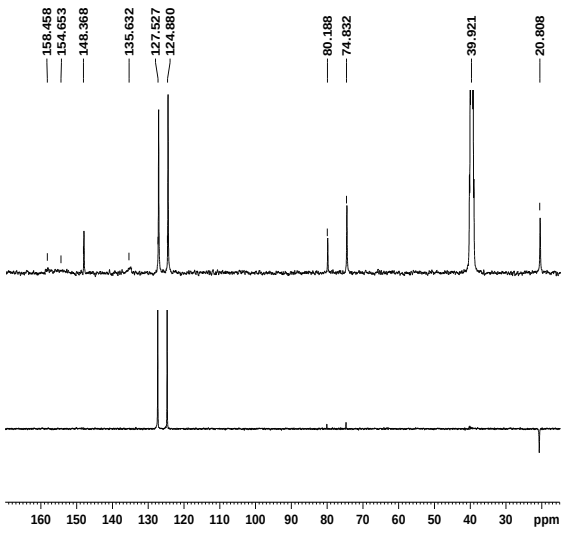

Fig.3A.6: *Comparison of t ^{13}C DEPT (lower) and ^{1}H decoupled ^{13}C spectrum (upper) of compound 1b (100 MHz, DMSO-d_6, 298 K).*

A combination of HSQC and HMBC spectra (Fig.3A.7) was helpful in obtaining assignments of various carbons and protons. Besides, ^{1}H-^{15}N HSQC did not show any cross peaks due to faster decay of signal during the polarization transfer delay employed.

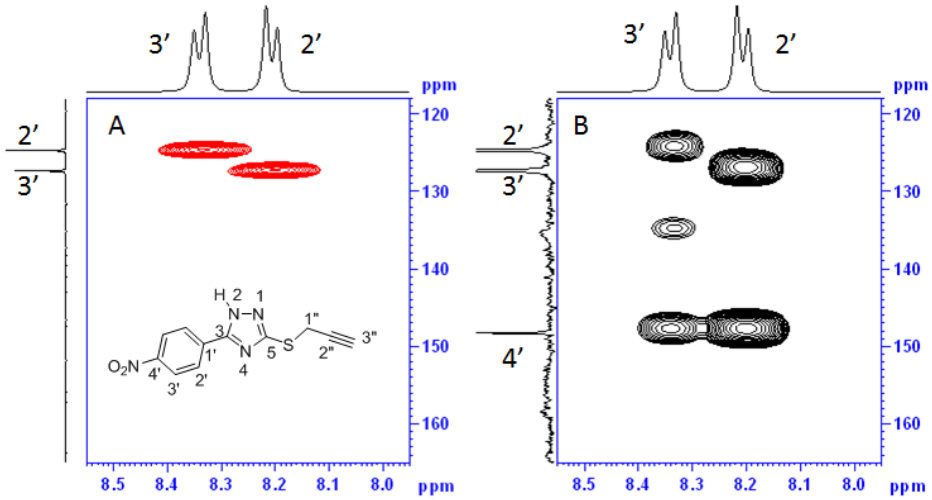

Fig.3A.7: *^{1}H-^{13}C HSQC (A) and HMBC (B) correlations of 1b: Only expanded HMBC spectrum showing correlations of aromatic protons and propargyl groups are shown.*

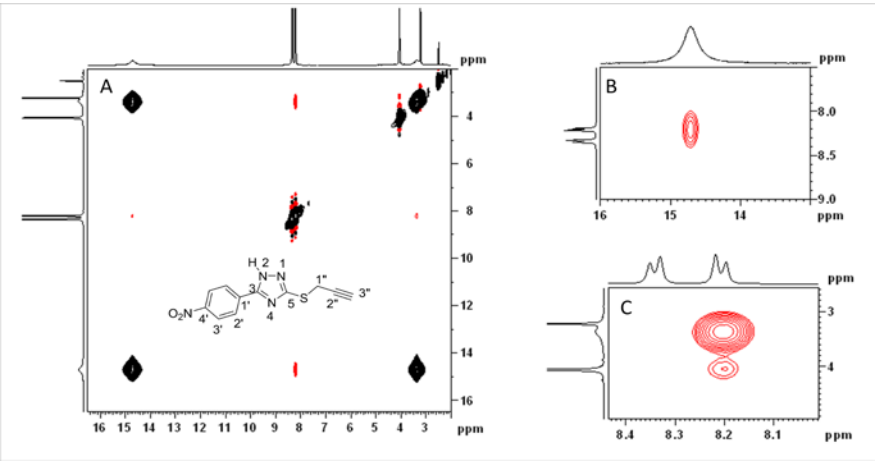

Fig.3A.8: *NOESY NMR spectrum (A) of compound 1b. (400 MHz, DMSO-d_6, 298 K). Negative and positive cross peaks are differentiated by red and black color, respectively. Expanded plots show nOe of aromatic protons to NH (B) and water, CH_2 protons (C).*

NOESY spectrum in DMSO is presented in Fig.3A.8 and shows the presence of exchange cross peak (strong and positive) for NH with water and negative nOe cross peak with shielded aromatic proton (H2', 8.20 ppm). These aromatic protons are closer to triazole rings and also shows weak nOe to the propargyl CH_2 protons (4.06 ppm) and a relatively strong nOe cross peak with water at 3.37 ppm (Fig.3A.8C). The latter cross peak indicates proximity of water molecule to aromatic ring/triazole moiety.

It is observed that the nature of ^{1}H spectrum changes with time. Fig.3A.9 shows a comparison of ^{1}H spectra recorded immediately after preparation of the solution and after about a week. Triazole NH peak splits into two signals of unequal intensity (~ 60:40 ratio appearing at 14.58 and 14.96 ppm, respectively) accompanied by broadening of one set of deshielded aromatic protons (8.34 ppm, H3') and the propargyl proton signals (4.06, 3.23 ppm). Narrowing of the deshielded NH proton and water signals (3.38 ppm) indicates slowing down of the dynamics which is also evident from the observation of ^{1}H-^{15}N HSQC cross peaks (Fig.3A.10). The major cross peak has a ^{15}N chemical shift of -165.89 ppm and shows correlation with the proton resonating at 14.58 ppm while the nitrogen chemical shift of the minor NH is -170.3 ppm.

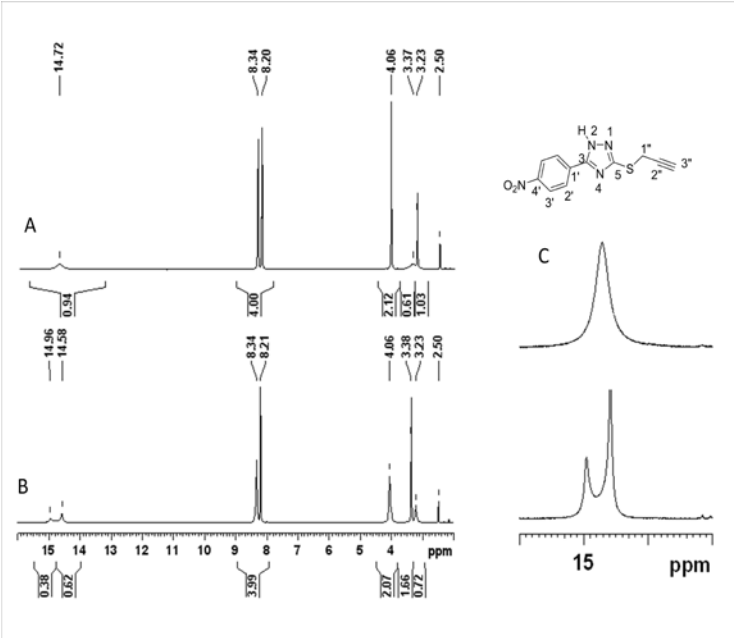

Fig.3A.9: *^{1}H NMR spectrum of compound 1b recorded at two time intervals. Immediately after preparation (A) and after one week (B). Expanded plot of NH region is also shown. (400 MHz, DMSO-d_6, 298 K)*

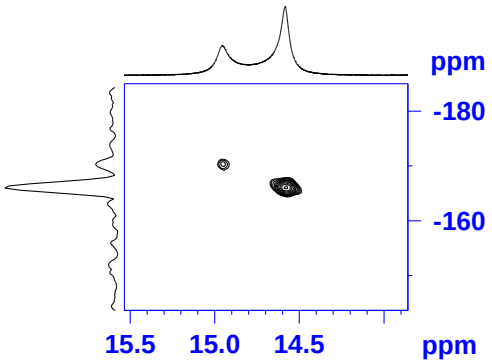

Fig.3A.10: *^{1}H-^{15}N HSQC spectrum of compound 1b obtained after ~ one week of aging, (40 MHz, DMSO-d_6, 298 K).*

The NH signal in the ^{1}H spectrum further broadened with time as shown in Fig.3A.11, though two environments are still present. Another noticeable observation is the relative content of the water molecules present, which is quite high in the spectrum recorded after three months of sample preparation. This is likely to be due to absorption of water molecules arising from exposure of the sample to the environment. Further, the

broadening of NH peaks may be resulting from their chemical exchange with a large pool of water. Nevertheless, the ^{13}C spectrum recorded for this sample is very similar to the freshly prepared sample with some additional broadening of the propargyl carbon signals at 79.9, 74.6 and 20.6 ppm (Fig.3A.12).

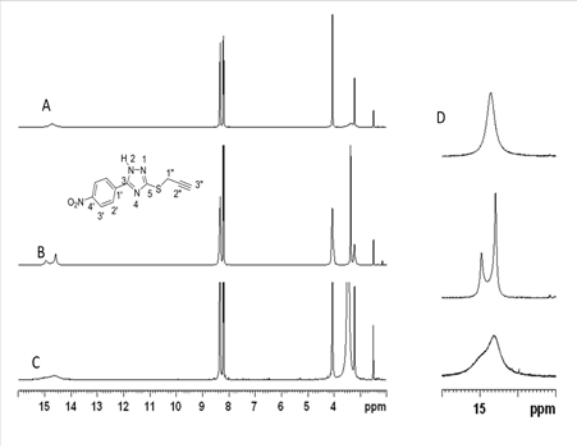

Fig.3A.11: *^{1}H NMR of the compound 1b. A) freshly prepared; B) after one week and C) after ~ 3 months. (400MHz, DMSO-d_6, 298 K) D) Expanded plot of NH region.*

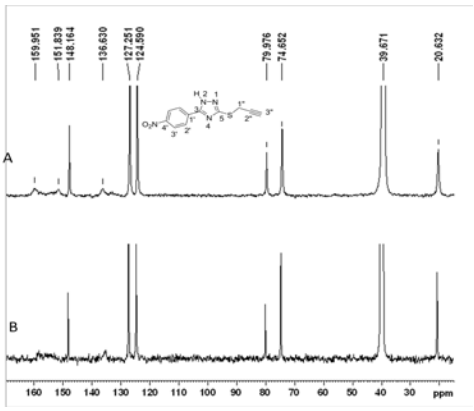

Fig.3A.12: *^{13}C NMR of compound 1b. A) freshly prepared B) recorded after ~ 3months, (100 MHz, DMSO-d_6, 298 K).*

These observations clearly demonstrate the existence of a dynamic equilibrium probably involving different tautomers in DMSO solution. It is not very clear whether

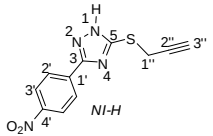

water molecules play a role, however the nOe cross peaks observed with aromatic protons do suggest the proximity of water molecules to the triazole ring. It is interesting to note that such time dependent spectral behavior was not noticed for thione systems discussed in Chapter II. Based on these observations, the presence of two species, probably two tautomers (3a and 3b, Scheme.3A.1) can be envisaged. The chemical shift assignments are tabulated in Table 3A.2.

Table 3A.2: *Chemical shift Assignments of compound 1b.*

Atom	Chemical Shift (ppm)	Atom	Chemical Shift (ppm)
1	-	1’	δ_C 135.3
2	δ_H 14.58 δ_N -165.89	2’	δ_H 8.2 δ_C 126.93
3	δ_C 151.9	3’	δ_H 8.34 δ_C 124.31
4	-	4’	δ_C 147.95
5	δ_C 160.0	1’’	δ_H 4.06 δ_C 20.36
		2’’	δ_C 79.74
		3’’	δ_H 3.22 δ_C 74.36

3.4.3 Compound 2: *p*-Fluorophenyl, *S*-propargyl 1,2,4 triazole

^{1}H NMR spectrum (Fig.3A.13) of a freshly prepared solution of this compound (*p* FPh, *S*-propargyl) showed two broad peaks of unequal intensity which are very close to each other for the NH proton of triazole ring, indicating an unequal distribution of two tautomeric species in solution.

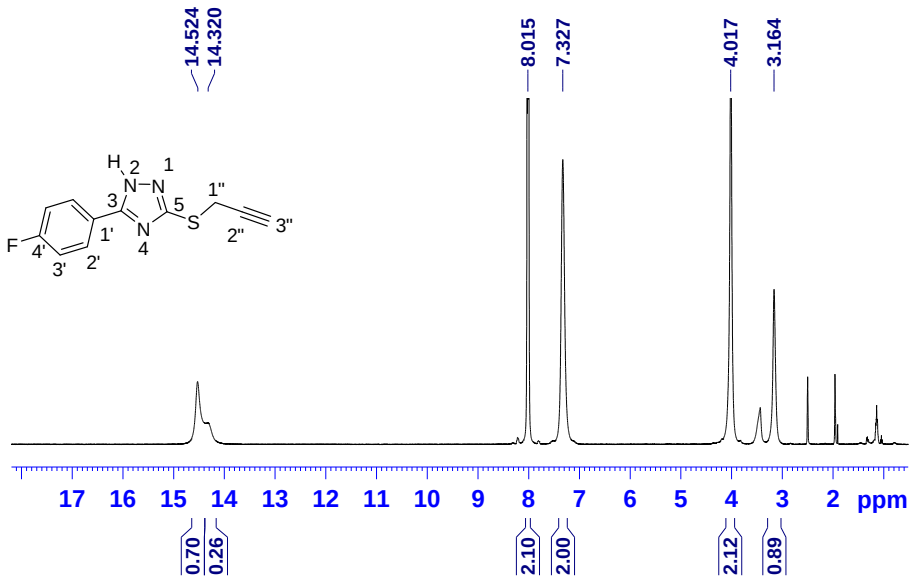

Fig.3A.13: *^{1}H NMR spectrum of compound 2. (400 MHz, DMSO-d_6, 298 K)*

The major NH signal appears at 14.52 ppm and the minor at 14.32 ppm. The ratio of the two peaks estimated from ^{1}H NMR spectrum is 70:30. ^{1}H chemical shift separation between the major and the minor tautomer is not at all visible for other proton resonances. In addition, ^{1}H NMR signals are also found to be broad and suggests slow exchange between species in solution even at the measurement temperature of 298K. For example one set of the signals from aromatic protons (7.32 ppm, assigned to H3') is very broad. The ^{1}H-^{19}F scalar coupling ($^{3}J_{H\text{-}F}$) can also contribute to line broadening to a certain extent for this resonance.

^{13}C NMR spectrum (Fig.3A.14) of this compound also shows effects of exchange broadening, and additional signals are seen for most of the carbons due to the coexistence of two tautomers. Multiplicity of some of the carbons belonging to *p*-FPh moiety (C4', C3', C2') is more due to scalar coupling with the fluorine atom ($^{1}J_{19F\text{-}C}$, $^{2}J_{19F\text{-}C}$ and $^{3}J_{19F\text{-}C}$). For example, the carbon to which fluorine atom is attached (C4') appears as a doublet with $^{1}J_{19F\text{-}C}$ of ~ 250Hz. The spectral assignments as shown in Table 3A.3 have been accomplished by means of ^{1}H-^{13}C HSQC and HMBC experiments. Correlations of NH protons to triazole ring carbons could not be obtained in the HMBC spectrum due to the decay of the NH signals during the long polarization transfer delay. Nevertheless, C3

carbon signal of the major isomer could be assigned on the basis of its HMBC correlation to H2' aromatic protons appearing at 8.02 ppm (Fig.3A.14C). Hence, the assignment of C5 carbon could be made by default since the C4' carbon could easily be identified from the HMBC correlation with H2' as well as its doublet nature due to $^{1}J_{19F\text{-}C}$ coupling. Chemical shift differences observed for the major and minor signals from C3 and C5 carbons of the triazole ring is noticeable. Major signal from C3 carbon is shielded (155.14 ppm) compared to the minor (161.58 ppm) while, the major C5 resonance is deshielded (158.98 ppm) compared to the minor (150.83 ppm). This clearly indicates that the chemical shifts of the triazole carbons are very sensitive to the nature of tautomer. That is in the major tautomeric form C3 is shielded by ~ 6.4 ppm compared to the minor form. Similarly, the C5 carbon is deshielded by ~ 8.1 ppm in the major tautomer than the minor tautomer. These observations imply that in the major tautomer C3 is closer to a *sp3* nitrogen atom (NH) while in the minor tautomer, C5 is adjacent to *sp3* nitrogen atom (NH). This in turn implies that the major tautomer is *N2-H* form (3b) and the minor tautomer is *N1-H* (3a) form. A careful look at the ^{13}C spectrum also identified two signals for C1' carbon, aromatic carbon linked to triazole ring, at 123.8 ppm (major) and 127.9 ppm (minor). Observation of ^{1}H-^{15}N HSQC cross peaks shown in Fig.3A.15 confirms slowing down of dynamics associated with triazole NH. Both NH protons show correlation to nitrogen resonating at -174.26 ppm, chemical shift of which corresponds to sp^3 hybridized nitrogen. Chemical shift assignments are shown in Table 3A.3.

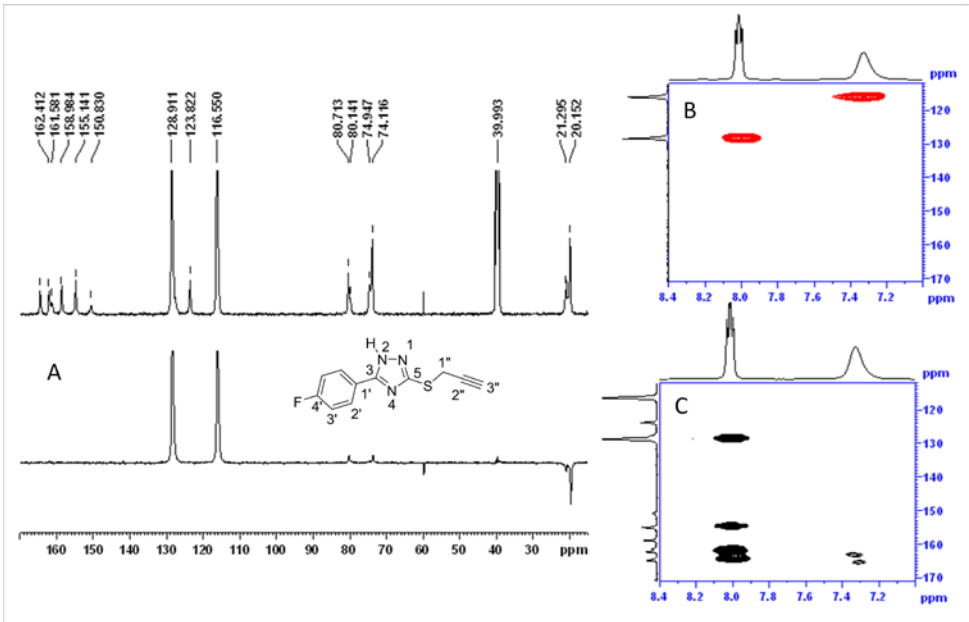

Fig.3A.14: *Comparison of the ^{13}C DEPT 135 and ^{1}H decoupled ^{13}C spectrum (A) of compound 2. (100 MHz, DMSO-d_6, 298 K); Selected regions of ^{1}H-^{13}C HSQC (B) and HMBC (C) spectrum.*

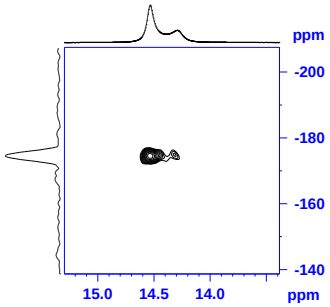

Fig.3A.15: *^{1}H- ^{15}N HSQC spectrum of compound 2. (400 MHz, DMSO-d_6, 298 K).*

As in the previous cases, NOESY spectrum (Fig.3A.16A) showed both positive and negative cross peaks due to chemical exchange and nOe contacts, respectively. The exchange peaks between the two NH protons are visible in the spectrum. These exchange cross peaks between NH protons can arise from the exchange between two tautomeric species 3a and 3b (Scheme.3A.1). Both the minor and the major NH peaks show similar exchange peaks with residual water peak (Fig.3A.16B). This further shows that water molecules can also indirectly contribute to the cross peak between the two NH protons by mediating a three site exchange involving both NH protons and water. nOe cross peak between NH proton and aromatic proton at 8.02 ppm not only confirms the assignment of the aromatic proton as H2' but also provides some insight to the nature of tautomers. Cross peak of NH with propargyl CH_2 protons at 4.02 ppm is very weak (Fig.3A.16B) compared to that observed with deshielded aromatic protons at 8.02 ppm (H2'). The inter molecular cross peak between residual water and these aromatic protons at 8.02 ppm (Fig.3A.16C) is stronger than the intra molecular nOe cross peaks with propargyl CH_2 protons at 4.02 ppm. However, the most intriguing observation is the cross peak of the major and the minor NH peaks with H2' aromatic protons (Fig.3A.16D). Both the NH show cross peaks of nearly equal strength, taking into account their population difference.

This is difficult to explain considering the presence of only the *N1-H/N2-H* (3a/3b) tautomers in the dynamic equilibrium.

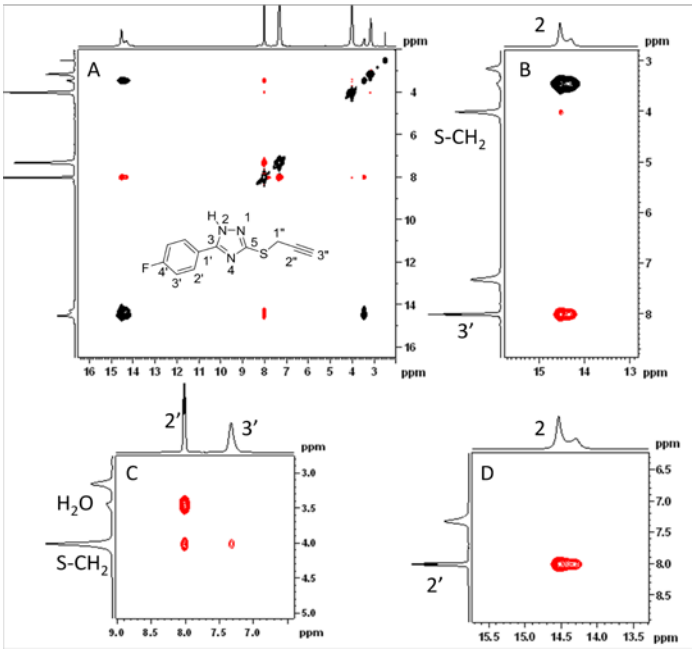

Fig.3A.16: *NOESY spectrum of compound 2(A). (400MHz, DMSO-d_6, 298 K). Expanded plots (B,C,D) of important regions are shown (see text).*

Table 3A.3: *Chemical shift assignments of compound 2.*

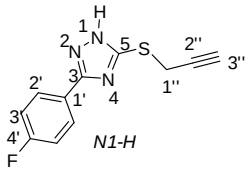

Atom	Chemical Shift (ppm)	Atom	Chemical Shift(ppm)
1	-	1’	δ_C 150.83
2	δ_H 14.52 δ_N -174.26	2’	δ_H 8.02 δ_C 128.42
3	δ_C 155.07	3’	δ_H 7.32 δ_C 116.03
4	-	4’	δ_C 163
5	δ_C 161.53	1’’	δ_H 4.02 δ_C 19.64
		2’’	δ_C 80.35
		3’’	δ_H 3.16

			δ_C 73.62

3.4.4 Compound 3: *p*-Nitrophenyl, *S*-allyl 1,2,4 triazole

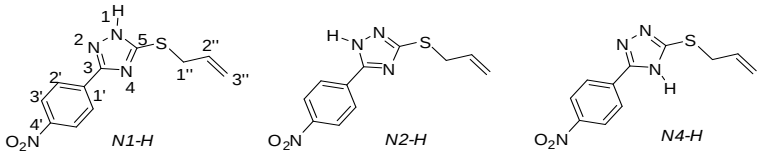

Presence of two types of NH signals at 14-15 ppm is clearly seen in the ^{1}H NMR spectrum of a freshly prepared solution of this compound (*para*-NO_2Ph, *S*-Allyl). But, they are very broad and nearly overlap (Fig.3A.17). Broadening of three of the quaternary carbons, two from triazole ring (160.47, 152.91 ppm; C3, C5 respectively) and one from aromatic ring (137.42 ppm, C1'), are noticed in the ^{13}C spectrum (Fig.3A.18). C3 and C5 carbons have been identified as those appearing at 160.47 ppm and 152.91 ppm, respectively from their HMBC correlations with aromatic H2' protons (8.11 ppm) and the allylic CH_2 protons (H1") at 3.81 ppm. The C1' carbon of *p*-NO_2Ph moiety appears at 137.38 ppm. All the three carbon signals are broad suggesting that they are involved in dynamic events. The expected cross peaks of NH protons to triazole carbons could not be seen in the ^{1}H-^{13}C HMBC spectrum due to the dynamics involving the NH proton.

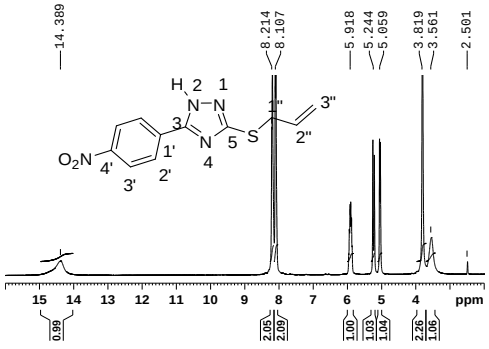

Fig.3A.17: *^{1}H NMR spectrum of compound 3. 400 MHz, DMSO-d_6, 298 K).*

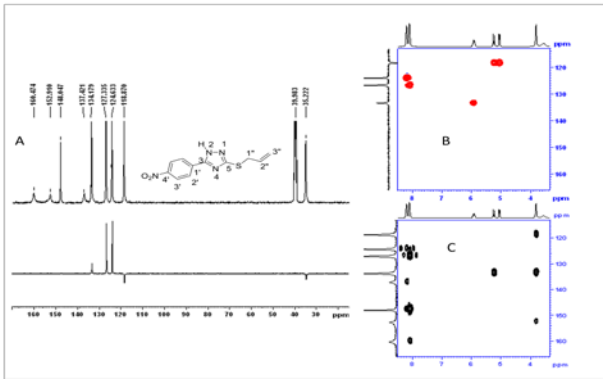

Fig.3A.18: *Comparison of the ^{13}C DEPT (lower) and ^{13}C spectrum (upper) (A) of compound 3. (100 MHz, DMSO-d_6, 298 K); Selected regions of ^{1}H-^{13}C HSQC (B) and ^{1}H-^{13}C HMBC (C) spectrum.*

NOESY spectrum (Fig.3A.19) is very useful to differentiate the aromatic protons since NH proton shows cross peak with only one set of aromatic protons in the region 8.04-8.14 ppm. The major NH peak shows nOe contact with the aromatic protons at 8.11 and maybe assigned to H2' (Fig.3A.19B). In addition to the expected intra molecular nOe cross peaks, inter molecular cross peaks due to interaction of water molecules and aromatic protons are also seen for the same set of protons (Fig.3A.19C). Cross peaks could not be obtained in the ^{1}H-^{15}N HSQC spectrum as a result of the dynamic nature of NH signal.

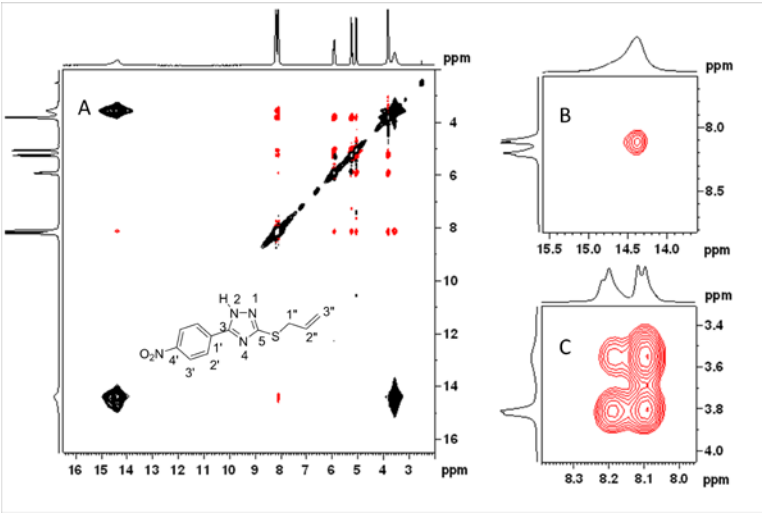

Fig.3A.19: *NOESY spectrum (A) of compound 3. (400 MHz, DMSO-d_6, 298 K). nOe cross peaks of aromatic protons to NH (B) and water molecule (C) are highlighted in the expanded plot.*

Sharpening and separation of ^{1}H resonances are observed with time. In Fig.3A.20, ^{1}H NMR spectrum taken after aging of the solution is compared with the ^{1}H spectrum discussed above. Most of the signals split in ~ 70:30 ratio and is particularly clear in the case of NH signals. Sharpening of the water signal at 3.37 ppm is also noticeable.

Similar changes are also observed in the ^{13}C NMR spectrum, a comparison of which is shown in Fig.3A.21, where sharpening of the resonance associated with the 1,2,4 triazole moiety (C3, C5, and C1', 161-150 ppm region) is very evident. ^{1}H-^{13}C HMBC correlations for NH protons to triazole ring carbons could also be obtained, which helps to identify the triazole ring carbons (Fig.3A.22).

All these observations point to slowing down of the rate of dynamic exchange with time. The carbon signal at 160.46 ppm (major signal) has HMBC correlations with NH proton and aromatic proton at 8.20 (C2') and hence it is assigned to C3. Minor signal of it is shielded appearing at 153.83 ppm (Fig.3A.21B). The C5 carbon in major tautomer is identified at 152.77 ppm by its correlation with allylic CH_2 (C1") appearing at 3.89 ppm and the minor C5 resonates at 160.46 ppm (Fig.3A.21B).

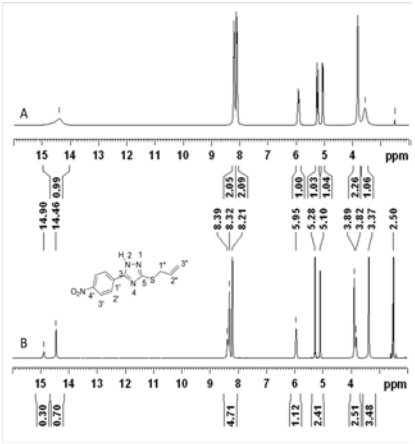

Fig.3A.20: *Comparison of ^{1}H NMR spectra of compound 3 recorded at two different time intervals in DMSO-d_6, 298 K. A) freshly prepared (400 MHz) and B) after ~ 6 months. (700 MHz*)

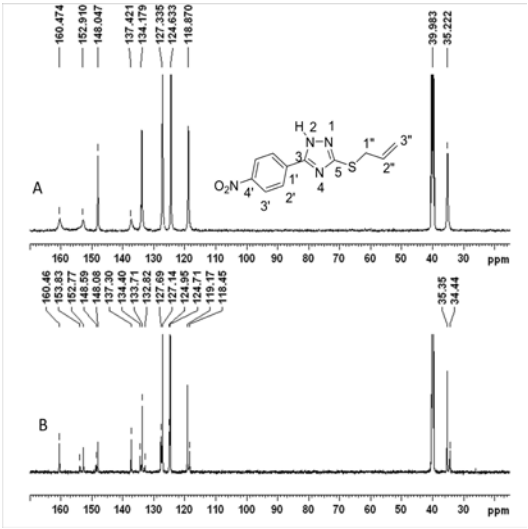

Fig.3A.21: *Comparison of ^{13}C NMR spectra of compound 3 recorded at two different time intervals in DMSO-d_6 at 298 K. A) freshly prepared (100 MHz) and B) after ~ 6 months. (175 MHz).*

It is interesting to note that the C3 carbon of the major tautomer in the present case is more deshielded than the minor tautomer, which is opposite to what is seen for the *para*-F Ph case (compound 2). In *para* FPh case, the major C3 carbon of the major tautomer appears at 155.14 ppm, which is close to the minor signal of *para*-NO_2Ph allyl compound (compound 3). This unambiguously proves that the tautomer populations are reversed in this case. That is the major tautomer in compound 3 is in the *N1-H* form (3a) rather that the *N2-H* form (3b). Similar inference can also be arrived at by comparing the chemical shifts of C5 carbons of compound 2 and compound 3. Thus, the chemical shift of C3 and C5 carbons carry the signature of the tautomer present. The C1' carbon also shows two signals at 134.39 ppm (major) and 132.82 ppm (minor) which also implies reversal of tautomer populations compared to compound 2.

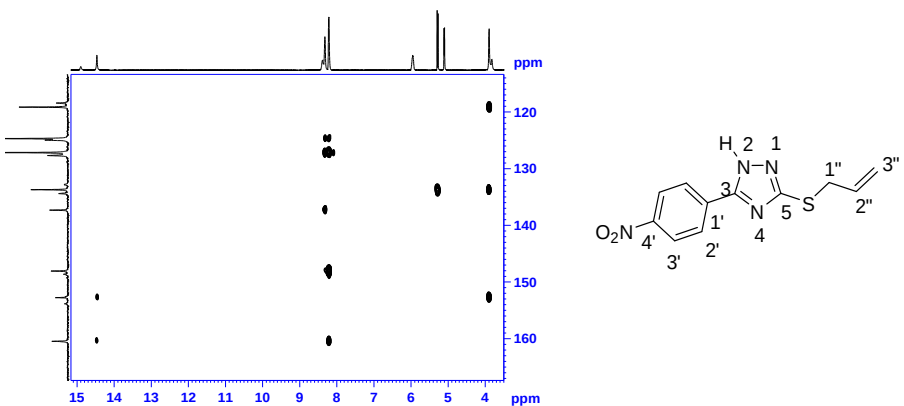

Fig.3A.22: *Expanded ^{1}H-^{13}C HMBC spectrum of compound 3 showing correlations of C3 and C5 carbons.*

It is interesting to note in passing that the NH protons also shows the trend of reversal in these two compounds (compound 2 and 3) and implying that the NH signal of the 3a tautomer (*N1-H* form) is more shielded than the 3b tautomer (*N2-H* form).

For this sample (compound 3), slowing of the dynamic events allows ^{1}H-^{15}N HSQC as well as HMBC correlations to be observed (Fig.3A.23). The major and minor NH chemical shifts obtained from the HSQC spectrum are -166.6 and -170.5 ppm respectively. The major NH signal at 14.46 ppm also shows an HMBC cross peak with a nitrogen at -89.6 ppm, which is typical of a *sp2* type nitrogen atom, *i.e*. N4. Chemical shift assignments of various nuclei are given in Table 3A.4.

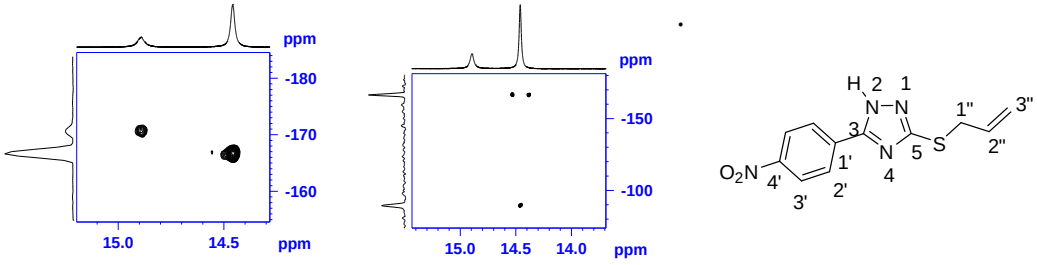

Fig.3A.23: *^{1}H-^{15}N HSQC and HMBC spectrum of an aged solution of compound 3 recorded on a 700 MHz spectrometer in DMSO-d_6 at 298 K.*

Table 3A.4: *Chemical shift assignments of compound 3.*

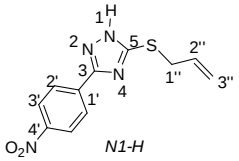

Atom	Chemical Shift (ppm)	Atom	Chemical Shift(ppm)
1	δ_H 14.46 δ_N -166.6	1’	δ_C 137.38
2	δ_N -89.6	2’	δ_H 8.11

			δ_C 126.72
3	δ_C 160.47	3’	δ_H 8.2 δ_C 124.04
4	-	4’	δ_C 147.48
5	δ_C 152.91	1’’	δ_H 3.81 δ_C 34.74
		2’’	δ_H 5.92 δ_C 133.4
		3’’	δ_H 5.05 δ_H 5.24 δ_C 118.37

3.4.5 Compound 4: *p*-Chlorophenyl, *S*-propargyl 1,2,4 triazole

Two well separated NH signals at 14.64 and 14.36 ppm, in the ratio 60:40, are seen in the ^{1}H NMR spectrum (Fig.3A.24) of a freshly prepared solution of this *para* chloro phenyl and *S*-propargyl substituted 1,2,4-triazole (*p*-ClPh, *S*-propargyl). Partial superimposition of two signals in similar ratio could be ascertained from other proton resonances that are also relatively broad. The broadness is very noticeable for one set of aromatic proton signals in the region 7.5 to 7.6 ppm.

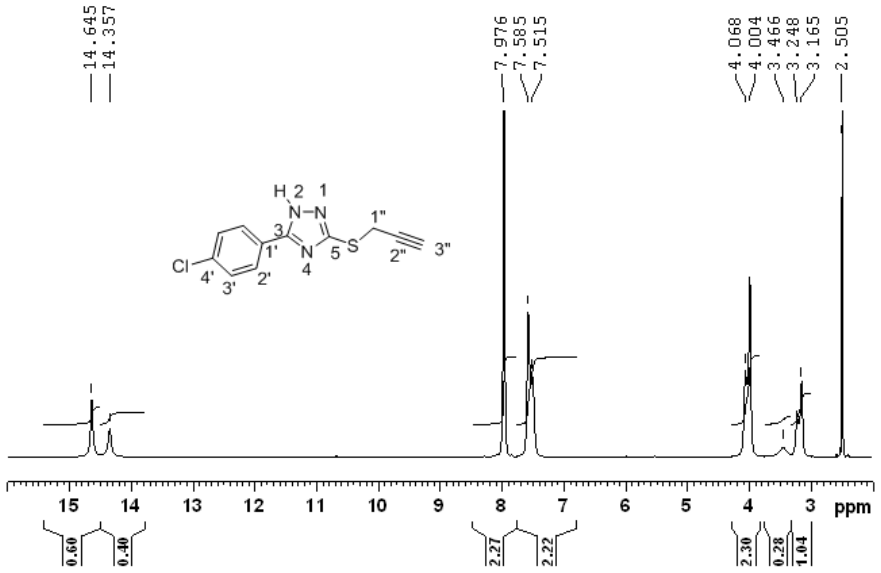

Fig.3A.24: *^{1}H NMR spectrum of compound 4. (700 MHz, DMSO-d_6, 298K).*

The ^{13}C NMR spectrum (Fig.3A.25A) is also relatively sharper in comparison with the *para* nitro analogue, compound 1b (Fig.3A.25B.) and suggests a slower dynamics in the present *para* chloro case. Additional signals for most of the carbons in the molecule are clearly visible. Assignments of signals, given in Table 3A.5 and 6, have been achieved on the basis of correlations seen in ^{1}H-^{13}C HSQC and ^{1}H-^{13}C HMBC spectra (Fig.3A.26). Here, HMBC correlations of NH protons, aromatic protons and propargyl CH_2 protons with triazole ring carbons have been used for unambiguous assignments. The chemical shift of C3 carbon (HMBC correlation to NH and aromatic protons H2' at 7.97 ppm) for the major and minor forms, are 155.0 and 161.49, respectively. Corresponding C5 carbon (HMBC correlation to NH and CH_2 protons H1" at 4.07 ppm) chemical shifts are 159.17 ppm (for major) and 151.22 ppm (for minor tautomer).

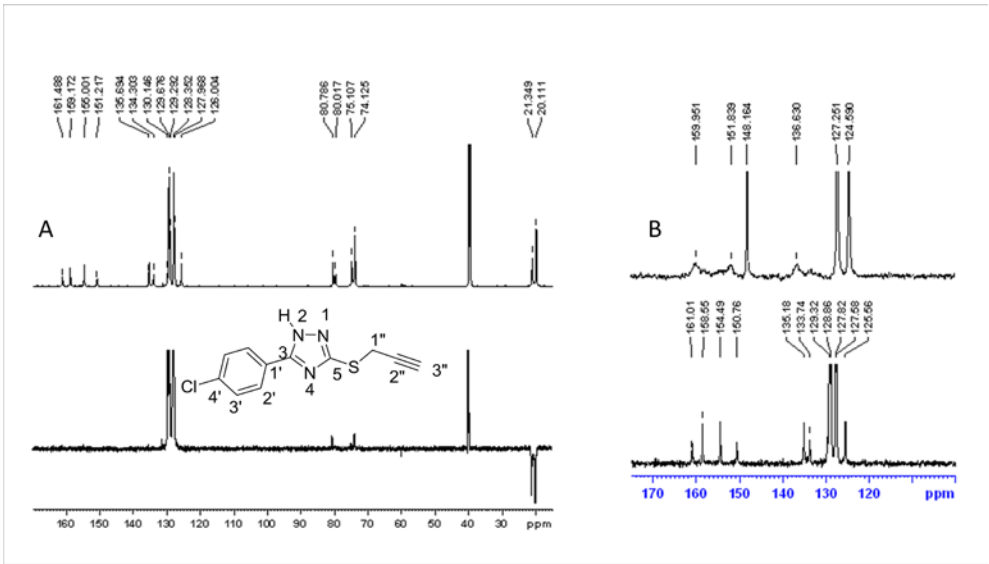

Fig.3A.25: *Comparison of the ^{13}C DEPT and ^{13}C spectra (A) of the compound 4 (175 MHz, DMSO-d_6, 298 K) and comparison of 100 MHz ^{13}C NMR spectrum (B) of para chloro compound (compound 4) with the para nitro analogue (compound 1b).*

The chemical shift differences observed between the major and minor signals are 6.69 and 7.95 ppm, respectively for C3 and C5 carbons. The minor environment is deshielded in the case of C3 carbon, while for C5 carbon it is shielded. From the previous discussions, it is clear that in this case *N2-H* tautomer (3b) is more populated than *N1-H* tautomer (3a). Here also, *N2-H* proton (14.64 ppm) is more deshielded than *N1-H* proton (14.36 ppm). Even though compound 4 was studied before, unequivocal evidence for the presence of *N1-H* and *N2-H* tautomers was not obtained. [24]

Table 3A.5: *Chemical shift assignments of compound 4 major tautomer.*

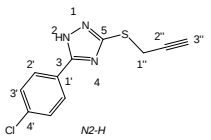

Atom	Chemical Shift (ppm)	Atom	Chemical Shift (ppm)
1	-	1’	δ_C 126.00
2	δ_H 14.64 -173.05	2’	δ_H 7.97 δ_C 128.30
3	δ_C 155.0	3’	δ_H 7.58 δ_C 129.72
4	-	4’	δ_C 135.66
5	δ_C 159.17	1’’	δ_H 3.99 δ_C 20.11
		2’’	δ_C 80.08
		3’’	δ_H 3.16 δ_C 74.17

Table 3A.6: *Chemical shift assignments of compound 4, minor tautomer.*

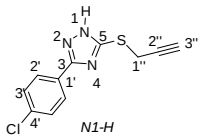

Atom	Chemical Shift (ppm)	Atom	Chemical Shift (ppm)
1	δ_H 14.36 -168.00	1’	δ_C 130.15
2	-	2’	δ_H 7.97 δ_C 127.97
3	δ_C 161.49	3’	δ_H 7.51 δ_C 129.28
4	-	4’	δ_C 134.31

5	δ_C 151.22	1''	δ_H 4.07 δ_C 21.3
		2''	δ_C 80.02
		3''	δ_H 3.24 δ_C 75.15

The differences observed for other carbons are of lesser magnitude except for the quaternary aromatic carbon attached to the triazole ring (C1') which shows a difference of ~ 4 ppm (minor signal at 130.15 ppm and major signal at 126.00 ppm). This also suggests that the chemical shift of C1' carbon atom also reflects the nature of tautomers present in solution. Presence of *N2-H* type of tautomer leads to shielding of this carbon in comparison with *N1-H* tautomer.

^{1}H-^{15}N HSQC spectrum (Fig.3A.27) indicates the presence of two NH nitrogen atoms at -173.05 ppm (for major) and -168.00 ppm (for minor tautomer). With prolonged data collection (~ 50,000 scans) at higher magnetic field (70 MHz) a ^{1}H decoupled ^{15}N 1D spectrum could be recorded which clearly shows six nitrogen signals confirming the presence of two types of species (tautomers) in solution.

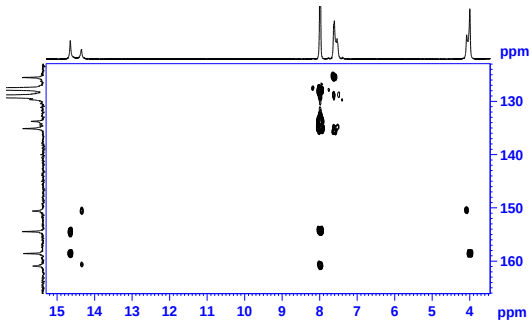

Fig.3A.26: *^{1}H-^{13}C HMBC spectrum of compound 4 (100 MHz, DMSO-d_6, 298 K) indicating important correlations of NH, aromatic and propargyl protons.*

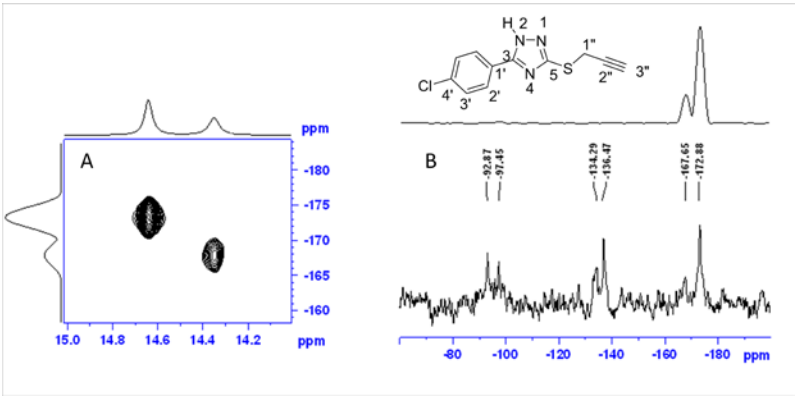

Fig.3A.27: *^{1}H-^{15}N HSQC spectrum (A) and comparison of ^{1}H decoupled ^{15}N spectrum & F1 projection of the HSQC spectrum for compound 4 recorded on a 700 MHz spectrometer in DMSO-d_6 at 298 K.*

NOESY spectral features are characterized by exchange and nOe cross peaks (Fig.3A.28). Both NH protons indicate nOe contacts with aromatic protons closer (H2', 7.97 ppm) to triazole ring (Fig.3A.28B) in addition to their weak nOes with the *S*-propargyl -CH_2 protons at ~ 4.0 ppm (Fig.3A.28C). Inter molecular nOe is noticed for water molecule and the deshielded H2' aromatic protons at 7.97 ppm (Fig.3A.28D).

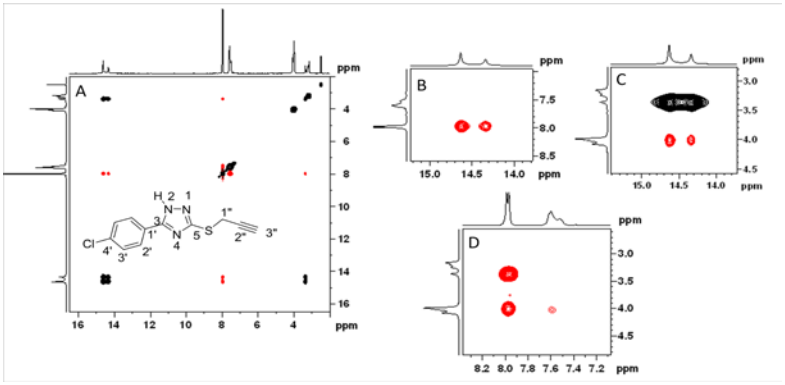

Fig.3A.28: *NOESY NMR spectrum of compound 4 (400 MHz, DMSO-d_6, 298 K). (A). Full spectrum; B, C and D are expanded regions of spectrum of interest (see text).*

The dynamic nature of the system was also studied by variable temperature NMR experiments (298K to 323K) and the ^{1}H NMR response is depicted in Fig.3A.29. Collapse or sharpening of signals belonging to the propargyl group and aromatic protons (7.5-7.6 ppm) is observed at 323K. Separation between the NH signals decreases with increase in temperature besides the broadening. Broadening of water resonances due to faster exchange with NH protons could also be noticed in the spectra. On cooling, the system tends to come back to the equilibrium state and thus shows the reversible nature of this dynamic system.

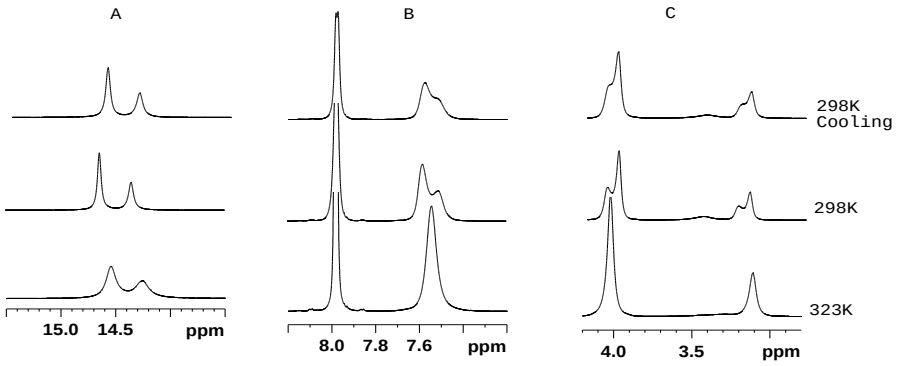

Fig.3A.29: *Variable temperature ^{1}H NMR of compound 4 (700 MHz, DMSO-d_6): A) NH region, B) aromatic region and C) aliphatic region.*

3.4.6 Compound 5: *p*-Chlorophenyl, *S*-allyl 1,2,4 triazole

^{1}H NMR spectrum (Fig.3A.30) of this compound is very similar to *para* nitro allyl case (compound 3) except for chemical shift changes in the aromatic region resulting from the change of substituent. A broad NH signal appears at 14.38 ppm. The high field aromatic signal at 7.56 ppm is broad though the other signals are reasonably well resolved. Broadness of the signals of triazole carbons in ^{13}C spectrum and the difficulty in obtaining ^{1}H-^{15}N HSQC spectrum demonstrated the dynamic nature of the molecule.

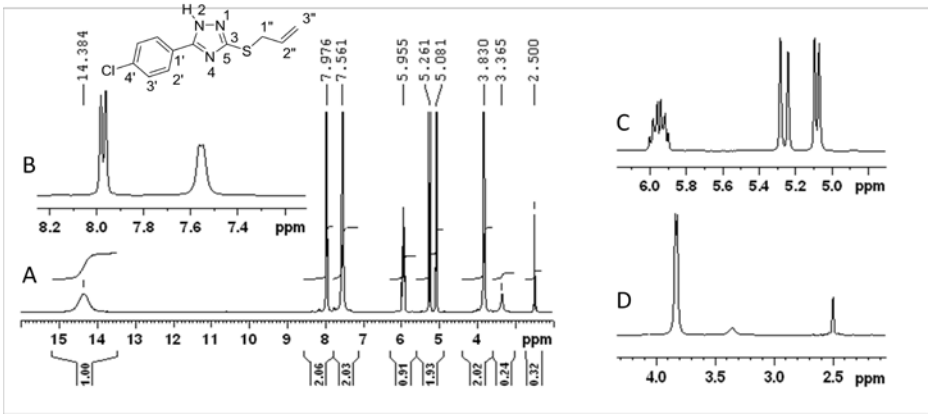

Fig.3A.30: *^{1}H NMR of compound 5 (A) at 400 MHz, DMSO-d_6, 298 K. Inset (B) shows expanded aromatic region. Expanded spectra of the olefinic region (C) as well as the aliphatic region (D) are also shown.*

This sample (compound 5) showed changes in its ^{1}H and ^{13}C NMR spectral features on aging. The NH signal splits into two equally populated peaks (Fig.3A.31A, B) and the other parts of ^{1}H spectrum is also modified, though the differences seen are not as evident as for the NH protons (Fig.3A.31C, D, E, F). Both NH signals show the same intensity indicating equal population of both the tautomers 3a and 3b.

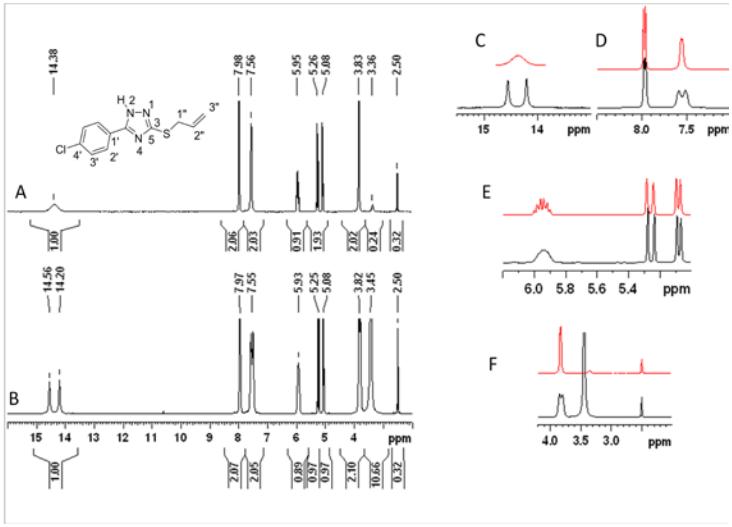

Fig.3A.31: *^{1}H NMR of the compound 5 recorded at two different times. Spectrum B is recorded after ~two months aging compared to A (400 MHz, DMSO-d_6, 298 K). Expanded spectra of different regions are shown in C, D, E and F where black traces depict the spectrum recorded after aging of the solution and red traces show the spectrum of the fresh solution.*

The NOESY spectral features are also found to be very similar in both cases except for the resolution associated with NH signals (Fig.3A.32).

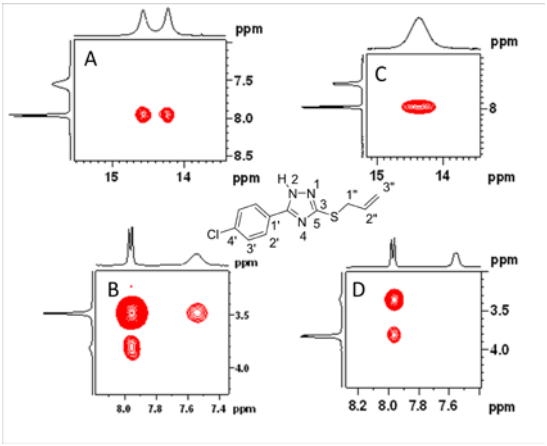

Fig.3A.32: *Comparison of the expanded NOESY spectra of compound 5 recorded at two different time intervals. The plots on the left side (A, B) are obtained after two months of aging compared to the spectra shown on the right side (C ,D) (400 MHz, DMSO-d_6, 298 K).*

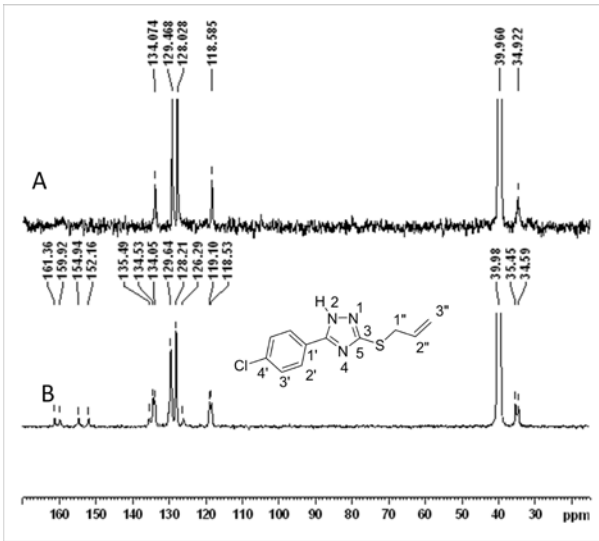

Fig.3A.33: *^{13}C NMR of the compound 5, recorded at two different time intervals. Spectrum B is recorded after ~ 2 months aging compared to A. (400 MHz, DMSO-d_6, 298 K).*

The quaternary carbons (C3, C5 and C1'), which were initially very broad, could be seen clearly in the ^{13}C spectrum of the aged sample (Fig.3A.33) though they are not very sharp. This sample did not show a good ^{1}H-^{13}C HMBC spectrum. Only the hetero nuclear correlations from the aromatic protons could be observed (Fig.3A.34A) which were sufficient to identify the C3 chemical shifts as 161.36 ppm and 154.94 ppm corresponding to the *N1-H* (3a) and *N2-H* (3b) tautomeric forms, respectively. C5 carbons of these two tautomers appear at 152.16 and 159.92 ppm respectively. As expected, these two signals are of the same intensity due to their equal population. Observed chemical shifts of C1' carbons are 126.29 and 130.25 ppm for *N2-H* and *N1-H* tautomers, respectively. ^{1}H-^{15}N HSQC spectrum (Fig.3A.34B) showed two cross peaks at -169.14 and -174.19 ppm, respectively correlating to the NH protons at 14.22 and 14.57 ppm. ^{1}H-^{15}N HMBC measurements did not show any detectable cross peaks at various

polarization transfer delays, corresponding to the long range coupling constant of 7-12 Hz, employed. The assignments are given in Table 3A.6.

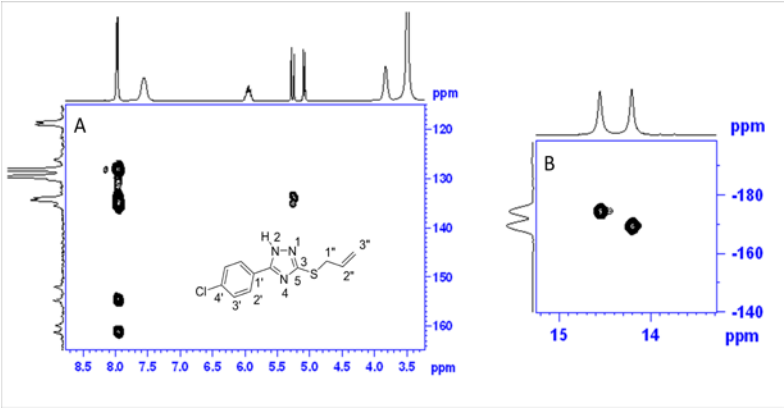

Fig.3A.34: *^{1}H-^{13}C HMBC (A) and ^{1}H-^{15}N HSQC (B) spectra of compound 5 (400 MHz, DMSO-d_6, 298 K).*

Table 3A.6: *Chemical shift assignments of compound 5 for N1-H (3a) tautomeric form*

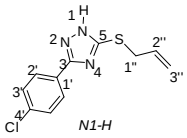

.

Atom	Chemical Shift (ppm)	Atom	Chemical Shift (ppm)
1	δ_H 14.22 δ_N -169.14	1’	δ_C 130.25
2	-	2’	δ_H 7.96 δ_C 128.1 or 128.19
3	δ_C 161.36	3’	δ_H 7.54 δ_C 129.45 or 129.71
4	-	4’	δ_C 135.53
5	δ_C 152.16	1’’	δ_H 3.82 δ_C 34.5 or 35.39
		2’’	δ_H 5.93 δ_C 133.89 or 134.49
		3’’	δ_H 5.25 and 5.07 δ_C 118.38 or 119.07

Table 3A.7: *Chemical shift assignments of compound 5 for N2-H (3b) tautomeric form.*

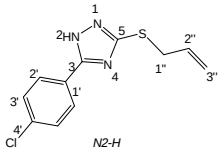

Atom	Chemical Shift (ppm)	Atom	Chemical Shift(ppm)
1	-	1’	δ_C 130.25
2	δ_H 14.57 δ_N -174.19	2’	δ_H 7.96 δ_C 128.1 or 128.19
3	δ_C 154.81	3’	δ_H 7.54 δ_C 129.45 or 129.71
4	-	4’	δ_C 135.53
5	δ_C 159.94	1’’	δ_H 3.82 δ_C 34.5 or 35.39
		2’’	δ_H 5.93 δ_C 133.89 or 134.49
		3’’	δ_H 5.25 and 5.07 δ_C 118.38 or 119.07

3.4.7 Compound 6: Furyl, *S*-propargyl 1,2,4 triazole

^{1}H NMR spectrum of compound 6 (furyl, *S*-propargyl) shown in Fig.3A.35 exhibits two peaks in the NH region at 14.65 and 14.35 ppm, indicating the presence of two environments (tautomers) for NH in approximately 65:35 mole ratio, as seen from the integrals of the peaks. This suggests co-existence of two tautomeric species in solution since only one NH signal is expected. Most of the other protons also appear with additional resonances in the same ratio. From the forgoing discussions on the other systems investigated, the more populated NH signal, being more deshielded, is assigned to the *N2-H* (3b) tautomer.

The peaks of the major form are more deshielded compared to those of the minor form for both NH and aromatic protons of furyl group while the aliphatic protons of the minor form are more deshielded. ^{1}H signals of the major and minor form have better separation in this case compared to the other systems discussed before. Nevertheless, it is

difficult to verify the details of the structural features of the major and minor species present in the system from the ^{1}H NMR spectrum. A standard COSY spectrum is employed to assign the protons of the furyl ring.

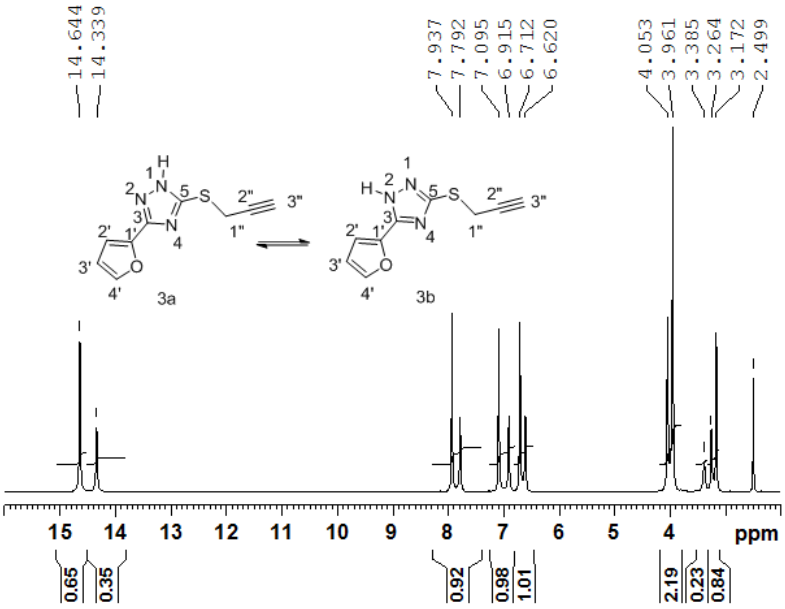

Fig.3A.35: *^{1}H NMR of the compound 6 (400 MHz, DMSO-d_6, 298 K).*

Though this compound has only nine carbons, ^{13}C NMR spectrum (Fig.3A.36) showed 18 peaks indicating that two species are present in the compound. Even though ^{13}C NMR is not quantitative, the relative intensities of peaks still give an idea that the two species are present in unequal amounts. Unlike many of the systems discussed, the ^{13}C signals, including those of the triazole moiety (C3 and C5), are found to be relatively sharper. ^{1}H-^{13}C HSQC and HMBC measurements have been performed for obtaining complete assignments of carbons and protons.

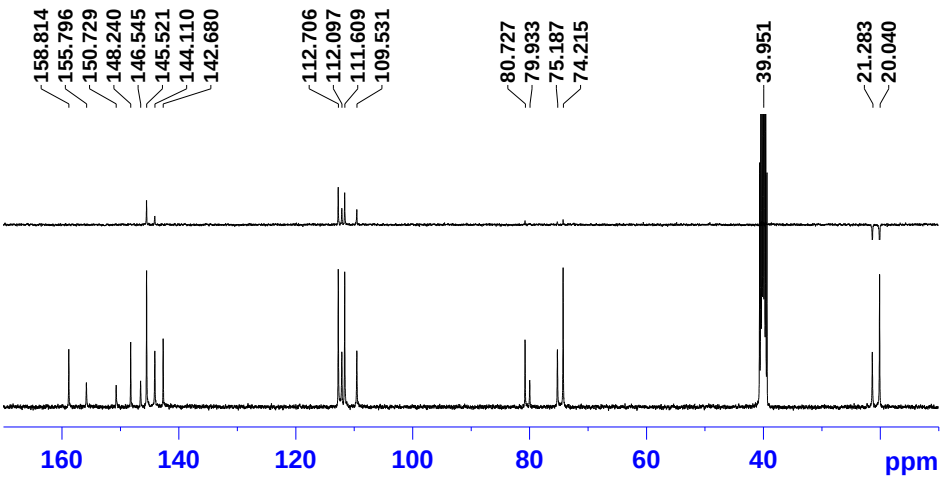

Fig.3A.36: *Comparison of the ^{13}C DEPT (upper) and ^{13}C spectra (lower) of compound 6 (100 MHz, DMSO-d_6, 298 K).*

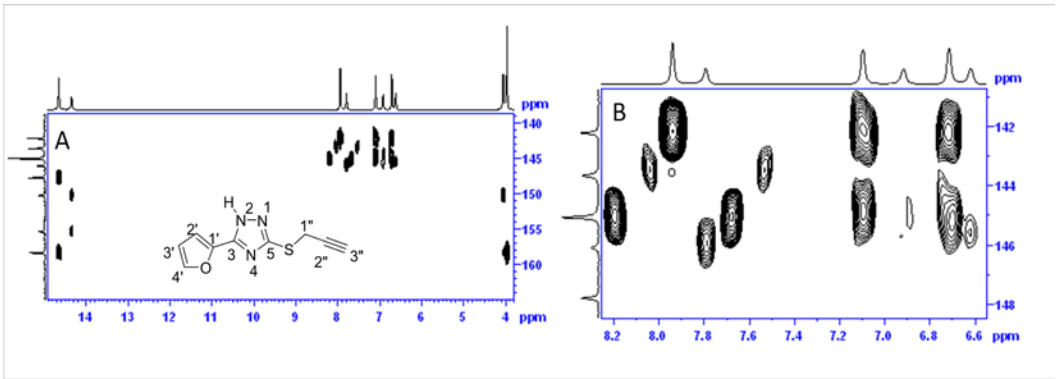

Fig.3A.37: *Expanded ^{1}H-^{13}C HMBC spectrum of the compound 6. Aromatic carbon ^{1}H correlations (A) and furyl (B). (400 MHz, DMSO-d_6, 298 K).*

HMBC correlations (Fig.3A.37) of the NH and *S*CH_2 protons are useful in identifying triazole ring carbons. The propargyl CH_2 protons (H1") from major tautomer at 3.96 ppm shows correlation with carbon at 158.82 ppm and the CH_2 proton from minor tautomer at 4.05 ppm shows correlation to the carbon at 150.73 ppm. Hence both these carbons are assigned to C5. The major and minor signals at 148.24 ppm and 155.79 ppm belong to C3 carbons of the major and minor tautomer, respectively.

Shielding nature of the major C3 carbon compared to the minor one confirms that the major tautomer is the *N2-H* form (3b). This inference is the same as the one obtained from the NH region of the ^{1}H NMR spectrum where the more populated NH is deshileded. Similarly, the major signal of the C1' carbon of the furyl ring is shielded (142.68 ppm) in comparison with the minor one (146.54 ppm).

Thus in nut shell, the deshielding nature of NH proton, shielding nature of C3 and C1' carbons and deshielding of C5 carbons are signatures of the *N2-H* form (3b) of tautomers, while shielding of NH proton, deshielding of C3 and C1' carbons and shielding of C5 carbon signal are characteristic of the *N1-H* (3a) tautomer.

^{1}H-^{15}N HSQC spectral analysis showed that the nitrogen chemical shift of the major tautomer (3b) is -174.29 ppm while that of the minor tautomer (3a) is -168.42 ppm (Fig.3A.38). ^{1}H-^{15}N HMBC spectrum failed to show any cross peak under the standard measurements conditions employed (1/2J delays corresponding to 4-10 Hz) as a result of the dynamic nature of the system. Complete assignments are shown in Table 3A.8 and 3A.9.

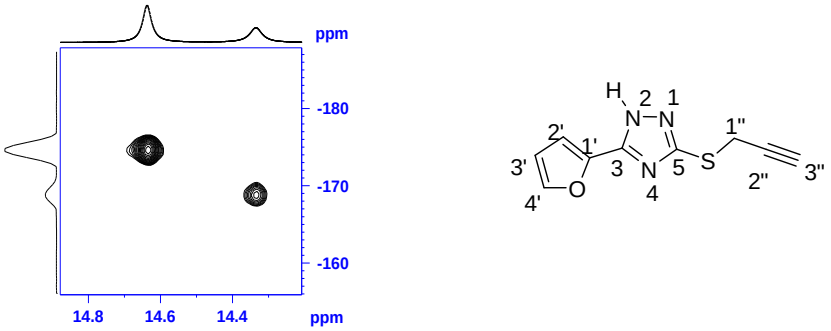

Fig.3A.38: *^{1}H-^{15}N HSQC spectrum of compound 6 (400 MHz, 40 MHz, DMSO-d_6, 298 K).*

Table 3A.8: *Chemical shift assignments of compound 6 corresponding to the N1-H (3a) tautomeric form.*

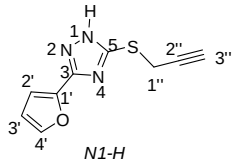

N1-H

Atom	Chemical Shift (ppm)	Atom	Chemical Shift (ppm)
1	δ_H 14.35 δ_N -168.42	1’	δ_C 146.54
2	-	2’	δ_H 6.92 δ_C 109.55
3	δ_C 155.79	3’	δ_H 6.62 δ_C 112.12
4	-	4’	δ_H 7.79 δ_C 144.13
5	δ_C 150.73	1’’	δ_H 4.05 δ_C 21.29
		2’’	δ_C 79.93
		3’’	δ_H 3.26 δ_C 75.19

Table 3A.9: *Chemical shift assignments of compound 6 corresponding to N2-H (3b) tautomeric form.*

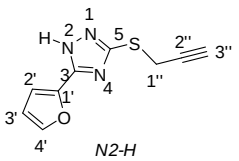

N2-H

Atom	Chemical Shift (ppm)	Atom	Chemical Shift (ppm)
1	-	1’	δ_C 142.68
2	δ_H 14.65 δ_N -174.29	2’	δ_H 7.09 δ_C 111.63
3	δ_C 148.24	3’	δ_H 6.71 δ_C 112.74
4	-	4’	δ_H 7.93 δ_C 145.53
5	δ_C 158.82	1’’	δ_H 3.96 δ_C 20.04
		2’’	δ_C 80.73
		3’’	δ_H 3.17 δ_C 74.24

NOESY spectrum (Fig.3A.39) of this compound is very interesting. It shows positive and negative cross peaks. Strong positive cross peaks are seen between signals of the major and minor tautomer signals and clearly demonstrates the presence of exchange equilibrium between two species. Triazole NH proton of both the species also show strong exchange cross peaks with trace amount of water (at 3.38 ppm) present in the solvent (Fig.3A.39A) in addition to the cross peaks between them. The exchange cross peaks between NH protons can also be mediated by intermolecular exchange involving water molecule. But, water molecule cannot mediate the exchange cross peak seen for the other major and minor peaks arising from the protons attached to various carbons in the molecule. Various exchange cross peaks are shown in Fig.3A.39B.

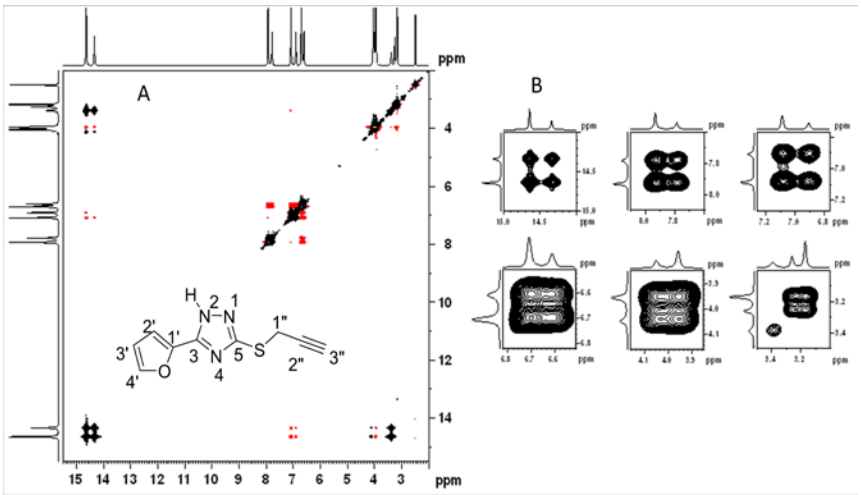

Fig.3A.39: *NOESY spectrum of compound 6 (400 MHz, DMSO-d_6, 298 K). A) Full spectrum and B) expanded plots near diagonal region showing exchange peaks (black colour contours) between the major and minor resonances. Negative nOe cross peaks are represented by red contours*.

Further proof for the exchange dynamics of the system is obtained from ^{1}H and ^{13}C variable temperature NMR measurements (Fig.3A.40) carried out in the temperature range 298K-368K. As expected, at higher temperature, coalescence of the exchanging proton signals is noticed due to increase in exchange rates. Variable temperature ^{13}C NMR spectra also reflect dynamics effects. ^{13}C signals become broader at higher temperature (Fig.3A.41).

The negative cross peaks in the NOESY spectrum are due to actual nOe contacts. The protons on the furyl rings show the expected nOe cross peaks (Fig.3A.42A). This corresponds to the nOe contact of 4'H (7.93, 7.79 ppm) to 3'H (6.71, 6.62 ppm) which in turn shows a cross peak with 2'H (7.09, 6.92 ppm).

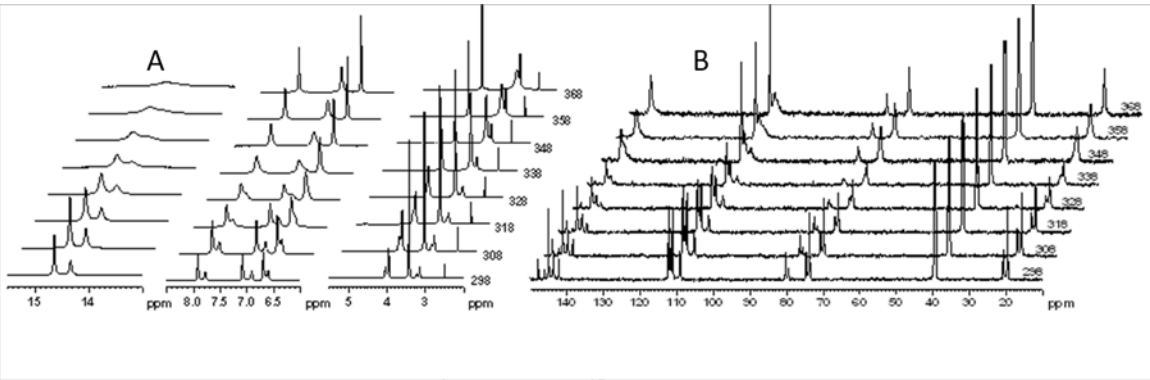

Fig.3A.40: *Variable temperature ^{1}H (A) and ^{13}C (B) NMR measurements of compound 6. Temperature of measurement is shown on the plot (700 MHz, DMSO-d_6, 298* K*).*

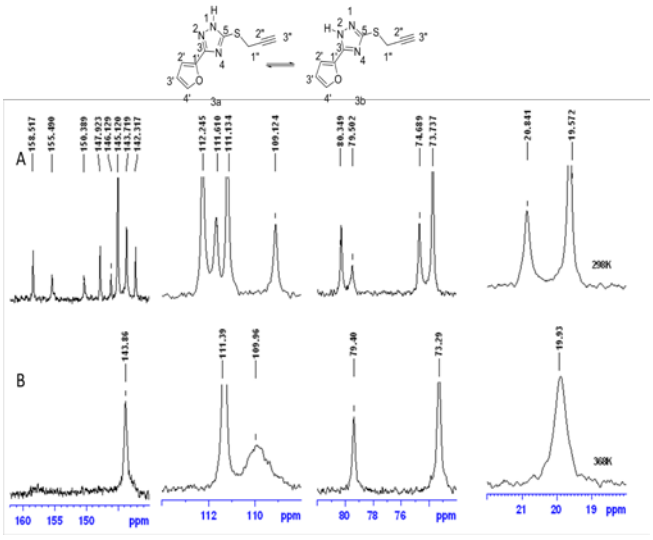

Fig.3A.41: *Expanded ^{13}C NMR spectrum of compound 6 at 298K (A) and 368K. (700 MHz, DMSO-d_6, 298 K).*

But, the intriguing observation is the negative cross peak seen between the major and the minor peaks (Fig.3A.42A). For example the major 4'H proton at 7.93 ppm is expected to show cross peak with the major 3'H at 6.71 ppm. But, in addition to this, it shows nOe cross peak also to the minor 3'H proton at 6.62 ppm. Similarly, the minor 4'H signal appearing at 7.79 ppm has correlation with both the major and minor 3'H protons. Same nOe pattern is observed for cross peaks of the 3'H and 2'H protons as well. Both the major and minor NH peaks show equally strong nOe cross peaks with 2'H protons of furyl unit (Fig.3A.42B) in addition to the cross peaks with *S*-propargyl CH_2 proton at 4.05 and 3.96 ppm (Fig.3A.42C). Propargyl CH and CH_2 protons also exhibit similar nOe patterns (Fig.3A.42D).

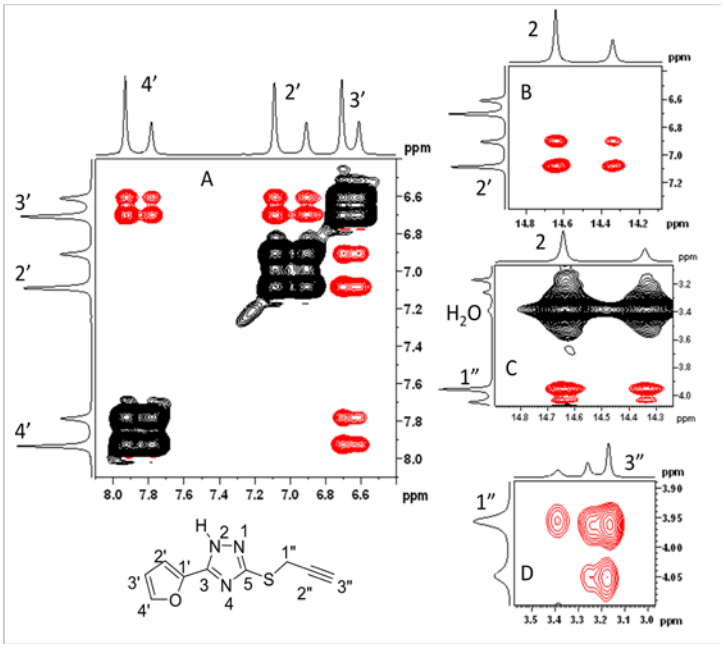

Fig.3A.42: *NOESY spectrum of compound 6 (400 MHz, DMSO-d_6, 298 K). A) Furyl region; B) NH to H2'region; C) NH to propargyl CH_2 region and D) among the propargyl protons. Positive exchange cross peak are shown as black contours. Negative nOe cross peaks are represented by red contours.*

These cross peaks are difficult to explain. The NOESY data indeed suggests that both the major and minor forms not only undergo chemical exchange but are also within nOe distance of 5Å. Such a situation can arise only if a dimeric structure involving both these environments together with exchange of protons is envisaged. The two environments are the two tautomers 3a and 3b with NH proton either on N1 or N2 respectively and the NH proton hops between N1 and N2 as shown in Fig.3A.43. The two triazole molecules may be close enough in space to show inter molecular nOe during this process and the life time of the transition state may also be long enough to manifest nOe contacts. Further, the negative cross peak also suggest that the molecular system as such still experiences dynamics corresponding to short correlation times.

These observations do not rule out the possibility of the presence of the *N4-H* tautomer even though theoretical calculations suggest it may be unstable (see Chapter V). Hence, this possibility has not been considered. Moreover, the close nature of ^{15}N chemical shifts observed for the two forms also favours a situation where in the chemical shifts are not much disturbed. The *N4-H* nitrogen atom in 1,2,4 triazole thiones discussed in the last chapter is usually more shielded than the *N1-H* nitrogen atom. Even the ^{13}C NMR data on the systems investigated is also in favour of a co existence of *N1-H* and *N2-H* tautomers. Taking all these into consideration the following dynamic model (Fig.3A.44) involving the two tautomers is proposed for this compound.

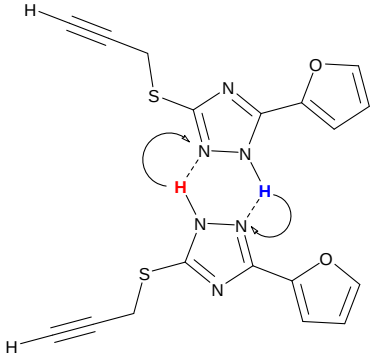

Fig.3A.43: *A dimeric model involving exchange of N1-H (3a) and N2-H (3b) tatuomer proposed in DMSO solution on the basis of nOe and ^{13}C NMR data for compound 6.*

The amount of water molecules is unlikely to play a crucial role in this dynamic equilibrium involving the two tautomers except modification of inter molecular exchange of triazole NH and water molecules. It is worthwhile to recall the inter molecular nOes observed between water molecules and aromatic protons. Such inter molecular nOe are observed even in 1,2,4-triazole thiones discussed in Chapter II. As an example in Fig.3A.45, the inter molecular nOe cross peaks observed for *para* fluoro thione and the corresponding *S*-propargyl derivate are shown. Few reports are also available in literature that suggest dimeric or trimeric nature in the solid as well as solution state for the triazole systems. [55, 56, 57, 58]

Proton and ^{13}C NMR spectra of the furyl system in $CDCl_3$ did not show any additional signals (Fig.3A.46) and clearly demonstrate the role of solvent in tautomerism. The NH signal is very broad and the NOESY data fail to show any correlations other than the usual intra molecular contacts. A difference in the chemical shift (~ 5ppm) for the NH proton is noticeable and indicates the effect of solvent on a good hydrogen bond donor group like NH. Sulphone group in DMSO is a good hydrogen bond acceptor and hence induces a downfield shift of the NH proton resonance.

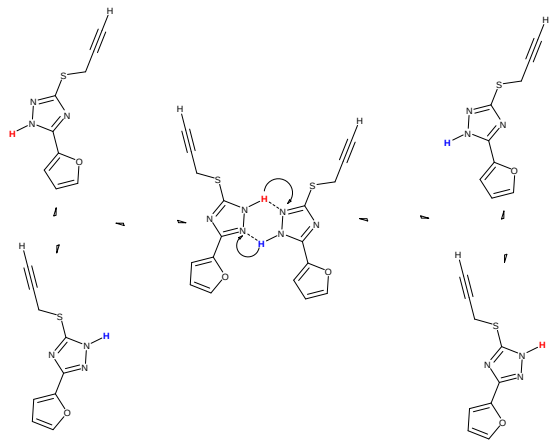

Fig.3A.44: *Proposed dynamic equilibrium involving formation of dimeric structure comprising N1-H (3a) and N2-H (3b) tatuomer in DMSO solution on the basis of NMR studies for compound 5.*

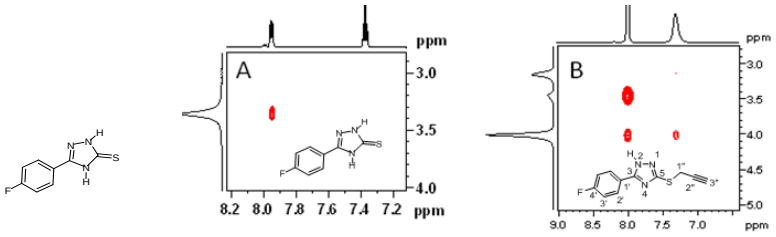

Fig.3A.45: *Inter molecular NOESY cross peaks observed for water and aromatic protons in para fluoro triazole thione (A) and its S-propargyl derivative compound 2 (B), (400 MHz, DMSO-d_6, 298 K).*

A comparison of the ^{1}H chemical shifts of NH peaks in the systems investigated is given in Table 3A.10. It is noted that the NH signal from the 3b *N2-H* tautomer is more deshielded than *N1-H* proton. Hence, this itself can be used as a quick way to differentiate the nature of tautomer in solution without any detailed investigations. On the basis of this, it is obvious that, in most of the cases *N2-H* tautomer is more populated. In the case of *p*-Cl-*S*-allyl compound (compound 4) both tautomers are equally populated. *N1-H* tautomer is more populated in *p*-NO_2Ph, *S*-allyl (compound 3) and *p*-NO_2Ph, *S*-propargyl (compound 1b) cases .

.

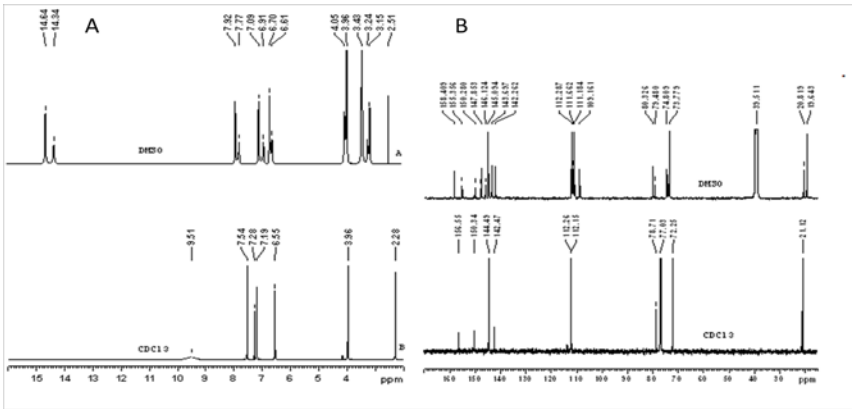

Fig.3A.46: *Comparison of the ^{1}H (A) and ^{13}C (B) NMR spectra of compound 5 in $CDCl_3$ and DMSO-d_6.*

Table: 3A. 10: *^{1}H Chemical shift of NH peaks of tautomers in DMSO*.

Compound	*N2-H* form 3b (ppm)	*N1-H* form 3a; (ppm)
1a, *p*-NO2Ph, *SO2*-Propargyl	15.67	15.67
1b, *p*-NO_2Ph, *S*-Propargyl	14.96 (minor)	14.58(major)
2, *p*-FPh, *S*-Propargyl	14.52 (major)	14.32 (minor)
3, *p*-NO_2Ph, *S*-Allyl	14.90 (minor)	14.46 (major)
4, *p*-ClPh, *S*-Propargyl	14.64 (major)	14.36 (minor)
5, *p*-ClPh, *S*-Allyl	14.56 (major)	14.20 (minor)
6, Furyl, *S*-Propargyl	14.64 (major)	14.34 (minor)

From these observations, it is envisaged that, *p*-NO_2Ph, *S*-propargyl system (compound 1b) has a higher population of the *N1-H* tautomer (3a) since the major NH signal is shielded (14.58 ppm) compared to the minor signal (14.96 ppm). Detailed structural investigations could not be performed on this system due to its unfavourable dynamic nature in DMSO. This further suggests that the nature of the substituent on the aromatic ring also contributes to the nature of tautomer present in solution. *N1-H* population is more in the *para* nitro phenyl substituted cases. In all other cases, the dominant tautomer is *N2-H*. In view of this it is likely that for the sulfone compound, *p*-NO_2Ph, *SO_2*-propargyl system, population of the tautomer is more weighted by *N1-H* form. The appreciable deshielding of the NH signal (15.67 ppm) is likely to result from the stabilization of the *N1-H* tautomer by a five membered intra molecular hydrogen bond with sulfone oxygen. A glimpse of ^{1}H NMR spectra of various systems investigated is presented in Fig.3A.47A and Fig.3A.47C.

It is also interesting to note that in the *para* substituted aromatic systems studied, in the ^{1}H NMR spectrum, one set of protons (H3', *ortho* to the substituent) is always

found to be broader than the other one (Fig.3A.47 C). The exact reason for this behavior is not very clear and is probably due to some kind of modification of the local environment during the process of proton jump from one molecule to other.

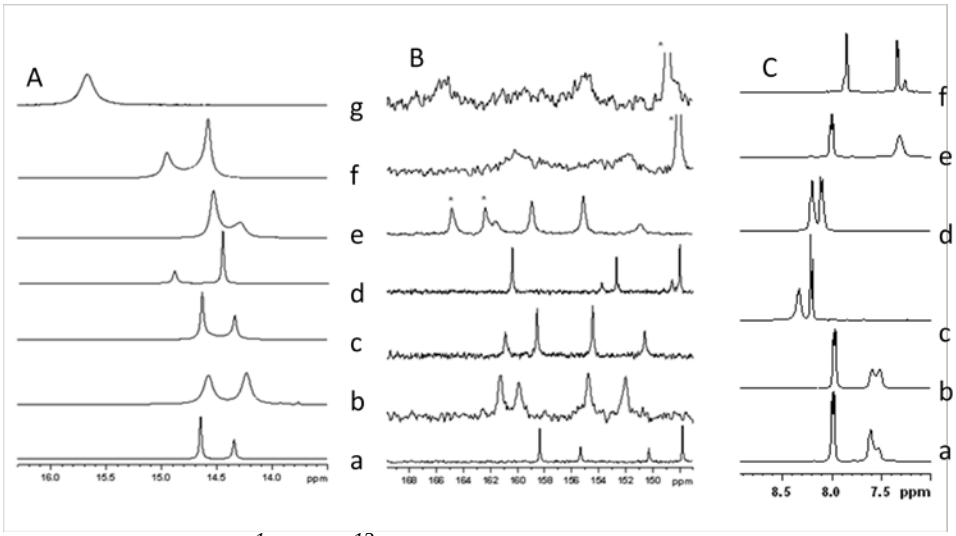

Fig.3A.47: *Comparison of ^{1}H and ^{13}C NMR spectra of various systems (a-g) investigated. A) NH region of proton spectra. B) Triazole ring carbon region in ^{13}C spectra. The systems are a) p-NO2Ph, SO2-Propargyl, b) p-NO_2Ph, S-Propargyl, c) p-FPh, S-Propargyl, d) p-NO_2Ph, S-Allyl, e) p-ClPh, S-Propargyl, f) p-ClPh, S-Allyl and g) Furyl, S-Propargyl. Fig.C shows aromatic region of various samples investigated to show specific broadening of one set of protons for p- methyl S-propargyl (a), p-FPh S-propargyl (b), p-NO_2Ph S-allyl,(c), p-NO_2Ph S-propargyl (d), p-ClPh-S-allyl (e) and p-ClPh S-propargyl (f).*

A comparison of the ^{13}C chemical shifts of triazole ring carbons (C3 and C5) and C1' observed for *N1-H* and *N2-H* tautomers is presented in Table 3A.11. The ^{13}C NMR spectra of the triazole ring carbon region are depicted in Fig.3.47B. In general it is noticed that the carbon adjacent to NH proton always experiences a shielding effect. Thus, in *N2-H* tautomer, C3 is always shielded and C5 is deshielded while in the *N1-H* tautomer C5 carbon is shielded and C3 is deshielded. C1' carbon also shows response to structure of the tautomers. *N2-H* form leads to shielding of C1'. Hence these features can be employed to predict the nature of tautomers in solution. A shielded signal in the region 150-152 ppm is the signature of *N1-H* tautomer. Unambiguous assignments could not be made for two of the systems viz. *p*-NO2Ph, *SO_2*-Propargyl (compound 1a) and *p*-NO_2Ph, *S*-Propargyl (compound 1b) due to exchange broadening of the triazole carbons.

Nevertheless, from the other NMR spectral features discussed above, a higher population of *N1-H* tautomer is expected in these systems.

Table 3A.11: *^{13}C Chemical shift C3,C5 and C1' carbons of tautomers in DMSO*.*

Compound	*N2-H* form 3b (ppm)			*N1-H* form 3a (ppm)		
	C3	C5	C1'	C3	C5	C1'
2, *p*-FPh, *S*-Propargyl	155.1	159.0	136.6	161.6	150.8	136.6
3, *p*-NO_2Ph, *S*-Allyl	153.8	160.5	123.8	160.5	152.8	127.9
4, *p*-ClPh, *S*-Propargyl	155.0	159.2	132.8	161.5	151.2	134.4
5, *p*-ClPh, *S*-Allyl	154.9	159.9	126.0	161.4	152.2	130.3
6, Furyl, *S*-Propargyl	147.9	158.4	142.3	155.4	150.3	146.1
1a, *p*-NO2Ph, *SO2*-Propargyl	165*	154*	132.7*	165*	154*	132.7*
1b, *p*-NO_2Ph, *S*-Propargyl	159.9*	151.8*	123.8*	159.9*	151.8*	127.9*

* For *p*-NO_2Ph, *SO_2*-Propargyl and *p*-NO_2Ph, *S*-Propargyl cases, unambiguous assignments could not be achieved due to broadness of the signals. The former compound showed exchange averaged signals at 165 ppm (C3) and 154 ppm (C5) and for the latter case, they were 159.9 ppm (C3) and 151.8 ppm (C3).

All the systems discussed so far exist in a dynamic equilibrium involving two tautomeric species in DMSO solution. The tautomers considered are present as *N1-H* and *N2-H* tautomeric form. The population of these tautomers varies with the system. In some of the cases studied, the dynamics seems to slow down with time. Variable temperature NMR measurements shows that the dynamics is very slow on the NMR time scale and the equilibrium is reversible in nature. ^{13}C NMR chemical shifts of the triazole ring carbons (C3 and C5) and C1' of the substituent are sensitive to the nature of the tautomers present. Triazole ring carbons adjacent to the ring NH is always found to be shielded. The NH proton of the *N2-H* tautomer is more deshielded than that of the *N1-H*

form. The NOESY data clearly shows the presence of inter molecular interactions between tautomers on the basis of which a dynamic equilibrium involving the two tautomers and a long living dimeric state is envisaged (Fig.3A.48).

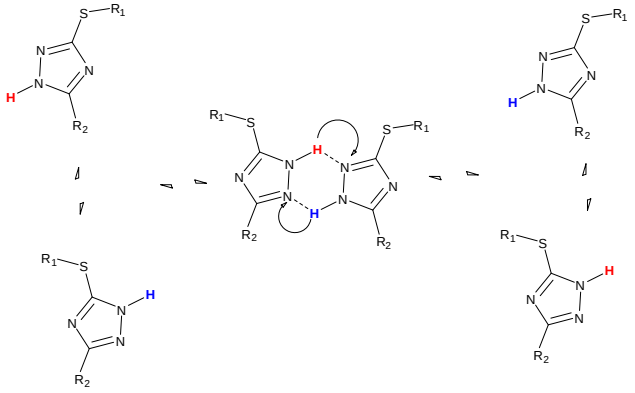

Fig.3A.48: *Proposed general dynamic model involving formation of dimeric structure comprising N1-H (3a) and N2-H (3b) tatuomer in DMSO solution on the basis of NMR studies for C,S disubstututed sulfanyl 1,2,4 triazoles.*

3.5 Part B: Tautomerism in disubstituted sulfanyl-1,2,4-triazole derivatives in solid state

The dynamic nature of the tautomeric species in solution and the related problems in their characterization has been discussed in the previous section. Solid state NMR technique is very handy in such situation for characterization. Of course, it will reflect the nature of tautomer present in the solid state which may or may not differ from that present in solution. A number of disubstitued sulfanyl 1,2,4-triazole systems have been investigated by ^{13}C CP-MAS, ^{15}N CP-MAS and ^{1}H MAS and the observations are discussed here. The systems studied are shown in Scheme.3B.1.

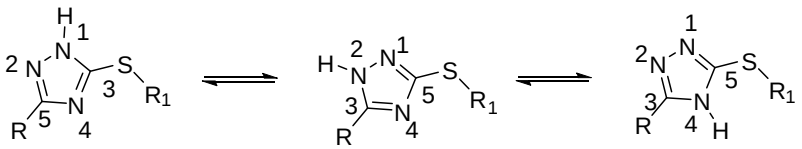

2a 2b 2c

1) R = H

2) R = CH_3

3) R = t-Bu

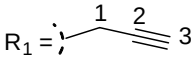

4) R = p-Chloro-phenyl

5) R = 4-fluoro-phenyl

6) R = 6a) 4-nitrophenyl and 6b) it's sulphone derivative

7) R = Furyl

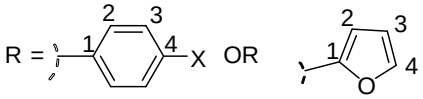

X = H, NO2, F.

8) R = 4-chlorophenyl

9) R = 4-nitrophenyl

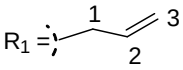

Scheme.3B.1: *Tautomers of S-substituted derivatives of the 3-substituted-1,2,4-triazole-5-thiones.*

Nine sulfanyl derivatives of 1,2,4 triazole have been investigated in solid state by ^{1}H MAS, ^{13}C CP-MAS and ^{15}N-CP-MAS experiments and the results of these studies are given below.

3.5.1 Compound 1: *S*-Propargyl sulfanyl 1,2,4 triazole

A 300 MHz ^{1}H MAS spectrum of compound 1 at 30 kHz spinning provided three signals at 17.45, 9.31 and at ~4.2 ppm (Fig.3B.1A.) The signal at 17.45 ppm corresponds to NH proton of 1,2,4-triazole ring while the signal resonating at 9.31 ppm is from the triazole ring proton H3. The propargyl group protons could not be differentiated. The narrow signal at 5.57 may be due to trace amount of water from the sample. Only an expanded center band of ^{1}H spectrum is shown in the figure. Hence the spinning side bands, which span either side of the center band, are not seen in the spectrum.

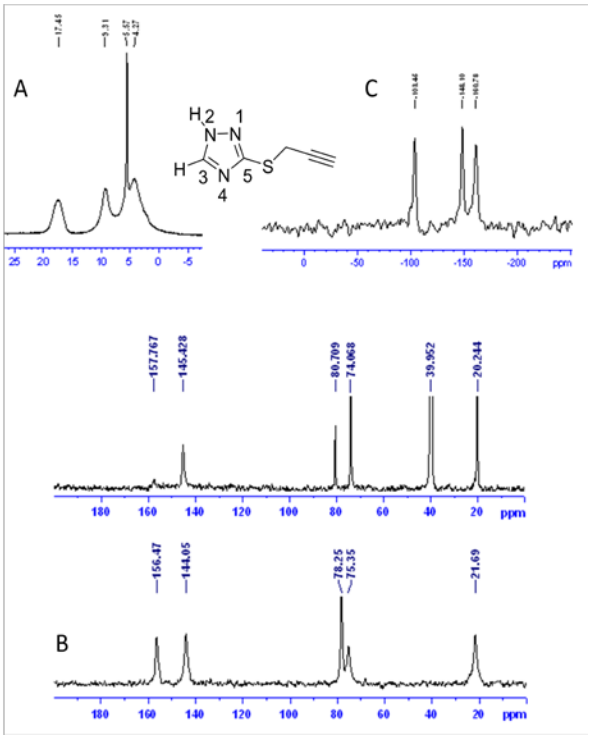

Fig.3B.1 : *^{1}H MAS (A, 300 MHz, spinning speed, ν_r= 30 kHz), ^{13}C CP-MAS (B, 75 MHz, ν_r= 8 kHz) and ^{15}N CP-MAS (C, 30 MHz, ν_r= 8 kHz) spectra of compound 1 (H-propargyl) at 298K. Solution state ^{13}C spectrum (100 MHz) in DMSO is also shown in B (upper trace) for comparison.*

Five resonance signals are seen in the ^{13}C CP-MAS spectrum which may be assigned by a comparison with the solution state NMR spectrum in DMSO (Fig.3B.1B).The most downfield carbon (156.47 ppm) is C5 while the signal at 144.05 ppm is C3. Assignment of the carbons of propargyl CH_2 group (21.69 ppm) and *sp* carbons (74-79 ppm) is straight forward. Attempts have not been made to differentiate the quaternary *sp* carbon. Similarity of chemical shift in solution and solid state is very

much evident from the Fig.3B.1B, which clearly shows that the same tautomer is present in both cases. In the solution state the *N2-H* (3b) tautomer is proposed on the basis of nOe between H3 and NH proton.[24]

The ^{15}N CPMAS spectrum (Fig.3B.1C) of the compound shows three peaks resonating at -160.78 ppm corresponding to N1, -103.45 (N2) and 148.10 ppm (N4). Chemical shifts obtained in the solution state were -173.6 (N1) and -101.6 ppm (N2). Chemical shift for N4 could not be obtained from solution state NMR. The difference seen for N1 is due to solvation effect. These chemical shifts can be considered as typical for the tautomeric form 3b in the solid state.

3.5.2 Compound 2: Methyl,*S*-Propargyl sulfanyl 1,2,4 triazole

In the ^{1}H MAS spectrum (Fig.3B.2A), NH proton resonates at 16.64 while the most upfield signal resonating at 3.45 ppm is from methyl protons. Other protons of propargyl group appear in the region 4-6 ppm . All the six carbons present in the compound are resolved in ^{13}C CPMAS spectrum (Fig.3B.2B). Solid state chemical shifts are very similar to that seen in solution state and hence the assignments are straight forward. Besides, it also suggests the similarity of the tautomer present in the solution (3b, confirmed by NOESY of CH_3 protons with NH proton) and solid state. ^{15}N chemical sifts of this compound are very similar to the previous case (Fig.3B.2C) and the changes in the chemical shifts seen are attributed to the substituent effect. The observed N1, N2 and N4 nitrogen chemical shifts are -166.21, -109.90, and -147.20, respectively while the solution state chemical shifts are -169.2 and -132.2 ppm for N1 and N4 (chemical shift of N2 signal could not be obtained in the solution state) .

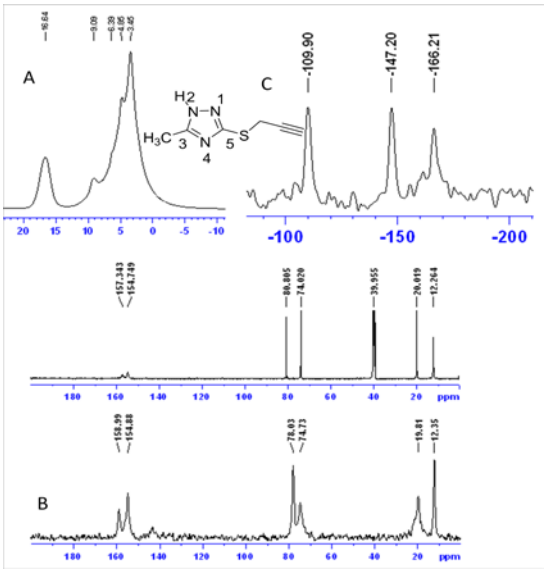

Fig.3B.2 :*[1]H MAS (A, 300 MHz, spinning speed, v_r= 30 kHz),[13]C CP-MAS (B, 75 MHz,v_r= 8 kHz) and [15]N CP-MAS (C, 30 MHz, v_r= 8 kHz) spectra of compound 2 (Me-propargyl) at 298K. Solution state [13]C spectrum (100 MHz) in DMSO is also shown in B (upper trace) for comparison.*

3.5.3 Compound 3: t Butyl,*S*- Propargyl sulfanyl 1,2,4 triazole

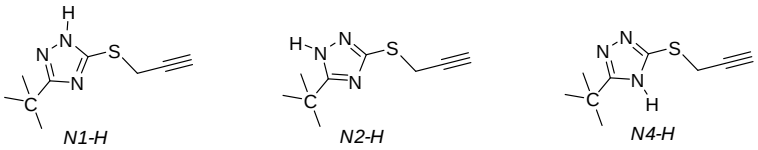

Sample spinning at 40 kHz is good enough to resolve all the proton resonances as shown in Fig.3B.3A. Only one deshielded NH signal is seen at 15.20 ppm. The shielded signal at 0.99 ppm is from protons of tertiary butyl group. The other signals corresponding to methylene and the alkynic protons appear in the range 2-4 ppm. A comparison of the solution state ^{13}C NMR spectrum and solid state CP-MAS spectrum is given in Fig.3B.3B which shows that ^{13}C chemical shifts are very close in both cases and indicate similar type of tautomer (3b as reported earlier) in solution as well as solid state. The assignments in solid state CP-MAS spectrum is accomplished by comparison with the solution state spectrum. Three different peaks seen in the ^{15}N CP-MAS spectrum (Fig.3B.3C) are assigned to N1 (-169.74 ppm) N2 (-100.74 ppm) and N4 (-

145.74 ppm) and are close to the values seen in the solution state HMBC spectrum (-174.2 ppm for N-1 and –102.1 ppm for N-2).

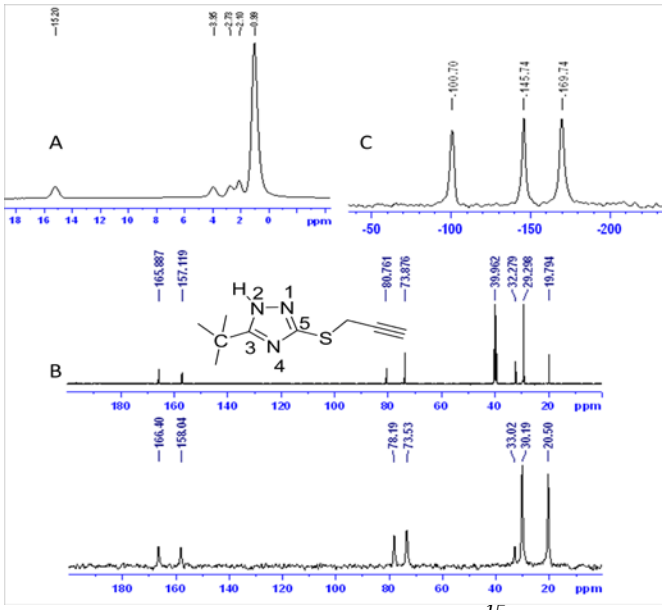

Fig.3B.3 : *^{1}H MAS (A, 700 MHz, spinning speed, ν_r= 40 kHz), ^{13}C CP-MAS (B, 75 MHz, ν_r= 8 kHz) and ^{15}N CP-MAS (C, 30 MHz, ν_r= 8 kHz) spectra of the compound 3 (t Bu-propargyl) at 298K. Solution state ^{13}C spectrum (100 MHz) in DMSO is also shown in B (upper trace) for comparison.*

3.5.4 Compound 4: *p* ClPh,*S*- Propargyl sulfanyl 1,2,4 triazole

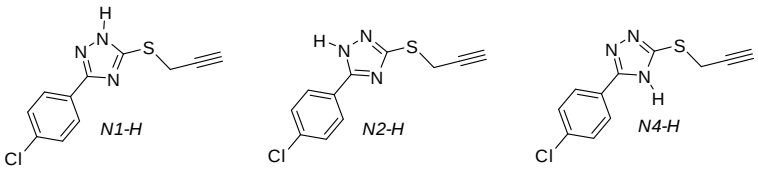

The ^{1}H solution state NMR spectrum of this compound showed the presence of two species in unequal intensity for NH protons while in the ^{1}H MAS spectrum (Fig.3B.4A) only one peak is observed in the downfield region corresponding to NH indicating that only one tautomeric form is present in the solid state. Aromatic protons resonate in the range 7-8.5 ppm while propargyl group protons resonate in the region 2.7-4 ppm. ^{13}C CPMAS spectrum (Fig.3B.4B) also supports that only one tautomer is

present in the solid state. A comparison with the solution state spectrum clearly demonstrates this.

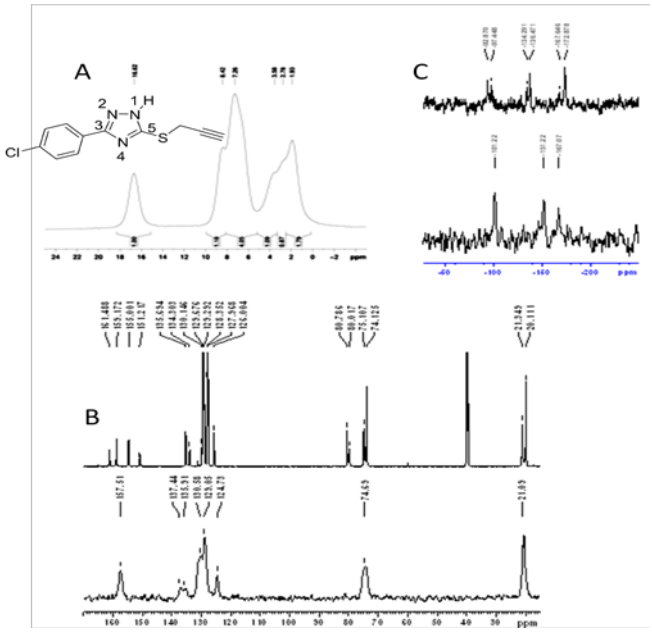

Fig.3B.4 : *^{1}H MAS (A, 700 MHz, spinning speed, ν_r= 40 kHz),^{13}C CP-MAS (B, 175 MHz,ν_r= 40 kHz) and ^{15}N CP-MAS (C, 40 MHz, ν_r= 8 kHz) spectra of compound 4 (p-Cl Phenyl-S-propargyl) at 298K. Solution state ^{13}C spectrum (175 MHz) in DMSO is also shown in B (upper trace) for comparison. ^{15}N NMR spectrum in solution state is also shown in C as the upper trace (70.97, DMSO-d6, 298K).*

Multiplicity of the C5 and C3 carbons (162-150 ppm region) seen in solution is no longer seen in the solid state. Moreover, both these carbons show same chemical shift (157.51 ppm) in the CP-MAS spectrum. Another interesting feature noticed in the CP-MAS spectrum is the overlap of the *sp* hybridized carbons of the propargyl group. ^{15}N CP-MAS spectrum (Fig.3B.4C) shows the presence of three signals corresponding to N1 (-167.1), N2 (-101.2) and N4 (-151.2). The solution state NMR showed six nitrogen signals (Fig.3B.4C, top trace). Solid state ^{15}N chemical shifts are comparable with those in solution except for N4 which is deshielded in solution by ~16 ppm. Unlike in solution, the *para* chloro derivative exists in one tautomeric form in solid state. But, it is difficult to judge the nature of the tautomer on the basis of ^{13}C due to the overlap of the

triazole carbons. Solution state NMR studies show a signal at ~ 151 ppm for the C5 carbon for the *N1-H* tautomer 3a. The absence of a signal around 150-152 ppm, supports the presence of *N2-H* tautomer in solid state.

3.5.5 Compound 5: *p* FPh,*S*-Propargyl sulfanyl 1,2,4 triazole

Solution state NMR studies of this compound, discussed in the previous section, (compound 2) indicted the coexistence of two tautomeric species 3a and 3b in DMSO solution. ^{1}H MAS spectrum (Fig.3B.5A) of this compound shows only one type of NH peak at 13.76 ppm. However, ^{13}C CP-MAS spectrum of this compound showed more number of signals than expected. A comparison of this with corresponding solution state NMR spectrum is shown in Fig.3B.5B. Multiplicity is clearly visible for the protonated aromatic carbons. For example, carbons *ortho* to fluorine (C3') appear at 116.5 ppm in solution while it showed two peaks at 115.8 and 118.7. Carbons *meta* to Fluorine substituent (C2') appears at 132.9 and 127.4 ppm compared to a signal at 128.9 in solution. C4' carbon shows a doublet feature in the region 165-160 ppm. The carbons of propargyl group do not exhibit any additional resonances.

Since the ^{13}C CP-MAS spectrum is recorded only with proton decoupling, the ^{19}F-^{13}C dipolar interactions will still persist. However, these interactions will be averaged at high spinning speeds at magic angle. Hence, at a spinning speed of 40 kHz employed in the experiment, only the $^{1}J_{CF}$ (~250Hz) is expected to survive. This will mainly affect the carbon atom to which the fluorine is bonded (C4'). Hence, the additional signals seen in the spectrum can either be due to two tautomers or due to various crystallographic arrangements of molecules in the unit cell. Multiplicity of signals in solid state NMR can arise due to polymorphism, solavtomorphism or due to the presence of more than one molecule in the unit cell which are inequivalent. Another possibility is the existence of the system as tautomeric polymorphs or tautomorphs i.e. crystal structure which contains different tautomeric structures. The exact reason for the

multiplicity of ^{13}C signals could not be ascertained due to lack of crystal structure for this compound. Attempts to crystallize this compound using various solvents did not provide good quality crystals. Absence of a signal at ~ 150 ppm in the CP-MAS spectrum is noticeable.

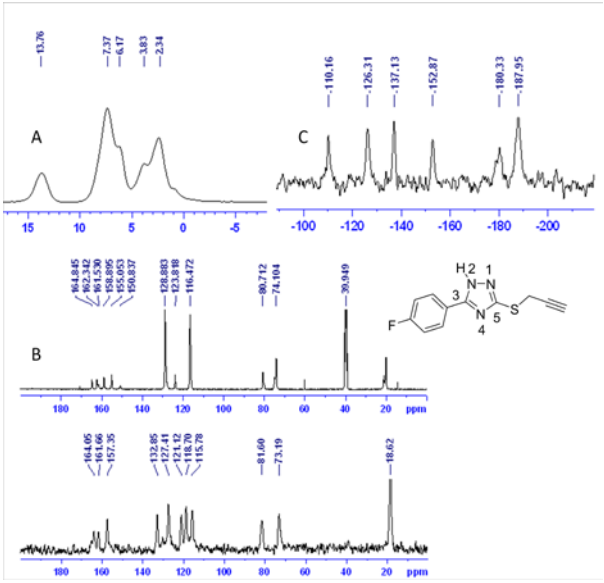

Fig.3B.5 : *^{1}H MAS (A, 700 MHz, spinning speed, ν_r= 40 kHz), ^{13}C CP-MAS (B, 175 MHz, ν_r= 8 kHz) and ^{15}N CP-MAS (C, 40 MHz, ν_r= 8 kHz) spectra of compound 5 (p-F-Ph,S-propargyl) at 298K. Solution state ^{13}C spectrum (100 MHz) in DMSO is also shown in B (upper trace) for comparison.*

Six well separated signals are observed in the ^{15}N CPMAS spectrum (Fig.3B.5C) indicating the presence of two chemically inequivalent molecules in the system which may be the two tautomeric forms (3a and 3b). Assignment of all the peaks to individual tautomers is difficult, although groups of signals for a particular type of nitrogen atom can be identified. Two most shielded signals, resonating at -187.95 and -180.33 ppm, are from the *sp3* hybridized nitrogen N-1 The most downfield signals resonating at -110.16 and -126.31 ppm are from the *sp2* hybridized nitrogen N-2 and the signals resonating at -137.13 and -152.87 ppm are from N-4. The observed chemical shift differences in the two forms of the molecules are very large which varies from ~6 to 16 ppm. The solution state chemical shift of N1 is -174 ppm.

3.5.6 Compound 6a: *p* NO_2Ph,*S*- Propargyl sulfanyl 1,2,4 triazole

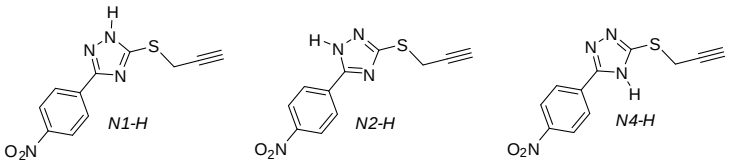

Proton MAS spectrum of compound 6a (Fig.3B.6A) shows two deshielded signals (12 to 14 ppm) which can be assigned to two types of NH protons. The solution state NMR measurements clearly demonstrated the presence of two tautomeric species. The integration of the NH signals indicated ~65:35 ratio, which is very close to what is observed in the solution state.

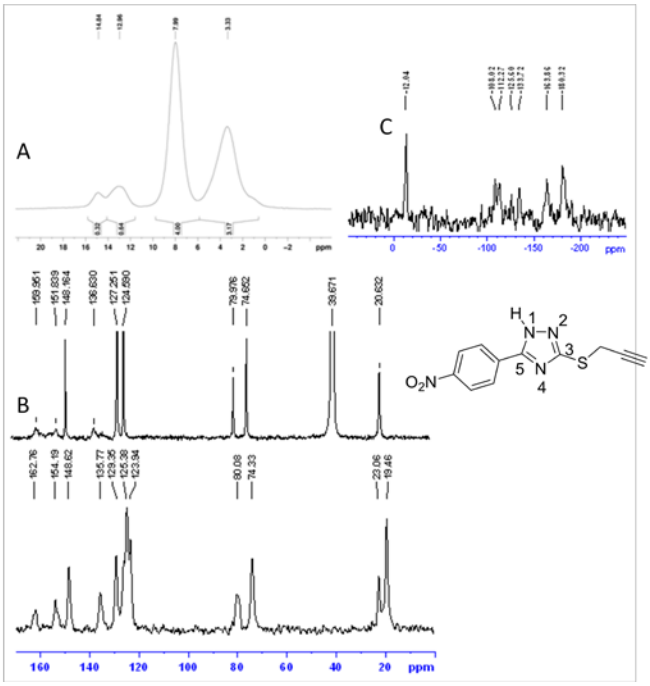

Fig.3B.6 : *^{1}H MAS (A, 700 MHz, spinning speed, o_r= 40 kHz),^{13}C CP-MAS (B, 175 MHz, v_r= 8 kHz) and ^{15}N CP-MAS (C, 40 MHz, v_r= 8 kHz) spectra of compound 6a (p-NO_2-Ph,S-propargyl) at 298K. Solution state ^{13}C spectrum (100 MHz) in DMSO is also shown in B (upper trace) for comparison.*

High speed (40 kHz) ^{13}C CP-MAS NMR spectrum (Fig.3B.6B) showed more signals than expected from the structure which has 9 chemically inequivalent carbons. The presence of two signals (19.53 and 22.74 ppm) corresponding to the *S*-methylene

group is striking, indicating that more than one tautomeric species is present in this compound. Aromatic carbon signals are also suggestive of coexistence of at least two chemically distinct molecules. In addition, the features (broadness with shoulder peak) of triazole C3 and C5 carbons favour this possibility. The ^{13}C CP-MAS spectrum is comparable with that in solution state, which is probably dominated by the *N1-H* tautomer, and indicates similarities in the nature of molecules.

The above conclusions are confirmed from ^{15}N CPMAS in Fig.3B.6C which show six signals for nitrogens corresponding to the two different 1,2,4-triazole moieties. However, only one signal for the aromatic nitro group is found, at ~ -12 ppm, probably due to its location which is away from the center of tautomerism. As discussed before, additional signals can also be expected due to reasons other than tautomerism such as polymorphism, solavtomorphism, etc. The question of solavtomorphism does not arise here as no signal from any solvent molecule is observed. The extra signals due to polymorphs can arise from different inter molecular hydrogen bonding patterns or as a result of different intermolecular arrangements of the aromatic rings. Inter molecular hydrogen bond patterns is known to alter ^{15}N chemical shifts considerably in solid state. Chemical shifts of a donor NH nitrogen undergo deshieling while that of a nitrogen acceptor, like *sp2* nitrogen, experience shielding effects. The donor- acceptor capability of various tautomers could be different and can thus shift resonances to different extents. The NH of the 1,2,4-triazole ring can form hydrogen bond either with triazole ring nitrogen of another molecule or with the oxygen of the nitro group in this system. In the former case, in which NH proton of one molecule forms a hydrogen bond with nitrogen of another molecule, it is less likely to affect the chemical shifts of all the three nitrogen atoms of the 1,2,4-triazole ring. Polymorphism involving hydrogen bonding of the triazole ring NH of one molecule with nitro group of another molecule should result in alteration of nitro group chemical shifts in different polymorphs. This is not observed in the present case since only one signal is seen for NO_2 group. Polymorphism due to different arrangements of the aromatic ring should also affect the chemical shifts of the nitro group. The above observations indicates that the extra signals observed for three nitrogen atoms of the 1,2,4-triazole ring are from the two different tautomeric species (tautomorphs) present in the system which is same as observed in the solution state. The

chemical shift obtained for N1 from solution state NMR is -170.2 (minor) and -166 (major). The chemical shifts observed for triazole ring nitrogen atoms are very similar to that observed in the *para* fluoro case discussed above.

3.5.7 Compound 6b: *p* NO_2Ph,SO_2 Propargyl sulfanyl 1,2,4 triazole

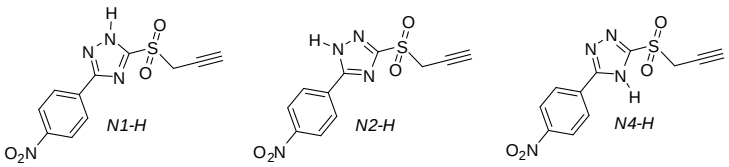

The solution state NMR studies on this suflone derivative showed indications of the existence of a dynamic situation even though separate resonance signals could not be seen. ^{13}C CP-MAS of the compound measured at 100 MHz at a spinning speed of 8 kHz is compared with the solution state NMR spectrum in Fig.3B.7A. A lot of spinning side bands are seen in the spectrum due to the large chemical shift anisotropy (CSA) associated with the aromatic group. Nevertheless, all the carbons of the molecule could be identified and assigned on the basis of solution state data. But, the resolution was not good enough to make any comments on the presence of additional signals.

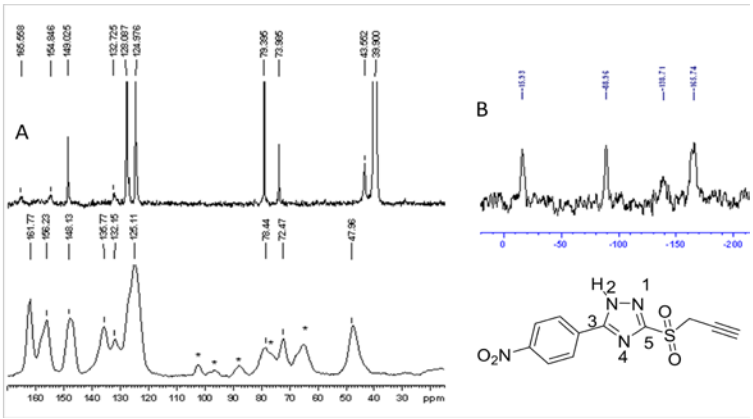

Fig.3B.7: *^{13}C CP-MAS (A, 100 MHz,v_r= 8 kHz) and ^{15}N CP-MAS (B, 40 MHz, v_r= 8 kHz) spectra of compound 6b (p-NO_2-Ph,SO_2-propargyl) at 298K. Solution state ^{13}C spectrum (100 MHz) in DMSO is also shown in A (upper trace) for comparison. Spinning side bands are marked by * in A.*

The ^{15}N CPMAS spectrum (Fig.3B.7B) of the compound shows four peaks indicating that only one type of molecule is present in solid state. However, the two

shielded signals, observed for N1 (-165.74 ppm) and N4 (-138.71 ppm), are relatively broader. The *sp2* hybridized nitrogen N2 shows a chemical shift of -88.96 ppm while the most downfield signal at -15.93 ppm is of the nitro group.

3.5.8 Compound 7: Furyl,*S* Propargyl sulfanyl 1,2,4 triazole

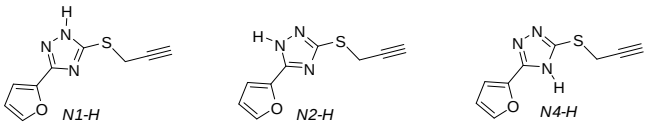

This furyl derivative showed the most dramatic behavior in solution state among all the systems studied, which has been discussed in the previous section. ^{1}H MAS spectrum (Fig.3B.8) of the compound shows one deshielded signal at 13.92 ppm assignable to NH proton of 1,2,4-triazole ring while the peaks corresponding to the furyl ring resonates in the region 6-8 ppm and the most upfield signals resonating at 2-4 ppm are from protons of propargyl group.

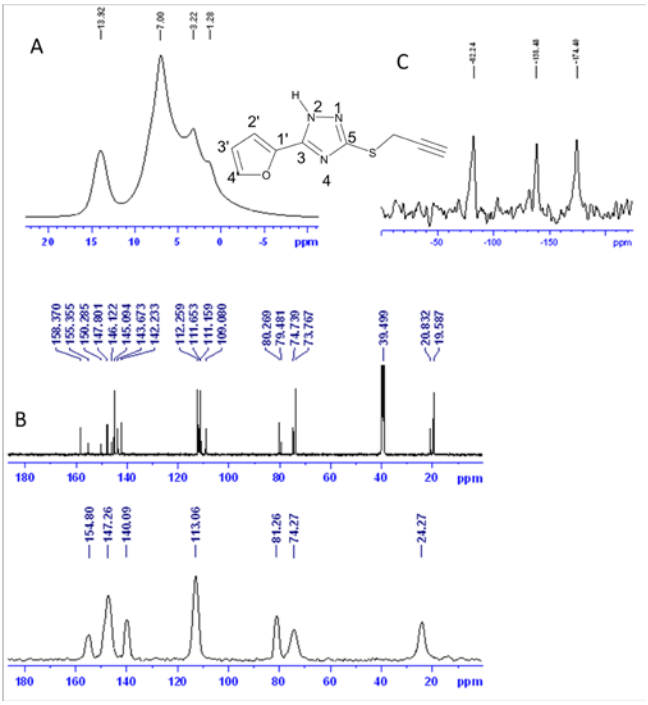

Fig.3B.8: *^{1}H MAS (A, 300 MHz, spinning speed, ν_r= 30 kHz),^{13}C CP-MAS (B, 75 MHz, ν_r= 8 kHz) and ^{15}N CP-MAS (C, 30 MHz, ν_r= 8 kHz) spectra of compound 7 (Furyl S-propargyl) at 298K. Solution state ^{13}C spectrum (100 MHz) in DMSO is also shown in B (upper trace) for comparison.*

^{13}C CP-MAS spectrum of this compound (Fig.3B.8B) showed fewer signals than expected due to the overlap of signals in the aromatic region (100-160ppm). The deshielded signals at 154.8 and 147.3 ppm can be assigned unambiguously to the traizole carbons C3 and C5. Furyl C4' carbon also appears at ~ 147 ppm. Absence of signals below 155 ppm suggest the presence of *N1-H* form in solid state. This chemical shift (154.8ppm) nearly matches with that of the minor *N1-H* tautomer (155.36 ppm) present in solution state. Assignments of the other signals are straight forward. The ^{13}C signals are found to be broad and may have to do with lack of crystalline behavior of the system. Usually, ^{13}C resonance signals of poorly ordered or amorphous systems are broader than their crystalline analogues.

The ^{15}N CPMAS spectrum (Fig.3B.8C) of the compound clearly shows the presence of only one type of environment as only three signals at -174.56 ppm (N1) at -138.82 ppm (N4) and -82.31 ppm (N2) are observed. The chemical shift observed for N1 in solution state is -174.63 (major) and -168.58 (minor), which is very close to what is measured in the CP-MAS spectrum.

3.5.9 Compound 8: *p* ClPh,*S*- Allyl sulfanyl 1,2,4 triazole

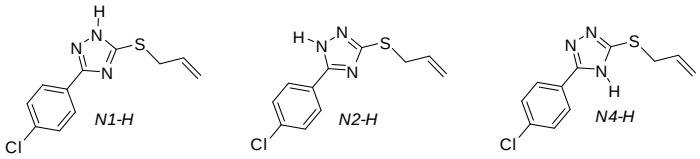

The solid state ^{13}C CP- MAS spectrum (Fig.3B.9A) supports the presence of one tautomer in the solid state. It is very evident from the figure that only two triazole carbons are seen in the low field region (159.96 and 157.18 ppm) compared to four signals in the solution state. Signals in the range 140 to 118 ppm are of aromatic carbons of the *para* nitro phenyl group. The absence of signals in the 155-150 ppm for C3/C5 carbon atoms favours the *N2-H* tautomer. The C5 chemical shift of *N1-H* tautomer in DMSO is 152.16 ppm.

^{15}N CP-MAS spectrum (Fig.3B.9B) of this compound showed only three peaks (-170.52 ppm for N-1, -153.14 ppm for N4 and -102.45 ppm for N2) and thereby confirms the presence of only one tautomer in the solid state. However, solution state spectra clearly showed that the molecule exists in a dynamic equilibrium involving two equally populated tautomers 3a and 3b. The N1 chemical shifts are comparable with those observed in the solution state (-174.3 and -169.2 ppm).

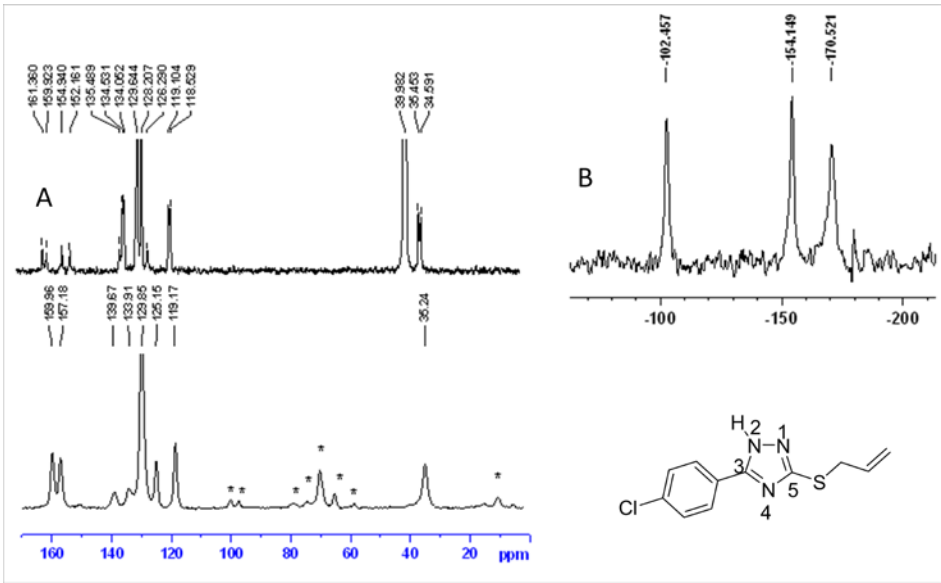

Fig.3B.9 : *^{13}C CP-MAS (A, 100 MHz, ν_r= 8 kHz) and ^{15}N CP-MAS (B, 40 MHz, ν_r= 8 kHz) spectra of compound 8 (p-Cl-Ph,S-allyl) at 298K. Solution state ^{13}C spectrum (100 MHz) in DMSO is also shown in A (upper trace) for comparison. Spinning side bands are marked by * in A. Full ^{13}C CPMAS spectrum is not shown and hence the SSB on the low field regions are not shown.*

3.5.10 Compound 9: *p* NO_2Ph,*S*- Allyl sulfanyl 1,2,4 triazole

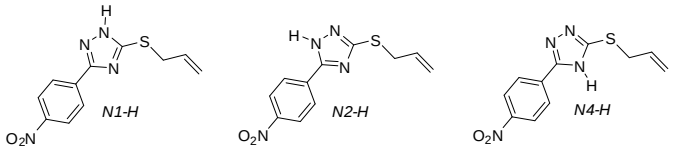

In Fig.3B.10, a comparison of ^{13}C CP-MAS spectrum of the *para* nitro, *S*-allyl compound recorded at two different magnetic fields at two different spinning speeds are shown to emphasize the advantage of sample spinning at higher speed. Spinning side

bands (SSB) flanking either side of the isotropic peak can clearly be seen in the spectrum obtained at 8 kHz spinning (at 100 MHz), whereas the spectrum at 40 kHz spinning is completely devoid of SSB's . Other spectral features are nearly identical except for the sharpening of the CH_2 carbon signal at ~40 ppm due to better ^{1}H decoupling in the spectrum recorded at 175 MHz. The ^{13}C CP-MAS spectrum (Fig.3B.11A) does not show any additional lines and indicates the presence of one type of tautomer which is also in agreement with the ^{15}N CP-MAS spectrum (Fig.3B.11B) that

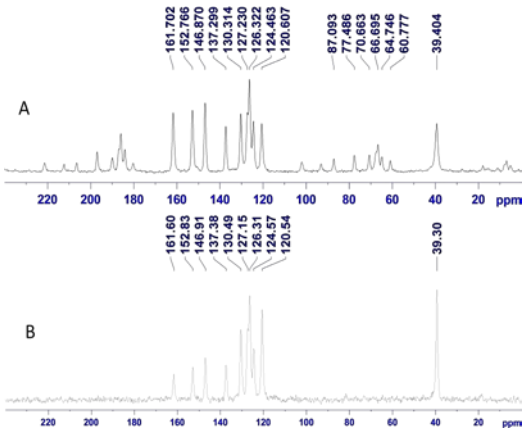

Fig.3B.10 : *Comparison of ^{13}C CPMAS spectra of compound 9 at two magnetic fields and spinning speeds. A)100 MHz at 8 kHz spinning and B)175 MHz, 40 kHz*

showed four peaks (three from the triazole ring and one from NO_2 group). The chemical shifts obtained from solid state ^{15}N and ^{13}C spectra nearly match with those from solution state NMR (Fig.3B.11A,B). Exact nature of the tautomer could not be ascertained from the ^{13}C chemical shifts of triazole ring carbons due to the overlap of resonances of C3/C5 carbons of *N1-H/N2-H* tautomers. Solution state measurements showed that C5 chemical shift of *N2-H* form (160.5 ppm) is close to C3 chemical shift of *N1-H* form (160.5 ppm) and C3 chemical shift of *N2-H* form (153.8ppm) is also close to C5 carbon of *N1-H* form (152.8 ppm). The ^{1}H MAS of the compound shown in Fig.3B.11C, indicates the presence of one NH signal at 13.26 ppm.

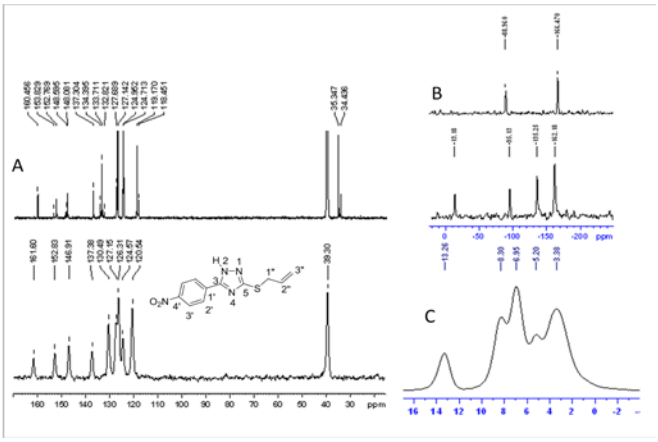

Fig.3B.11: *^{13}C CP-MAS (A, 175 MHz, ν_r= 8 kHz) and ^{15}N CP-MAS (B, 70 MHz, ν_r= 8 kHz) and ^{1}H MAS (C, 700 MHz, spinning speed, ν_r= 40 kHz), spectra of compound 9 (p-NO_2-Ph,S-allyl) at 298K. Solution state ^{13}C spectrum (100 MHz) in DMSO is also shown in B (upper trace) for comparison.*

A comparison of the ^{1}H chemical shifts observed for the NH protons of all the compounds in solution and solid state is shown in Table 3B.1. ^{1}H chemical shift of proton donors like NH group is very sensitive to its hydrogen bonding with other acceptors. They experience downfield shift in presence of acceptors and the magnitude of the shift provides a measure of hydrogen bond strength. In DMSO solution, solvent molecules also act as inter molecular hydrogen bond acceptor and the observed chemical shift is more dominated by this. In solid state intermolecular interaction is the source of hydrogen bond acceptors. In solution NH proton chemical shifts of the compound studied span a range of ~1.2 ppm (13.7 to 14.9 ppm) whereas in the ^{1}H MAS spectrum it is ~4.5 ppm (13 to 17.5 ppm). Maximum deshielding is observed for the unsubstituted case (*S*-propargyl 1,2,4 triazole) while the minimum is for one of the NH protons of the *p*-NO2 propargyl derivative. It is interesting to note that the ^{1}H chemical shift of the donor NH group is relatively shielded in the molecular systems which showed the presence of more than one tatuomer in solution, suggesting weaker inter molecular interactions in the solid state. Besides, solution state NMR shows that *N1-H* protons are shielded compared to *N2-H* protons.

Table 3B.1: *Comparison of ^{1}H Chemical shifts of NH in solid state and solution state.*

Substituent	^{1}H, δ_{NH} solild	^{1}H, δ_{NH} solution
H, *S* propargyl	17.45	14.14
Me, *S* propargyl	16.64	13.69
tBu, *S* propargyl	15,50	13.67
p-Cl-Ph, *S* propargyl	16.62	14.64,14.36
p-F-Ph, *S* propargyl	13.71	14.56,14.30
p-NO_2-Ph, *S* propargyl	14.48,12.96	14.96,14.54
furyl, *S* propargyl	13.92	14.64,14.34
p-NO_2-Ph, *S* allyl	13.26	14.90,14.46

Comparison of the ^{15}N chemical shifts (Table 3B.2) in solid state also provides some interesting insights. N1 of *S* propargyl 1,2,4 triazole case (unsubstituted) is found to be the most deshileded (~-160 ppm) while that of the furyl derivate is the most shielded (-174.6 ppm) among the systems that gave only one set of signals (*p*-NO2 propargyl and *p*-F-propargyl are excluded) in ^{15}N CP-MAS spectrum. This is also in agreement with the ^{1}H chemical shift observed for the corresponding NH protons. The *para* fluoro propargyl cases show two N1 nitrogen signals which are considerably shielded at -187 and -180 ppm while in the corresponding *para* NO_2 case, two signals appear at -163.9 and -180.3 ppm. The N2 chemical shift also shows similar variations. N2 of the furyl is most deshielded at -82.3 ppm while that of the methyl is the most shielded (-109.9), if the *para* nitro propargyl and *para* fluoro propargyl cases are excluded. The N2 nitrogen is a hydrogen bond acceptor and hence suggests that N2 of the furyl case is a weaker acceptor. In the *para* fluoro (-110.16, -126.3ppm) and *para* nitro (-108.0, -112.27) propargyl cases, the N2 is more shielded than even the methyl case. The N4 chemical shift varied from -135 ppm (for *p*-NO2-Ph, *S* -allyl) to -153 ppm (*p*-Cl-Ph, *S*- allyl) for the systems studied. The furyl case (-138.8ppm) it is closer to the deshielded side while in the methyl case (-147ppm) to the shielded side. It is likely that the substituent in the phenyl ring may also contribute to the chemical shift by modification of the electron density on N4. Nitro group is a strong electron withdrawing group while chloro group attached to aromatic ring is electron donating by mesomeric effect. Comparison of the N4 chemical shift of *p*-Cl-Ph, *S* -propargyl (-151.2 ppm) and *p*-Cl-Ph, *S* -allyl (-153.14 ppm) demonstrate that the substituent on the sulphur atom does not alter the chemical

shift. It is worthwhile to have a comparison of the N4 chemical shift of *p*-NO_2-Ph, *S*-allyl and *p*-NO_2-Ph, *S*- propargyl systems since both have the same substituent on the aromatic ring and hence should have similar effect on the triazole ring. The *p*-NO_2-Ph, *S*- propargyl compound shows two signals at -125.6,-133.7 ppm. One of them (-133.7 ppm) is very close to the N4 chemical shift observed for *p*-NO_2-Ph, *S*-allyl case (-135.3 ppm) and indicate similarities in their structural features. The other signal (-125.6 ppm) of *p*-NO_2-Ph, *S*-propargyl is deshielded by ~10 ppm suggesting a site with weaker hydrogen bond acceptor capability. Similarly in the *p*-F-Ph, *S* -propargyl case, which also show two resonances for N4 (at -137.13, -152.87 ppm), the shielded signal is closer to that observed for the *p*-Cl-Ph, *S* propargyl system, the nearest analogue that has been studied. In short, the ^{15}N chemical shifts provide information about the differences in the solid state structural features in the systems investigated which will also have implications in their solution state behavior. Two of the systems investigated, *viz,* the *para* fluoro and *para* nitro propargyl cases, definitely behave differently from others.

Table 3B.2: *Comparison of ^{15}N Chemical shifts of triazole ring nitrogen atoms in solid state and solution state.*

Substituent	^{15}N, δ_{NH} solid (solution)		
	N1	N2	N4
H, *S* propargyl	-160.76 (-173.6)	-103,45 (-101.6)	-148.10
Me, *S* propargyl	-166 (-169.2)	-109.9	-147 (-132)
tBu, *S* propargyl	-169.7 (-174.2)	-100.7 (-102.1)	-145.7
Furyl, *S* propargyl	-174.6 (-174.6,-168.6)	-82.3	-138.8
p-Cl-Ph, *S* propargyl	-167.1 (-167.6,-172.9)	-101.2 (-92.9,-97.5)	-151.2 (-134,3,-136.5)
p-Cl-Ph, *S* allyl	-170.5 (-174.3,-169.2)	-102.4	-153.14
p-NO_2-Ph, *S* allyl	-162.2 (-166)	-95.1 (-88)	-135.3
p-NO_2-Ph, *S* propargyl	-180.3,-163.9 (-170,-166)	-108.0,-112.27	-125.6,-133.7
p-F-Ph, *S* propargyl	-187, -180 (-174)	-110.16,-126.3	-137.13,-152.87

Comparison of the ^{13}C chemical shifts of the triazole ring carbons and the carbon of the substituent attached to triazole ring in solid state and solution is given in Table 3B.3. In general they are found to be comparable except in the cases where more than one signal is seen in the solution state. The effect of solvation is not as pronounced as those observed in the case of ^{15}N NMR since the carbon atoms are not directly involved in interaction with the solvent.

Table 3B.3: *Comparison of ^{13}C Chemical shifts of C3, C5 and C1' carbon atoms in solid state and solution state.*

Substituent	^{13}C, δ solid (solution)		
	C3	C5	C1'
H, *S* propargyl	156.47 (157.76)	144.05 (145.42)	-
Me,*S* propargyl	158.99 (157.34)	154.88 (154.75)	19.81 (20.01)
t-Bu,*S* propargyl	158.08 (157.12)	166.40 (165.39)	30.19 (32.20)
furyl,*S* propargyl	154.80 (158.37, 150.28)	147.26 (147.8, 155.35)	140.09 142.26,146.12)
p-Cl-Ph,*S* propargyl	157.51 (150.83,158.90)	157.51 (161.53,155.05)	135.91,137.44 (134.24,135.64)
p-Cl-Ph, *S* allyl	157.18 (159.87,152.02)	159.96 (161.28,154.6)	139.67, 133.9 (135.5,134.0)
p-NO_2-Ph,*S* allyl	152.76 (152.76)	161.60 (160.38)	137.8 (137.23)
p-NO_2-Ph,*S* propargyl	154.59 (151.84)	162.76 (159.65)	135.77 (135.77)
p-F-Ph,*S* propargyl	157.35 (158.90,150.83)	157.51 (155.0,161.47)	121.82 (123.8,128.7)

3.6 Conclusions:

From the above studies it can be concluded that *S*-propargylated/allylated derivatives of 1,2,4-triazole thione and some of the substituted 1,2,4-triazole thiones (methyl, tertiary butyl, p-chloro-phenyl, furyl etc.) exist only in one tautomeric form 3b in the solid state while when the substituent is *p*-fluoro-phenyl and *p*-nitro phenyl, both the tautomeric forms 3a and 3b exist.

3.7 Overall conclusion of the solution and solid NMR studies:

It is clear from the discussions in this chapter that in most of the disubstituted sulfanyl derivates of 1,2,4 triazoles studied, two tatutomeric forms in dynamic equilibrium coexist in DMSO which is likely to be same in solid state, at least in two cases studied. In DMSO, the dynamics between the tautomers seem to slow down with time and give rise to separate ^{1}H, ^{13}C and ^{15}N resonances. Only two of the tautomeric forms (3a and 3b) corresponding to *N1-H* and *N2-H* forms, respectively have been considered in the equilibrium. A dimeric model involving these two tautomers is proposed on the basis of the inter molecular nOe cross peaks. Comparison of ^{1}H,^{13}C and ^{15}N chemical shifts obtained in the solid and solution state provides useful insights into the molecular environments.

References:

[1]. Dhiman; S.; Anna; R.; Prabhakar; A,; Joshi, R. R.; Khedkar, V. M.; **Jul 7, 2016** WO 2016108249 A1**.**

[2]. Francesco, D.; Maria E. J., Heffernan, P.; Hamilton, T.; Matthew L. W.; Soth, M. P.; Burke, J. P.; Le, Kang; C., Christopher L.; Palmer, W.; Lewis, R.; McAfoos, T.; Czako, B.; Liu, G.; Theroff, J.; Herrera, Z.; Yau, A. **Jan 7, 2016** WO 2016004404 A2**.**

[3]. Michael;S. K.; Pham, S. M.; Williams, D. C.; **Apr 4, 2013** WO 2013049591 A2**.**

[4]. Papakonstantinougaroufalia, S.S.; Tani, E.; and Todoulou, O.; *J. Pharm. Pharmacol.*, **1998**, ***1***, 117.

[5]. Chorab, M. M.; El-Sharief, A. M. Sh.; and Ammar, J.A.; *Phosphorus Sulfur Silicon Relat. Elem.*, **2001**, *173*, 223.

[6]. Chu, C.H.; Zhang, Y.; and Zhang, Z.Y.; *Indian J. Chem., Sect. B,* **2000**, *39*, 791.

[7]. US Patent no. 6 919 342, 2005; *Ref. Zh., Khim.*, **2006**, *9* 107.

[8]. Shaker, R.M.; Mahmoud, A.F.; and Abdal-Lafit, F.F.; *Phosphorus, Sulfur Silicon*, **2005**, *180*, 397.

[9]. Chu, C.H.; Zhang, Y.; Zhang, Z.Y.; Li, Z.-C.; and Liao, R. A.; *Indian J. Chem., Sect. B*, **2000**, 39, 791.

[10]. Aldoshin, S.M.; Sanina, N.A.; Rakova, O.A.; Shilov, G.V.; Kulikov, A.V.; Shul'ga, Yu.M.; and Ovanesyan, N.S.; *Izv. Ross. Akad. Nauk, Ser. Khim*., **2003**, 8, 1614.

[11]. Oprean, L.; David, L.; Zaharia, V.; Conisa, A.; and Oprean, R.; *Stud. Univ. Babes-Bolyai, Chem*., **2002**, *47*, 179

[12]. Trzhtsinskaya, B.V.; Aleksandrova, A.E.; and Apakina, E.V.; *Khim.-Farm. Zh*., **1991**, *25*, 25.

[13]. Mir, I. and Siddigui, M.T.; *Tetrahedron*, **1970**, *26*, 5235.

[14]. Ersan, S.; Nacak, S.; and Berkem, R.; *Farmaco*, **1998**, *53*, 773.

[15]. Amir, M. and Kumar, S.; *Pharmazie*, **2005**, *60*,175

[16]. Szilagyi, G.; Somorai, T.; Bozo, E.; Lango, J.; Nagy, G.; Reiter, J.; Janaky, J.; and Andrasy, F.; *Eur. J. Med. Chem*., **1990**, *25*, 95.

[17]. Wujec, M.; Pitucha, M.; Dobosz, M.; Kosikowkcu, U.; and Malm, A.; *Acta Pharm. (Croatica)*, **2004**, *54*, 251; *Ref. Zh., Khim*., **2005**, 291.

[18]. El-Barbary, A.A. and Abou-El-Ezz, A.Z.; *Phosphorus, Sulfur Silicon*, **2004**, *179*, 1497.

[19]. US Patent no. 6 600 057, **2003**.

[20] Kalman, A. and Argay G. Y.; *Journal of Molecular Structure*, **1983**, *102*, 391.

[21] Siedle, A. R.; Robert J.; Webb, R. A.; Newmark, M. B.; David A.; Weil, K. E; Fred. E.; Behr, V. G.; Young J.; *Journal of Fluorine Chemistry* , **2003**, *122*, 175.

[22]. Phalgune,U. D. ;Vanka, K.;and Rajamohanan P, R.; *Magn. Reson. Chem*. **2013**, *51*, 767.

[23]. Buzykin, B. I.; Mironova, E. V.; Nabiullin, V. N.;. Azancheev, N. M.; Avvakumova, L. V.; Rizvanov, I. Kh.; Gubaidullin, A. T.; Litvinov, I. A and Syakaev, V. V.; *Russian Journal of General Chemistry*, **2008**, *78*,461.

[24]. Preeti M.; Chaudhary, S. R.; Chavan, M.; Kavitha, S. P.; Maybhate, S. R.; Deshpande, A. P.; and Rajamohanan P. R.; *Magn. Reson. Chem.* **2008**, *46*, 1168.

[25]. Minkin, V.I.; Garnovskii, A.D.; and Elguero, J.; *Adv. Heterocycl. Chem.,* **2000**, 76, 157.

[26]. Claramunt, R.M.; Elguero, J.; and Katritzky, A.R.; *Adv. Heterocycl. Chem.,* **2000**, 77, 1.

[27]. Kubota, S. and Uda, M.; *Chem. Pharm. Bull.*, **1975**, *23*, 955.

[28]. Litchman, W.M.; *J. Heterocycl. Chem.,* **1982**,*19*, 1235.

[29]. Sorescu, D.C.; Bennett, C.M.; and Thompson, D.L.; *J. Phys. Chem. A,* **1998**, *102*, 10348.

[30]. Claramunt, R.M.; Lopez, C.; Garcia, M.A. and Otero, M.D., *New J. Chem.,* **2001**, *25*, 1061.

[31]. Katritzky, A.R.; Lue, P.; and Yannakopoulou, K.; *Tetrahedron,* **1990**, *46*, 641.

[32]. Maretina, I.A.; *Russ. J. Org. Chem.,* **2005**, *41*, 1.

[33]. Lipson, V.V.; Desenko, S.M.; Borodina, V.V.; Shirobokova, M.G.; and Musatov, V.I., *Russ. J. Org.Chem.,* **2005**, *41*, 114.

[34]. Buzykin, B. I.; Mironova, E. V.;Nabiullin, V. N.; Gubaidullin, A. T. and Litvinov, I. A.; *Russian Journal of General Chemistry,* **2006**, *76, 1471*.

[35]. Goldstein, P.; Ladell, J.;and Abowitz, G.; *Acta Crystallogr., Sect. B,* **1969**, *25*, 135.

[36]. Starova, G.L.; Frank-Kamenetskii, O.V.; Makarskii, V.V.; and Lopyrev, V.A.; *Kristallografiya,* **1978**, *23*, 849.

[37]. Evrard, G.; Durant, F.; and Michel, A.; *Bull. Soc. Chim. Belg.*, **1984**, *93*, 233.

[38]. Delage, C.; Lagorce, J.-F.; and Raby, C.; *Acta Crystallogr., Sect. C,* **1988**, *44*, 2187.

[39]. Nieuwenhuyzen, M.; Keirse, R.; Shaw, B.; and Vos, J.G.; *Acta Crystallogr., Sect. C,* **1999**, *55*, 264.

[40]. Aouial, M.; Viallefont, P.; and Ammari, L.El.; *Acta Crystallogr., Sect. C,* **1991**, *47*, 1866.

[41]. Garcia, E. and Lee, K.-Y.; *Acta Crystallogr., Sect. C,* **1992**, *48*, 1682.

[42]. Borbulevych, O.Ya.; Shishkin, O.V.; and Desenko, S.M.; *Acta Crystallogr., Sect. C,* **1998**, *54*, 442.

[43]. Nikitina, E.V.; Starova, G.L.; Frank-Kamenetskaya, O.V.; and Pevzner, M.S.; *Kristallografiya,* **1982**, *27*,485.

[44]. Rusinov, V.L.; Pilicheva, T.L.; and Tumashev, A.A.; *Khim. Geterotsikl. Soedin.*, **1990**,*12*, 1632.

[45]. Wawrzycka, I.; Koziol, A.E.; and Walesa, K.G.; *Z. Kristallogr.*, **2000**, *215*, 766.

[46]. Prins, R.; Birker, P.J.M.W.L.; and Verschoor, G.C.; *Acta Crystallogr., Sect. B*, **1982**, *38*, 2934.

[47]. Starova, G.L.; Frank-Kamenetskaya, O.V.; and Shibanova, E.F.; *Kristallografiya*, **1980,** *25*, 1292.

[48]. Bradshaw, J.S., Nielsen, R.B., and Tse, P.-K., *J. Heterocycl. Chem.*, **1986**, *23*, 361.

[49]. Siedle, A.R., Webb, R.J., and Newmark, R.A., *J. Fluorine Chem.*, **2003**, *122*,175.

[50]. Nieuwenhuyzen, M., Keyes, T.E., Gallagher, J.F., and Vos, J.G., *Acta Crystallogr., Sect. C*, **1997**, *53*, 1873.

[51]. Starova, G.L., Frank-Kamenetskaya, O.V., and Makarskii, V.V., *Kristallografiya*, **1990**, *35*,769.

[52]. Vereshchagin, A.N; Moscow: Nauka, **1988**.

[53]. Hansch, C., Leo, A., and Taft, R.W., *Chem. Rev.*, **1991**, *91*, 165.

[54]. (a) Olofson, R. A.;. Kendall, R. V.; *J. Org. Chem.* **1970**, *35*, 2246; (b) Zoltewicz, J. A.; Deady, L. W.; *J. Am. Chem. Soc.* **1972**, *94*, 2765.

[55]. Starova, G.L., Frank-Kamenetskaya, O.V., and Makarskii, V.V., *Kristallografiya*, **1990**, *35*, 769.

[56]. Kereselidze, Dzh.A., Zarkua, T.Sh., and Kikalishvili, T.Dzh., *Usp. Khim.*, **2002**, *71*,1120.

[57]. Lebedev, A.V., Lebedeva, A.B., Sheludyakov, V.D., Kovaleva, E.A., Ustinova, O.L., and Kozhevnikov, I.B., *Russ. J. Gen. Chem.*, **2005**, *75*, 782.

[58]. Nikulin, V.V., Artamonova, T.V., and Koldobskii, G.I., *Russ. J. Org.* Chem., **2005**, *41*,444.

CHAPTER IV:

NMR studies on the mixed hybrid derivatives of 1,2,4 and 1,2,3-triazoles.

Aim: The aim of this part of the thesis is to characterize hybrid molecular systems that contains 1,2,3-triazole and 1,2,4-triazole moieties in the same molecule using nuclear magnetic resonance techniques. Self assembling behavior of these systems is also examined in addition to their binding ability to halogen atoms.

Introduction

Triazoles are synthetic heterocyclic compounds which finds applications in various research fields including biological sciences,[1] materials chemistry,[2] medicinal chemistry,[3] and synthetic organic chemistry.[4] Triazoles are key intermediates for the synthesis of many biologically active heterocycles like thiazolo-triazoles [5a] and bistriazoles[5b] and many triazole derivatives are used as drugs, a few of which are shown in Scheme.4.1. Many hybrid triazoles, which contain triazole moiety along with another pharmacophore in the same molecule, are also being investigated for their biological activity, especially to overcome the problem of drug resistance.[6] Hybrid triazoles are also known to be molecular systems of considerable interest.[7]

In the present work, characterization of some hybrid triazole derivatives using NMR spectroscopic techniques are discussed in addition to their self assembling property and interaction with halogen ions. This chapter is divided into two parts. Part A deals with the structural characterization of hybrid triazoles and their self assembling nature and part B discusses their interaction with halogen atoms.

Scheme.4.1**:** A few triazole based biologically active derivatives.

Experimental

Synthesis: The triazoles derivatives were synthesized by following reported procedures. [8,9].

4.2.1 Method of synthesis:

a. Preparation of 1-formylthiosemicarbazide: To a stirred solution of thiosemicarbazide 10 g (1 equivalent) in 30 ml of water, formic acid (25 ml) was added (see eq 1). The reaction mixture was heated at 80^0C and was stirred for an hour after reaching the desired temperature. The completion of the reaction was checked by TLC. The reaction mixture was then cooled and filtered. The product formed (Scheme 4.2), 1-

formylthiosemicarbazide, is soluble in water.hence, water was removed from the filtrate using a rotary evaporator at 60^0C and again filtered to get 1-formylthiosemicarbazide (white coloured solid 10.243 gm) which was used as such without further purification in the preparation of 1,2,4-triazole-5-thione (Scheme.4.2).

b. Preparation of 1,2,4-triazole-5-thione:- 1-formylthiosemicarbazide(10.243 gm) was taken in R.B. and 30 ml of 10% NaOH was added to it. The resulting mixture was heated at 80^0C and stirred for 3 hours. Completion of the reaction was checked by the TLC. The solution was cooled and acidified with conc. HCl, following which, 1,2,4-triazole-5-thione precipitates on cooling.

Scheme.4.2: Synthesis of a model 1,2,4-triazole.

c. General experimental protocol for propargylation of triazole thiols : To stirred solution of thiones (1mmol) in DMF (10ml) in a round bottom flask, potassium carbonate (2.4 mmol) was added followed by addition of propargyl bromide (2.2 mmol). The reaction mixture was stirred at room temperature for 4-6 hrs (Scheme.4.3). Completion of the reaction was monitored by TLC. DMF was removed under vacuum; reaction mixture was partitioned between ethyl acetate and water. Organic phase was washed with water and brine, dried over sodium sulphate, and then concentrated to get the crude product. Column chromatographic separation of the crude product on silica gel furnished mono and dipropargylated products.

These regioisomers were utilized for the preparation of hybrid systems with 1,2,3-triazole by Huisgens (1 +3)Cu(1)catalyzed dipolar cycloaddition with benzyl azide to obtain hybrid triazoles (Scheme 4.4) studied in this chapter. .

Synthesis of benzyl azide:

Safety Comment: Sodium azide is very toxic, hence precautions should be taken since low molecular weight organic azides are potential explosives Generally, when the total number of carbon (*N*C) plus oxygen (*N*O) atoms is less than the total numbers of nitrogen atoms (*N*N) by a ratio of three, i.e., (*N*C + *N*O) / *N*N < 3, the compound is considered as an explosive hazard. In those instances, the compound was prepared immediately before use. A standard PVC blast shield was used when necessary.

Procedure: Benzyl bromide (2 gm, 1 eq.) was dissolved in acetone and sodium azide was added followed by catalytic amount of TEBA (Scheme.4.3). The resulting reaction mixture was stirred at 65°C for 5 hours. The completion of the reaction was checked by TLC. Benzyl bromide and benzyl azide have the same RF value on TLC but benzyl azide becomes yellowish after charring.

Workup:- Acetone was removed using rotary evaporator and the compound was dissolved in the organic layer (ethylacetate) which was washed successively with water and brine. The crude compound was dried over sodium sulphate and purified by column chromatography to obtain 70-83% yield.

Reaction:

Scheme.4.3: Synthesis of the benzyl azide.

The general procedure for the synthesis of triazoles is as follows:

General experimental protocol for preparation of 1,2,3 triazoles: To a stirred solution of propargylated derivatives **(**1 mmol) and benzyl azide (1mmol) in 10 ml of t-butanol /water (8:2) in a round bottom flask; copper sulphate (24mg, 5 mole%) and sodium ascorbate (40 mg, 10 mol%) was added. The reaction mixture was stirred at room temperature for 4 to 12 hrs. Completion of the reaction was monitored by TLC. Tertiary

butanol was removed under reduced pressure and the reaction mixture was extracted with ethyl acetate. The organic phase was washed with water and brine, dried over sodium sulphate and concentrated to furnish the pure product. Cu(1) catalysed reactions, can give rise to undesired oxidized products. Exclusion of oxygen is required to prevent these by-products, therefore a reducing agent Na ascorbate is used along with the copper salt $CuSO_4.5H_2O$.

NMR

4.2.2 General Experimental: All the NMR measurements were carried out on a Bruker AV 400 MHz (unless otherwise stated) spectrometer operating at 400.13, 100.62, and 40.55 MHz for ^{1}H, ^{13}C,and ^{15}N nuclei, respectively. Experimental conditions are same as given in Chapter -II. For the dilution studies a concentrated solution of the compound (100 mM) was made and after recording ^{1}H nmr spectrum, the sample was subsequently diluted by adding the solvent. This procedure was repeated till the 1mM concentration is achieved.

4.3 Part A: NMR characterization of the hybrid derivatives of 1,2,4 and 1,2,3-triazoles

Result and discussions:

In this chapter, we have studied three major kinds of mixed triazoles depending on the position of the substituent and the triazoles moieties as shown in Scheme.4A.1.

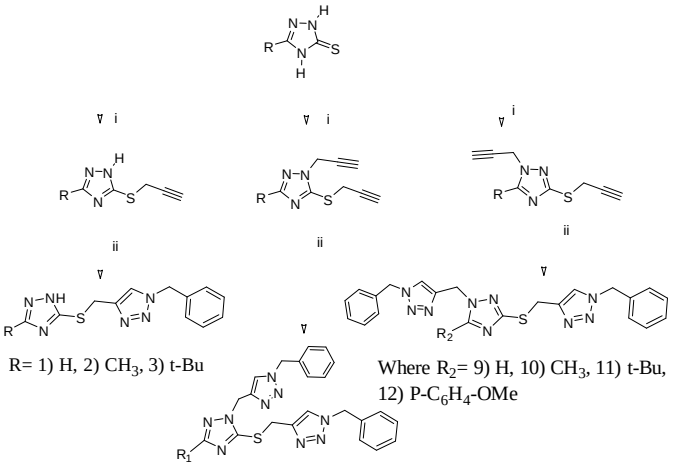

R= 1) H, 2) CH_3, 3) t-Bu

Where R_2= 9) H, 10) CH_3, 11) t-Bu, 12) P-C_6H_4-OMe

R_1 = 4) H, 5) CH_3, 6) t-Bu, 7) p-C_6H_4-Cl, 8) p-C_6H_4-OMe.

Reagents:

i) K_2CO_3, dry DMF, proporgyl bromide, ii) Benzyl azide, Na ascorbate, CuSO4, t-BuOH, H_2O.

Scheme.4A.1: *General scheme for the synthesis of hybrid triazole derivatives studied.*

It can be seen from the Scheme.4A.1 that the molecules 4-12, have four methylene groups linked to triazole rings. Out of these, two methylene groups are linked to triazole nitrogen atoms as well as to an aromatic ring. One of the remaining methylene groups is attached to a sulphur atom that connects two triazole rings while the remaining CH_2 group, links the two triazole rings through a carbon atom. The chemical shift of the methylene group directly bonded to sulphur is expected to appear up field compared with those bonded to nitrogen. However, identification of the chemical shifts for the remaining three methylene groups is very difficult from a 1D spectrum alone as each group forms one bond with nitrogen and a second bond with the aromatic ring. Similarly, assignments of triazole ring carbons and nitrogens are also not straight forward. The present investigation describes the use of homonuclear and heteronuclear 1D and 2D NMR experiments to arrive at unambiguous assignments of all the protons, carbons and nitrogens in the systems investigated shown in Scheme.4A.2 and3.

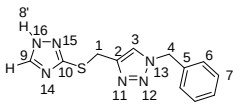

comp. 1

4-(((1 *H*-1,2,4-triazol-5-yl)thio)methyl) -1-benzyl-1 *H*-1,2,3-triazole

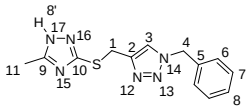

comp. 2

1-benzyl-4-(((5-methyl-1 *H*-1,2,4-triazol-3-yl)thio) methyl)-1*H*-1,2,3-triazole

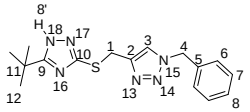

comp. 3

1-benzyl-4-(((5-(*tert*-butyl)-1 *H*-1,2,4-triazol-3-yl) thio)methyl)-1*H*-1,2,3-triazole

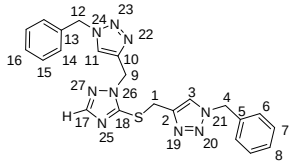

comp. 4

1-benzyl-4-(((1-((1-benzyl-1 *H*-1,2,3-triazol-4-yl)methyl) -1*H*-1,2,4-triazol-5-yl)thio)methyl)-1 *H*-1,2,3-triazole

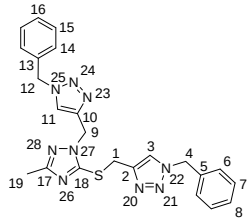

comp. 5

1-benzyl-4-(((1-((1-benzyl-1 *H*-1,2,3-triazol-4-yl)methyl) -3-methyl-1 *H*-1,2,4-triazol-5-yl)thio)methyl)-1 *H*-1,2,3-triazole

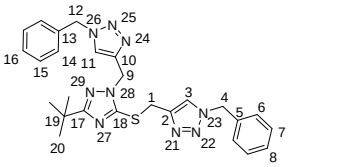

comp. 6

1-benzyl-4-(((1-((1-benzyl-1 *H*-1,2,3-triazol-4-yl)methyl)-3- (*tert*-butyl)-1 *H*-1,2,4-triazol-5-yl)thio)methyl)-1 *H*-1,2,3-triazole

Scheme.4A.2: *The numbering pattern adopted and the IUPAC names of the compounds 1-6.*

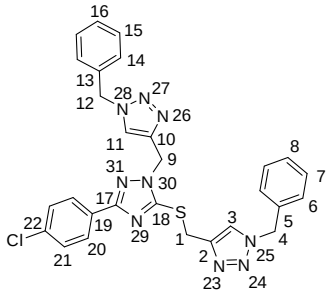

comp. 7

1-benzyl-4-(((1-((1-benzyl-1 *H*-1,2,3-triazol-4-yl)methyl)-3-(4-chlorophenyl) -1*H*-1,2,4-triazol-5-yl)thio)methyl)-1 *H*-1,2,3-triazole

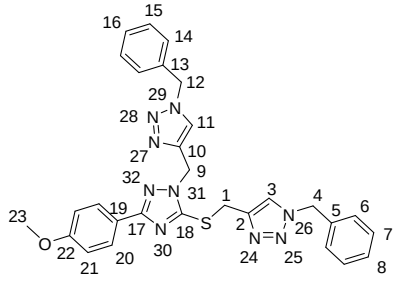

comp. 8

1-benzyl-4-(((1-((1-benzyl-1 *H*-1,2,3-triazol-4-yl)methyl)-3-(4-methoxyphenyl)-1 *H*-1,2,4-triazol-5-yl)thio)methyl)-1 *H*-1,2,3-triazole

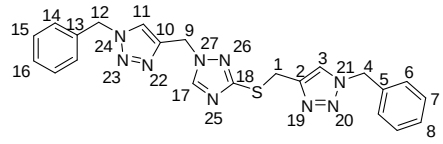

comp. 9

1-benzyl-4-(((1-((1-benzyl-1 *H*-1,2,3-triazol-4-yl)methyl) -1*H*-1,2,4-triazol-3-yl)thio)methyl)-1 *H*-1,2,3-triazole

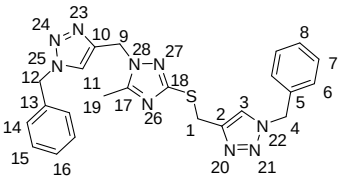

comp. 10

1-benzyl-4-(((1-((1-benzyl-1 *H*-1,2,3-triazol-4-yl)methyl) -5-methyl-1*H*-1,2,4-triazol-3-yl)thio)methyl)-1 *H*-1,2,3-triazole

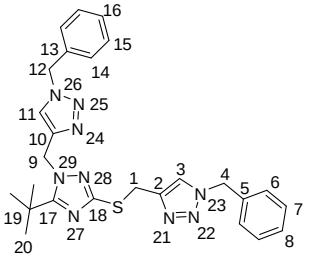

comp. 11

1-benzyl-4-(((1-((1-benzyl-1 *H*-1,2,3-triazol-4-yl)methyl)-5-(*tert*-butyl)-1*H*-1,2,4-triazol-3-yl)thio)methyl)-1 *H*-1,2,3-triazole

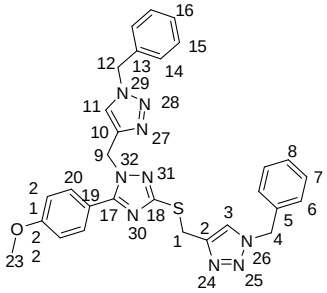

comp. 12

1-benzyl-4-(((1-((1-benzyl-1 *H*-1,2,3-triazol-4-yl)methyl)-5-(4-methoxyphenyl)-1 *H*-1,2,4-triazol-3-yl)thio)methyl)-1 *H*-1,2,3-triazole

Scheme.4A.3: *The numbering pattern adopted and the IUPAC names of the compounds 7-12.*

4.3.1 Compound 1: 4-(((1H-1,2,4-triazol-5-yl)thio)methyl)-1-benzyl-1H-1,2,3-triazole:

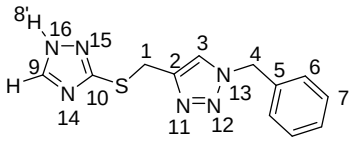

comp. 01

4-(((1 *H*-1,2,4-triazol-3-yl)thio)methyl)-1-benzyl-1 *H*-1,2,3-triazole

^{1}H and ^{13}C NMR chemical shifts:

^{1}H NMR (400 MHz, 298^{0}K; solvent $CDCl_3$ δ=7.27 ppm) , δ = 4.36 ppm (s, 2H), 5.41 ppm (s, 2H), 7.16 ppm (m, 2H), 7.26 to 7.30 ppm (m, 3H), 7.53 ppm (s, 1H), 8.17 ppm (s, 1H), 11.08 ppm (s, 1H).

^{13}C NMR (100 MHz, 298^{0}K; solvent $CDCl_3$, δ = 77.00 ppm), δ = 26.67 ppm, 54.07 ppm, 122.79 ppm, 127.87 ppm, 128.57 ppm, 128.89 ppm, 134.1 ppm, 144.62 ppm, 146.57 ppm, 155.88 ppm.

The ^{1}H and ^{13}C NMR spectral details are given in Figs.4A.1 and 4A.2. Though the compound can exist in two tautomeric forms (Chapter III), detailed investigations are not performed to identify its nature in solution. Only the major tautomeric form is considered here. The chemical shifts of different protons, carbons and nitrogens in compound 1 are assigned on the basis of the observations made from the various 1D/2D NMR experiments as discussed below.

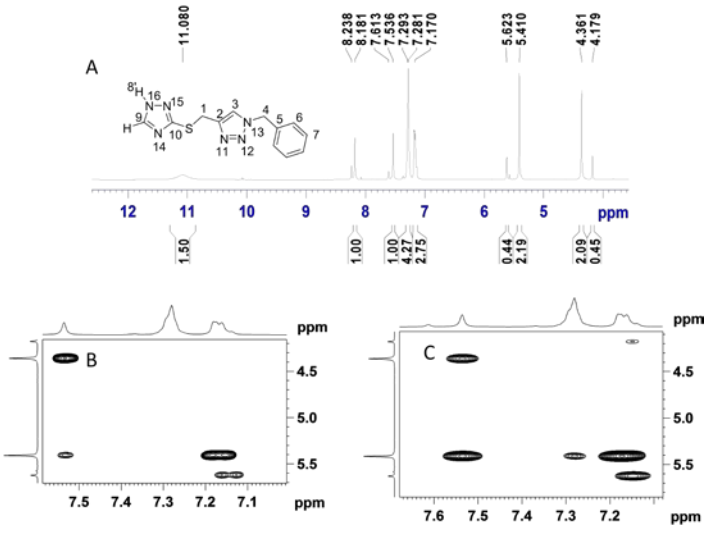

Fig.4A.1: A)*[1]H NMR spectrum of compound 1. B) Expanded COSY (B) and NOESY (B) spectrum showing Correlations of CH_2 protons with aromatic protons. (400 MHz, $CDCl_3$, 298 K).*

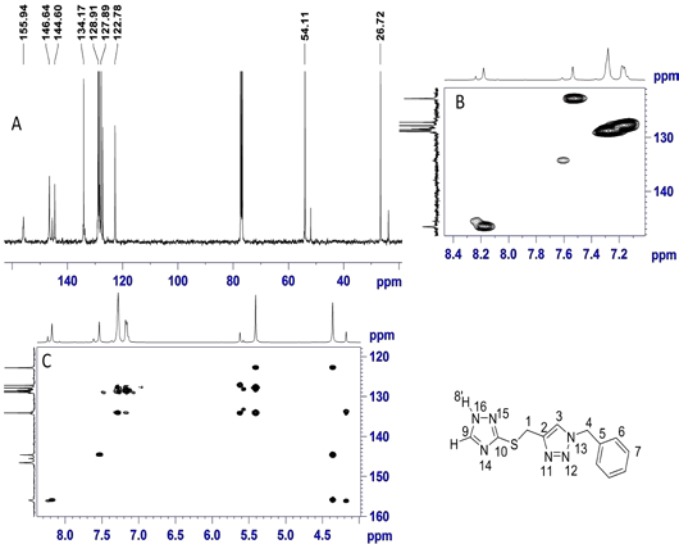

Fig.4A. 2: *100 MHz ^{13}C NMR spectrum (A) and selected ^{1}H-^{13}C HSQC (B) and HMBC (C) spectra of compound 1 ($CDCl_3$, 298 K).*

The ^{1}H spectrum (Fig.4A.1) does not show any visible splitting due to scalar couplings which can usually be employed for signal assignments. In this molecule there are two methylene protons. Out of these one at higher field (4.36 ppm) is assigned to *S*-CH_2 group (H-1) and the other (5.41ppm) to the methylene group attached to nitrogen (H-4). There are two triazole ring protons on each of the triazole rings. The COSY spectrum of the compound is shown in Fig 4A.1B. Stronger cross peaks are seen only for some protons in the aromatic region. But, weak cross peaks due to long range couplings are noticed between the protons in the aromatic region and CH_2 protons.

The proton on the 1,2,3 triazole ring (H-3) is expected to show long range J coupling with the *S*-CH_2 (H-1) as well as the Ar-CH_2 protons (H-4) and hence is assigned to the signal at 7.53 ppm (H-3). This helps in the assignment of Ar-CH_2 protons (H-4) at 5.41 ppm. Weak correlation of this with *ortho* protons of the aromatic ring (H-6

at 7.16) is also observable. The remaining singlet at 8.17 ppm is the 1,2,4 triazole ring proton (H-9). The H-3 protons show NOE correlations with H-1 as well as H-4 indicating that these groups are spatially closer (Fig.4A.1C). The H-6 shows NOE correlations with the H-4 protons. The cross peak from the NH signal could not be observed probably due to exchange with residual water in $CDCl_3$ solvent. The homonuclear correlations are summarized in Table 4A.1

Table 4A.1: *Homonuclear correlations observed for compound 1*.

The Carbon and the proton number	^{1}H chemical shifts (ppm)	correlation with (ppm)	Remarks
1	4.36	7.53	COSY/NOESY
3	7.53	5.41	COSY/NOESY
4	5.41	7.16	COSY/NOESY

One of the carbon signals at 143.24 is found to be broad. ^{1}H-^{13}C HSQC spectrum (Fig.4A.2B) \ shows that this corresponds to C9 of the triazole ring. The broadness is due to co existence of two tautomers in which the NH protons hops between N16 and N15 (see numbering in the molecule). ^{1}H-^{13}C HSQC spectrum further shows that the methylene protons in each group are equivalent. C-10 carbon shows the 3-bond ^{1}H-^{13}C HMBC correlations (Fig.4A.2C) with H-9 as well as H-1. C-2 to H-1 & H-3(2-bond correlations), C-3 to H-1(3-bond correlations) C-4 to H-3 & H-6 (three bond correlations), H-4 to C-5 & C-6 correlations are observed which are used for unambiguous assignments of all the carbons and protons in the molecule (Table 4A.2).

Table 4A.2: *^{1}H-^{13}C HSQC/HMBC correlations obtained for compound 1.*

The Carbon and the proton number	^{1}H chemical shifts (ppm)	^{13}C chemical shifts (ppm)	Remarks
1	4.36	26.67 144.62, 122.79, 155.88	HMBC
3	7.53	122.79 144.62, 54.07	HSQC HMBC
4	5.41	54.07 122.79, 134.1, 127.87	HSQC HMBC

6	7.16	127.87 54.07	HSQC HMBC
9	8.17	146.57 155.88	HSQC HMBC

^{1}H-^{15}N HMBC: Polarization transfer delay in the experiment is optimized for 2-3 bond heteronuclear correlations corresponding to a long range coupling of coupling constant of 8 Hz. The ^{1}H-^{15}N HMBC experiment (Fig.4A.3) is very useful in confirming assignments as well as to obtain the ^{15}N chemical shifts of various nitrogen atoms from the F1 projection. N-11 shows 3-bond correlations with H-1 and H-3. N-13 shows 2-bond correlations with H-3 as well as H-4 protons and from its chemical shifts (-132.75 ppm) it is clear that it is sp^3 hybridized nitrogen. N-12 also shows 3-bond correlations with H-4 and appears at -20.8 ppm. The chemical shift of N-12 is typical of sp^2 hybridized nitrogen flanked by the two nitrogens which results in deshielding. The 1,2,4-triazole ring

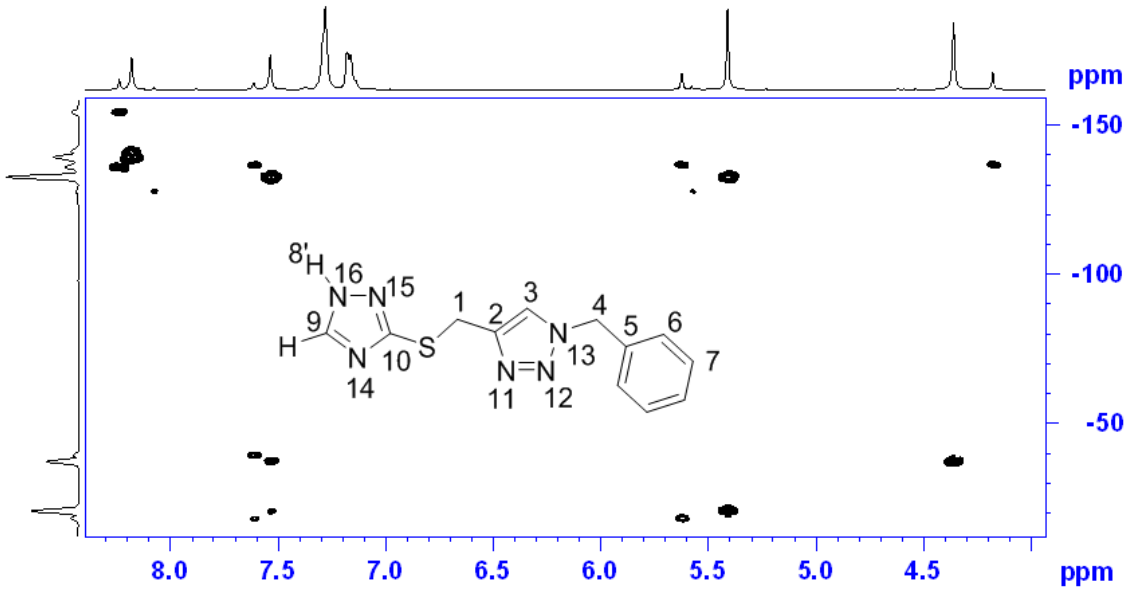

Fig.4A. 3: *^{1}H-^{15}N- HMBC spectrum of the compound 1 (400 MHz, $CDCl_3$, 298 K).*

Nitrogen atoms N-14 and N-15 shows two bond correlations with H-9. Out of these two nitrogens, N-15 is expected to show relatively downfield shift since it is directly bonded with another nitrogen, therefore, it has a chemical shift of -139.28 ppm and the N-14 has

a chemical shift of -141.03 ppm. Various ^{1}H-^{15}N NHBC correlations are presented in Table 4A.3 and the complete assignment is given in Table 4A.4. Scheme. 4A.4 represents some of the important correlations observed schematically.

Table 4A.3:*^{1}H-^{15}N HMBC correlations observed for compound 1*:

Nitrogen atom	^{1}H chemical shifts (ppm)	^{15}N chemical shifts (ppm)
11	4.36	-37.1
12	5.41	-20.8
13	7.53, 5.41	-132.75
14	8.17	-141.03
15		-139.28
16	-	-

Scheme.4A.4: *Pictorial representation of the various correlations obtained for the compound 1.*

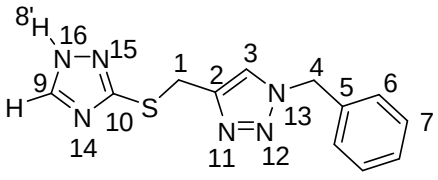

comp. 01

Table 4A.4: *Chemical shift assignment of compound 1*

Atom number	δ_H ppm	δ_C or δ_N ppm	Atom number	δ_H ppm	δ_C or δ_N ppm
1	4.36	26.67	9	8.17	146.57
2		144.62	10	-	155.88
3	7.53	122.79	11	-	-37.1
4	5.41	54.07	12	-	-20.8
5		134.1	13	-	-132.75
6	7.16	127.87	14	-	-141.03
7	-	-	15	-	-139.28
8	-	-	16	-	-
8’	11.08	-			

4.3.2 Compound 2: 1-benzyl-4-(((5-methyl-1H-1,2,4-triazol-3-yl)thio)methyl)-1H-1,2,3-triazole:

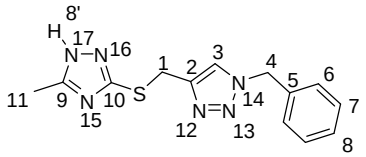

comp. 02

1-benzyl-4-(((5-methyl-1 *H*-1,2,4-triazol-3-yl)thio) methyl)-1*H*-1,2,3-triazole

^{1}H and ^{13}C NMR chemical shifts

^{1}H NMR (400 MHz, 298^{0}K; solvent $CDCl_3$ δ=7.27 ppm), δ = 2.29 ppm (s, 3H), 4.28 ppm (s, 2H), 5.38 ppm (s, 2H), 7.14 ppm (s, 2H), 7.23 ppm to 7.28 ppm (m, 3H), 7.49 ppm (s, 1H).

^{13}C NMR (100 MHz, 298^{0}K; solvent $CDCl_3$, δ = 77.00 ppm), δ = 11.55 ppm, 26.33 ppm, 53.97 ppm, 122.61 ppm, 127.60 ppm, 128.35 ppm, 128.69 ppm, 134.10 ppm, 144.54 ppm, 155.29 ppm, 156.74 ppm.

The ^{1}H NMR spectrum of compound 2 (Fig.4A.4A) is very similar to the previous sample except for the absence of 1,2,4 triazole ring proton and the presence of a methyl signal at 2.30ppm. The H-4, H-1 and H-6 signals are assigned on the basis of weak COSY(Fig.4A.4B) and NOESY (Fig.4A.4C)cross peak due to long range coupling (Table 4A.5).

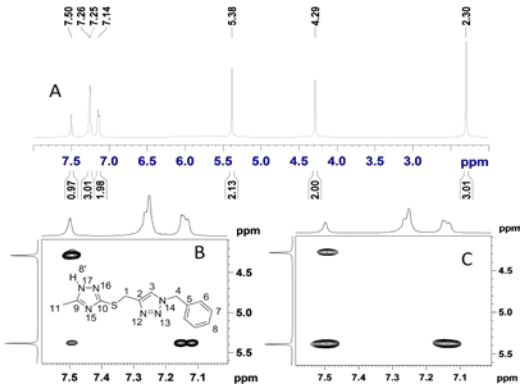

Fig.4A.4: *A)^{1}H NMR spectrum of compound 2. B) Expanded COSY (B) and NOESY (B) spectrum showing Correlations of CH_2 protons with aromatic protons. (400 MHz, $CDCl_3$, 298 K).*

Various carbons are assigned on the basis of HSQC and HMBC (Fig.4A.5 A,B) experimental data which are summarized in Table 4A.6 The two carbons from the 1,2,4-triazole ring are the most deshielded carbons. Out of these C-9 shows 2-bond HMBC correlations with the methyl protons, H-11, and hence could be assigned to the carbon at 155.29. The three bond correlation of the *S*-CH_2 protons to the 1,2,4 triazole carbon (C-10) is also observed. All the assignments are given in Table 4A.7. ^{1}H-^{15}N HMBC spectrum is shown in Fig.4A.6 and the correlations are shown in the pictorial form in Scheme.4A.5.

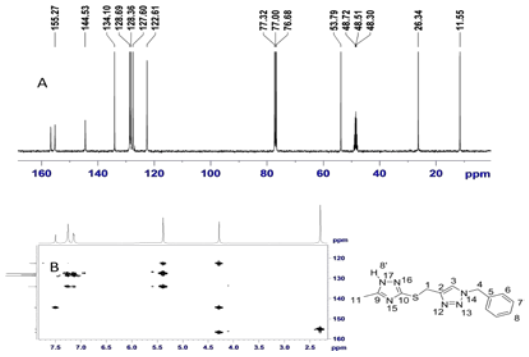

Fig.4A. 5: *100 MHz ^{13}C NMR spectrum (A) and HMBC (B) spectrum of compound 2 ($CDCl_3$+ Methanol d_4, 298 K).*

Table 4.6: *Homonuclear correlations observed for compound 2.*

^{13}C and ^{1}H No.	^{1}H chemical shifts (ppm)	correlation with (ppm)	Remarks
1	4.28	7.49	COSY/NOESY
3	7.49	5.38	COSY/NOESY
4	5.38	7.14	COSY/NOESY

Table 4A.7: *^{1}H-^{13}C HSQC/HMBC correlations obtained for compound 2.*

The Carbon and the proton number	^{1}H chemical shifts (ppm)	^{13}C chemical shifts (ppm)	Remarks
1	4.28	26.33 156.74, 144.54, 122.61	HSQC HMBC HMBC
3	7.49	122.61 144.54, 53.97	HMBC
4	5.38	53.97 122.61, 134.10, 127.60	HSQC HMBC
6	7.14	127.60 53.97, 134.10	HSQC HMBC
7	7.26	128.69 134.10	HSQC HMBC
11	2.29	11.55 155.29	HSQC HMBC

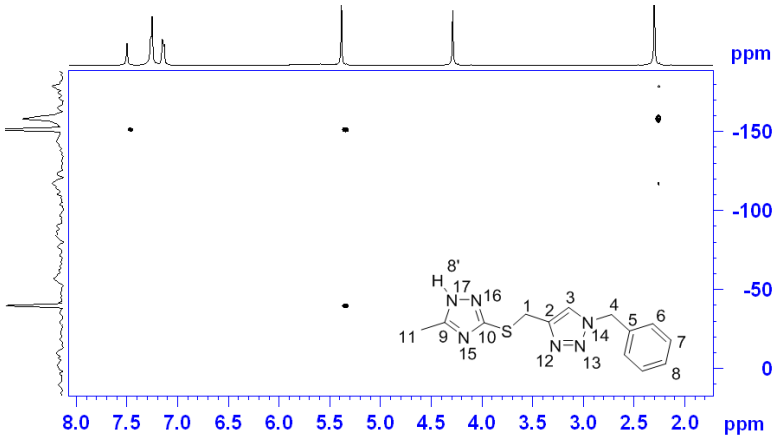

Fig.4A. 6: *^{1}H-^{15}N- HMBC spectrum of the compound 2 (400 MHz, $CDCl_3$, 298 K).*

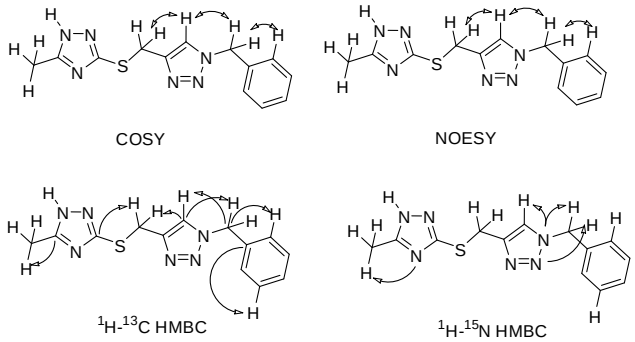

Scheme.4A.5: *Pictorial representation of the various correlations obtained for the compound 2 .*

Table .4A.8: *Assignments of the chemicals shifts for different protons and carbons.*

Atom number	δ_H ppm	δ_C or δ_N ppm	Atom number	δ_H ppm	δ_C or δ_N ppm
1	4.28	26.33	10		156.74
2	-	144.54	11	2.29	11.55
3	7.49	122.61	12		-
4	5.38	53.97	13		-39.6
5	-	134.1	14		-151.13
6	7.14	127.6	15		-157.9
7	7.26	128.69	16		-
8	-	-	17	-	-
9		155.29	18		

4.3.3 Compound 3: 1-benzyl-4-(((5-(tert-butyl)-1H-1,2,4-triazol-3-yl)thio)methyl)-1H-1,2,3-triazole:

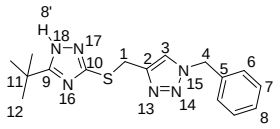

comp. 03

1-benzyl-4-(((5-(*tert*-butyl)-1 *H*-1,2,4-triazol-3-yl) thio)methyl)-1 *H*-1,2,3-triazole

Observed ^{1}H and ^{13}C chemical shifts:

^{1}H NMR (400 MHz, 298^{0}K; solvent $CDCl_3$ δ=7.27 ppm), δ = 7.48 ppm (s, 1H), 7.12 ppm (m, 2H), 7.25 ppm (m, 3H), 5.36 ppm (s, 2H, 4.28 ppm (s, 2H), 1.24 ppm (S, 9H).

^{13}C NMR (100 MHz, 298^{0}K; solvent $CDCl_3$, δ = 77.00 ppm), δ = 28.68 ppm, 26.55 ppm, 53.92 ppm, 122.63 ppm, 127.75 ppm, 128.45 ppm, 128.79 ppm, 32.07 ppm, 167.16 ppm, 156.75 ppm, 144.97 ppm, 134.16 ppm.

The chemical shifts of the different protons, carbons and the nitrogens in compound 3 are assigned on the basis of the observations made from 1D and 2D experiments (Fig. 4A.7 and 4A.8). The homonuclear and heteronuclear correlations observed are presented in Tables 4A.9 and 4A.10. The t-butyl group at 1.24 ppm (H-12) shows nOe correlations with the H-1, H-4 protons and also the phenyl protons (H-6, H-7) which is present at the other side of the molecule (Fig.4A.7D). Such nOe's are unexpected and needs more investigation.

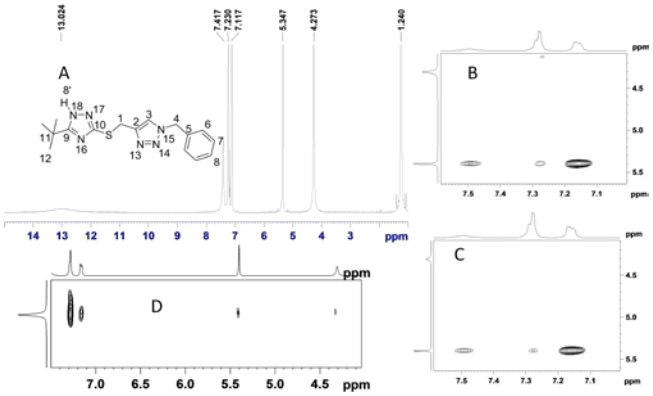

Fig.4A.7: A) *^{1}H NMR spectrum of compound 3. B) Expanded COSY (B) and NOESY (C) spectrum showing correlations of CH_2 protons with aromatic protons. D) NOESY cross peak of methyl protons of t-Butyl group (400 MHz, $CDCl_3$, 298 K).*

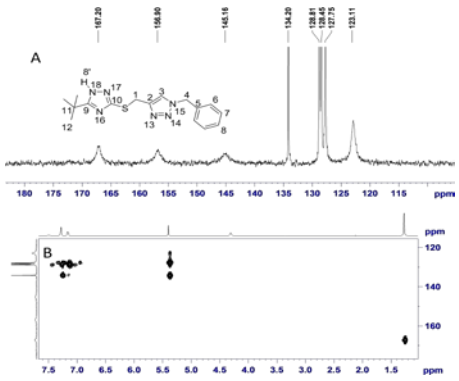

Fig.4A. 8: *100 MHz ^{13}C NMR spectrum (A) and HMBC (B) spectrum of compound 3 ($CDCl_3$+ Methanold4, 298 K).*

Some of the ^{13}C resonance signals (Fig.4A.8A) especially those related to triazole ring are found to be broad due to tautoeric equilibrium present in 1,24 triazole ring moety. ^{1}H-^{13}C HSQC and HMBC data indicated that the tertiary butyl protons at 1.24 ppm (H-12) shows long range heteronuclear correlations with the carbons resonating at 32.07 (C-11) and 167.16 ppm (C-9) indicating two bond and three bond correlations with the aliphatic and aromatic quaternary carbons respectively. However, the quaternary carbons at 156.75 (C-10) and 144.97 ppm (C-2) did not show any cross peaks with any of the protons under the present experimental conditions.

Table .4A.9:*Homonuclear correlations observed for compound 3.*

The Carbon and the proton number	^{1}H chemical shifts (ppm)	correlation with (ppm)	Remarks
3	7.48	5.36	NOESY
4	5.36	7.12	COSY/NOESY
6	7.12	7.24	COSY/NOESY
12	1.24	7.12, 7.24	NOESY

Table 4A.10 : *^{1}H-^{13}C HSQC/ HMBC correlations obtained for compound 3.*

The Carbon and the	^{1}H chemical shifts	^{13}C chemical shifts	Remarks

proton number	(ppm)	(ppm)	
1	4.28	26.55 122.63	HSQC HMBC
4	5.36	53.92 122.63, 127.75, 134.16	HSQC HMBC
6	7.12	127.75 53.92, 127.79, 134.16	HSQC HMBC
7	7.24	134.16	HMBC
12	1.24	32.07, 167.16	HMBC

Out of the six nitrogen atoms present, three nitrogens of the 1,2,4-triazole ring do not show any HMBC correlations (Fig.4A.9) under the measurement conditions. The NH signal could not be obtained as the measurements were done in $CDCl_3$-Methanol-d_4 mixture. The nitrogen atoms on the 1,2,3-triazole rings are assigned on the basis of HMBC correlations with H-1, H-3 and H-4 at -36.59 ppm (N-13), -20.13 (N-14) and -133.02 ppm (N-15). (Table 4A.11) . A pictorial representation of the homonuclear and heteronuclear correlations used are shown in Scheme.4A.6 and the chemical shift assignments are summarized in Table 4A.12.

Table 4A.11:*^{1}H- ^{15}N HMBC correlations obtained for compound 3.*

Nitrogen atom	^{1}H chemical shifts (ppm)	^{15}N chemical shifts (ppm)
13	4.28	-36.59
14	5.36	-20.13
15	7.48, 5.36	-133.02

Scheme.4A.6: *Pictorial representation of the various correlations obtained for the compound 3 .*

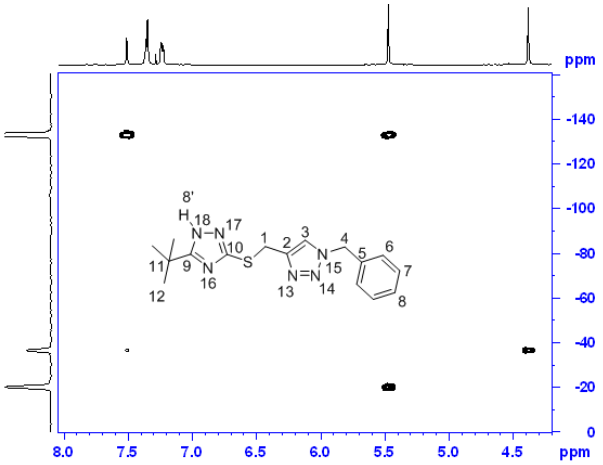

Fig.4A.9: *^{1}H-^{15}N HMBC spectrum of compound 3 ($CDCl_3$, 298 K).*

Table 4A.12: *Chemical shift assignment of compound 3*

Atom number	δ_H ppm	δ_C or δ_N ppm	Atom number	δ_H ppm	δ_C or δ_N ppm
1	4.28	26.55	10		156.75
2		144.97	11		32.07
3	7.48	122.63	12	1.24	28.68
4	5.36	53.92	13		-36.59
5		134.16	14		-20.13
6	7.12	127.75	15		-133.02
7	7.24	128.45	16		-
8	7.25	128.79	17		-
9		167.16	18		-

4.3.4 Compound 4: 1-benzyl-4-(((1-((1-benzyl-1H-1,2,3-triazol-4-yl)methyl)-1H-1,2,4-triazol-5-yl)thio)methyl)-1H-1,2,3-triazole:

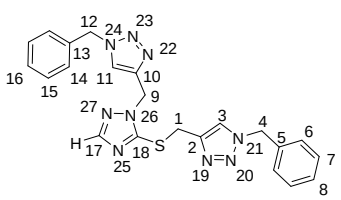

comp. 04

1-benzyl-4-(((1-((1-benzyl-1 *H*-1,2,3-triazol-4-yl)methyl) -1*H*-1,2,4-triazol-5-yl)thio)methyl)-1 *H*-1,2,3-triazole

Observed ^{1}H and ^{13}C chemical shifts:

^{1}H NMR (400 MHz, 298^{0}K; solvent $CDCl_3$ δ=7.27 ppm), δ = 7.82 ppm (s, 1H), 7.43 ppm (s, 2H), 7.35 ppm (m, 6H), 7.18 ppm (m, 2H), 7.25 ppm (m, 2H), 4.45 ppm (S, 2H), 5.29 ppm (S, 2H), 5.43 ppm (S, 2H), 5.46 ppm (S, 2H).

^{13}C NMR (100 MHz, 298^{0}K; solvent $CDCl_3$, δ = 77.00 ppm), δ = 28.29 ppm, 44.03 ppm, 54.09 ppm, 54.21 ppm, 122.75 ppm, 127.90 ppm, 128.08 ppm, 128.71 ppm, 128.80 ppm, 129.06 ppm, 129.09 ppm, 134.19 ppm, 134.35 ppm, 151.08 ppm, 151.61 ppm.

Compound 4 contains two additional methylene groups compared to the previous samples and one 1,2,3-triazole moiety. All the four -CH_2- protons are well resolved in the ^{1}H NMR spectrum (Fig.4A.10A) and they can be identified from the COSY cross peaks to the triazole ring protons and the aromatic protons of the phenyl rings. (Fig.4A.10B) Only H-17 does not show COSY cross peaks. (See Table 4A.13,4A.14). Important NMR correlations are shown in Scheme.4A.7) and the complete assignments are given in Table 4A.15.

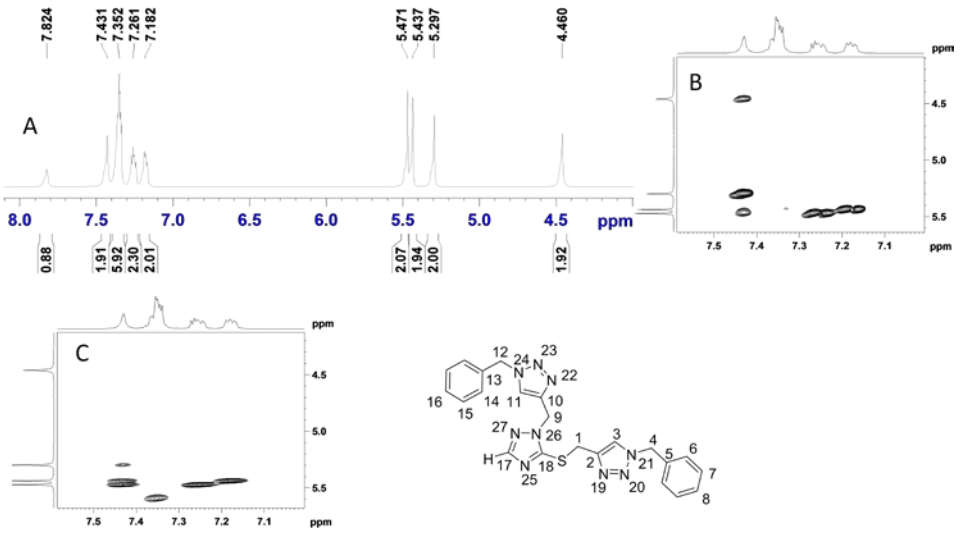

Fig.4A.10: *A)^{1}H NMR spectrum of compound 4. B) Expanded COSY (B) and NOESY (C) spectrum showing correlations of CH_2 protons with aromatic protons. (400 MHz, $CDCl_3$, 298 K).*

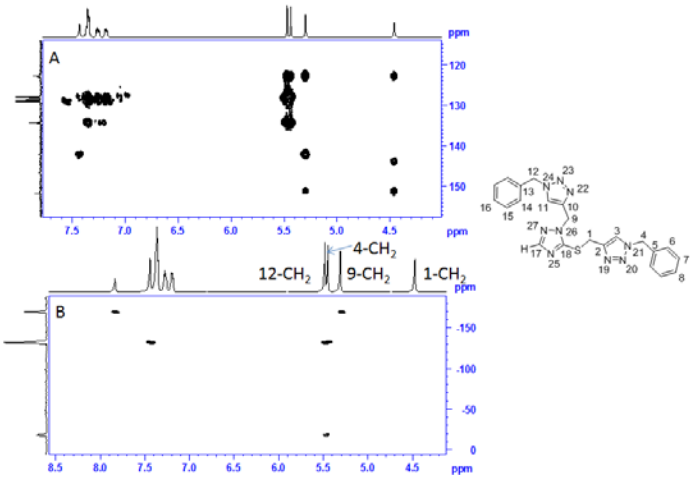

Fig 4A.11: *^{1}H-^{13}C HMBC (A) ^{1}H-^{15}N HMBC(B) spectra of compound 4*

Table 4A.13: *Homonuclear correlations observed for compound 4.*

The Carbon and the proton number	^{1}H chemical shifts (ppm)	correlation with (ppm)	Remarks
3	7.43	4.45, 5.43	COSY
3	7.43	5.43	NOESY
4	5.43	7.18, 7.43	COSY/NOESY
11	7.43	5.29, 5.46	COSY
11	7.43	5.46	NOESY
12	5.46	7.25	COSY/NOESY

Table .4A.14: *^{1}H-^{13}C HSQC/HMBC correlations obtained for compound 4.*

The Carbon and the proton number	^{1}H chemical shifts (ppm)	^{13}C chemical shifts (ppm)	Remarks
1	4.45	28.29 151.08, 143.93, 122.75	HSQC HMBC
4	5.43	54.09 122.75, 134.35	HSQC HMBC
6	7.18	127.90	HSQC

		128.71	HMBC
9	5.29	44.03 151.08, 122.75	HSQC HMBC
11	7.43	122.75 142.02	HSQC HMBC
12	5.46	54.21 122.75, 134.19	HSQC HMBC
14	7.25	128.08 128.80	HSQC HMBC
17	7.82	151.08	HMBC

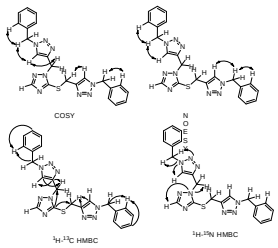

Scheme.4A.7: *Pictorial representation of the various correlations obtained for the compound 4*

The nOe correlations from the NOESY data is found to be in agreement with the single crystal X-ray structure which shows (Fig.4A.12) a zig-zag "anti" conformation of the triazole moieties which is also reported in the literature for other triazoles.[10, 11] (Single crystal is obtained by slow evaporation of the solution in chloroform)

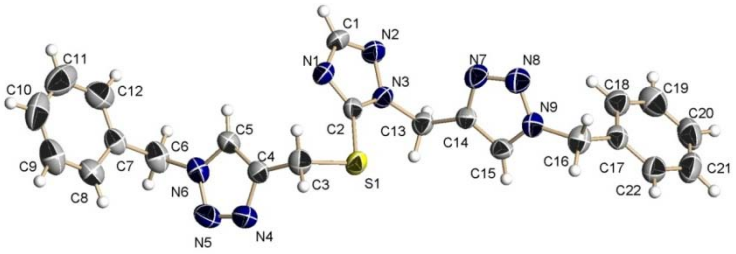

Fig. 4A.12: *ORTEP diagram of X-ray structure of the compound 4.*

Table 4A.15: *Chemical shift assignment of compound 4*

Atom number	δ_H ppm	δ_C or δ_N ppm	Atom number	δ_H ppm	δ_C or δ_N ppm
1	4.45	28.29	15	-	-
2		143.93	16	-	128.80
3	7.43	122.75	17	7.82	151.61
4	5.43	54.09	18	NA	151.08
5		134.35	19	NA	-
6	7.18	127.90	20	NA	-
7	7.35	-	21	NA	-
8	-	128.71	22	NA	-
9	5.29	44.03	23	NA	-18.2
10		142.02	24	NA	-131.36
11	7.43	122.75	25	NA	-
12	5.46	54.21	26	NA	-169.41
13		134.19	27	NA	-
14	7.25	128.08	28		

4.3.5 Compound 5: 1-benzyl-4-(((1-((1-benzyl-1H-1,2,3-triazol-4-yl)methyl)-3-methyl-1H-1,2,4-triazol-5-yl)thio)methyl)-1H-1,2,3-triazole:

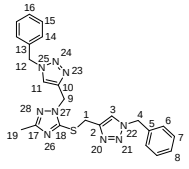

comp. 05

1-benzyl-4-(((1-((1-benzyl-1 *H*-1,2,3-triazol-4-yl)methyl) -3-methyl-1 *H*-1,2,4-triazol-5-yl)thio)methyl)-1 *H*-1,2,3-triazole

Observed ^{1}H and ^{13}C chemical shifts

^{1}H NMR (400 MHz, 298^{0}K; solvent $CDCl_3$ δ=7.27 ppm), δ = 2.19 ppm (s, 3H), 4.36 ppm (s, 2H), 5.15 ppm (s, 2H), 5.37 ppm (s, 2H), 5.39 ppm (s, 2H), 7.10 ppm (m, 2H), 7.18 ppm (m, 2H), 7.24 to 7.30 ppm (m, 6H), 7.39 ppm (s,1H), 7.41 ppm (s,1H).

^{13}C NMR (100 MHz, 298^{0}K; solvent $CDCl_3$, δ = 77.00 ppm), δ = 13.79 ppm, 28.29 ppm, 43.59 ppm, 53.81 ppm, 53.92 ppm, 122.516 ppm, 122.631 ppm, 127.70 ppm,

127.87 ppm, 128.45 ppm, 128.50 ppm, 128.84 ppm, 134.16 ppm, 134.25 ppm, 142.07 ppm, 143.58 ppm, 150.47 ppm, 160.69 ppm.

The NMR spectral correlations of compound 5 is given in Table 4A.16 and 17 based on the various NMR spectral (Fig.4A.13 and 4A.14) data.

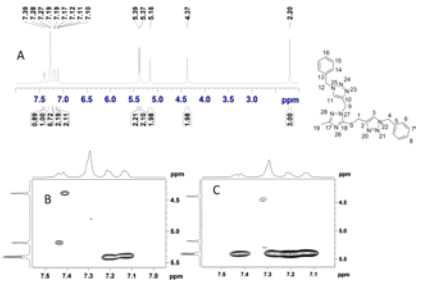

Fig.4A.13: *A)^{1}H NMR spectrum of compound 5. B) Expanded COSY (B) and NOESY (C) spectrum showing correlations of CH_2 protons with aromatic protons. (400 MHz, $CDCl_3$, 298 K).*

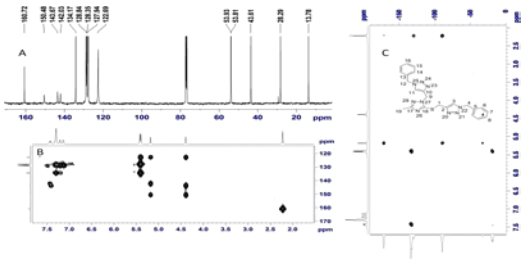

Fig.4A. 14: *100 MHz ^{13}C NMR spectrum (A), ^{1}H-^{13}C HMBC (B) and ^{1}H-^{15}N HMBC spectra of compound 5($CDCl_3$298 K).*

Table .4A.16: *Homonuclear correlations observed for compound 5.*

The Carbon and the proton number	^{1}H chemical shifts (ppm)	correlation with (ppm)	Remarks
1	4.36	7.39	COSY
4	5.37	7.10	COSY
4	5.37	7.39, 7.10	NOESY
9	5.15	7.41	COSY
12	5.39	7.18	COSY/NOESY

Table 4A.17: *^{1}H-^{13}C,HSQC HMBC correlations obtained for compound 5.*

The Carbon and the proton number	^{1}H chemical shifts (ppm)	^{13}C chemical shifts (ppm)	Remarks
1	4.36	28.29 150.47, 143.58, 122.63	HSQC HMBC
3	7.39	122.631 143.58, 53.81	HSQC HMBC
4	5.37	53.81 122.63, 134.25, 127.70	HSQC HMBC
6	7.10	127.70 53.81	HSQC HMBC
9	5.15	43.59 150.47, 142.07, 122.516	HSQC HMBC
11	7.41	122.516 142.07	HSQC HMBC
12	5.39	53.92 134.16, 127.87	HSQC HMBC
14	7.18	127.87 53.92, 134.16	HSQC HMBC
19	2.19	13.79 160.69	HSQC HMBC

^{1}H-^{15}N HMBC: Compound 5 has a total of 9 nitrogen atoms, 3 from the 1,2,4-triazole ring and 3 each from the two different 1,2,3-triazole rings which are present in the side chains of C-18 and N-27. All the 9 signals can be extracted from the HMBC spectrum (Fig.4A.14C) of compound 5. In the *S*-substituted side chain, H-1 shows 3-bond correlations with only one of the nitrogen atoms (N-20 resonating at -31.98 ppm). Out of the remaining two nitrogens N-21 is sp^2 which resonates at -18.92 ppm and the sp^3 hybridized N-22, appears at -133.06 ppm. N-22 shows 2-bond correlations with H-3 as well as H-4 whereas N-21 shows 3-bond correlations with H-4. H-9 protons show correlations with N-23 (-32.29 ppm) from 1,2,3-traizole ring. H-9 also shows correlations with N-27 (-171.38 ppm, sp^3 hybridized), and N-28 (-89.18 ppm, sp^2 hybridized). The basis for assigning the other two nitrogens to the 1,2,4-triazole ring is as follows. Only one nitrogen from the 1,2,3-triazole ring can show correlations with H-9, therefore the remaining two nitrogens must be from the 1,2,4-triazole ring. N-24 (-17.48 ppm) and N-25 (- 131.72 ppm,) both shows correlations with H-12. One of the nitrogens (N-26, -

129.99 ppm) from the 1,2,4-triazole ring shows the 3-bond correlation with H-19. The ^{1}H-^{15}N HMBC correlations are summarized in Table 4A.18 and the complete assignments based on various correlations shown in Scheme.4A.8 is given in Table 4A.19.

Table 4A.18: *^{1}H-^{15}N HMBC correlations obtained for compound 5.*

Nitrogen atom	^{1}H chemical shifts (ppm)	^{15}N chemical shifts (ppm)
20	4.36	-31.98
21	5.37	-18.92
22	7.39, 5.37	-133.06
23	5.15	-32.29
24	5.39	-17.48
25	5.39	-131.72
26	2.19	-129.99
27	5.15	-171.38
28	5.15	-89.18

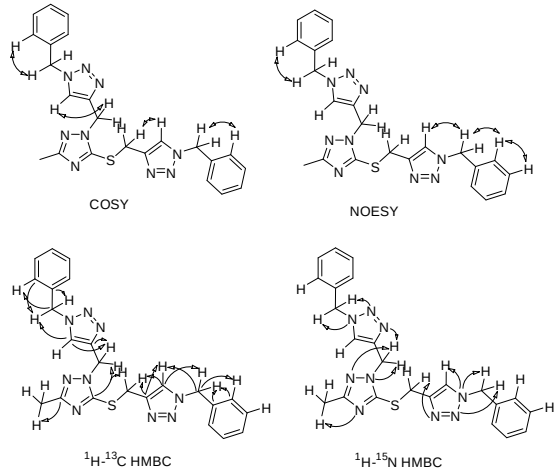

Scheme.4A.8: *Pictorial representation of the various correlations obtained for the compound 5*

Table.4A.19: *Chemical shift assignment of compound 5*

Atom number	δ_H ppm	δ_C or δ_N ppm	Atom number	δ_H ppm	δ_C or δ_N ppm
1	4.36	28.29	15	-	-
2		143.58	16	-	-
3	7.39	122.63	17		160.69
4	5.37	53.81	18		150.47
5		134.25	19	2.19	13.79

6	7.1	127.7	20		-31.98
7	-	-	21		-18.92
8	-	-	22		-133.06
9	5.15	43.59	23		-32.29
10		142.07	24		-17.48
11	7.41	122.516	25		-131.72
12	5.39	53.92	26		-129.99
13		134.16	27		-171.38
14	7.18	127.87	28		-89.18

4.3.6 Compound 6: 1-benzyl-4-(((1-((1-benzyl-1H-1,2,3-triazol-4-yl)methyl)-3-(tert-butyl)-1H-1,2,4-triazol-5-yl)thio)methyl)-1H-1,2,3-triazole:

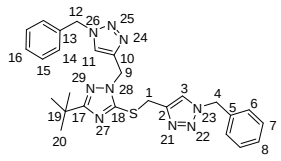

comp. 06

1-benzyl-4-(((1-((1-benzyl-1 *H*-1,2,3-triazol-4-yl)methyl)-3-(*tert*-butyl)-1*H*-1,2,4-triazol-5-yl)thio)methyl)-1 *H*-1,2,3-triazole

Observed ^{1}H and ^{13}C Chemical shifts:

^{1}H NMR (400 MHz, 298^{0}K; solvent $CDCl_3$ δ=7.27 ppm), δ = 7.38 ppm (s, 1H), 7.36 ppm (s, 1H), 7.09 ppm (m, 2H), 7.19 ppm (m, 2H), 7.26-7.31 ppm (m, 6H) , 5.40 ppm (s, 2H), 5.37 ppm (s, 2H), 5.18 ppm (s, 2H), 4.36 ppm (s, 2H), 1.19 ppm (s, 9H).

^{13}C NMR: (100 MHz, 298^{0}K; solvent $CDCl_3$, δ = 77.00 ppm), δ = 29.21 ppm, 43.75 ppm, 53.97 ppm, 28.28 ppm, 53.97 ppm, 122.80 ppm, 127.88 ppm, 127.83 ppm, 128.58 ppm , 128.91 ppm, 128.98 ppm, 171.74 ppm, 150.03 ppm, 142.48 ppm, 134.31 ppm, 144.33 ppm, 134.21 ppm.

NMR spectra for the compound 6 are shown in the Fig.4A.15 and 4A.16 .The assignments details are given in Tables 4A.20 to 4.23. In this case the CH carbons of both the triazole rings resonate at the same frequency hence distinguishing the benzyl group attached to the different triazole rings by ^{1}H-^{13}C HMBC becomes difficult. However, ^{1}H-^{15}N HMBC experiments (Fig.4A.16B) could be used for obtaining complete assignments.

The protons of the t-Bu group, H-20, show 4-bond correlations with the nitrogen resonating at the -90.8 ppm (N-29) from the 1,2,4-triazole ring. Proton H-9 shows correlations with the sp^3 hybridized nitrogen atom from the 1,2,4-triazole ring resonating at -173.66 ppm (N-28) and also with one of the sp^2 hybridized nitrogens from the 1,2,3-triazole ring at -32.45 ppm (N-24) which shows correlations with H-11 proton. Also, the nitrogen appearing at -18.8 ppm (N-25) shows correlations with H-11 proton and H-12 protons and thus confirms its position. The crucial evidence of the connectivity of the triazole unit with this benzyl group comes from the nitrogen resonating at -132.23 ppm (N-26), which shows correlations with H-11 as well as H-12 protons, and is useful for

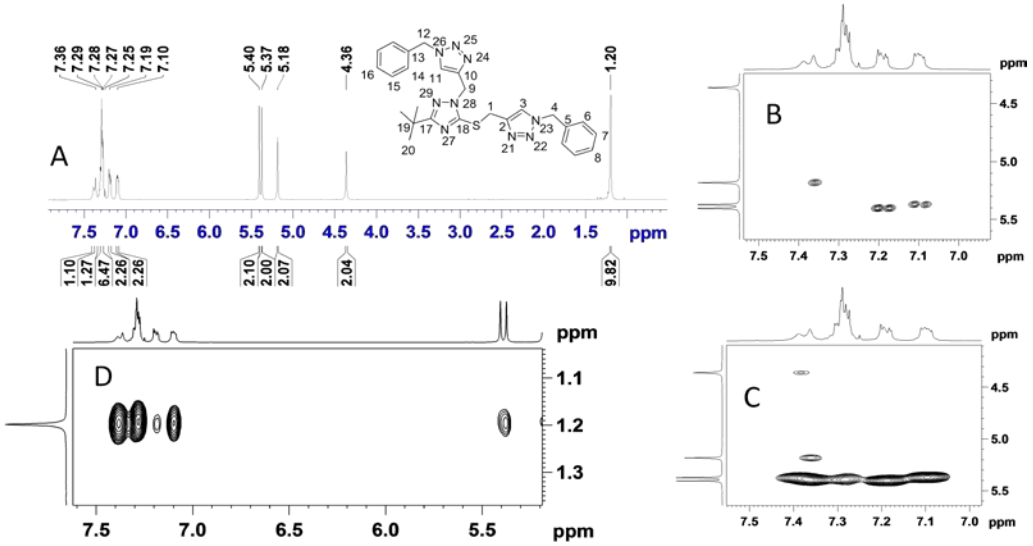

Fig.4A.15: *A)^{1}H NMR spectrum of compound 6. B) Expanded COSY (B) and NOESY (C) spectrum showing correlations of CH_2 protons with aromatic protons. D) NOESY cross peak of me thyl protons of t-Butyl group (400 MHz, $CDCl_3$, 298 K).*

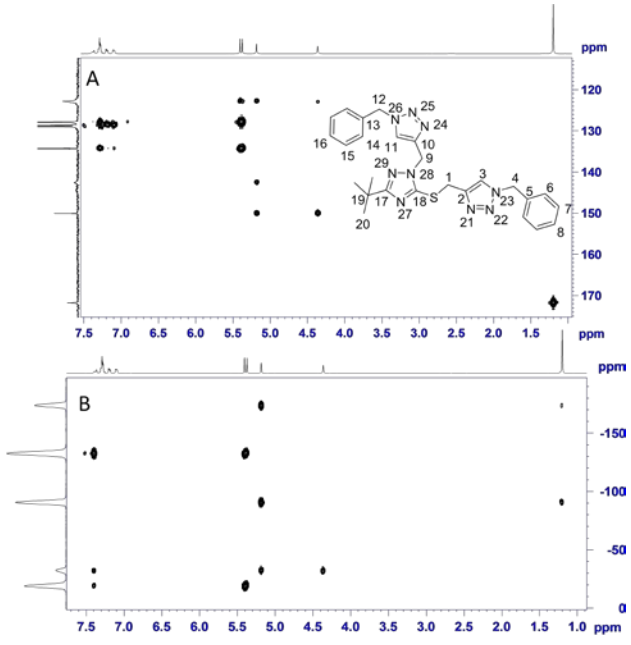

Fig 4A.16: *^{1}H-^{13}C HMBC (A) ^{1}H-^{15}N HMBC(B) spectra of compound 6*

Table .4A.20*: Homonuclear correlations observed for compound 6.*

The Carbon and the proton number	^{1}H chemical shifts (ppm)	correlation with (ppm)	Remarks
1	4.36	7.38	COSY/NOESY
3	7.38	5.37	NOESY
4	5.37	7.09	COSY/NOESY
6	7.09	7.27	COSY
11	7.36	5.18, 5.40	COSY/NOESY
12	5.40	7.19, 7.36	COSY/NOESY
14	7.19	7.29	COSY
20	1.19	7.38, 5.37, 7.09, 7.19	NOESY

Table 4A.21: *^{1}H-^{13}C HSQC/HMBC correlations obtained for compound 6.*

The Carbon and the proton number	^{1}H chemical shifts (ppm)	^{13}C chemical shifts (ppm)	Remarks
1	4.36	28.28 150.03, 144.33, 122.80	HSQC HMBC
4	5.37	53.97 122.80, 134.21	HSQC HMBC
6	7.09	127.83 53.97	HSQC HMBC
9	5.18	43.75 150.03, 142.48, 122.80	HSQC HMBC
11	7.36	122.80 142.48	HSQC HMBC

12	5.40	53.97 122.80, 134.31	HSQC HMBC
14	7.19	127.88 53.97	HSQC HMBC
20	1.19	29.21 171.74, 32.75	HSQC HMBC

distinguishing different benzyl groups bonded with different triazole units. H-1 protons are expected to show 3 bond correlation with only one of the nitrogens of the 1,2,3 trazole ring that resonates at -31.79 ppm (N-21). At the same time the nitrogens resonating at -19.6 (N-22) and -133.56 ppm (N-23) both shows correlations with the H-4 protons thereby confirming their positions as shown in the Scheme.4A.9 and Table-4A.23.

Table 4A.22: *^{1}H-^{15}N HMBC correlations obtained for compound 6.*

Nitrogen atom	^{1}H chemical shifts (ppm)	^{15}N chemical shifts (ppm)
21	4.36	-31.79
22	5.37	-19.6
23	5.37	-133.56
24	5.18, 7.36	-32.45
25	7.36, 5.40	-18.8
26	7.36, 5.40	-132.23
27	NA	-
28	5.18	-173.66
29	1.19	-90.8

Scheme.4A.9: *Pictorial representation of the various correlations obtained for the compound 6*

Table 4A. 23: *Chemical shift assignment of compound 6*

Atom number	δ_H ppm	δ_C or δ_N ppm	Atom number	δ_H ppm	δ_C or δ_N ppm
1	4.36	28.28	16	-	-
2		144.33	17		171.74
3	7.38	122.8	18		150.03
4	5.37	53.97	19		32.75
		134.21	20	1.19	29.2
6	7.09	127.83	21		-31.79
7	7.27	-	22		-19.6
8	-	-	23		-133.56
9	5.18	43.75	24		-32.45
10		142.48	25		-18.8
11	7.36	122.8	26		-132.23
12	5.4	53.97	27		-
13		134.31	28		-173.66
14	7.19	127.88	29		-90.8
15	7.29	-			

4.3.7 Compound 7: 1-benzyl-4-(((1-((1-benzyl-1H-1,2,3-triazol-4-yl)methyl)-3-(4-chlorophenyl)-1H-1,2,4-triazol-5-yl)thio)methyl)-1H-1,2,3-triazole:

Observed ^{1}H and ^{13}C Chemical shifts:

^{1}H NMR (400 MHz, 298^{0}K; solvent $CDCl_3$ δ = 7.27 ppm), δ = 4.48 ppm (s, 2H), 5.28 ppm (s, 2H), 5.37 ppm (s, 2H), 5.42 ppm (s, 2H), 7.11 ppm (m, 2H), 7.20 to 7.25 ppm (m, 5H), 7.29 to 7.33 ppm (m, 5H), 7.46 ppm (s, 1H), 7.48 ppm (s, 1H), 7.89 ppm (d, J = 8.49 Hz, 2H).

^{13}C NMR (100 MHz, 298^{0}K; solvent $CDCl_3$, δ = 77.00 ppm), δ = 28.26 ppm, 44.04 ppm, 53.81 ppm, 53.91 ppm, 122.66 ppm, 122.74 ppm, 127.23 ppm, 127.71 ppm, 127.82 ppm, 128.45 ppm, 128.79 ppm, 128.84 ppm, 134.09 ppm, 134.18 ppm, 134.84 ppm, 141.8 ppm, 143.6 ppm, 151.68 ppm, 160.72 ppm.

The spectral data given in Figs.4A.17 and 4A.18 are utilized to get a complete assignment of all the protons, carbons and nitrogens in compound 7 as shown in Tables 4A.24 to 4A.27.

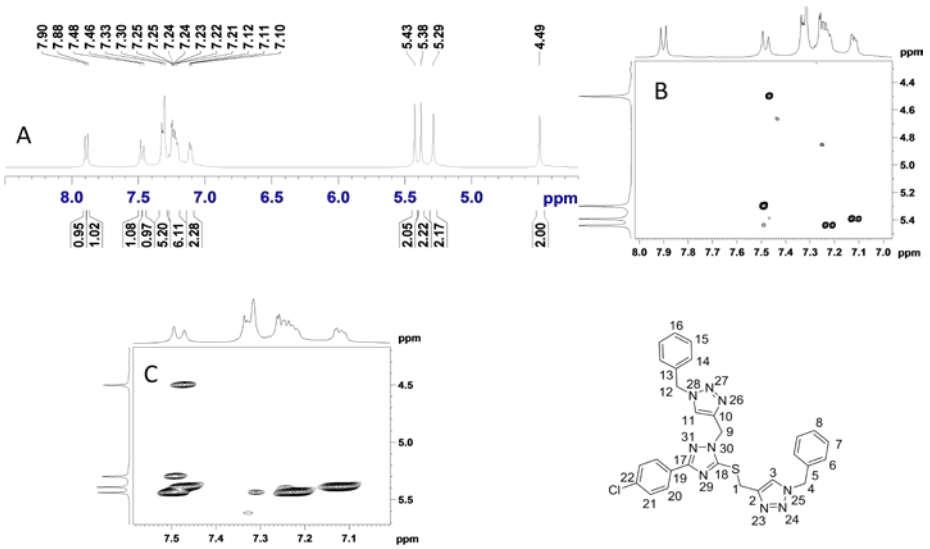

Fig.4A.17: A)^{1}H NMR spectrum of compound 7. B) Expanded COSY (B) and NOESY (C) spectrum showing correlations of CH_2 protons with aromatic protons. (400 MHz, $CDCl_3$, 298 K).

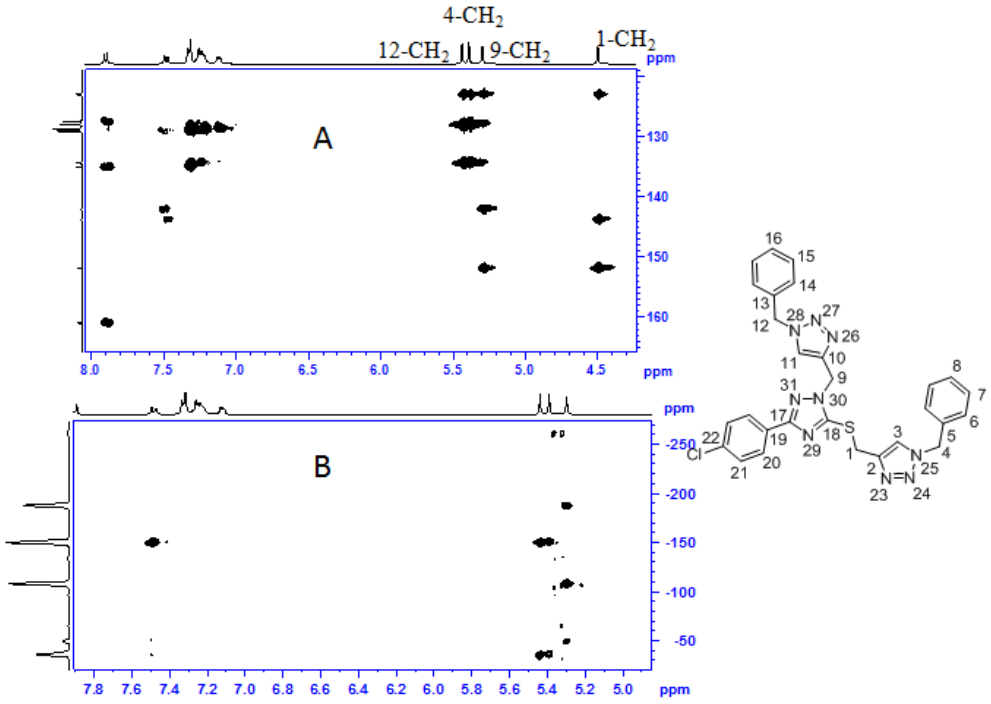

Fig 4A.18: *^{1}H-^{13}C HMBC (A) ^{1}H-^{15}N HMBC(B) spectra of compound 7*

Table 4A.24: *Homonuclear correlations observed for compound 7.*

The Carbon and the proton number	^{1}H chemical shifts (ppm)	correlation with (ppm)	Remarks
1	4.48	7.46	COSY/NOESY
3	7.46	7.11	NOESY
4	5.37	7.11	COSY/NOESY
9	5.28	7.48	COSY/NOESY
11	7.48	5.28, 5.42, 7.21	NOESY
12	5.42	7.21	COSY/NOESY
20	7.89	7.31	COSY/NOESY
20	7.89	4.48, 7.46. 5.28	NOESY

Table 4A.25: *^{1}H-^{13}C HSQC/ HMBC correlations obtained for compound 07.*

The Carbon and the proton number	^{1}H chemical shifts (ppm)	^{13}C chemical shifts (ppm)	Remarks
1	4.48	28.26 151.68, 143.6, 122.74	HSQC HMBC
3	7.46	122.74 143.6, 53.81	HSQC HMBC
4	5.37	53.81 122.74, 134.09	HSQC HMBC
6	7.11	127.71 134.09	HSQC HMBC
9	5.28	44.04 151.68, 141.8, 122.66	HSQC HMBC
11	7.48	122.66 141.8, 53.91	HSQC HMBC
12	5.42	53.91 122.66, 134.18	HSQC HMBC
14	7.21	127.82 53.91	HSQC HMBC
20	7.89	127.23 160.72, 134.84	HSQC HMBC

^{1}H-^{15}N-HMBC: In the ^{1}H-^{15}N HMBC spectrum (Fig.4A.18B), H-4 shows 3-bond correlations with N-24 (-19.02 ppm, sp^2 hybridized) and 2-bond correlations with N-25 (-132.73 ppm, sp^3 hybridized). H-9 shows correlations with three nitrogens N-26 (-32.17 ppm) , N-30 (-169.8 ppm,) and N-31 (-89.87 ppm). Out of these, sp^3 hybridized N-30 can be identified very easily from the relatively up field chemical shift (-169.8 ppm) compared to other two sp^2 hybridized nitrogen atoms. Out of the remaining two sp^2 hybridized nitrogens, the deshielded one is from the 1,2,3-triazole ring (N-26 ,-32.17 ppm). N-27(-18.09 ppm, sp^2 hybridized) shows a 3-bond correlation with H-11 while N-28 (-131.71 ppm, sp^3 hybridized) shows a 2-bond correlation with H-12. N-29 does not have any protons 2-bond or 3-bond away hence it does not show any cross peaks and its chemical shift could not be determined. N-23 also did not show any correlations under the experimental conditions. These results are tabulated (Table.4A.26) and schematically shown (Scheme.4A.10)

Scheme. 4A.10: *Pictorial representation of the various correlations obtained for the compound 7*

Table 4A.26: *^{1}H-^{15}N HMBC correlations obtained for compound 7.*

Nitrogen atom	^{1}H chemical shifts (ppm)	^{15}N chemical shifts (ppm)
23		-
24	5.37	-19.02
25	5.37	-132.73
26	5.28	-32.17
27	5.42	-18.09
28	5.42	-131.71
29	-	-
30	5.28	-169.8
31	5.28	-89.87

Table 4A.27Chemical shift assignment of compound 7

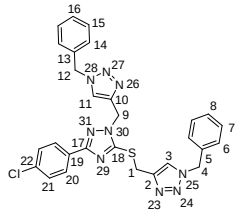

comp. 07

Atom number	δ_H ppm	δ_C or δ_N ppm	Atom number	δ_H ppm	δ_C or δ_N ppm

1	4.48	28.26	17		160.72
2		143.6	18		151.68
3	7.46	122.74	19		-
4	5.37	53.81	20	7.89	127.23
5		134.09	21	7.31	-
6	7.11	127.71	22		134.88
7	-	-	23		-
8	-	-	24		-19.02
9	5.28	44.04	25		-132.73
10		141.8	26		-32.17
11	7.48	122.66	27		-18.09
12	5.42	53.91	28		-131.71
13		134.18	29		-
14	7.21	127.82	30		-169.8
15	-	-	31		-89.87
16	-	-	32		

4.3.8 Compound 08: 1-benzyl-4-(((1-((1-benzyl-1H-1,2,3-triazol-4-yl)methyl)-3-(4-methoxyphenyl)-1H-1,2,4-triazol-5-yl)thio)methyl)-1H-1,2,3-triazole:

Observed ^{1}H and ^{13}C Chemical shifts:

^{1}H NMR (400 MHz, 298^{0}K; solvent $CDCl_3$ δ = 7.27 ppm), δ = 3.78 ppm (s, 3H), 4.47 ppm (s, 2H), 5.26 ppm (s,2H), 5.35 ppm (s, 2H), 5.39 ppm (s, 2H), 6.87 ppm (d, J= 8.39 Hz, 2H), 7.10 ppm (m, 2H), 7.19 ppm (m, 2H), 7.24 ppm (m, 3H), 7.29 ppm (m, 3H), 7.46 ppm (s, 1H), 7.48 ppm (s, 1H), 7.89 ppm (d, J = 8.39 Hz, 2H).

^{13}C NMR (100 MHz, 298^{0}K; solvent $CDCl_3$, δ = 77.00 ppm), δ = 28.32 ppm, 43.97 ppm, 53.79 ppm, 53.89 ppm, 55.07 ppm, 113.65 ppm, 122.9 ppm, 123.20 ppm, 127.37 ppm, 127.69 ppm, 127.80 ppm, 128.39 ppm, 128.46 ppm, 128.78 ppm, 128.81 ppm, 134.18 ppm, 134.23 ppm, 151.2 ppm, 160.30 ppm, 161.68 ppm.

Tables 4A.28 and 4A.29 depicts the correlations observed to arrive at the assignments given in Table 4A.30 . The 1D and 2D spectra are shown in Figs. 4A.18.I and 4A.19

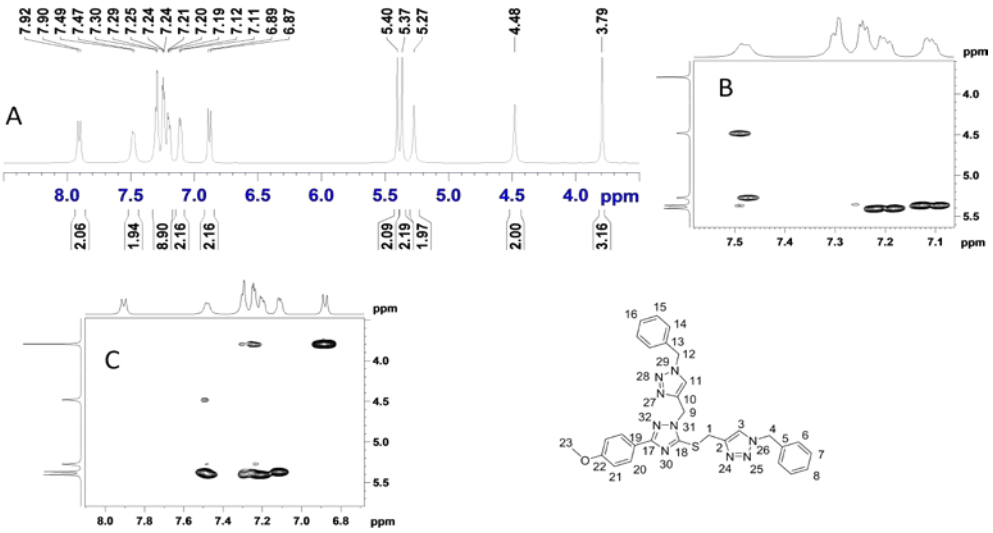

Fig.4A.18.I: A)^{1}H NMR spectrum of compound 8. B) Expanded COSY (B) and NOESY (C) spectrum showing correlations of CH_2 protons with aromatic protons. (400 MHz, $CDCl_3$, 298 K).

^{13}C NMR spectrum of compound 8 (Fig.4A.20A) show broadening of a few resonances (C11,C10, C2 and C3) associated with 1,2,3 trazole moieties and suggests occurrence of slow dynamics involving them. Efforts have not been made to get details on the exact nature of dynamic events present. It is likely to be due to slow rotation about the C-C bond connecting the 1,2,3 triazole moieties to 1,2,4 triazole ring. This dynamic events present also hampered the efforts to get ^{1}H-^{15}N HMBC spectrum of it. 2D NMR correlations observed are also shown schematically (Scheme.4A.11)

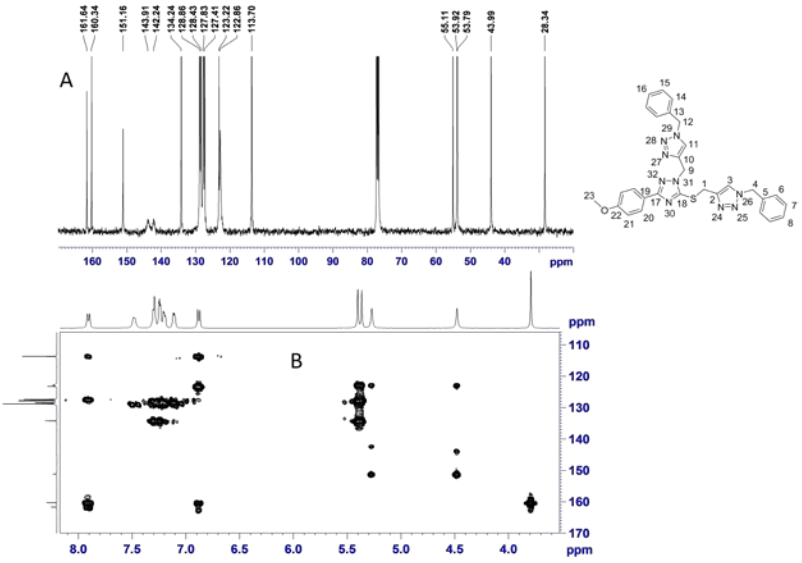

Fig.4A.19: *100 MHz ^{13}C NMR spectrum (A) and ^{1}H-^{13}C HMBC spectrum (B) of compound 8($CDCl_3$298 K).*

Table. 4A. 28: *Homonuclear correlations observed for compound 8.*

The Carbon and the proton number	^{1}H chemical shifts (ppm)	correlation with (ppm)	Remarks
3	7.48	4.47, 5.35	COSY
4	5.35	7.10, 7.48	COSY/NOESY
9	5.26	7.46	COSY
12	5.39	7.19	COSY
12	5.39	7.46, 7.19	NOESY
20	7.89	6.87	COSY/NOESY
21	6.87	3.78	NOESY

Table 4A.29: *^{1}H-^{13}C HSQC/HMBC correlations obtained for compound 8.*

The Carbon and the proton number	^{1}H chemical shifts (ppm)	^{13}C chemical shifts (ppm)	Remarks
1	4.47	28.32 151.2, 143.86, 122.9	HSQC HMBC
4	5.35	53.79 122.9, 134.18	HSQC HMBC
6	7.10	127.69	HSQC

		53.79	HMBC
9	5.26	43.97 151.2, 142.28. 122.9	HSQC HMBC
12	5.39	5.39 122.9, 134.23	HSQC HMBC
14	7.19	127.80 53.89	HSQC HMBC
20	7.89	127.37 161.68, 160.30	HSQC HMBC
21	6.87	113.65161.68, 160.30	HSQC HMBC
23	3.78	55.07 160.30	HSQC HMBC

Scheme.4A.11: *Pictorial representation of the various correlations obtained for the compound 8* .

Table 4A.30: *Chemical shift assignment of compound 8*

Atom number	δ_H ppm	δ_C or δ_N ppm	Atom number	δ_H ppm	δ_C or δ_N ppm
1	4.47	28.32	17		161.68
2		143.86	18		151.2
3	7.48	122.9	19		123.2

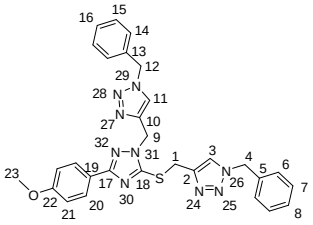

comp, no. 8.

4	5.35	53.79	20	7.89	127.37
5		134.18	21	6.87	113.65
6	7.1	127.69	22		160.3
7	-	-	23	3.78	55.07
8	-	128.39	24		-
9	5.26	43.97	25		-
10		142.28	26		-
11	7.46	122.9	27		-
12	5.39	53.89	28		-
13		134.23	29		-
14	7.19	127.8	30		-
15	-	-	31		-
16	-	128.47	32		-

4.3.9 Compound 9: 1-benzyl-4-(((1-((1-benzyl-1H-1,2,3-triazol-4-yl)methyl)-1H-1,2,4-triazol-3-yl)thio)methyl)-1H-1,2,3-triazole:

Observed ^{1}H and ^{13}C Chemical shifts.

^{1}H NMR (400 MHz, 298^{0}K; solvent $CDCl_3$ δ = 7.27 ppm), δ = 4.08 ppm (s, 2H), 5.12 ppm (s, 2H), 5.18 ppm (s, 2H), 5.25 ppm (s, 2H), 6.96 ppm (m, 2H), 7.03 ppm (m, 2H), 7.05 to 7.11 ppm (m, 6H), 7.41 ppm (s, 1H), 7.59 ppm (s, 1H), 8.03 ppm (s, 1H).

^{13}C NMR (100 MHz, 298^{0}K; solvent $CDCl_3$, δ = 77.00 ppm), δ = 25.7 ppm, 44.08 ppm, 53.39 ppm, 53.63 ppm, 122.86 ppm, 123.43 ppm, 127.34 ppm, 127.57 ppm, 128.03 ppm, 128.22 ppm, 128.40 ppm, 128.50 ppm, 133.92 ppm, 134.25 ppm, 141.4 ppm, 144.24 ppm, 144.25 ppm, 159.43 ppm.

All the relevant NMR spectra of compound 9 are shown in the Figs.4A.20 and 4A.21. The spectra of this compound was obtained in CDCl3- methanol-d_4 solvent mixture. Various correlations are observed and the assignments are given in Tables 4A.31to 4A.35 and Scheme 4A.12.

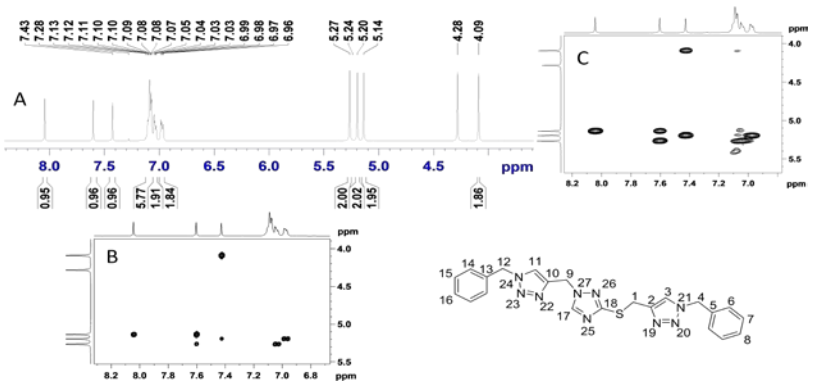

Fig.4A.20: *A)^{1}H NMR spectrum of compound 9. B) Expanded COSY (B) and NOESY (C) spectrum showing correlations of CH_2 protons with aromatic protons. (400 MHz, $CDCl_3$+ Methanol-d4, 298 K).*

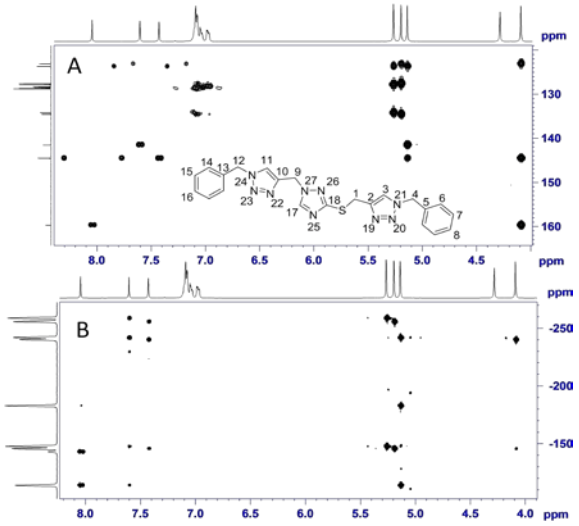

Fig.4A.21: *^{1}H-^{13}C HMBC (A) ^{1}H-^{15}N HMBC(B) spectra of compound 9*

Table .4A.31: *Homonuclear correlations observed for compound 9.*

The Carbon and the proton number	^{1}H chemical shifts (ppm)	correlation with (ppm)	Remarks
3	7.41	4.08, 8.18	COSY/NOESY
3	7.41	6.96	NOESY
4	5.18	7.41, 6.96	COSY/NOESY

9	5.12	8.03, 7.59	COSY/NOESY
11	7.59	7.03	NOESY
12	5.25	7.59, 7.03	COSY/NOESY

Table .4A.32: *^{1}H-^{13}C HSQC HMBC correlations obtained for compound 9.*

The Carbon and the proton number	^{1}H chemical shifts (ppm)	^{13}C chemical shifts (ppm)	Remarks
1	4.08	25.7 159.43, 144.24, 122.86	HSQC HMBC
3	7.41	122.86 144.24, 53.39	HSQC HMBC
4	5.18	53.39 134.25, 127.34	HSQC HMBC
6	6.96	127.34 53.39	HSQC HMBC
9	5.12	44.08 141.4, 123.43	HSQC HMBC
11	7.59	123.43 53.63, 141.4, 44.08	HSQC HMBC
12	5.25	53.63 123.43, 133.92, 127.57	HSQC HMBC
14	7.03	127.57 53.63	HSQC HMBC
17	8.03	144.25 159.43, 44.08	HSQC HMBC

Table 4A.34: *^{1}H-^{15}N HMBC correlations obtained for compound 9.*

Nitrogen atom	^{1}H chemical shifts (ppm)	^{15}N chemical shifts (ppm)
19	-	-38.5
20	5.18	-23.1
21	5.18	-133
22	-	-36.6
23	5.25	-19.9

24	5.25, 7.59	-131
25	-	-135.67
26	5.12	-96.08
27	5.12, 8.03	-165.07

Scheme.4A.12: *Pictorial representation of the various correlations obtained for the compound 9*

Table 4A.35: *Chemical shift assignment of compound 9*

Atom number	δ_H ppm	δ_C or δ_N ppm	Atom number	δ_H ppm	δ_C or δ_N ppm
1	4.08	25.7	15	-	-
2		144.24	16	-	-
3	7.41	122.86	17	8.03	144.25

4	5.18	53.39	18		159.43
5		134.25	19		-38.5
6	6.96	127.34	20		-23.1
7	-	-	21		-133
8	-	-	22		-36.6
9	5.12	44.08	23		-19.9
10		141.4	24		-131
11	7.59	123.43	25		-135.67
12	5.25	53.63	26		-96.08
13		133.92	27		-165.07
14	7.03	127.57	28		NA

4.3.10 Compound 10: 1-benzyl-4-(((1-((1-benzyl-1H-1,2,3-triazol-4-yl)methyl)-5-methyl-1H-1,2,4-triazol-3-yl)thio)methyl)-1H-1,2,3-triazole:

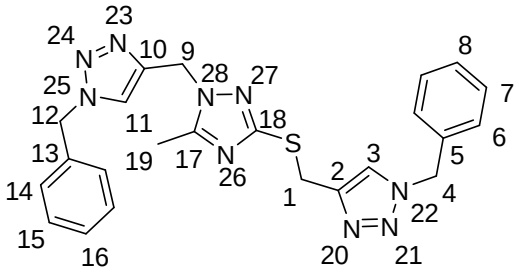

Observed ^{1}H and ^{13}C Chemical shifts:

^{1}H NMR (400 MHz, 298^{0}K; solvent $CDCl_3$ δ = 7.27 ppm), δ = 2.46 ppm (s, 3H), 4.33 ppm (s, 2H), 5.25 ppm (s, 2H), 5.41 ppm (s, 2H), 5.47 ppm (s, 2H), 7.18 ppm (s, 2H), 7.26 ppm (s, 2H), 7.30 to 7.35 ppm (m, 6H), 7.47 ppm (s, 1H), 7.60 ppm (s, 1H).

^{13}C NMR (100 MHz, 298^{0}K; solvent $CDCl_3$, δ = 77.00 ppm), δ = 11.91 ppm, 26.67 ppm, 44.03 ppm, 53.94 ppm, 54.17 ppm, 122.51 ppm, 123.05 ppm, 127.88 ppm, 128.09 ppm, 128.57 ppm, 128.76 ppm, 128.95 ppm, 129.05 ppm, 134.25 ppm, 134.57 ppm, 142.37 ppm, 145.36 ppm, 153.53 ppm, 158.16 ppm.

The NMR spectra for the compound **10** are shown in the Figs.4A.22 and 4A.23.The chemical shifts of different protons, carbons and the nitrogens (Table 4A.39) in the compound **10** are assigned on the basis of the 2D correlations given in Tables 4A.36 to 4A.38 and Scheme.4A.13.

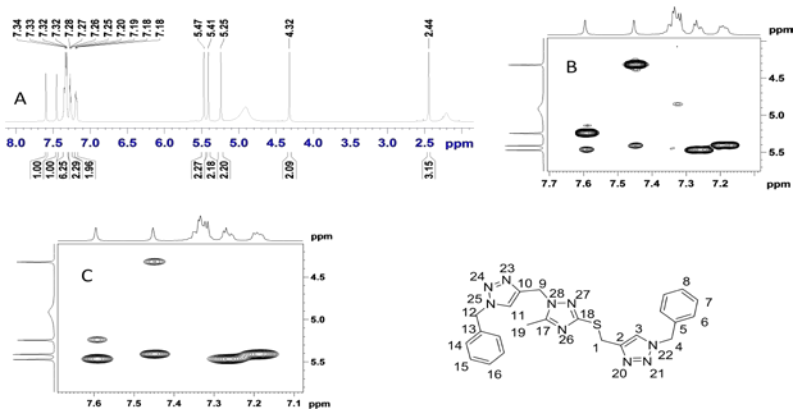

Fig.4A.22: *A)*^{1}*H NMR spectrum of compound 10. B) Expanded COSY (B) and NOESY (C) spectrum showing correlations of* CH_2 *protons with aromatic protons. (400 MHz,* $CDCl_3$*+ Methanol-d4, 298 K).*

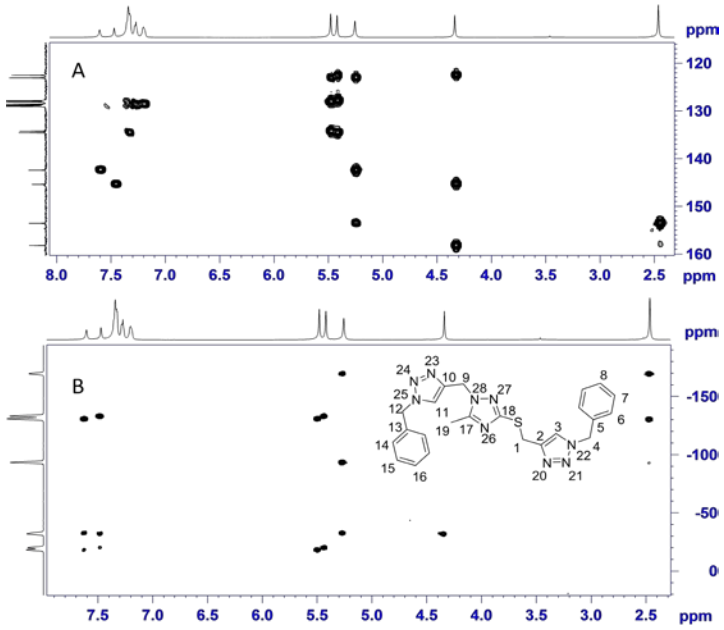

Fig 4A.23: ^{1}*H-*^{13}*C HMBC (A)* ^{1}*H-*^{15}*N HMBC(B) spectra of compound10*

Table .4A.36: *Homonuclear correlations observed for compound 10.*

The Carbon and the proton number	^{1}H chemical shifts (ppm)	correlation with (ppm)	Remarks
1	4.33	7.47	cosy/noesy
3	7.47	5.41	noesy
4	5.41	7.18	cosy/noesy
9	5.25	2.46, 7.60	noesy
11	7.60	5.25, 5.47	cosy/noesy
12	5.47	7.26	cosy/noesy

. Table .4A.37: *^{1}H-^{13}C HSQC HMBC correlations obtained for compound 10.*

The Carbon and the proton number	^{1}H chemical shifts (ppm)	^{13}C chemical shifts (ppm)	Remarks
1	4.33	26.67 158.16, 145.36, 122.51	HSQC HMBC
3	7.47	122.51 145.36, 53.94	HSQC HMBC
4	5.41	53.94 122.51, 134.57, 127.88	HSQC HMBC
6	7.18	127.88 128.57, 53.94	HSQC HMBC
9	5.25	44.03 153.53, 142.37, 123.05	HSQC HMBC
11	7.60	123.05 142.37, 54.17	HSQC HMBC
12	5.47	54.17 123.05, 128.09	HSQC HMBC
14	7.26	128.09 54.17, 128.76	HSQC HMBC
19	2.46	11.91 153.53	HSQC HMBC

Table 4A.38: *^{1}H-^{15}N HMBC correlations obtained for compound 10.*

Nitrogen atom	^{1}H chemical shifts (ppm)	^{15}N chemical shifts (ppm)
20	4.33, 7.47	-31.92
21	7.47, 5.41	-20
22	7.47, 5.41	-133.07
23	5.25, 7.60	-32.53
24	5.47, 7.60	-18.14
25	5.47, 7.60	-130.8
26	2.46	-130.36
27	5.25	-93.4
28	5.25, 2.46	-169.51

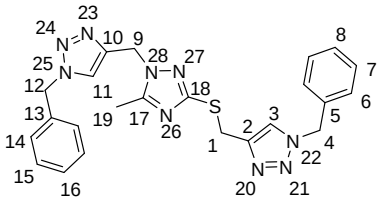

Table 4A.39: *Chemical shift assignment of compound 10*

Atom number	δ_H ppm	δ_C or δ_N ppm	Atom number	δ_H ppm	δ_C or δ_N ppm
1	4.33	26.67	15	-	-
2	-	145.36	16	-	128.76
3	7.47	122.51	17		153.53
4	5.41	53.94	18		158.16
5		134.57	19	2.46	11.91
6	7.18	127.88	20		-31.92
7	-	-	21		-20
8	-	128.57	22		-133.07
9	5.25	44.03	23		-32.53
10		142.37	24		-18.14
11	7.6	123.05	25		-130.8
12	5.47	54.17	26		-130.36
13		134.25	27		-93.4
14	7.26	128.09	28		-169.51

Scheme.4A.13: *Pictorial representation of the various correlations obtained for the compound 10*

4.3.11 Compound 11: 1-benzyl-4-(((1-((1-benzyl-1H-1,2,3-triazol-4-yl)methyl)-5-(tert-butyl)-1H-1,2,4-triazol-3-yl)thio)methyl)-1H-1,2,3-triazole:

^{1}H NMR (400 MHz, 298^{0}K; solvent $CDCl_3$ δ = 7.27 ppm), δ = 7.64 ppm (s, 1H), 7.44 ppm (s, 1H), 7.15 ppm (m, 2H), 7.22 ppm (m, 2H), 7.26-7.29 ppm (m, 6H), 5.43 (s, 2H), 5.37 (s, 2H), 5.41 (s, 2H), 4.28 (s, 2H), 1.34 ppm (s, 9H).

^{13}C NMR (100 MHz, 298^{0}K; solvent $CDCl_3$, δ = 77.00 ppm), *δ* = 29.26 ppm, 4.28 ppm, 5.41 ppm, 5.37 ppm, 5.43 ppm, 122.55 ppm, 123.53 ppm, 127.87 ppm, 128.52 ppm, 128.89 ppm, 32.60 ppm, 134.51 ppm, 134.56 ppm, 145.65 ppm, 143.12 ppm, 157.06 ppm, 163.32 ppm.

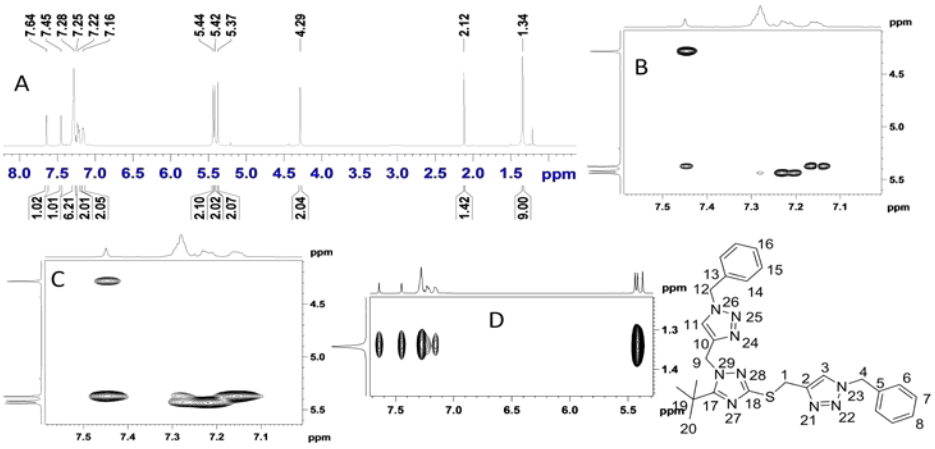

Fig.4A.24: *A) ^{1}H NMR spectrum of compound 11. B) Expanded COSY (B) and NOESY (C) spectrum showing correlations of CH_2 protons with aromatic protons. D) NOESY cross peak of methyl protons of t-Butyl group (400 MHz, $CDCl_3$, 298 K).*

All the relevant assignments of ^{1}H, ^{13}C and ^{15}N nuclei are made on the basis of the 1D and 2D data collected and the correlations observed. They are presented in Tables 4A.40 to 4A.43, Scheme.4A.14 and the spectral details are shown in Figs.4A.24 and 4A.25.

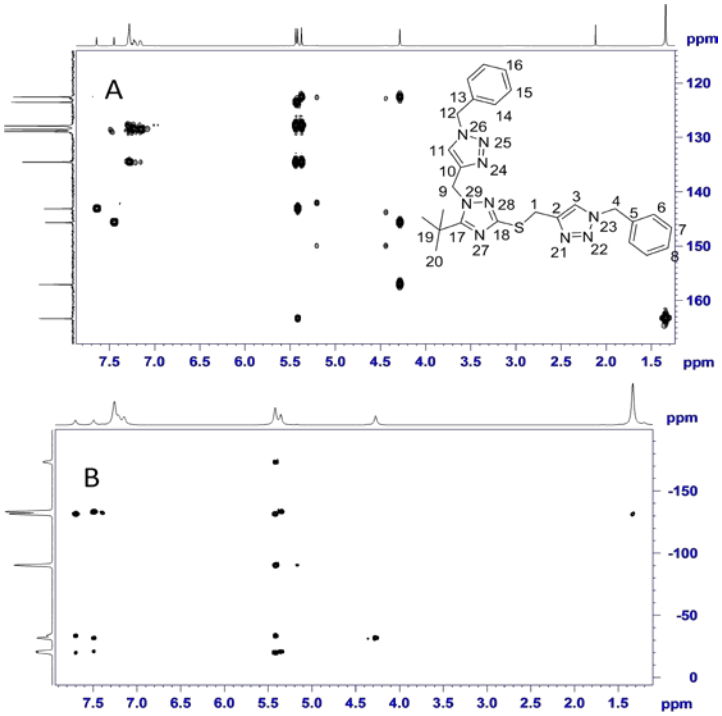

Fig. 4A.25: *^{1}H-^{13}C HMBC (A) ^{1}H-^{15}N HMBC(B) spectra of compound11*

Table .4A.40: *Homonuclear correlations observed for compound 11.*

The Carbon and the proton number	^{1}H chemical shifts (ppm)	correlation with (ppm)	Remarks
3	7.44	4.28, 5.37	COSY/NOESY
4	5.37	7.15	NOESY
9	5.41	7.64	COSY
12	5.43	7.22	COSY/NOESY
20	1.34	7.44, 5.37, 7.15, 5.41, 7.64	NOESY

Table .4A.41: *^{1}H -^{13}C HSQC/HMBC correlations obtained for compound 11.*

The Carbon and the proton number	^{1}H chemical shifts (ppm)	^{13}C chemical shifts (ppm)	Remarks
1	4.28	26.54	HSQC

		157.06, 122.55	HMBC
3	7.44	122.55 145.65, 53.87	HSQC HMBC
4	5.37	53.87 122.55, 134.51, 127.87	HSQC HMBC
9	5.41	46.02 163.32, 143.12, 123.53	HSQC HMBC
11	7.64	123.53 143.12, 53.96	HSQC HMBC
12	5.43	53.96 134.56, 127.87	HSQC HMBC
20	1.34	29.26 32.60, 163.32	HSQC HMBC

Table 4A.42: *^{1}H-^{15}N HMBC correlations obtained for compound 11.*

Nitrogen atom	^{1}H chemical shifts (ppm)	^{15}N chemical shifts (ppm)
21	4.28, 7.44	-31.83
22	7.44, 5.37	-21.06
23	7.44, 5.37	-133.42
24	5.41, 7.64	-33.79
25	7.64, 5.43	-20.16
26	7.64, 5.43	-131.61
27	-	-
28	5.41	-90.31
29	5.41	-173.42

It is interesting to note the NOE correlations of the t-butyl group H-20 with H-1, H-3, H-6 and H-11 (Fig.4A.24D) indicating that these groups are spatially close thus providing important information about the three dimensional structure of the molecule. A molecular dynamics calculation of this molecule shows a structure wherein the 1,2,4-triazole ring comes closer to the phenyl rings.

Table 4A.43: *Chemical shift assignment of compound 11*

Atom number	δ_H ppm	δ_C or δ_N ppm	Atom number	δ_H ppm	δ_C or δ_N ppm
1	4.28	26.54	16	-	128.52
2		145.65	17		163.32

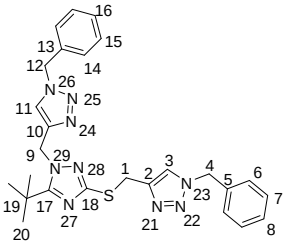

comp. 11

3	7.44	122.55	18		157.06
4	5.37	53.87	19		32.6
5		134.51	20	1.34	29.26
6	7.15	127.87	21		-31.83
7	-	-	22		-21.06
8	-	128.52	23		-133.42
9	5.41	46.02	24		-33.79
10		143.12	25		-20.16
11	7.64	123.53	26		-131.61
12	5.43	53.96	27		-
13		134.56	28		-90.31
14	7.22	127.87	29		-173.42
15	-	-	30		

Scheme.4A.14: *Pictorial representation of the various correlations obtained for the compound 11*

4.3.12 Compound 12: 1-benzyl-4-(((1-((1-benzyl-1H-1,2,3-triazol-4-yl)methyl)-5-(4-methoxyphenyl)-1H-1,2,4-triazol-3-yl)thio)methyl)-1H-1,2,3-triazole:

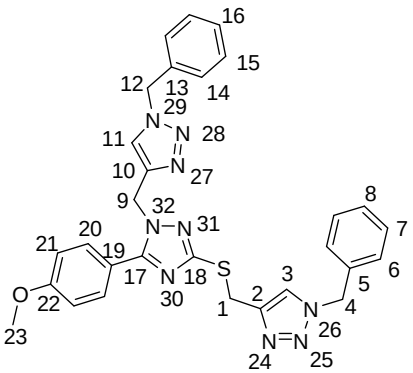

comp. 12.

Compound 12 is a regio isomer of compound 8 which differ in the position of substituent on the 1,2,4-triazole ring.

Observed ^{1}H and ^{13}C Chemical shifts:

^{1}H NMR (400 MHz, 298^{0}K; solvent $CDCl_3$ δ = 7.27 ppm), δ = 3.82 ppm (s, 3H), 4.38 ppm (s, 2H), 5.35 ppm (s, 2H), 5.39 ppm (s, 2H), 5.47 ppm (s, 2H), 6.96 ppm (d, J = 8.88 Hz, 2H), 7.17 ppm (m, 2H), 7.23 to 7.29 ppm (m, 5H),7.30 to 7.34 ppm (m, 3H), 7.50 ppm (s, 1H), 7.65 ppm (d, J = 8.88 Hz, 2H), 7.69 ppm (s, 1H).

^{13}C NMR (100 MHz, 298^{0}K; solvent $CDCl_3$, δ = 77.00 ppm), δ = 26.46 ppm, 44.73 ppm, 53.82 ppm, 54.02 ppm, 55.25 ppm, 114.21 ppm, 119.04 ppm, 122.58 ppm, 123.54 ppm, 127.81 ppm, 127.97 ppm, 128.44 ppm, 128.59 ppm, 128.83 ppm, 128.91 ppm, 130.32 ppm, 134.32 ppm, 134.52 ppm, 142.71 ppm, 145.36 ppm, 155.86 ppm, 158.89 ppm, 161.09 ppm.

Figs. 4A.25 and 4A.26 and Tables 4A.44 to 4A.47 provide all the NMR spectral details and correlations observed for the assignment of the chemical shifts. Important correlations are also shown schematically (Scheme.4A.15).

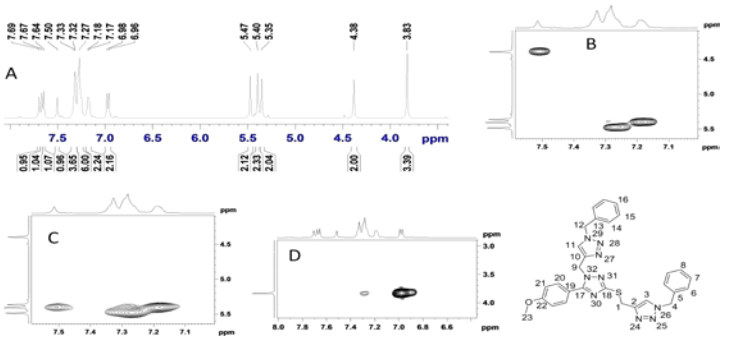

Fig.4A.26: *A) ^{1}H NMR spectrum of compound 12. B) Expanded COSY (B) and NOESY (C) spectrum showing correlations of CH_2 protons with aromatic protons. D) NOESY cross peak of methoxy protons (400 MHz, $CDCl_3$, 298 K).*

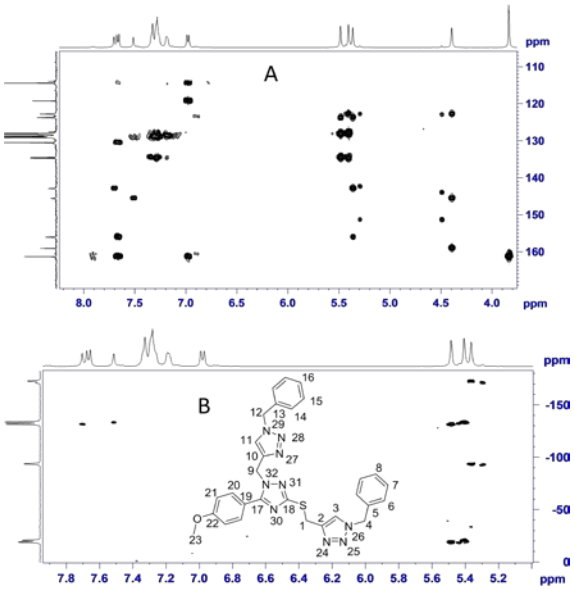

Fig 4A.27: *^{1}H-^{13}C HMBC (A) ^{1}H-^{15}N HMBC(B) spectra of compound11*

Table .4A.44: *Homonuclear correlations observed for compound 12.*

The Carbon and the proton number	^{1}H chemical shifts (ppm)	correlation with (ppm)	remarks
3	7.50	4.38, 5.39	cosy
4	5.39	7.17	cosy/noesy
9	5.35	7.69	cosy
12	5.47	7.25	cosy/noesy
20	7.65	6.96	cosy/noesy
21	6.96	3.82	noesy

Table .4A.45: *^{1}H-^{13}C HSQC/ HMBC correlations obtained for compound 12.*

The Carbon and the proton number	^{1}H chemical shifts (ppm)	^{13}C chemical shifts (ppm)	Remarks
1	4.38	26.46 158.89, 145.36, 122.58	HSQC HMBC

3	7.50	122.58 145.36, 53.82	HSQC HMBC
4	5.39	53.82 122.58, 134.52, 127.81	HSQC HMBC
6	7.17	127.81 53.82	HSQC HMBC
9	5.35	44.73 155.86, 142.71, 123.54	HSQC HMBC
11	7.69	123.54 142.71, 54.02	HSQC HMBC
12	5.47	54.02 123.54, 134.32, 127.97	HSQC HMBC
14	7.25	127.97 54.02	HSQC HMBC
20	7.65	130.32 155.86, 161.09	HSQC HMBC
21	6.96	114.21 119.04, 161.09	HSQC HMBC
23	3.82	55.25 161.09	HSQC HMBC

Table .4A.46: *^{1}H-^{15}N HMBC correlations obtained for compound 12.*

Nitrogen atom	^{1}H chemical shifts (ppm)	^{15}N chemical shifts (ppm)
24	4.38	-31.89
25	5.39	-21.18
26	7.50, 5.39	-133.34
27	5.35	-33.49
28	5.47	-18.93
29	7.69, 5.47	-131.61
30	-	-
31	5.35	-93.78
32	5.35	-172.73

Scheme.4A.15: *Pictorial representation of the various correlations obtained for the compound 12*

It is interesting note that the ^{13}C NMR spectrum obtained for this compound is much sharper than that of its regio isomer (compound 8) discussed before. A comparison of them is shown in Fig.4A.28. In compound 12 the 1,2,3 triazole units are further separated (attached to C18 and N32) compared to compound 8 (C18 and N31). Hence, it is very clear that the observed broadening of some of the carbon signals in compound 8 is motional restriction induced due to the steric effect of the substituent.

Table .4A.47 Chemical shift assignment of compound 11

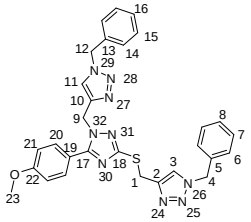

Atom number	δ_H ppm	δ_C or δ_N ppm	Atom number	δ_H ppm	δ_C or δ_N ppm
1	4.38	26.46	17		155.86
2		145.36	18		158.89
3	7.5	122.58	19		119.04
4	5.39	53.82	20	7.65	130.32
5	-	134.52	21	6.96	114.21

6	7.17	127.81	22		161.09
7	-	-	23	3.82	55.25
8	-	-	24		-31.89
9	5.35	44.73	25		-21.18
10		142.71	26		-133.34
11	7.69	123.54	27		-33.49
12	5.47	54.02	28		-18.93
13		134.32	29		-131.61
14	7.25	127.97	30		-
15	-	-	31		-93.78
16	-	-	32		-172.73

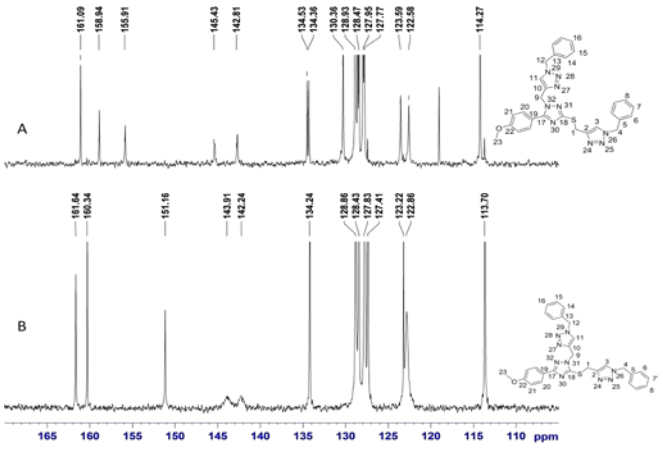

Fig 4A.28: Comparison of ^{13}C NMR spectra compound11 (A) and 8.

Comparison of ^{13}C chemical shifts (Table.4A.48) of regio isomers also brings out interesting features. The two triazole carbons C17, C18 and C19 show characteristic changes. The ^{13}C signal of 1,2,4 triazole ring which is close to the substituent (α to substituent) , is always shielded while the other ring carbon experiences deshielding. These are depicted in Scheme.4A.16. Similar effects are seen for region isomers shown in Schemes.4A.17-20. These observations are very similar to the changes in chemical shifts observed for the two tautomers discussed in Chapter III. As in the case of tautomers, the regio isomers also affect changes in the chemical shift of C19 carbon in compound 8 and 12. The proximity of substituent leads to shielding of it and it can be used as quick way to identify regiosiomers without going into detailed NMR investigations.

Table 4A.48: *Comparison of the chemical shifts of compound 12 with its regiomer compound 08.*

Atom number	δ_H ppm comp. 12	δ_H ppm comp. 08	δ_C ppm comp. 12	δ_C ppm comp. 08
1	4.38	4.47	26.46	28.32
2			145.36	143.86
3	7.5	7.48	122.58	122.9
4	5.39	5.35	53.82	53.79
5	-		134.52	134.18
6	7.17	7.1	127.81	127.69
7	-	-	-	-
8	-	-	-	128.39
9	5.35	5.26	44.73	43.97
10			142.71	142.28
11	7.69	7.46	123.54	122.9
12	5.47	5.39	54.02	53.89
13			134.32	134.23
14	7.25	7.19	127.97	127.8
15	-	-	-	-
16	-	-	-	128.47
17			155.86	161.68
18			158.89	151.2
19			119.04	123.2
20	7.65	7.89	130.32	127.37
21	6.96	6.87	114.21	113.65
22			161.09	160.3
23	3.82	3.78	55.25	55.07

Scheme.4A.16: *Comparison of chemical shifts of regioisomers compound 8 and 12*

Scheme.4A.17: *Comparison of chemical shifts of regioisomers compound 4 and 9*

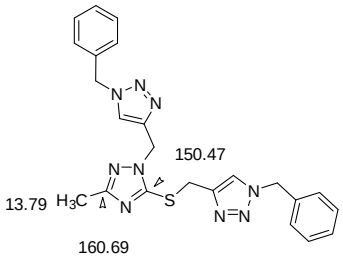

comp. 05
Regiomer A

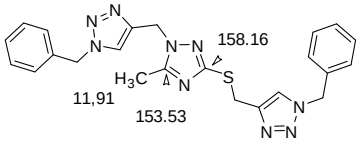

comp. 10
Regiomer B

Scheme.4A.18: *Comparison of chemical shifts of regioisomers compound 5 and 10*

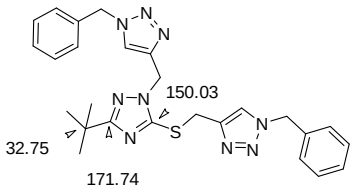

comp. 06
Regiomer A

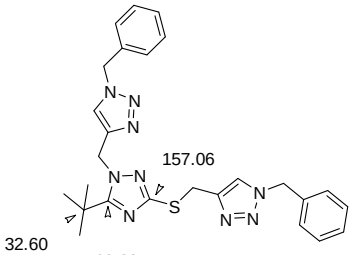

comp. 11
Regiomer B

Scheme.4A.19: *Comparison of chemical shifts of regioisomers compound 6 and 11*

4.4 Evaluation of the NOESY cross peaks obtained in 3, 6 and 11 triazole derivatives:

The NOESY spectrum provides a measure of ^{1}H-^{1}H spatial distances up to 5 Å. This information is useful for determining the 3-dimensional structure of molecules. In compounds 3, 6 and 11, the 2D NOESY spectra, recorded at 64 to 80 mM concentrations with a mixing time of 1s, shows cross peak between atoms which are far apart and is difficult to explain (Scheme.4A.20. It could result either from an intermolecular interaction (self assembling) or a conformation which is intra molecular in nature. For example, the NOESY spectrum of compound 3 is shown in Fig.4A.29

Scheme.4A.20: *Pictorial representation of the key long range nOe's in compounds 3, 6, and 11.*

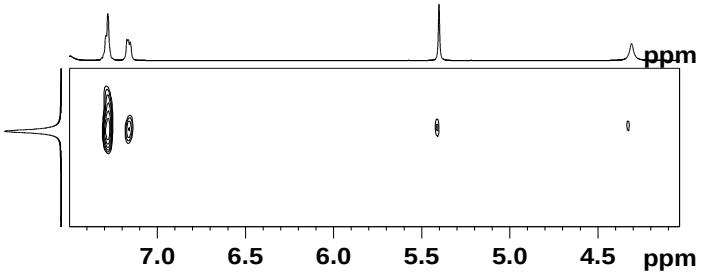

Fig.4A.29:*The expanded 2D NOESY spectra of compound 3 showing the NOESY correlations with the other protons in the molecule.*

In the case of compound 3, 1,2,4-triazole ring is aromatic and planar. The t-Bu group substituent at C-9 of the 1,2,4-triazole ring, exhibits NOESY cross peaks with H-1, H-3, H-4, H-6, and H-7 protons which are located almost on the opposite side of the t-Bu substituent. The nOe contacts between them indicate that the t-Butyl group and protons of the benzyl group are within the 5Å distance. However the X-ray structure of the compound (Fig.4A.30) shows that the groups which show NOE cross peaks are not oriented spatially close to each other. Hence, the nOe pattern obtained is either from intermolecular interactions or from a solution state structure which is different from the solid state structure. This triggered our interest to study self-assembly (intermolecular interactions) in these triazoles.

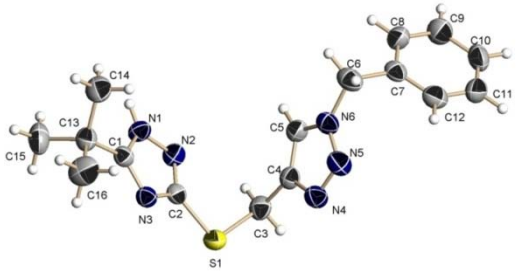

Fig.4A.30: *ORTEP diagram of X-ray structure of the compound 3.*

Similarly, compound 6 also shows cross peaks between the t-Bu and H-1, H-3, H-4, H-6, H-9, H-14 protons (Fig. 4A.31). The noticeable difference between compounds 3 and 6 is that in the latter the same side chain is also attached to 1,2,4 triazole nitrogen (N-28) as well as to sulphur atom as in compound 3. This gives the new substituent a different spatial position but the NOE cross peaks between H-9, H-14 as well as H-6 and the t-Bu group are still observed. The similar kind of long range nOe's obtained in the compounds 11 is shown in the Fig.4A.32

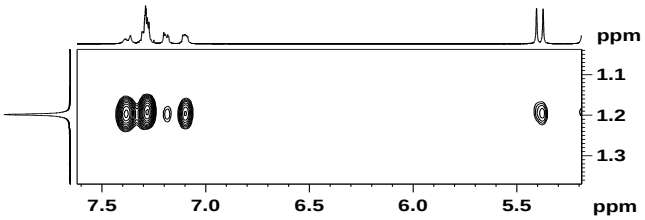

Fig.4A.31: *The expanded 2D NOESY spectra of compound 6 showing the NOESY correlations of the t-Bu group with the other aliphatic protons in the molecule.*

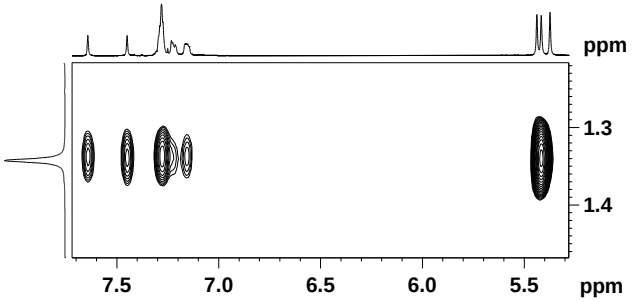

Fig.4A.32: *The expanded 2D NOESY spectrum of compound 11 showing the NOESY correlations of the t-Bu group with the aromatic protons in the molecule.*

In these cases the NOESY cross peaks are difficult to rationalize. One of the possibilities is t intermolecular nOe due to self-aggregation. Organic molecules, which posses the properties of self-aggregation can show such intermolecular nOe's [12-15] and self-aggregation is a known phenomenon in triazole derivatives [16-18].

4.5 Conclusions.

Characterization of hybrid triazole molecules containing 1,2,3 and 1,2,4 trazole moieties by a combination of various 1 and 2 dimensional NMR techniques helps to identify hierarchical order of the magnitude and ranges of the chemical shifts for the different atoms. COSY cross peak arising from long range scalar coupling are shown to be very useful for assignments of various methylene bridges in these hybrid molecules. ^{15}N-^{1}H HMBC along with the ^{13}C-^{1}H HMBC is very useful for obtaining unambiguous assignments. Unexpected long range NOESY cross peaks were observed for some of the compounds which needs to be investigated in detail.

4.6 Part B: Studies on self-assembly of flexible triazoles and non-covalent bidentate contacts with halide anions.

Aim of the study: In this study we examine the self-assembling properties of the new hybrid triazoles containing both 1,2,3 and 1,2,4-triazole rings and the ability of these systems to form non covalent complexes with various halide anions *via*. 1,2,3-triazole CH---halogen ion interactions in solution.

It has been shown that aromatic protons can play a supporting role in binding halide anion along with triazole CH in aryl substituted traizoles.[19] for example the triazole macrocycles [20] and foldamers [21] containing polarized CH in the 1,2,3-triazole ring in which the hydrogen can be allowed to interact with the halide ions which are highly charged.[22] Flood *et al*. reported that the small fluoride anion can bind with two triazole units and one phenylene CH. [20 b] It is known that the binding of the anion with triazole could be enhanced if the system contains hydrogen atoms bound to an electronegative heteroatom[23], aryl proton[24] , aliphatic hydrogen[25] flanked between

the strongly withdrawing atoms or groups etc. The self-assembling nature of molecules affects their properties. The 1,4-substituted triazole rings are known to show π-stacking.[26] It is also known that triazoles can self-assemble into supramolecular structures whose shape, size and function can be controlled by external factors. Triazole macrocycles also possess interesting self-assembling properties.[27] Whitesides *et al*. have described a wide range of applications for materials possessing self-assembling properties.[28]

Results and discussion:

The ^{1}H NMR spectra of triazole derivatives discussed in the previous section shows that the spectra are somewhat broad at higher concentrations and a few of the observed long range NOE cross peaks are difficult to rationalize. These could be the result of intermolecular interactions in the triazole systems studied. This triggered our interest in the study of self-assembling behavior of model triazoles in $CDCl_3$ solution.

In this section, the self-assembling nature of some of triazole systems (Scheme.4B.1) discussed in the previous section has been examined through the effect of temperature and concentrations on the ^{1}H NMR chemical shift and also by following the changes in diffusion coefficients with concentration.

Scheme.4B.1: *Structures of the compounds used for the studies with the adopted numbering.*

NMR studies:

Structures of all the four compounds shown in Scheme.4B.1 have been completely characterized by a combination of ^{1}H, ^{13}C and ^{15}N 1D/2D NMR experiments as explained in the previous section. ^{1}H NMR spectra of all the compounds were found to be broader than expected which is likely to be due to either restricted molecular rotation/motion and/or self assembling of the molecules in solution. In order to obtain more insights and a deeper understanding of the contribution from these factors the ^{1}H NMR spectrawere monitored as a function of temperature and dilution.

4.6.1 Temperature effect: Temperature affects the degree of intermolecular hydrogen bonding or other types of intermolecular interactions leading to aggregation, and this is likely to be accompanied by chemical shift changes. Generally on increasing the temperature, the intermolecular interactions are weakened (lengthened on average) and the protons are shifted upfield. Also, if the temperature of a solution is increased, the magnitude of thermal fluctuations becomes larger, which results in an increase in the average distance between the atoms and weakening of inter molecular interactions. The chemical shifts of protons involved in intermolecular interactions display temperature

dependence. Temperature coefficient (Δδ/ΔT), defined as the ratio of chemical shift change with temperature is widely employed to study the strength of hydrogen bonds and thus to differentiate the intra and inter molecular hydrogen bonds.[29]

It should also be noted that for molecules that are conformationally flexible, the populations of conformers change with temperature. If the chemical shifts of various conformations are different, it will vary with temperature and the observed chemical shift is the weighted average of the shifts of the individual conformations.

Compound 1:

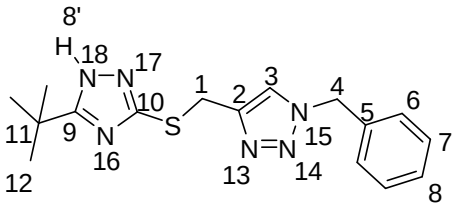

Fig.4B.1 summarizes the effect of temperature on the ^{1}H NMR spectrum of compound 1. It indicates that the H-8' (NH) of compound 1, shows a large upfield shift by $\Delta\delta = 2.90$ ppm with increase in temperature from 243 to 318 Kleading to a temperature coefficent of -38.6 ppb/K. This indicates that at lower temperature H-8'is invlolved in some kind of intermolecular hydrogen bonding. As the temperature increases, there is a decrease in intermolecular interactions, which results in an upfield shift for the NH (H-8') proton. The considerable change in the magnitude of the NH chemical shift ($\Delta\delta/\Delta T$=-38.6ppb/K) indicates that the NH is involved in some type of intermolecular interactions. One of the possibilities of intermolecular interaction is with trace amount of water present in the solvent employed for measurement. The NH proton can, in principle, undergo slow chemical exchange with these water molecules, which also involves inter molecular

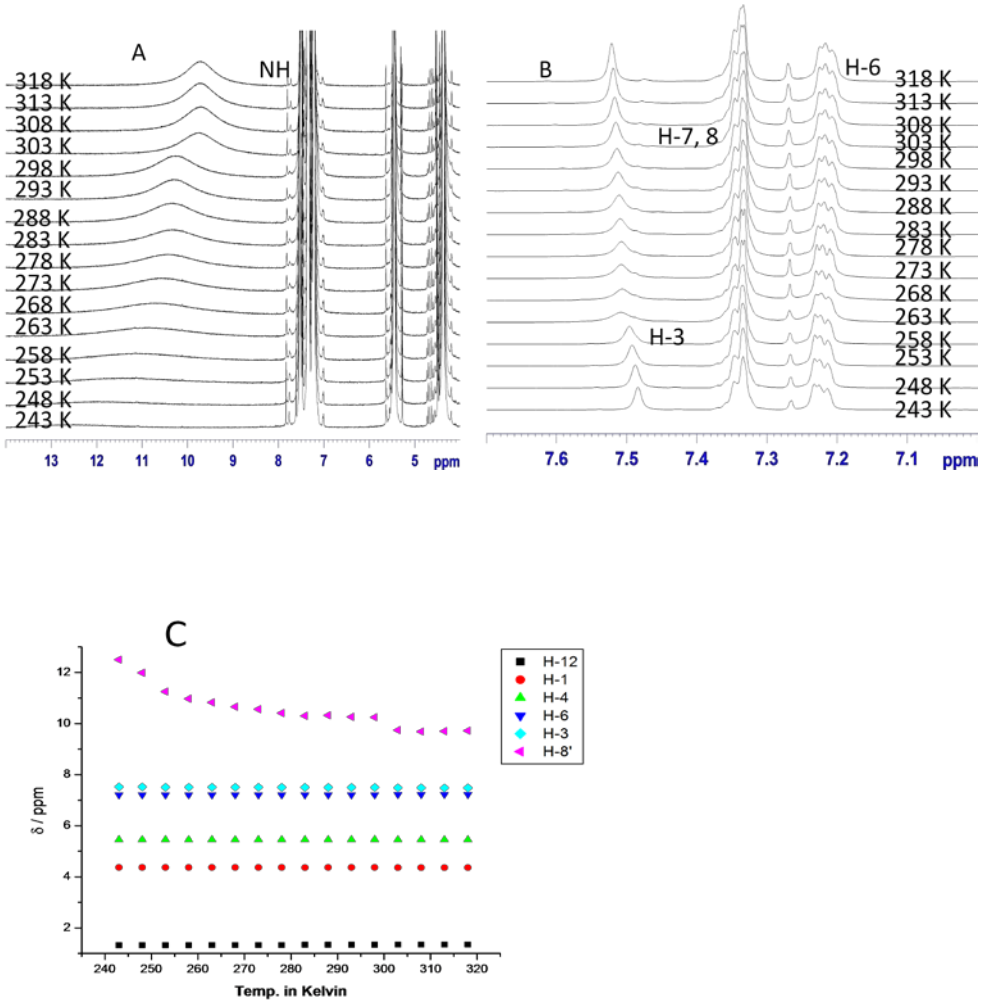

Fig.4B.1: *Effect of temperature on the ^1H NMR spectrum of compound 1 in $CDCl_3$ solution (400 MHz) A) triazole ring NH, B) aromatic protons and C) plot of ^1H chemical shift verses temperature.*

hydrogen bonding with water. These intermolecular hydrogen bonds break at higher temperature and result in faster chemical exchange. This will also lead to an upfield shift of the NH proton (as observed) as well as line broadening , which was not observed. Temperature response of the ^{1}H NMR spectrum is shown in Fig.4B.1 It can be seen from the figure that as the temperature increases, broadening of the NH signal decreases. The presence of any dynamic process (exchange) with water taking place at room temperature is expected to become faster at higher temperature and would have resulted in broadening of the NH signal. However, the observed sharpening of the NH signal suggests the presence of a dynamic process other than chemical exchange with water.

Appreciable broadening of NH signal at lower temperature suggests its participation in intermolecular interactions with other triazole molecules. The triazole H-3 proton of compound. 1 exhibits a weak upfield shift of $\Delta\delta$ = 0.04 ppm with an increase in temperature from 243 to 318 K ($\Delta\delta/\Delta T$=-0.53 ppb/K) implying very weak intermolecular interactions involving the triazole CH.

The ^{13}C chemical shifts of compound 1 are practically unaffected (Fig.4B.2) in the temperature range studied (243 to 318 K) and shows that the ^{13}C nuclei are not directly involved in any intermolecular interactions

.

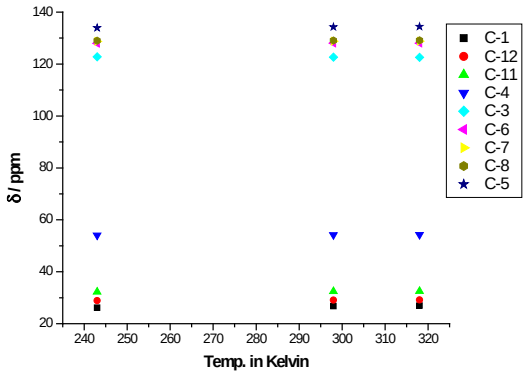

Fig.4B.2: *Plot of ^{13}C chemical shift verses temperature (right) for the compound 1 in $CDCl_3$ solution.*

Compound 3:

Variable temperature ^{1}H NMR:

The ^{1}H NMR spectra obtained at various temperatures are shown in Fig. 4B.3A,E). A plot of chemical shift vs temperature (Fig.4B.3B,C.) indicates that the triazole CH proton, H-11, shows a slight upfield shift by $\Delta\delta$ = 0.022 ppm with increase in temperature from 253 to 323 K (-0.31 ppb/K). This suggests the prescece of very weak intermolecular interactions associated with the 1,2,3-triazole moiety containg H-11.

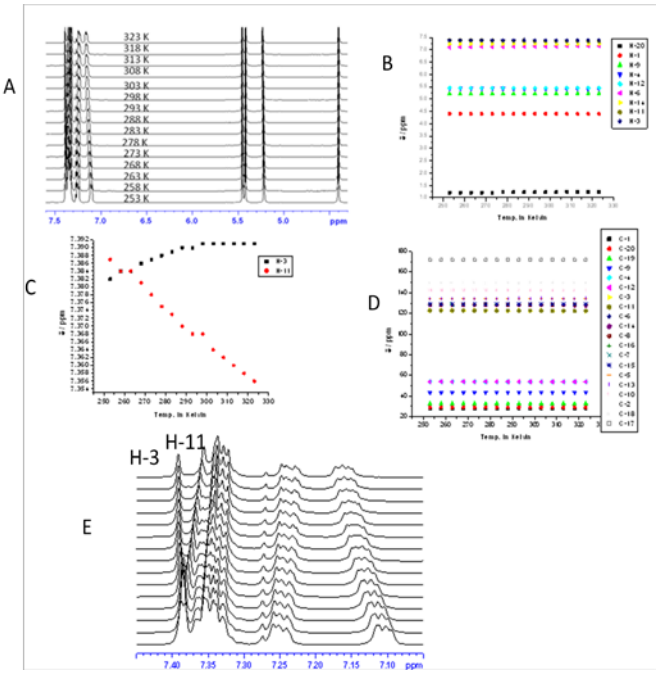

Fig.4B.3: *Effect of temperature (253K-323K) on the ^1H NMR spectrum of compound 3 in $CDCl_3$ solution. A)^1H spectrum at different temperatures with temperature increasing form bottom to top, B) plot of ^1H chemical shift versus temperature, C) plot of chemical shift versus temperature for H3 and H11, D) expanded ^1H NMR spectrum at different temperature. The temperature increases from bottom to top. E) plot of aromatic proton chemical shift versus temperature.*

On the other hand, the other triazole ring proton, H-3 shows a very weak downfield shift by $\Delta\delta = 0.004$ ppm with increase in temperature (+0.057 ppb/K). This minor change in chemical shift indicates that the H-3 is not involved in intermolecular interactions and the down field shift could result from the disruption of weak π-π ineractions. The π-π interaction results in shielding and usually shows postive temperature coefficient (deshielding at higher temperature). The possibility of of an intramolecular CH-----N type of interaction of H-3 with either of the N-24, N-25 or N-26 of the same molecule cannot be ruled out. It is also known that triazole CH forms weak intramolecular C-H...O hydrogen bond with suitably placed heteroatoms having the capacity to form hydrogen bonding. [30]. No noticeable temperature dependent changes were observed for the various carbons in the molecule. (Fig.4B.3D)

Compound 4:

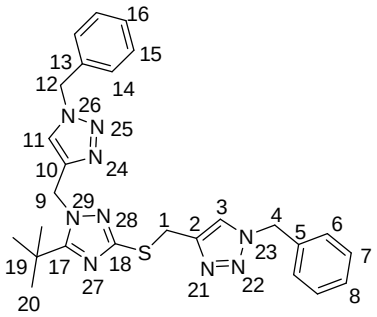

Variable temperature ^{1}H NMR measurements of compopund 4 show very negligible changes in chemical shifts (Fig.4B.4). The feature of triazole ring protons H-3 and H-11are higlighted in Fig.4B.4C.

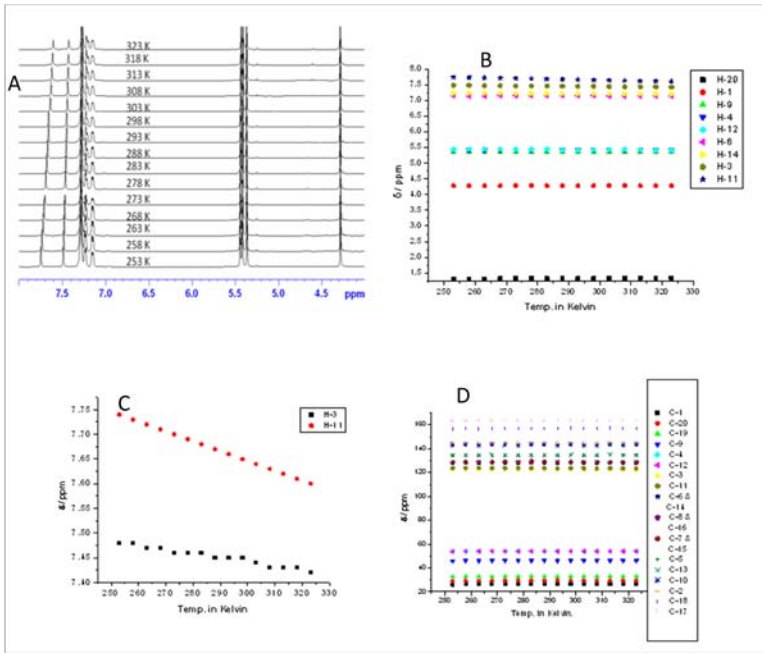

Fig. 4B.4: *Effect of temperature (253K-323K) on the ^{1}H NMR spectrum of compound 4 in $CDCl_3$ solution. A)^{1}H spectrum at different temperature, B) plot of ^{1}H chemical shift verses temperature, C) plot of chemical shift versus temperature for H3 and H11,D) plot of ^{13}C chemical shift versus temperature.*

Both of them show minor upfield shiftsof $\Delta\delta$ = 0.062(-0.88 ppb/K) and 0.143 ppm (-2.04 ppb/K), respectively with increase in temperature suggesting the possibility of weak intermolecular interactions involving triazole CH in this compound and that the involvement of H-11 is more than that of H-3. As in the previous cases, ^{13}C chemical shifts were not affected by change in temperature (Fig.4B.4D)

In general, some of the triazole ring C-H protons show minor negative temperature coefficients (shielding with increase in temperature) indicating very weak intermolecular interactions. One of the triazole CH (H-3) protons in compound 3 shows minor deshielding effect with temperature. The NH proton, if present in the molecule, has a major role to play in the inter- molecular interactions. The ^{13}C signals are practically unaffected by change in temperature. Also, the ^{13}C chemical shifts are likely to change only in the cases involving breakage of very strong self-assemblies with increase in temperature, since the carbon atoms are affected to a lesser extent by solvent, temperature and other external conditions when compared to protons.

Smaller values of temperature coefficients can be encountered if the intermolecular interactions are either too strong so that the temperature range used (which is limited by the solvent $CDCl_3$) is not enough to break these intermolecular interactions or if the intermolecular interactions are very weak or absent. The maximum effect is observed for the triazole NH proton in compound 1. This can also arise from intermolecular interactions with trace amount of water present in the solvent.

The exact nature of intermolecular interactions could not be confirmed from these studies even though it favours the presence of very weak intermolecular interactions involving triazole C-H. Nevertheless, these measurements definitely rules out the possibilities of strong π-π stack interactions which would have resulted in an appreciable upfield shift of protons on cooling. Dilution experiments were performed to obtain more insights into the self-assembly phenomenon in these compounds.

4.6.2 Dilution effect:

Introduction:

Measurement of ^{1}H NMR chemical shift as a function of concentration is generally employed to differentiate inter and intra molecular interactions, especially in systems involving hydrogen bonds. Concentrated solutions have less number of solvent molecules compared to dilute solutions and hence will have more intermolecular interactions. In other words, more of the solute molecules are exposed to solvent in dilute

solutions. These changes in the solute-solvent and solute-solute interactions usually modify ^{1}H chemical shifts of the solute molecules.

Result and discussions:

The changes in ^{1}H NMR spectra of compounds 1, 2 and 03 were studied in the concentration range 100 to 10 mM. (Fig.4B5)Shielding or broadening of ^{1}H NMR signals at higher concentrations is characteristic of aggregation or self assembling process. For compound 01, H-8'(NH) and the H-3 (1,2,3-triazole CH), both experience a downfield shift at 100 mM by $\Delta\delta$ = +1.29 and $\Delta\delta$ = +0.04 ppm, respectively due to intermolecular interactions compared to the chemical shifts at 1mM, a concentration at which the solute -solute intermolecular interactions are very weak. At higher concentration the NH protons show a downfield shift ($\Delta\delta$ = +1.29) with broadening of the signal indicating its role in intermolecular interactions. This is very similar to what was noticed on lowering of temperature.. The small change in $\Delta\delta$ = +0.04 ppm seen for the triazole C-H may be originating from weak intermolecular interactions. The aromatic protons H-6 experience an up field shift by 0.03 ppm ($\Delta\delta$ = -0.03 ppm) indicating that these groups interact through very weak intermolecular π –π stacking at 100 mM concentration.

On a closer examination of the data shown in Fig.4B.5B it is clear that NH protons show down field shifts while the aromatic protons H-6, H-7 and H-8 show up field shifts with increasing concentration. The up field shift of the aromatic protons with increase in concentration is a signature of π-π stacking interaction in solution.[31]

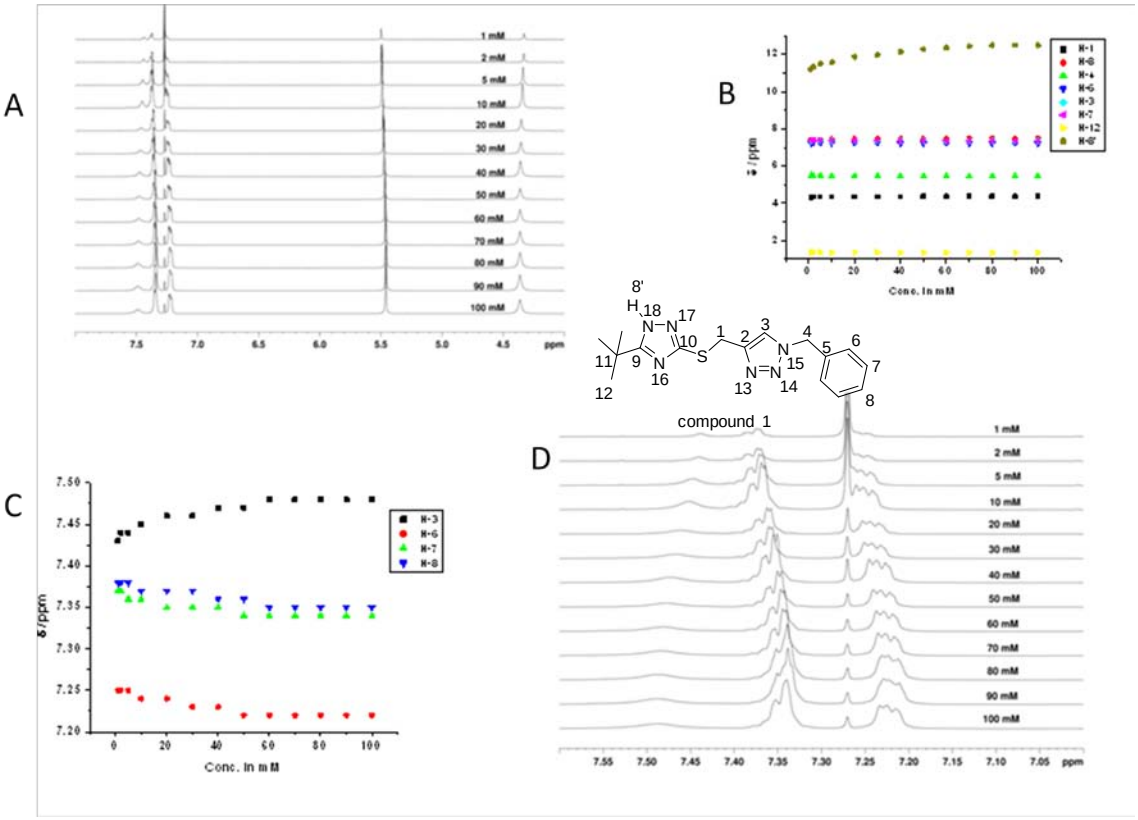

Fig. 4B.5: *A,D: Effect of solute concentration (100-1mM) on the* ^{1}*H NMR spectrum of compound .1 (400 MHz,* $CDCl_3$*, 298K). B, C Plot of* ^{1}*H chemical shift verses concentration 100 to 1mM.*

Compound 3:

For compound 03, at higher concentration (100 mM), both H-3 and H-11 experience an up field shift of 0.26 and 0.149 ppm, respectively compared to the chemical shifts at 10 mM concentration (Fig.4B.6). In contrast, the aromatic protons experience very minor change (down field shift by 0.027 ppm) with the same change in concentrations (Fig.4B.6C.) These observations indicate that H-3 and H-11 plays some

role in the weak CH-π type of intermolecular interactions at higher concentrations. With gradual decrease in concentration, at 10 mM these intermolecular interactions are disrupted and H-3 and H-11 tend to show chemical shifts devoid of the effects of intermolecular interactions.

As shown in Fig.4B.6 at a lower concentration of 10 mM the peaks of the *S*-CH_2 and the triazole protons resonate relatively down field but as the concentration of the triazole compound 3 is increased the S-CH_2 and the triazole protons show slightly up field shifts due to the increase in intermolecular interactions. The slight broadening of these signals may also be attributed to the increased intermolecular interactions between the triazole moieties due to weak CH-π interactions.

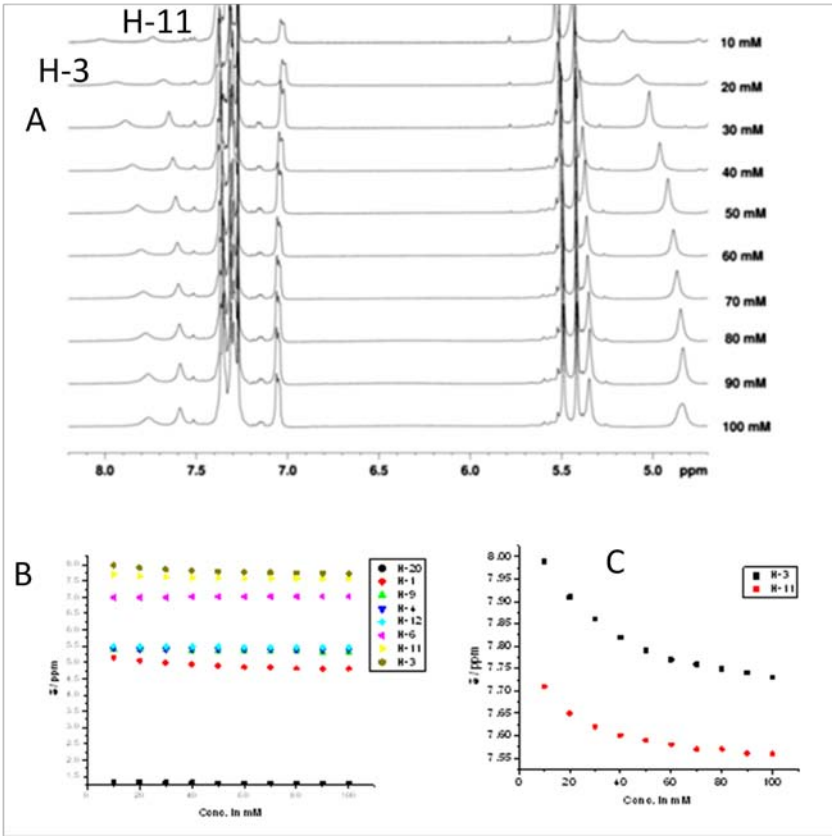

Fig. 4B.6: *A) Effect of solute concentration on the ^1H NMR chemical shifts of compound 3 (400 MHz, $CDCl_3$, 298K). B, C Plot of ^1H chemical shift versus concentration in the range 100 mM to 1 mM.*

The behavior of compound 2 is very similar to that of compound 3 i.e. both H-3 and H-11 experience up field shifts of $\Delta\delta$ = 0.147 and $\Delta\delta$ = 0.375 ppm respectively

(Fig.4B.7) The S-CH_2 and the H-17 in compound 02 also show a slight up field shift due to the increase in concentration as noticed in compound 3 which were also attributed to the increase in the intermolecular interactions of the CH-π type. Similarly, upfiled shift with increasing concentration indicates that the compound has either CH-π or π-π stack interactions. The lower magnitude of the change in chemical shift indicates weaker interactions. [3

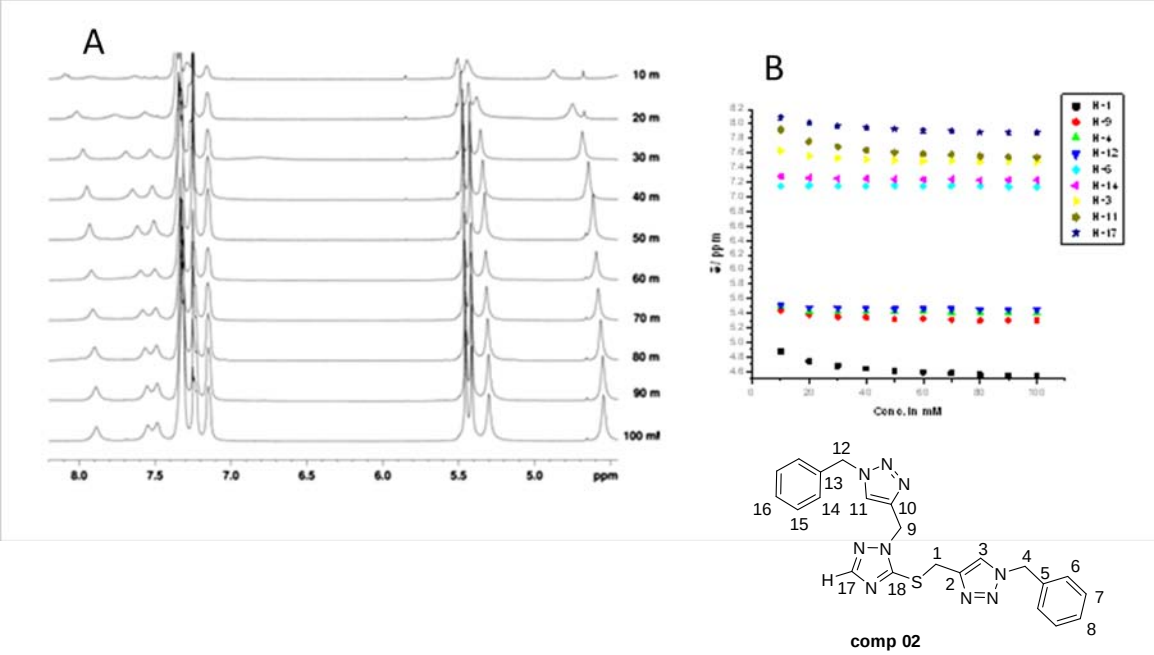

Fig.4B.7: *A Effect of solute concentration on the ^1H NMR spectrum of compound 2 (400 MHz, $CDCl_3$, 298K). Plot of 1H chemical shift verses concentration.*

Overall conclusions of the dilution study:

From the variable temperature and dilution experiments it is clear that the triazole ring C-H has some role in the intermolecular interactions of these compounds. The magnitude of chemical shift changes suggests that the inter molecular interactions, if present, are very weak in nature. The intermolecular forces in all three compounds are probably dictated by the intermolecular CH-π interactions. To get more insight, NMR self diffusion coefficients measurements were performed on these samples at a few representative dilutions.

4.6.3 Diffusion studies:

The diffusion of molecules depends on physical parameters such as shapes and sizes of the molecules, temperature and viscosity. Small molecules diffuse faster than bigger ones. Hence, one would expect slower diffusion if the molecules aggregate in solution since molecular aggregates are of larger size than a single molecule. In the present investigation difference in the diffusion coefficients in concentrated and dilute solutions have been examined to evaluate the aggregation in triazoles 1 and 2 with the anticipation that aggregation of molecules leads to a proportional decrease of the self diffusion coefficients.

NMR diffusion measurements were carried out on solutions of 100, 10 and 5 mM concentrations. The diffusion coefficients are summarized in Table.4B.1. For compound 1 the diffusion coefficients are 6.382×10^{-10}, 6.548×10^{-10} and 7.872×10^{-10} m^2/s for 100, 10 and 5 mM solutions respectively. A similar trend is also seen for compound 2. A 10 fold increase in concentration from 10mM to 100mM does not change the diffusion coefficients to any greater extent, though the molecules in 5mM solution diffuse faster. These changes can be attributed to changes in viscosity or very weak association. The intermolecular interactions, even if present, do not lead to any molecular self assembly or bigger aggregates. Probably weak aggregates of small order are formed under the experimental conditions.

Table.4B.1: *Self diffusion coefficients (D) for compound 01 and 02 at the different concentrations.*

Conc. in mM	Comp. 01	Comp. 02
100	6.382×10^{-10} m^2/sec	7.697×10^{-10} m^2/sec
10	6.548×10^{-10} m^2/sec	7.853×10^{-10} m^2/sec
5	7.872×10^{-10} m^2/sec	8.461×10^{-10} m^2/sec

Taking into account minor changes in chemical shift with dilution or change in temperature the formation of strong self-assemblies or aggregates, which can result in the intermolecular nOe's observed for these molecular systems are ruled out. Therefore, the NOESY cross peaks obtained in these compounds are likely to be of intra molecular origin. In order to verify this, Molecular Dynamics (MD) studies were performed on compounds 1,2 and 3 and the following 3D structures were determined.

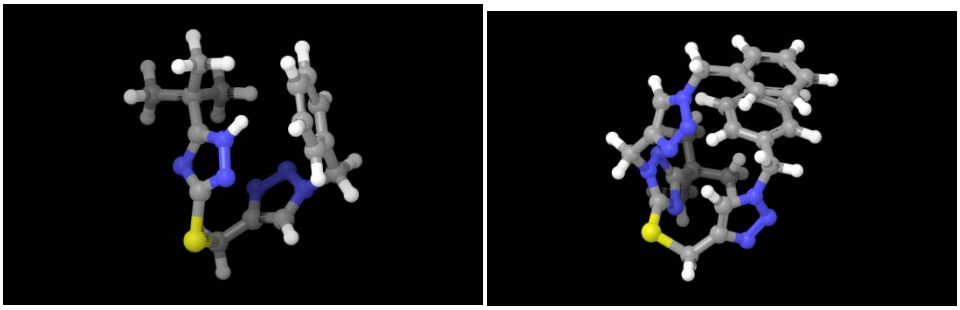

Fig.4B.8: *The energy optimized triazole derivative compound. 1 (left) and 3(right) by using the Jaguar version 7.9 from the Schrödinger software by utilizing the amber* force field and the 6-31g** ++ basis set.*

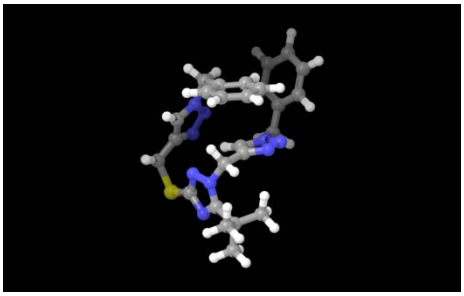

Fig. 4B.9: *The energy optimized triazole derivative compound. 4 by using the Jaguar version 7.9 from the Schrödinger software by utilizing the amber* force field and the 6-31g** ++ basis set.*

It can be seen from the optimized structures shown in Fig.4B8 and 4B.9 that the triazole molecules does not have a linear structure and the tertiary group being bulkier protrudes out and has a probability of a higher degree of spatial interactions with the groups around it. This could be one of the reasons for the observed nOe's under the experimental conditions in solution state.

4.6.4 Aggregation in the solid state by using the scanning electron microscopy (SEM) images:

The self-assembly of the triazoles has been studied in the solid state by scanning electron microscopy (Fig.4B.10). In case of triazoles interplay of attractive and repulsive interactions of non-covalent nature leads to rotational constrains around single bonds attached to the 1-and 4-positions and should therefore be able to induce well-defined conformational preferences in the triazoles. The supramolecular organization of these triazoles into irregular self-assemblies has been visualized by scanning electron microscopy (SEM) in the solid state. The lack of planarity of the different aromatic rings due to the presence of the labile methylene or benzylic groups hamper formation of regular three dimensional assemblies. These irregular assemblies are unlikely to persist in presence of a good solvent like $CDCl_3$ employed in NMR studies.

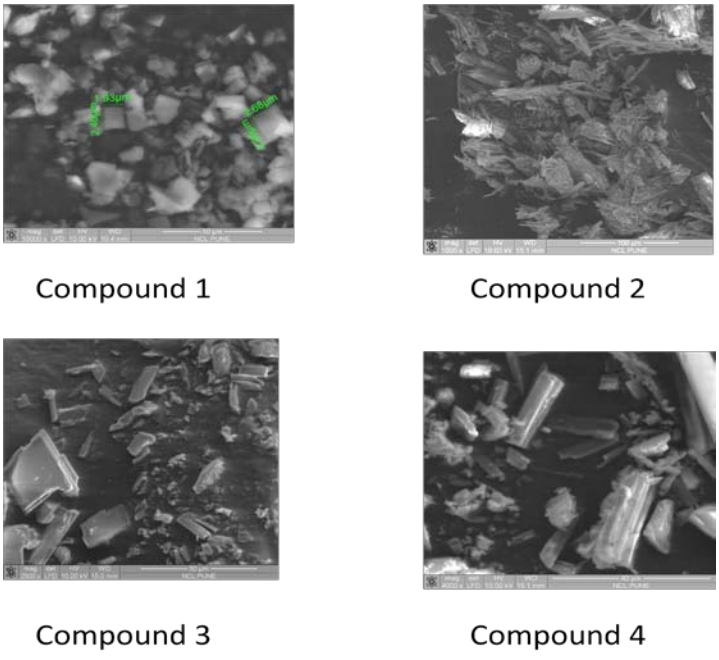

Fig.4B.10: *SEM images of compound 1,2,3 and 4 showing the irregular self-assemblies of different shapes.*

4.6.5 Binding studies of the triazole CH with the halide anions:

There are many reports on binding of halogen ions to rigid macrocyclic triazoles through aromatic CH- H-bonds. [20a, 17, 33] In such cases suitably placed aromatic protons of the aromatic moiety also assists in the binding of the halide anions as shown in the Scheme.4B.2 and 3.

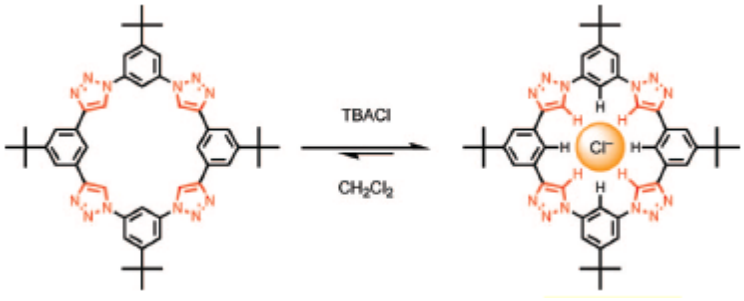

Scheme.4B.2 : *[3$_4$]Triazolophanes tightly encapsulating Cl^- ions in CH_2Cl_2.*

Open or flexible aryl triazoles are also known to bind with the halide anion through complexation induced conformational changes. In this case also, a suitably located aromatic protons takes part in the binding processes with the halide anion.[27]

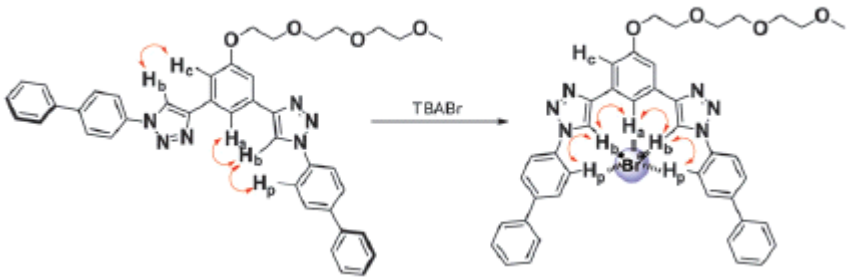

Scheme.4B. 3: *Chemical structures of the flexible aryl triazole receptors binding with the TBABr.*

Various studies demonstrating non covalent interactions of 1,2,3-triazoles such as triazolophane [34], triazole-based cyclic peptide [35] etc. have been reported. Flood et al

used model triads to show that the CH of 1,2,3-triazoles appear to approach the hydrogen bond strengths of the NH donors of pyrrole units[36]. They have also studied the CH···halide interactions by employing DFT calculations. A proper understanding of the nature of non covalent interactions of triazole moieties is very important for rational drug design since the number of synthetic, drug candidates containing triazoles moieties are ever increasing.

This part of the thesis deals with the study of halide ion binding capability of some of the triazoles that have been investigated for structural characterization. These triazol molecules are more flexible in nature compared to the structurally constrained macro cyclic cases and they also have aromatic rings as well as triazole C-H which can take part in binding with the halide ions. Triazole derivatives studied here also show antitubercular activity by selectively killing dormant pathogenic *tuberculi bacilli*.[9]

Result and the discussions:

Apart from the triazole C-H other aliphatic and the aromatic groups can also take part in binding with the halide anion. Computationally it is shown that the aryl CH…anion hydrogen bond strength is about half of that of the NH…anion bond.[37, 38] and takes a secondary role in binding.[20b] NMR spectroscopic studies were undertaken to obtain a better picture of CH- halogen interactions in triazoles derivatives 3 and 1. The anion binding properties of complexes of these compounds were monitored by ^{1}H NMR titration in $CDCl_3$ at 1mM concentrations with different halide ions (TBAX, X=F,Cl,Br,I) which are soluble in $CDCl_3$. The titrations were carried out by adding aliquots of halide solution to the NMR tube. The concentration of TBAX salt was increased gradually from 1 to 140 equivalents and the chemical shift of the triazole C-H and other protons were monitored. With the objective of excluding contribution from other atoms in the binding, the system chosen has mainly the triazole C-H entity to interact with the halide anion. In the molecules considered for this study, phenyl and methylene groups, which may contribute to binding in addition to the triazole C-H, are also present. The acyclic flexible triazole systems chosen exclude any forced structural constrains for binding as in the case of macrocyclic triazoles. The methylene spacers between the aromatic rings and triazole moieties are expected to reduce the participation

of the aromatic proton for binding. Hence, the chosen systems should provide information on the affinity of triazole C-H to form complexes with the halide ions.

The binding of the triazole CH with the halide anion generally results in a downfield shift of the triazole C-H due to the tight binding of the halide anion rather than a bulk dielectric effect [21b]. The compounds presented in this study are well characterized with various 1D and 2D homo and heteronuclear NMR spectroscopic techniques as discussed in the previous section. The titrations are done in $CDCl_3$ which is known to be a poor solvent to induce halogen binding. [21c, 24] This will help to reduce the assistance of solvent and thus provide a realistic picture of the affinity of triazole-halide interactions in the absence of any supporting factor.

Compound 3:

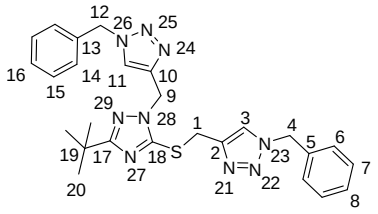

The titration of compound 03 with halide ions (TBAX , X= F, Cl, Br, I) did not induce any appreciable change in the chemical shift which indicates that the weak polarizing effect at the triazole centers itself is not sufficient to bind halide ions (Fig.4B.11-14). Generally the addition of the salt may result in a change in the chemical shift of the protons due to a change in the conformation.[39] In the case of compound 03 the chemical shift of the triazole protons (H-3 and H-11) remain almost unaltered even after the addition of different TBAX salts as seen from the Table.4B.2. This indicates that the interactions between the different salts and the triazole protons are not strong enough to induce changes in the chemical shifts of these protons. It is expected that the addition of the salt may change the conformations of the molecule, if it interacts, and should result in a change in the chemical shifts of the protons. However, in the present case almost no chemical shift change is observed. This kind of behavior is possible if these triazole protons are involved in intra molecular interactions. However the protons of tertiary butyl group show a downfield shift of 0.84 ppm indicating that it is interacting with the TBAX salt.

Table.4B.2 :*Variation in chemical shifts of the compound 3 with the addition of the salts.*

Comp.3	Change in chemical shift δ_H ppm for different protons								
salt	H-1	H-3	H-4	H-6	H-9	H-11	H-12	H-14	H-20
TBAF	-0.03	0.00	-0.02	-0.03	-0.03	+0.01	-0.02	-0.02	-0.36
TBACl	-0.05	0.00	-0.03	-0.04	-0.05	+0.01	-0.03	-0.04	+0.84
TBABr	-0.06	0.00	-0.04	-0.05	-0.06	-0.01	-0.04	-0.05	+0.54
TBAI	-0.06	+0.01	-0.03	-0.04	-0.06	0.00	-0.04	-0.04	+0.24

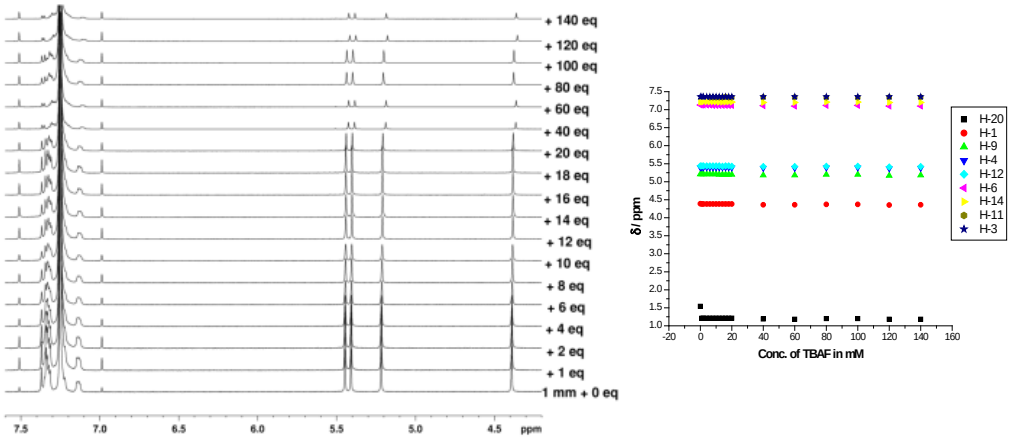

Fig.4B.11: *Stacked plot of the ^{1}H NMR spectrum of compound 03 in $CDCl_3$ (400 MHz) on addition of TBAF at 298 K. and the plot of change in 1H chemical shift with concentration of TBAF.*

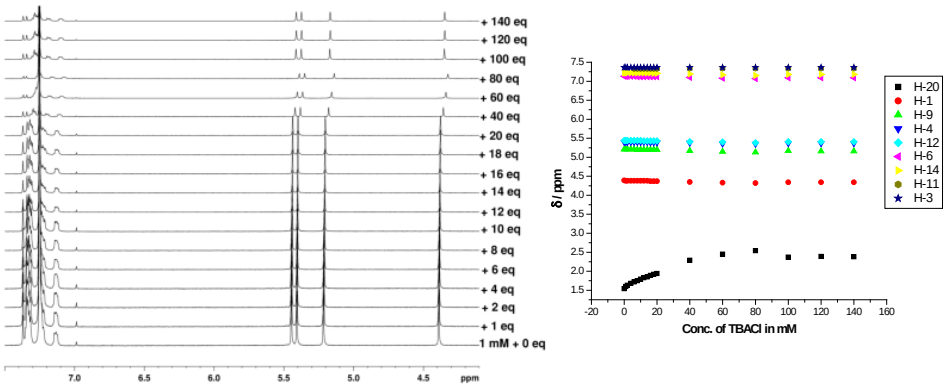

Fig.4B.12: *Stacked plot of the ^{1}H NMR spectrum of compound 03 in $CDCl_3$ (400 MHz) on addition of TBACl at 298 K and the plot of change in ^{1}H chemical shift with concentration of TBACl.*

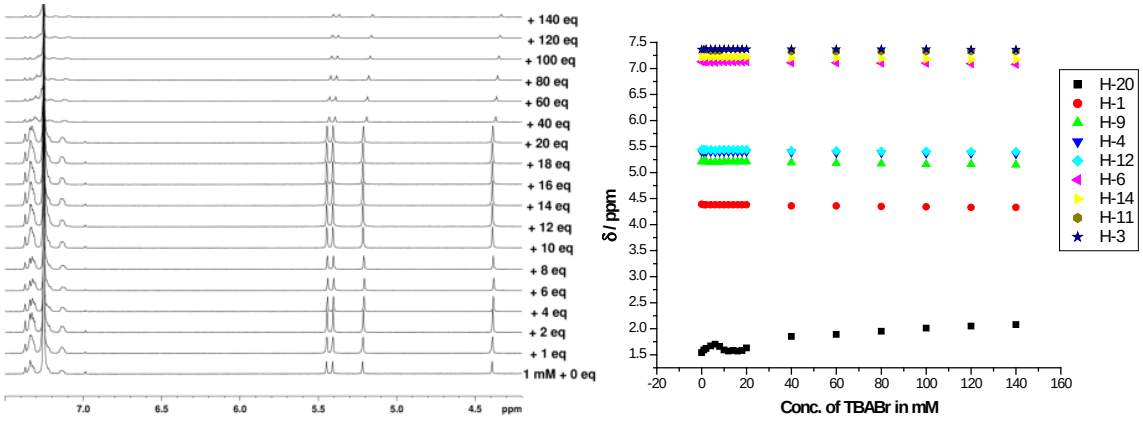

Fig.4B.13: *Stacked plot of the ^{1}H NMR spectrum of compound 03 in $CDCl_3$ (400 MHz) on addition of TBABr at 298 K. and the plot of change in 1H chemical shift with concentration of TBABr.*

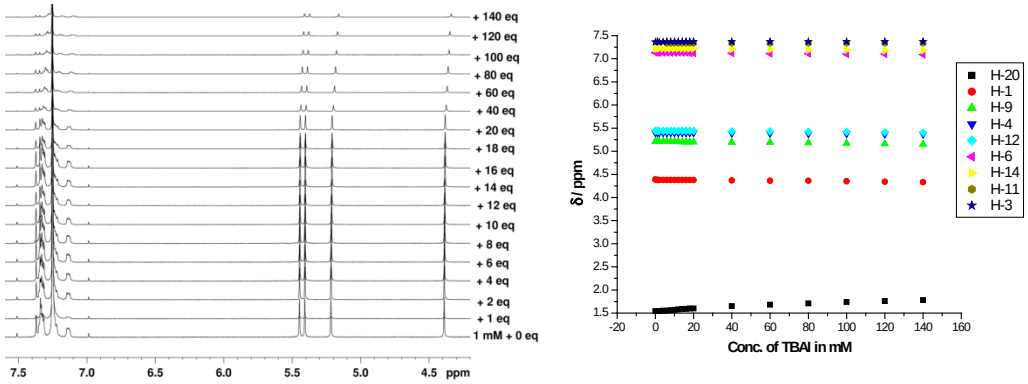

Fig.4B.14: *Stacked plot of the ^{1}H NMR spectrum of compound 03 in $CDCl_3$ (400 MHz) on addition of TBAI at 298 K. and the plot of change in 1H chemical shift with concentration of TBAI.*

In order to improve the strength of binding compound 1 is considered. The NH proton has the ability to bind with the halide anion due to its polar nature. However at low concentrations of 1 mM the NH signal could not be seen probably due to the exchange with the residual moisture in the deuterated solvent. Here, the triazole C-H signal shows slight downfield shift (0.09 ppm) after titration with the TBAI salt (Fig.4B.11) indicating that these triazole protons interact weakly with the added salt.

Compound 1:

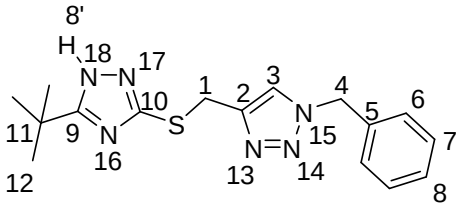

In the present case as well, the tertiary butyl group shows a downfield shift of 1.04 ppm suggesting its role in binding interactions with the salt. Such features of ^{1}H NMR spectra in halide ion titrations are consistent with the picture generated from the binding affinities.[21b]

Table.4B.3: *Variation in the chemical shifts of the compound 01 with the addition of the salts.*

Comp.1	Change in chemical shift δ_H ppm				
salt	H-1	H-3	H-4	H-6	H-12
TBAF	0.00	+0.05	-0.07	-0.02	-0.21
TBACl	-0.01	+0.09	-0.11	-0.10	+1.04
TBABr	-0.01	+0.07	-0.06	-0.05	+0.46
TBAI	-0.03	+0.09	-0.05	-0.05	+0.24

Some of the models proposed consider combined electro negativities of the three nitrogen atoms in triazole to polarize the C-H bond to make it a potent C-H bond donor [18, 21b, 33d] with its positive end orienting towards the H atom which interacts with halide. The present data clearly shows that the interaction between the triazole motif halide (I, Br, Cl, F) anions induce minor ^{1}H chemical shift changes in compound 1 of the triazole CH signal in the NMR spectra. In general, the data obtained shows that the halide additions induce very minor changes in the chemical shift of the triazole C-H and other protons and the association constants were too low to be determined by NMR. The observed weak binding can be justified on the basis that [20a] only very weak binding is observed even in favourable macro cyclic systems containing four triazole rings. (binding constant of 7 M^{-1}).[20a]

The anion binding, even if weak, can change the native structure of the triazole. DFT calculations show that compound 01 adopts a *syn* conformation of 1,2,3-triazole moiety upon halide complexation in order to form C–H ---- halide anion complex and the presence of the tetrabutyl counter ion disrupts the formation of organized supramolecular structures. It can also be seen from the graphs that except fluoride anion, all the other halide anions viz. chloride, bromide and iodide shows some binding interactions with the t-Bu substituent at the C-9 and C-17 in the case of the compound 1 and compound 3, respectively. A theoretical study on halide binding for compound 1 shows that the 1,2,3-triazole ring protons takes part in binding of the halide anion along with the NH of the 1,2,4-triazole ring as shown in the Fig.4B. 15. It can also be seen that the t-Bu group is orientated towards the halide anion due to which it can also have interactions with the halide anion.

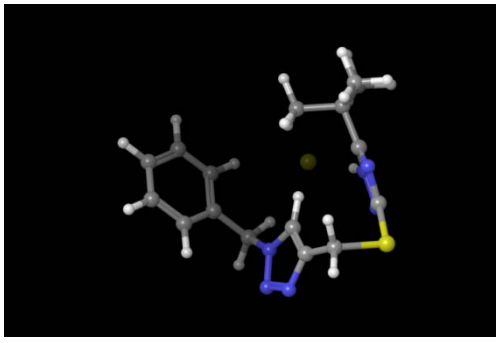

Fig.4B.15: *The complex of the compound 01 bound with the Br^- anion; an energy optimized structure using the Macromodel 7.9 from the Schrödinger software.*

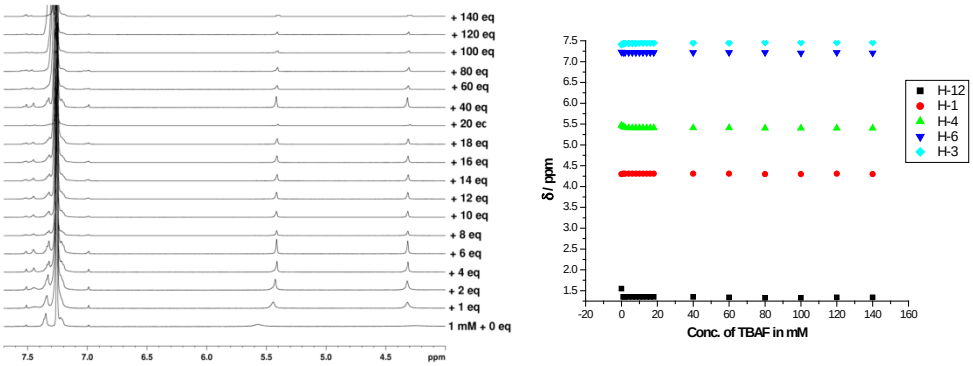

Fig.4B.16: *Stacked plot of the ^1H NMR spectrum of ompound 01 in $CDCl_3$ (400 MHz) on addition of TBAF at 298 K and the plot of change in 1H chemical shift with concentration of TBAF.*

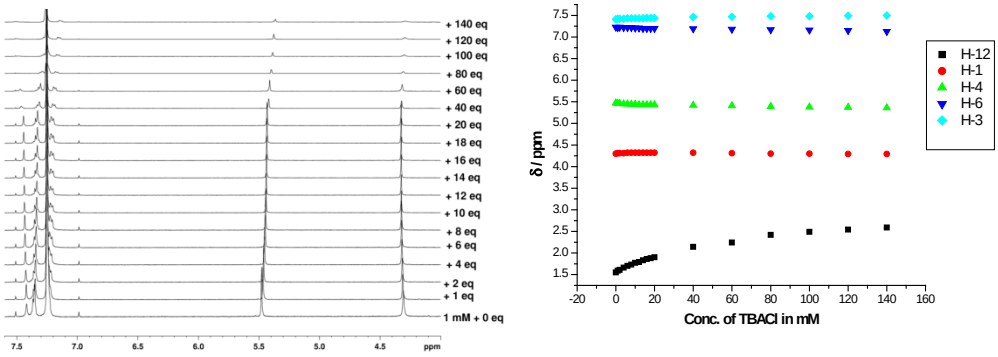

Fig. 4B.17: *Stacked plot of the ^{1}H NMR spectrum of compound 01 in $CDCl_3$ (400 MHz) on addition of TBACl at 298 K and the plot of change in ^{1}H chemical shift with concentration of TBACl.*

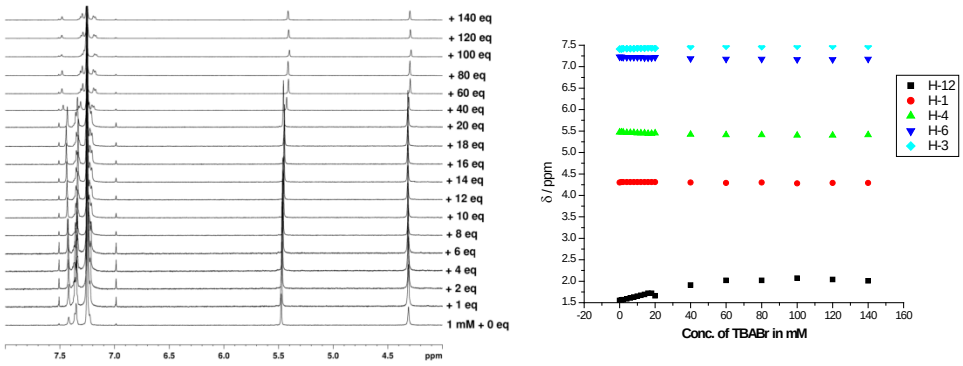

Fig.4B.18: *Stacked plot of the ^{1}H NMR spectrum of compound **01** in $CDCl_3$ (400 MHz) on addition of TBABr at 298 K and the plot of change in 1H chemical shift with concentration of TBABr.*

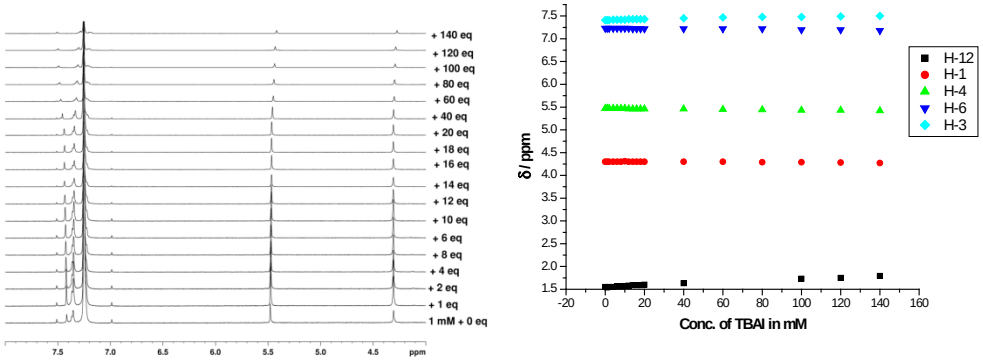

Fig. 4B.19: *Stacked plot of the ^{1}H NMR spectrum of compound 01 in $CDCl_3$ (400 MHz) on addition of TBAI at 298 K. and the plot of change in ^{1}H chemical shift with concentration of TBAI.*

It is clear from the study that addition of tetrabutylammonium salts of various anions to $CDCl_3$ solutions of triazoles result in minor alteration of chemical shift of the 1,2,3-

triazole C-H protons and other protons. This observation suggests that polarizing interactions of the triazole C-H with the halide anion are not strong enough to induce substantial changes in the chemical shifts under the present experimental conditions.[21b]

Conclusions:

Together, these results demonstrates that compound 03 and compound 01 are interesting systems to show that unsupported triazoles form weak intermolecular interactions with halide anions as observed by minor changes in the ^{1}H chemical shifts of the triazole protons. The study also supports formation of weak halogen bonds by triazoles through the C-H bonds in case of compound 01. The triazole derivatives studied by using scanning electron microscopy show irregular-aggregates of the different sizes and shapes.

References:

[1]. (a) Sivakumar K., F. Xie, B. M. Cash, S. Long, H. N. Barnhill, Q. Wang, *Org. Lett.* **2004**, 6, 4603; (b) Agard N. J., J. A. Prescher, C. R. Bertozzi, *J. Am. Chem. Soc.* **2004**, 126, 15046.

[2]. (a) Wu P., Feldman A. K., Nugent A. K., Hawker C. J., Scheel A., B. Voit, J. Pyun, J. M. J. Fre'chet, K. B. Sharpless, V. V. Fokin, *Angew. Chem. Int. Ed*. **2004**, 43, 3928; (b) Aucagne V., K. D. Ha"nni, D. A. Leigh, P. J. Lusby, D. B. Walker, *J. Am. Chem. Soc*. **2006**, 128, 2186.

[3]. (a) Kolb H. C., Sharpless K. B., *Drug Discovery Today* **2003**, 8, 1128; (b) Manetsch R., Krasiski A., Z. Radi, J. Raushel, P. Taylor, K. B. Sharpless, H. C. Kolb, *J. Am. Chem. Soc*. **2004**, 126, 12809.

[4]. (a) Wacharasindhu, S. Bardhan, Z. K. Wan, K. Tabei, T. S. Mansour, *J. Am. Chem. Soc.* **2009**, 131, 4174; (b) Y. Liu,W. Yan, Y. Chen, J. L. Petersen, X. Shi, *Org. Lett.* **2008**, 10, 5385.

[5]. (a) Heravi, M. Tajbaksh, M. Rahimizadeh, A. Davoodnia, K. Aghapoor, *Synth. Commun.* **1999**, *29*, 4417; (b) Y. Xia, Z. Fan, J. Yao, Q. Liao, W. Li, F. Qu, L. Peng, *Bioorg. Med. Chem. Lett.* **2006**, *16*, 2693.

[6]. Gupta D, Jain DK. J. Adv. Pharm. Technol Res. **2015** Jul-Sep, 6(3):141.

[7]. Keck TM, Banala AK, Slack RD, Burzynski C, Bonifazi A, Okunola-Bakare OM, Moore M, Deschamps JR, Rais R, Slusher BS, Newman AH *Bioorg Med Chem*. **2015** Jul 15, 23(14): 4000.

[8]. Preeti M. Chaudhary, Sayalee R. Chavan, M. Kavitha, Shailaja P. Maybhate, Sunita R. Deshpande, Anjali P. Likhite and P. R. Rajamohanan *Magn. Reson. Chem.* **2008**, *46*, 1168.

[9]. Sarkar D., Deshpande Sunita Ranjan, Maybhate Shailaja Pramod, Likhite Anjali Prabhakar, Sarkar Sampa, Khan Arshad, Chaudhry Preeti Madhukar, Chavan Sayalee Ramchandra. International publication number WO 2011/111077 A1 and PCT/IN2011/000172.

[10]. Hemraj J., Jeremy M. Lenhardt, Jose C. Castillo, Emily Zhao, Sibi Krishnamurthy, Ryan M. Jamiolkowski, Ki-Hyon Kim, and Stephen L. Craig *J. Org. Chem*. **2009**, 74, 8924.[11]. Fatima G., M. Rosario Torres, Emilio Matesanz, and Luis Sanchez *Chem. Commun*., **2011**, 47, 5016.

[12]. Minghui C., Aaron K. Holley and Michael Kruskamp ; *Chem. Commun*., **2007**, 168.

[13]. Fioroni, M. D. Diaz, K. Burger, and S. Berger; J. AM. CHEM. SOC. **2002**, 124, 7737.

[14]. Gustavo G., Pablo R. Sainz-Rozas, José Ramón Isasi, Andrés Guerrero-Martínez, and Gloria Tardajos ; *J. Phys. Chem. B* **2004**, *108,* 14154.

[15]. Jorge S., Christian Seel, Pilar Prados, and Javier de Mendoza; *J. Am. Chem. Soc*. **1996,** *118,* 277.

[16]. Fatima G., M. Rosario Torres, Emilio Matesanz and Luis Sánchez; *Chem. Commun*., **2011**, 47, 5016.

[17]. Haridas V., Kashmiri Lal, Yogesh K. Sharma, and Shailesh Upreti *Org. Lett*., 10, 8, **2008**, 1645.

[18]. Seth W., Maneesh K. Yadav, C. David Stout, and M. Reza Ghadiri; *J. AM. CHEM. SOC*. **2004**, 126, 15366.

[19]. Elsayed M. Zahran, Yuran Hua, Semin Lee, Amar H. Flood, and Leonidas G. Bachas,, *Anal. Chem*. **2011**, 83, 3455.

[20]. (a) Li Y. and Flood A. H., *Angew. Chem., Int. Ed*., **2008**, 47, 2649;

(b) Li Y. and Flood A. H., J. Am. Chem. Soc., **2008**, 130, 12111;

(c) Li Y., Pink M., J. A. Karty and A. H. Flood, J. *Am. Chem. Soc.*, **2008**, 130, 17293.

[21](a) Meudtner R. M., M. Ostermeier, R. Goddard, C. Limberg and S. Hecht, *Chem. Eur. J*., **2007**, 13, 9834; (b) Juwarker H., J. M. Lenhardt, D. M. Pham and S. L. Craig, *Angew. Chem., Int. Ed.*, **2008**, 47, 3740; (c) H. Juwarker H., Lenhardt J. M, J. C. Castillo, E. Zhao, S. Krishnamurthy, R. M. Jamiolkowski, K.-H. Kim and S. L. Craig, *J. Org. Chem*., **2009**, 74, 8924; (d) Hua Y. and Flood A. H., *J. Am. Chem. Soc*., **2010**, 132, 12838.

[22] Hua Y. and Flood A. H., *Chem. Soc. Rev*., **2010**, 39, 1262. [23]. Jonathan L. Sessler, Jiajia Cai, Han-Yuan Gong, Xiaoping Yang, Jonathan F. Arambula, and Benjamin P. Hay, *J. AM. CHEM. SOC*. **2010**, *132*, 14058.[24]. a. White G. and Paul D. Beer, *Supramolecular Chemistry* 24, No. 7, July **2012**, 473., b. Yuran H., Raghunath O. Ramabhadran, Esther O. Uduehi, Jonathan A. Karty, Krishnan Raghavachari, and Amar H. Flood *Chem. Eur. J*. **2011**, 17, 312.

[25]. Anjul K. and Pramod S. Pandey, *Org. Lett*., 10, No. 2, **2008**, 165.

[26]. Kolb H. C. and. Sharpless K. B, *Drug Discovery Today*, **2003**, 8, 1128.

[27]. a) Garcıa F., Torres M. R., Matesanz E. and Sanchez L., *Chem. Commun*., **2011**, 47, 5016; (b) Yu, T. B. Bai J. Z. and Guan Z., *Angew. Chem., Int. Ed*., **2009**, 48, 1097;
(c) Haridas V., Lal K., Sharma Y. K. and Upreti S., *Org. Lett*., **2008**, 10, 1645;
(d) Haridas V., Sahu S. and Venugopalan P., *Tetrahedron*, **2011**, 67, 727.

[28]. (a) Bowden N., Terfort A., Carbeck J. and Whitesides G. M., *Science*, 1997, 276, 233; (b) Boncheva M. and Whitesides G. M., *MRS Bull*., **2005**, 30, 736.

[29]. Kroon J., Kroon-Batenburg L.M.J, Leeflang B.R.,. Vliegenthart J.F.G, *Journal of Molecular Structure* **1994**, 322, 27.

[30]. Yuan Y. Z., Gui T. W., Ren X .W., and Zhan-Ting Li *Crystal Growth & Design*, 9, 11, **2009**, 4778.

[31]. Hui S., Yunfeng Z., Zhaowei H., Yue Wang, and Fei Li *J. Phys. Chem. A* **2008**, *112*, 11382.

[32]. Zhang, J. , Moore, J. S. *J. Am. Chem. Soc.* **1992**, *114*, 9701 and
Shetty, A. S.; Zhang, J.; Moore, J. S. *J. Am. Chem. Soc.* **1996**, *118*, 1019

[33]. (a) Chande, M. S.; Athalye, S. S. *Synth. Commun.* **1999**, *29*, 1711. (b) Chande, M. S.; Athalye, S. S. *Synth. Commun.* **2000**, *30*, 1667. (c) Ray, A.; Manoj, K.; Bhadbhade, M. M.; Mukhopadhyay, R.; Bhattacharjya, A. *Tetrahedron Lett.* **2006**, *47*, 2775. (d) Chande, M. S.; Barve, P. A.; Khanwelkar, R. R.; Athalye, S. S.; Venkataraman, D. S. *Can. J. Chem.* **2007**, *85*, 21.

[34]. Haridas, K. Lal, Y. K. Sharma and S. Upreti, *Org. Lett.,* **2008**, 10, 1645;

[35]. Horne, W. S.; Yadav, M. K.; Stout, C. D.; Ghadiri, M. R. *J. Am. Chem. Soc.* **2004**, *126*, 15366.

[36]. Indrajit B., Krishnan R., and Amar H. Flood, *Chem Phys Chem* **2009**, 10, 2535.

[37] Bryantsev, V. S.; Hay, B. P. *Org. Lett.* **2005**, 7, 5031.
[38] Bryantsev, V. S.; Hay, B. P. *J. Am. Chem. Soc*. **2005**, 127, 8282.
[39].Anthony B., Pierre M., and Shankar B. *J. Am. Chem. Soc.* ***2012***, 134, 19953.

CHAPTER: V

Theoretical calculations of geometry optimized structures and NMR shielding constants on substituted triazole thiones, disubstituted 1,2,4-triazole sulfanyl compounds and hybrid of 1,2,3 and 1,2,4-triazoles by Density Functional Theory

5.1 Introduction:

Tautomerism of 1,2,4-triazole thiones and other sulfanyl derivatives has already been discussed in Chapters II and III. It is also observed that triazole thiones exclusively exist as 1,4 dihydro tautomer in solids as well as in DMSO solutions. On the other hand, the sulfanyl derivatives of triazoles were found to be present in a dynamic equilibrium of tautomers in solution, while their solid state NMR studies indicated coexistence of two tautomers at least in two cases. These observations prompted us to study some of these systems by means of theoretical calculations which will provide information about the relative stability of different tautomers, their spatial geometry and other molecular properties. Besides, such an approach will also allow calculation of NMR chemical shifts for each tautomer and a comparison of these theoretical values with the experimentally determined chemical shift values will be useful in identifying the nature of tauomer/s observed in solution and solid state. It is necessary to note that the observed NMR chemical shifts in solution are a statistical average of all the dynamic events of the molecules (motion, diffusion, conformational exchange, chemical exchange etc.) inside the solution. However, by employing theoretical studies it is possible to compute chemical shifts for each of the different species involved in the dynamic events such as tautomerism. Hence, theoretical calculation of species specific chemical shifts is very useful in understanding the nature of dynamic events. With such a study, it is possible to find out the stable conformers and tautomers in the triazoles by comparing the experimental chemical shifts with the theoretically calculated chemical shifts. [1, 2]

Computational chemistry has developed in leaps and bounds in the past decade and has become an indispensable tool in design of drugs, materials etc. It is also used as a tool to predict chemical and physical properties of molecules. [3a] Various software packages are now available for computational chemistry applications. In the present work, the software package "Jaguar" is employed for theoretical calculations. "Jaguar" is an *ab initio* calculation software available as a module in "Schrodinger" package.[4] It is widely used for calculation of molecular properties such as dipole moment, electron density, electrostatic potential, polarizability, solvation, predicting spectral parameters of IR, NMR, UV etc. In this chapter, some of the systems discussed in Chapters 2, 3 and 4 are subjected to theoretical calculations based on Density Functional Theory to get minimum energy geometry optimized structures which are further used for calculation of shielding constants to extract ^{1}H, ^{13}C and ^{15}N theoretical chemical shifts. This chapter is divided into two parts- part A deals with theoretical studies on thiones and sulfanyl derivatives of 1,2,4 triazoles while part B is devoted to hybrid triazoles.

5.2 Experimental:

5.2.1 Geometry optimization of structures:

The first task for any theoretical calculation is geometry optimization of structure of the molecule under consideration using Hartree-Fock (HF) theory or density functional theory (DFT). In the present work DFT method [5] with the M06-2X functional and the ps 6-31G**++ basis set is chosen for calculation. First, the molecular structures of the molecule (triazoles in this case) were drawn and converted to the three dimensional structure and was refined by using the geometry clean-up tool provided with the maestro interface. Energy minimization and conformational search of the resulting structure is achieved by 'MacroModel' program, a force-field-based molecular modeling program available with the package. The 'conformational search' locates the low-energy conformations of a molecular structure. MacroModel program also employ continuum solvation models to account for solvent effects. DMSO, $CDCl_3$ or methanol is used as solvent for the calculation depending on the systems. MacroModel calculations were

prepared and launched from the Maestro GUI (graphical user interface) on a remote computer.

Conformational search by Monte Carlo Multiple Minimum (MCMM) is accomplished by using the following parameters:

Search variables: Ring closures; Steps per rotatable bonds: 100; Energy window for saving structures: 21.0 kJ/mol; Maximum deviation cutoff: 0.5 Å; Maximum number of steps: 200. The value of 0.05 was used for the "convergence threshold" with 500 iterations.

The output structures from MCMM contain all structures found below the specified 21.0 kJ/mol energetic window. 100 to 150 structures were generated during this exercise. These output structures are used as input for the serial MCMM Conformational Search. (Parameters Used: Torsion sampling options: Intermediate; Steps per rotatable bonds: 100; Energy window for saving structures: 21.0 kJ/mol; Maximum deviation cutoff: 0.5 Å; Maximum number of steps: 100.) This job took about 20 to 40 minutes and 9,000-15,000 structures were generated depending upon the complexity of the molecule.

All these structures are arranged in the ascending order of potential energy and the least energy structure is selected for the conformational search by DFT method in the 'Jaguar' using ps 6-31G**++ to get better refined structural output. (Convergence criteria used:-Maximum iterations: 48; Energy change: 5e-005 hartree; RMS density matrix change: 5e-006; SCF level shift:0.0 hartree; Thermal smearing: None; Convergence scheme: DIIS). This calculation took several days depending on the size of the molecule and the number of the local host computers available for the job. The converged structures obtained from the above exercise are used for chemical shift calculation.

5.2.2 Calculation of shielding constants:

All density functional theory (DFT) calculations were carried out by Schrödinger program package using the hybrid meta exchange-correlation M06-2X function in combination with standard ps 6-31G**++ basis set for tetramethylsilane (TMS), nitro methane and all the other compounds investigated. On geomerty optimized structure

from the previous step, single-energy calculations at the M06-2X/6-31G**++ level was performed to compute the ^{1}H, ^{13}C and ^{15}N shielding constants. The predicted ^{1}H, ^{13}C and ^{15}N NMR chemical shifts were derived from the equation $\delta = \sum_0 - \sum$, where δ is the chemical shift, $\sum$ is the absolute shielding and $\sum_0$ is the absolute shielding of the standard. [6-8]

The chemical shifts are referenced to TMS for ^{1}H and ^{13}C NMR and to nitro methane for ^{15}N NMR in both experimental and in theoretical calculations. $\sum_0$ values for the reference compounds are 31.77, 189.49 and -170.05 ppm, respectively for ^{1}H, ^{13}C and ^{15}N under M06-2X/6-31G**++ conditions. The effect of solvent on the theoretical NMR parameters was included using the standard Poisson-Boltzmann model, by choosing the PBF from the Solvent model option menu provided by Schrödinger. The PBF [9] solvent model incorporates the solvent effect with a dielectric constant of 4.806 and the probe radius of 2.52 Å for $CHCl_3$, a dielectric constant of 33.62 and the probe radius of 2.00 Å for methanol and a dielectric constant of 47.24 and the probe radius of 2.41 Å for DMSO solvent at 20^0C [10, 11] to calculate the NMR shielding constants.

5.3 Part A: Geometry optimized structure and calculation of the NMR shielding constants of mono substituted 1,2,4-triazole thione and disubstitutedsulfanyl-1,2,4-triazole derivatives by Density Functional Theory

The purpose of this part of the study is to calculate minimum energy tautomeric structure of various 1,2,4 triazole thiones discussed in Chapter II and their sulfanyl derivatives discussed in Chapter III. These structures are further compared with the structures predicted from the NMR studies. ^{1}H, ^{13}C and ^{15}N chemical shifts of all the tautomers are theoretically calculated and compared with the experimentally measured values to get information on the nature of tautomers present in solution and solid state. Scheme.5.1 shows various substituted triazole thione systems subjected to theoretical calculations and their tautomers.

Scheme.5.1: *Various tautomers of triazole thione systems investigated.*

The tautomer ID, the convergence criterion (CC), number of iterations required to complete the optimization, time taken for the convergence and the geometry optimized structures for a few representative cases are presented in Table 5.1.

Table 5.1: *Details of the theoretical calculations and geometry optimized structures obtained for furyl and phenyl substituted 1,2,4 triazole thiones.*

ID	CC	No.	Time (min)	geometry optimization energy (hartrees)	Optimized structure of the tautomer
Furyl-1	3	5	19	-869.142	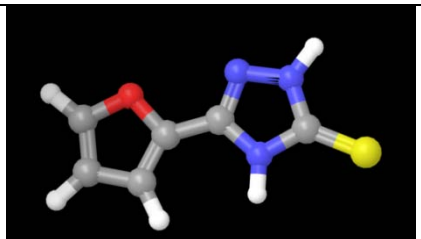
Furyl-2	0	11	33	-869.115	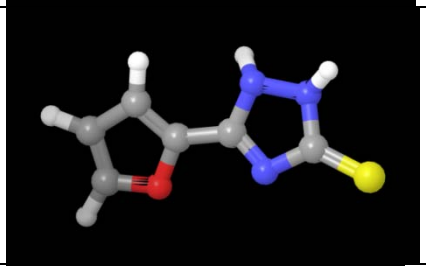
Furyl-3	3	5	18	-869.122	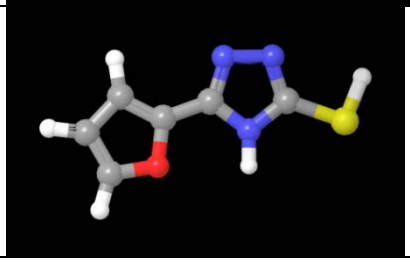

Furyl-4	0	5	12	-869.125	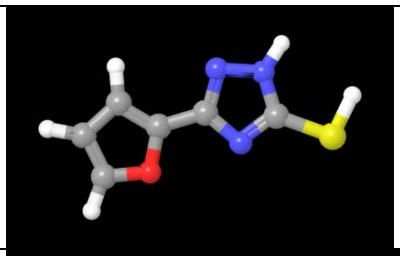
Furyl-5	0	5	13	-869.128	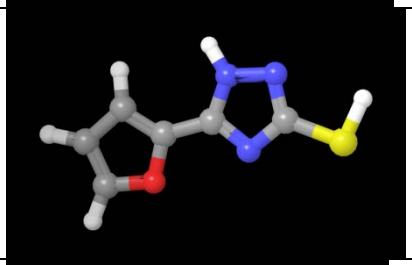
Ph-1	3	5	04	-871.338	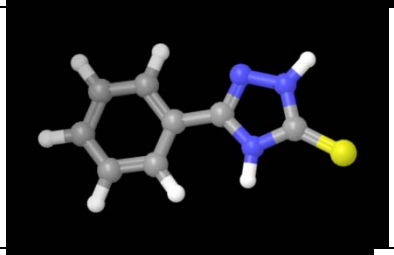
Ph-2	0	2	04	-871.311	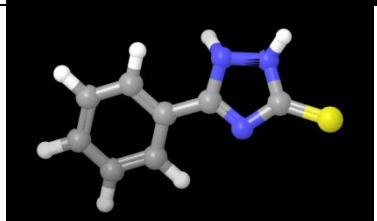
Ph-3	3	9	1h 15	-871.313	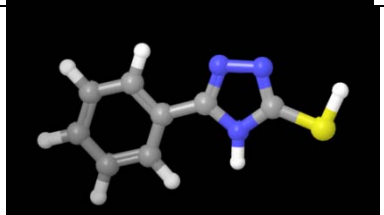
Ph-4	3	10	15	-871.321	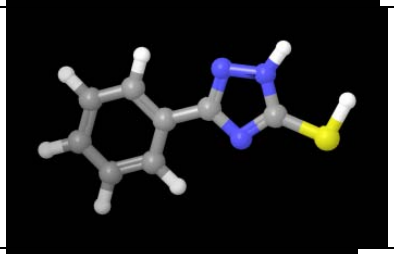
Ph-5	0	5	10	-871.324	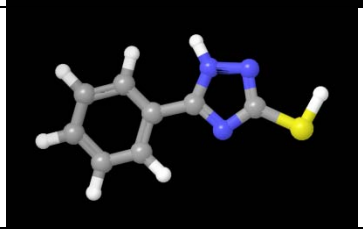

A comparison of the geometry optimization energies of the different tautomers shows that, 5a, (Scheme.5.1) has the least optimization energy (most negative value) in all the cases, irrespective of the substituents. This is perfectly in agreement with the results of solution and solid state NMR studies mentioned in Chapter II.

The chemical shifts for all the tautomers shown in the Scheme.5.1 are calculated in the solution state and compared with the experimental chemical shifts. ^{13}C chemical shifts are expected to be less affected by the nature of solvent. However, protons, being located on the periphery of the molecule, show larger solvation effects [11]. ^{15}N chemical shifts of nitrogen atoms containing the lone pair of electrons depends on the solvent properties, temperature [12] and concentration. To make a comparison with experimental observations, the calculations have been performed in the same solvent (DMSO) used for NMR measurements. A plot of the calculated chemical shifts to the observed chemical shifts for all the tautomers 5a, 5b, 5c, 5d and 5e show better correlation only with the chemical shifts of 5a tautomer (Fig.5.1).

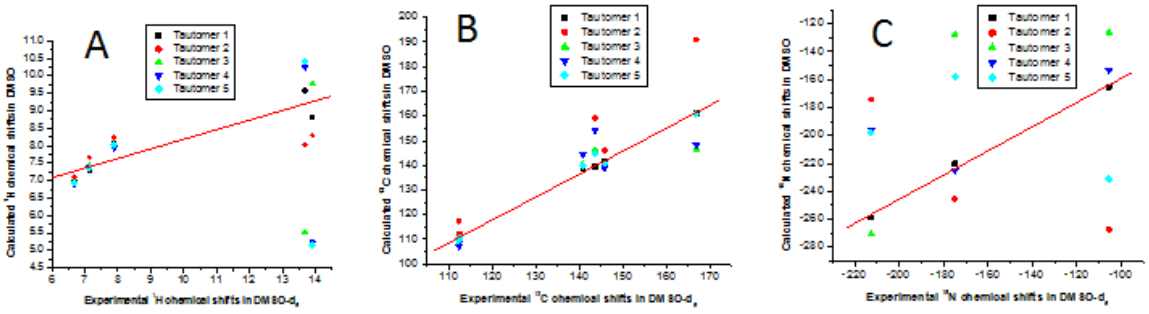

Fig.5.1 : *Correlation between the experimentally observed and the calculated ^{1}H (A), ^{13}C (B) and ^{15}N (C)chemical shifts for the furyl-thione triazoles.*

A comparison of the theoretical and observed chemical shifts for a representative case of furyl substituted 1,2,4 triazole thione is shown in Scheme.5.2.The scheme shows calculated ^{1}H, ^{13}C and ^{15}N chemical shifts for all the tautomers of the furyl substituted triazole thione along with the corresponding experimental chemical shifts.

The calculated ^{1}H chemical shifts of different tautomeric forms clearly show that thiol proton chemical shift is below 6 ppm for 5c, 5d and 5e, while for 5a and 5b the NH proton chemical shifts are above 8 ppm. The observed chemical shifts are well above 13 ppm and thus the presence of thiol forms of tautomers can be ruled out. Moreover, geometry optimized structure also indicates that the thiol forms are less stable.

Only two of the tautomers (5a and 5e) show calculated ^{13}C chemical shift of 160 ppm or more for C-5 carbon. However, between 5a and 5e, only 5a tautomer can be chosen to satisfy the ^{13}C chemical shift of C-5 carbon because the experimental chemical shift for C-5 carbon in this compound is 166.5 ppm and on the other hand, the thiol form

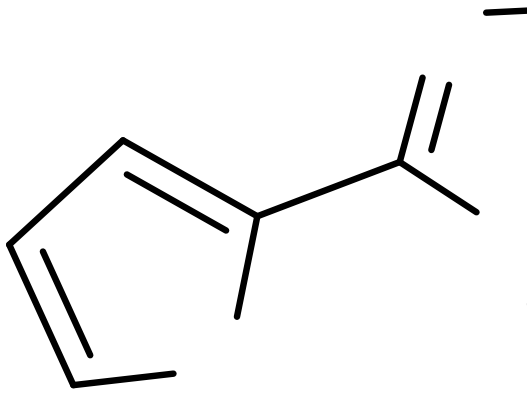

Scheme.5.2: *Comparison of predicted and experimental ^{1}H, ^{13}C and ^{15}N chemical shifts of furyl substituted 1,2,4-triazole thione. Various tautomers and numbering adopted for atoms are also shown. ^{13}C and ^{15}N chemical shifts are shown with the arrow pointing*

towards the atom to which they belong to while the ^{1}H chemical shifts are written close to the corresponding proton.

(5e) is already ruled out on the basis of ^{1}H chemical shifts. A quick comparison of the calculated and observed ^{15}N chemical shifts also rules out the possibility of any thiol tautomers since the observed values correspond to two *sp3* type of nitrogen atoms and the suitable candidates for this are 5a and 5b. Comparison of relative differences in chemical shift gives a better option than comparison of absolute values. For example, difference in the chemical shifts of two sp^3 hybridized nitrogens in tautomer-5b is 22 ppm while for tauotomer-5a it is 38 ppm according to theoretical calculations. The experimentally observed difference between the sp^3 hybridized nitrogens is about 38 ppm indicating that tautomeric form 5a is present in the solution state. A comparison of the calculated and experimental ^{1}H, ^{13}C and ^{15}N chemical shifts of all the systems investigated (Scheme.5.1) is presented in Tables 5.2-5.7.

Table 5.2: *Comparison of the experimental ^{1}H chemical shifts in the solution state and the theoretically calculated ^{1}H chemical shifts for the furyl triazole thione.*

Atom No	Expt. ^{1}H	Tauto-1 5a	Tauto-2 5b	Tauto-3 5c	Tauto-4 5d	Tauto-5 5e
4	13.91	8.82	8.3	9.77	5.23	5.16
1	13.68	9.58	8.04	5.52	10.25	10.42
2'	7.14	7.31	7.67	7.43	7.39	7.35
3'	6.68	6.97	7.09	6.96	6.89	6.94
4'	7.14	8.05	8.24	8.03	7.93	8.03

Table 5.3: *Comparison of the experimental ^{13}C chemical shifts in the solution state and the theoretically calculated ^{13}C chemical shifts for the furyl triazole thione.*

Atom No	Expt. ^{13}C solution	Expt. ^{13}C solid	Tauto-1 5a	Tauto-2 5b	Tauto-3 5c	Tauto-4 5d	Tauto-5 5e
3	143.6	148.35	139.47	159.09	146.22	154.32	144.59
5	166.5	164.98	161.06	190.99	146.64	148.31	160.86
1'	140.83	138.74	138.55	140.04	140.3	144.49	140.07
2'	111.89	111	110.92	117.43	108.36	107.25	109.74
3'	112.03	116	110.32	112.31	110.22	109.27	110.41
4'	145.37	144.80	141.66	145.95	139.97	138.9	140.73

Table 5.4: *Comparison of the experimental ^{15}N chemical shifts in the solution state and the theoretically calculated ^{15}N chemical shifts for the furyl triazole thione.*

Atom No.	Expt. ^{15}N solution	Expt. ^{5}N solid	Tauto-1 5a	Tauto-2 5b	Tauto-3 5c	Tauto-4 5d	Tauto-5 5e
1	-176.1	-178.10	-220.32	-245.39	-127.6	-225.01	-158.35
2	-109.3	-123.44	-165.17	-267.39	-126.21	-153.45	-231.16
4	-214	-213.54	-258.94	-174.24	-270.41	-196.09	-198.12

Table 5.5: *Comparison of the experimental ^{1}H chemical shifts in the solution state and the theoretically calculated ^{1}H chemical shifts for the phenyl triazole thione.*

Atom No.	Expt. ^{1}H	Tauto-1 5a	Tauto-2 5b	Tauto-3 5c	Tauto-4 5d	Tauto-5 5e
4	13.89	9.23	9.23	8.47	9.96	5.27
1	13.72	9.78	9.78	8.43	5.57	10.32
1'	7.91	8.04	8.04	8.17	8.08	8.29
2'	7.48	7.81	7.81	7.9	7.8	7.74
3'	7.48	7.75	7.75	7.98	7.7	7.62

Table 5.6: *Comparison of the experimental ^{13}C chemical shifts in the solution state and the theoretically calculated ^{13}C chemical shifts for the phenyl triazole thione.*

Atom No.	Expt. ^{13}C Solution	Expt. ^{13}C Solid	Tauto-1 5a	Tauto-2 5b	Tauto-3 5c	Tauto-4 5d	Tauto-5 5e
5	167.49	163.43	161.84	189.45	147.74	147.89	160.7
3	150.67	149.62	147.15	168.27	153.4	161.03	151.8
1'	125.9	124	121.65	123.2	122.91	127.47	122.7
2'	126.12	124.96	121.35	124.86	120.84	121.66	121.79
3'	129.554	127.27	125.06	125.68	124.93	124.36	125.11
4'	131.06	129.88	127.3	130.82	125.85	125.16	126.44

Table 5.7: *Comparison of the experimental ^{15}N chemical shifts in the solution state and the theoretically calculated ^{15}N chemical shifts for the phenyl triazole thione.*

Atom No.	Expt. ^{15}N solution	Expt. ^{15}N solid	Tauto-1 5a	Tauto-2 5b	Tauto-3 5c	Tauto-4 5d	Tauto-5 5e
4	-212.3	-210.2	-256.43	-169.46	-270.18	-191.9	-193.1
1	-174.9	-172.28	-218.49	-242.32	-128.22	-224.77	-156.29
2	-105.88	-105.51	-157.89	-262.01	-118.19	-148.85	-228.74

5.4 Theoretical calculations on disubstituted 1,2,4-triazole sufanyl derivatives:

A few of the disubstituted 1,2,4 triazole sulfanyl systems shown in Scheme.5.3 have been subjected to DFT calculations to get information on relative stabilities of tautomers and also to calculate ^{1}H, ^{13}C and ^{15}N chemical shifts. The tautomer ID, the convergence criterion (CC), number of iterations required to complete the optimization, time taken for the convergence and the geometry optimized structures for a few representative cases are presented in Tables 5.8- 5.10.

Scheme.5.3: *Tautomers of substituted triazole sulfanyl derivatives investigated.*

Table 5.8: *Details of theoretical calculations and geometry optimized structures obtained for p-chloro-phenyl S-propargyl, and furyl S-propargyl 1,2,4 triazole sulfanyls.*

ID	CC	No.	Time (min)	geometry optimization energy(hartrees)	Optimized structure
p-Cl-1	3	26	1h 16	-1446.305	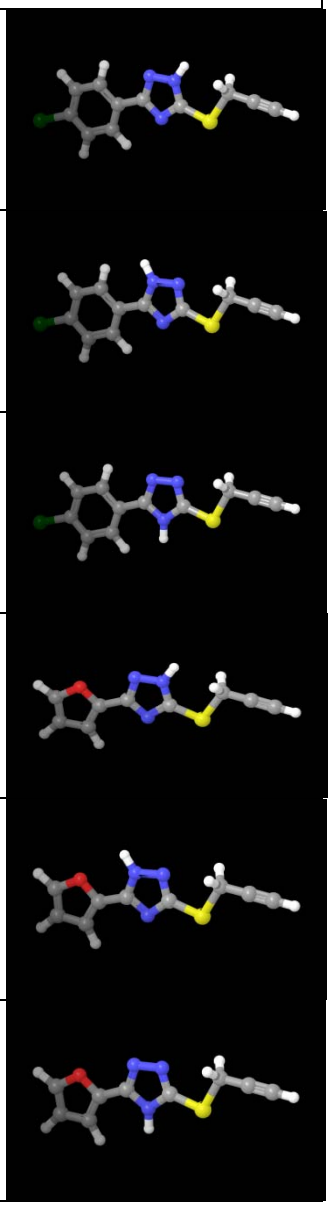
p-Cl-2	3	11	25	-1446.308	
p-Cl-3	3	39	1h 43	-1446.300	
Furyl-1	3	15	32	-984.526	
Furyl-2	3	2	04	-984.534	
Furyl-3	3	12	28	-984.520	

Table 5.9: *Details of theoretical calculations and geometry optimized structures obtained for p-fluoro-phenyl S-propargyl, p-nitro-phenyl-S-propargyl, and its sulphone derivative 1,2,4 triazole sulfanyls.*

ID	CC	No.	Time (min)	geometry optimization energy(hartrees)	Optimized structure
p-F-Ph-1	1	10	40 min	-1085.896	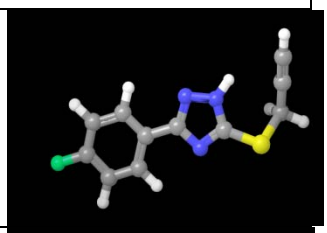
p-F-Ph - 2	3	71	11 days	-1085.946	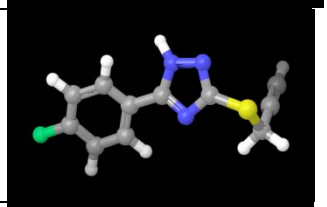
p-NO_2-1	3	13	43	-1191.221	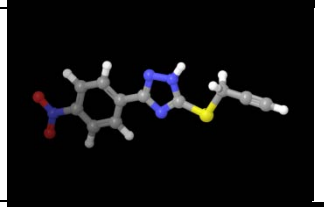
p-NO_2-2	3	31	1h 29	-1191.223	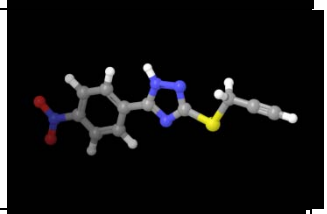
p-NO_2-3	3	22	52	-1191.215	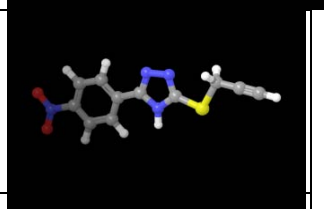
p-NO_2-Propargyl – suphone-1	3	15	2h 55 min	-1341.468	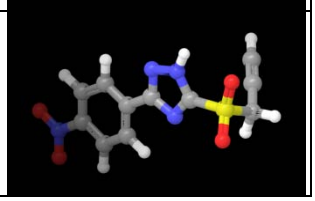

Table 5.10: *Details of theoretical calculations and geometry optimized structures obtained for p-Chloro-phenyl S-allyl, p-nitro-phenyl S-allyl 1,2,4 triazole sulfanyls*.

ID	CC	No.	Time (min)	Geometry optimization energy(hartrees) E	Optimized structure

p-Cl-allyl-1	1	11	46 min	-1447.511	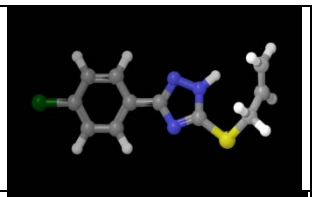
p-Cl-allyl -2	0	4	1h 23 min	-1447.546	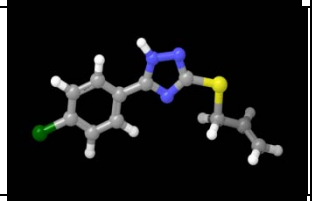
p-NO_2-allyl-1	3	13	2h 10 min	-1192.392	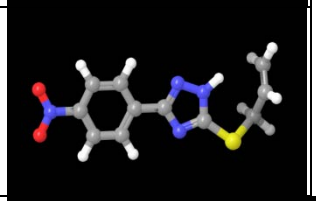
p-NO_2-allyl -2	3	5	3 days	-1192.416	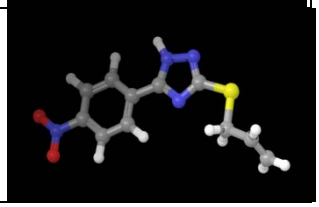

Geometry optimization studies performed on tautomers of disubstituted 1,2,4 triazole sufanyl derivatives show that the minimum energy is associated with 5f tautomer with the proton on N-2 (*N2-H* form) and hence is the most stable form of tautomer. Further, it is noticed that the difference in energy between 5g and 5f tautomers (*N1-H* and *N2-H* forms, respectively) is less (0.002 to -0.008 hartrees) compared with the energy difference between 5f and 5h (-0.008 to -0.014 hartrees) i.e. *N4-H* tautomer. For example, for compound 1, the difference between *N2-H* and *N1-H* form is -0.008 hartrees (E_{N2H}-E_{N1H}) while the difference between *N2-H* and *N4-H* (E_{N2H}-E_{N4H}) is -0.014 hartrees. Hence, co-existence of both the low energy forms is likely. Most of these systems indeed showed co-existence of *N2-H* (5f) and *N1-H* (5g) tautomers as studied by solution state NMR (Chapter III). Though theoretical calculation predicts *N2-H* form as the most stable tautomer, the actual populations of the tautomeric forms may depend on the nature of substituent on the triazole ring. For example, the free energy difference between 5f and 5g tautomers in *para* nitro *S*-propargyl triazole case is very little (0.002 hartrees). In agreement, a dominance of *N1-H* tautomer was noticed in solution state NMR of this

compound (Chapter III, Part A, compound 1b). These calculations also show that the possibility of *N4-H* tautomer is unlikely in any of the systems investigated.

Shielding constants are calculated in DMSO (using continuum solvation model) for the minimum energy optimized structures of the furyl *S*-propargyl 1,2,4-triazole sulfanyl, to extract theoretical ^{1}H, ^{13}C and ^{15}N chemical shifts. The chemical shift values thus obtained are compared with the experimentally observed chemical shifts. Correlation graphs obtained for calculated and experimental chemical shifts for all the tautomers of the representative compound are presented in (Fig 5.2). It can be seen from the figure that the proton chemical shifts in the 14-15 ppm corresponding to the tautomer 3 deviate more from linearity, which indicate that the tautomer 3 is the least stable among the three.

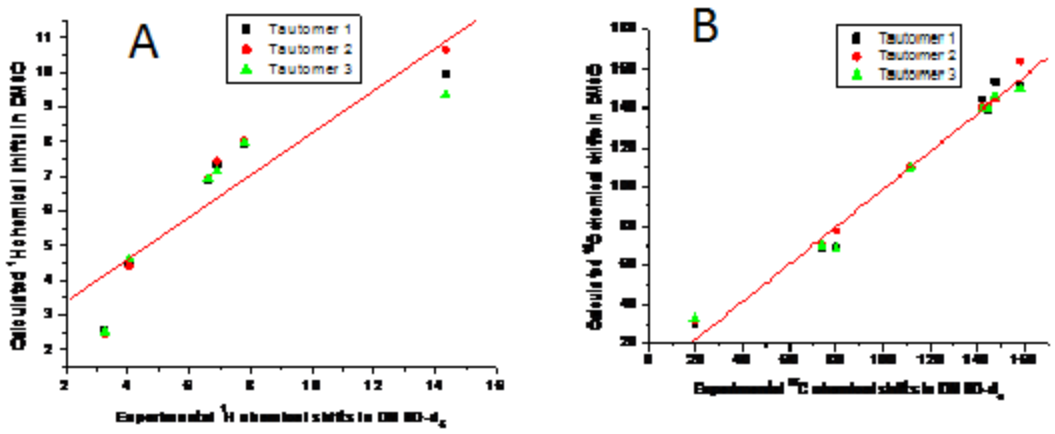

Fig. 5.2: *Correlation between the experimentally observed and the calculated ^{1}H (A), ^{13}C (B) chemical shifts for the tautomers of furyl S-propargyl sulfanyl 1,2,4 triazole.*

A comparison of the calculated and experimental ^{1}H, ^{13}C and ^{15}N chemical shifts of systems investigated is presented in Table 5.11-5.19 respectively.

Table 5.11: *Comparison of the experimental ^{1}H chemical shifts in the solution state and the theoretically calculated ^{1}H chemical shifts for the furyl S-propargyl sulfanyl 1,2,4-triazole.*

Atom No.	Expt. major	Expt. minor	Tauto-1,5f	Tauto-2,5g	Tauto-3,5h
1	14.65	14.35	9.97	10.66	9.35
1'	3.96	4.05	4.49	4.4	4.63
3'	3.17	3.26	2.57	2.46	2.52
2"	7.09	6.92	7.35	7.44	7.15

3"	6.71	6.62	6.87	6.96	6.94
4"	7.93	7.79	7.92	8.04	7.99

Table 5.12: *Comparison of the experimental ^{13}C chemical shifts in the solution state and the theoretically calculated ^{13}C chemical shifts for the furyl S-propargyl sulfanyl 1,2,4-triazole.*

Atom. No.	Expt. major	Expt. minor	Tauto-1,5f	Tauto-2,5g	Tauto-3,5h
3	148.24	155.79	153.91	144.33	145.66
5	158.82	150.73	152.23	163.63	150.1
1'	20.04	21.29	30.68	32.42	33.37
2'	80.73	79.93	68.94	70.54	70.18
3'	74.24	75.19	69.02	77.62	68.63
1"	142.68	146.54	144.67	140.8	139.94
2"	111.63	109.55	109.14	110.29	108.58
3"	112.74	112.12	109.31	110.05	109.83
4"	145.53	144.13	139.15	141.1	140.42

Table 5.13*: Comparison of the experimental ^{15}N chemical shifts in the solution state and the theoretically calculated ^{15}N chemical shifts for the furyl S-propargyl sulfanyl 1,2,4-triazole.*

Atom No.	Solution major	Solution minor	Solid	Tauto-1,5f	Tauto-2,5g	Tauto-3,5h
1	-	-168.42	-82.31	-230.48	-160.05	-129.5
2	-174.29	-	-174.56	-199.16	-202.63	-274.95
3	-	-	-138.82	-157.56	-231.15	-129.66

Table 5.14: *Comparison of the experimental ^{1}H chemical shifts in the solution state and the theoretically calculated ^{1}H chemical shifts for the p-fluoro-phenyl S-propargyl sulfanyl 1,2,4-triazole.*

Atom No.	Expt.	Tauto-1,5f	Tauto-2,5g	Tauto-3,5h*
3'	4.02	4.11	4.11	
1'	3.17	3.16	3.16	
2	14.52	12.24	12.24	
2"	8.02	9.76	9.76	
3"	7.34	8.6	8.6	

* The calculation did not converge

Table 5.15: *Comparison of the experimental ^{13}C chemical shifts in the solution state and the theoretically calculated ^{13}C chemical shifts for the p-fluoro-phenyl S-propargyl sulfanyl 1,2,4-triazole.*

Atom No.	Expt. major	Expt. minor	Tauto-1,5f	Tauto-2,5g	Tauto-3,5h*
1'	19.64	136.6	19.84	29.13	
2'	80.35	-	87.05	89	
3'	73.62	-	85.61	82.24	
3	155.07	161.6	163.66	169.38	
5	161.53	150.8	163.88	176.42	
1"	150.83	-	142.32	136.21	
2"	128.42	-	146.49	147.15	
3"	116.03	-	134.79	131.82	
4"	163	-	181.33	179.79	

* The calculation did not converge

Table 5.16: *Comparison of the experimental ^{15}N chemical shifts in the solution state and the theoretically calculated ^{15}N chemical shifts for the p-fluoro-phenyl S-propargyl sulfanyl 1,2,4-triazole.*

Atom. no.	Solution	Tauto-1 solid,5f	Tauto-2 solid, 5g	Tauto-1 5f	Tauto-2 5g	Tauto-3,5h*
1	-	-187.33	-110.16	-180.33	-126.31	
2	-174.26	-126.31	-180.33	-110.16	-187.95	
4	-	-137.13	-152.87	-152.87	-137.13	

* The calculation did not converge

Table 5.17: *Comparison of the experimental ^{1}H chemical shifts in the solution state and the theoretically calculated ^{1}H chemical shifts for the p-nitro-phenyl S-propargyl sulfanyl 1,2,4-triazole.*

Atom No.	Expt.	Tauto-1,5f	Tauto-2,5g	Tauto-3,5h*
2	14.7	12.43	12.75	
1'	4.06	4.23	3.08	
3'	3.22	3.14	4.21	
2"	8.2	9.89	9.69	
3"	8.34	9.81	10.1	

* The calculation did not converge

Table 5.18: *Comparison of the experimental ^{13}C chemical shifts in the solution state and the theoretically calculated ^{13}C chemical shifts for the p-nitro-phenyl S-propargyl sulfanyl 1,2,4-triazole.*

Atom No.	Expt.	Tauto-1,5f	Tauto-2,5g	Tauto-3,5h*
3	151.9	164.09	169.48	
5	160	165.04	176.39	
1'	20.36	19.92	29.18	
2'	79.74	86.6	88.78	
3'	74.36	85.6	82.19	
1''	135.3	155.82	149.25	
2''	126.93	144.83	145.9	
3''	124.31	146.05	142.06	
4''	147.95	168.33	162.43	

* The calculation did not converge

Table 5.19: *Comparison of the experimental ^{15}N chemical shifts in the solution state and the theoretically calculated ^{15}N chemical shifts for the p-nitro-phenyl S-propargyl sulfanyl 1,2,4-triazole.*

Atom no.	Solution	Solid-1	Solid-2	Tauto-1,5f	Tauto-2,5g*	Tauto-3,5h*
1	-	-180.31	-112.27	-213.16		
2	-165.89	-108.02	-163.86	-135.28		
4	-	-133.72	-125.6	-160.42		

* The calculations did not converge

Calculated ^{13}C and ^{15}N chemical shift values are found to be extremely useful for identification of tautomers in disubstituted sulfanyl triazole cases investigated. It is demonstrated for a representative case (furyl *S*-propargyl 1,2,4 triazole sulfanyl) studied. The calculated and experimental ^{13}C and ^{15}N chemical shifts for this system (compound - 1, Scheme.5.3) are shown in Scheme 5.4. Comparison of the ^{15}N chemical shift data immediately rules out the possibility of 5h tautomer (*N4-H*) since a relatively more shielded nitrogen signal is not observed in ^{15}N CP-MAS of ^{1}H-^{15}N HSQC spectra. However, this does not confirm whether the tautomeric form present is 5f or 5g.

Importance of triazole ring carbon (C-3 and C-5) chemical shifts in determination of nature of tautomer has already been discussed in Chapter III. This is also validated by the calculated chemical shifts, which shows that the carbon atom adjacent to triazole NH

always experiences more shielding. For example, the calculated chemical shift of C-3 carbon for *N1-H* tautomer (5g) is 153.91 ppm while for *N2-H* tautomer (5f) it is 144.33 ppm. Similarly, predicted chemical shift of C-5 carbon for *N1-H* (5g) tautomer is 152.23 compared to 163.63 ppm predicted for the *N2-H* (5f) tautomer. A comparison of this with the observed ^{13}C chemical shifts of C-3 and C-5 carbons of the major and minor forms (shown in Scheme.5.4) is very well in line with the predicted nature. Further, it also substantiates that the major tautomer present is indeed the *N2-H* form (5f). On going from *N1-H* to *N2-H* tautomer, the calculation predicts shielding for C-3 carbon by 9.58 ppm and shielding for C-5 carbon by -11.40 ppm. This is fairly in agreement with the observed values of +7.51 (δ_{minor}-δ_{major}) for C-3 and -8.09 (δ_{minor}-δ_{major}) for C-5. It is also interesting to recall the behavior of C-1′ carbons in two tautomeric forms discussed in Chapter III. A shielding of C-1′ carbon by 3.86 ppm is noticed for the *N2-H* tautomer in solution state NMR compared to *N1-H* tautomer. This similar behavior is observed also for the calculated chemical shifts, which predict a shielding by 3.87 ppm of C-1′ from *N1-H* to *N2-H*. .

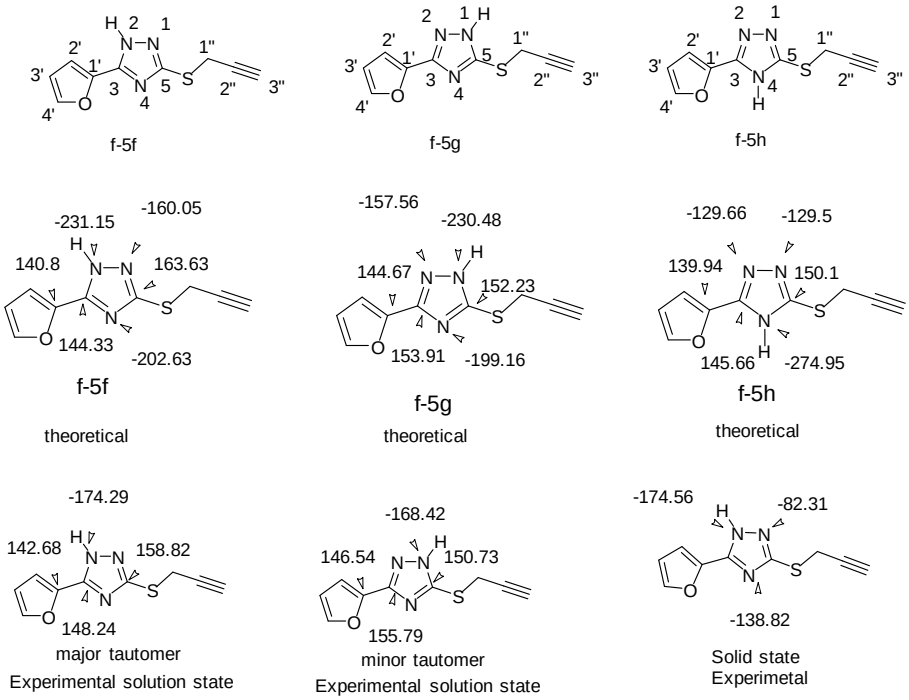

Scheme 5. 4: *Comparison of the predicted and experimental ^{13}C and ^{15}N chemical shifts of furyl substituted 1,2,4-triazole sulfanyl derivative. Various tautomers of the system and the numbering adopted for atoms are also shown.*

5.5 Conclusions:

Geometry optimization studies performed on tautomers of various triazole thiones indicated 1,4 dihydro tautomer (5a) as the most stable among the five possible tautomers. Calculated ^{13}C and ^{15}N chemical shifts correlated well with the values obtained for 1,4 dihydro tautomer from NMR studies. For disubstituted 1,2,4-triazole sufanyl derivatives, the least energy tautomer is found to be *N2-H* form (5f tautomer) but the difference in energy between this and the *N1-H* tautomer (5g) is relatively less (0.002 to -0.008 hartrees). Hence, co-existence of both the low energy forms is likely. Calculated ^{13}C and ^{15}N chemical shift values are found to be extremely useful for identification of tautomers in disubstituted sulfanyl triazole cases investigated. Importance of triazole ring carbon (C-3 and C-5) chemical shifts in determination of nature of tautomer noticed in solution state NMR studies is also validated by the calculated chemical shifts.

5.6 Part B: Geometry optimized structures and calculation of the NMR shielding constants of hybrid triazoles by Density Functional Theory

The work presented in this section is aimed to find out the minimum energy structure of the hybrid triazole molecules characterized in the previous Chapter IV and to compare the calculated chemical shifts with the measured values. In this part of the thesis quantum chemical calculations on hybrid triazole derivatives have been performed to get minimum energy conformations, which are then compared with the structural features envisaged from the solution state NMR studies. Same procedure as discussed in Part A is used to get energy optimized structures of hybrid triazole derivatives shown in Scheme 5.5 In addition, the ^{1}H, ^{13}C and ^{15}N NMR chemical shifts of the hybrid compounds have also been calculated using the density functional theory (DFT/M06-2X) method with the ps 6-31G**++ basis set, and compared with the experimental data. Geometry optimized structures of hybrid triazoles studied are given in Table 5.20 and other details of the calculation are summarized Table 5.21. The geometry optimized structures from the above calculations are used as inputs for calculations of shielding constants. The optimization process was followed by single point calculations at the M06-2X/6-31**++ level with ultrafine grids.

Scheme. 5.5: *The 1,2,4 and 1,2,3 mixed triazoles used for the theoretical studies.*

Table 5.20: *The energy optimized 1,2,3/1,2,4-mixed triazole derivative structures obtained on the Jaguar version 7.9 of the Schrödinger software by utilizing the amber* force field and the 6-31g** basis set.*

Comp. ID	Structure	Comp. ID	Structure
01	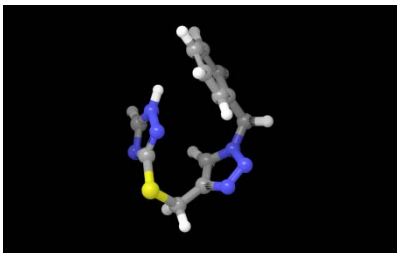	02	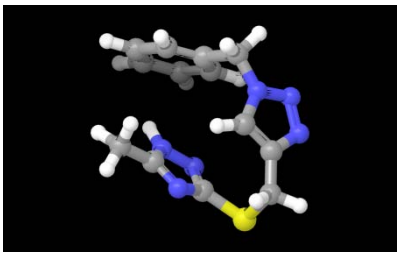
03	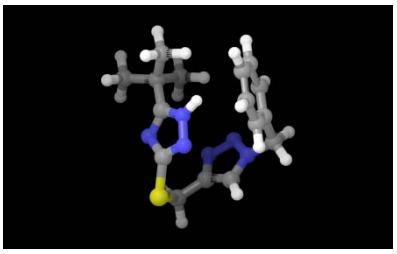	04	

05	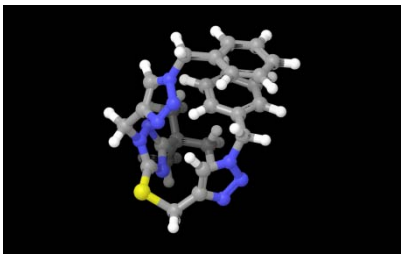	06	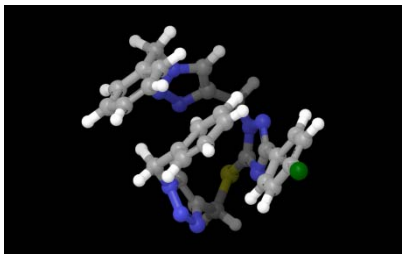
07	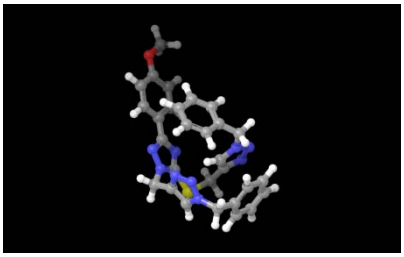	08	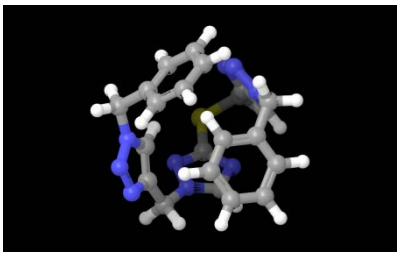
9	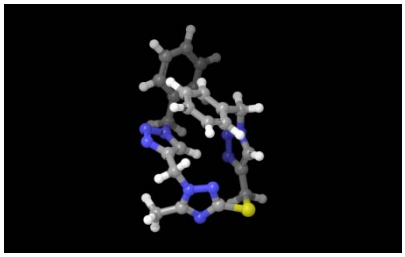	10	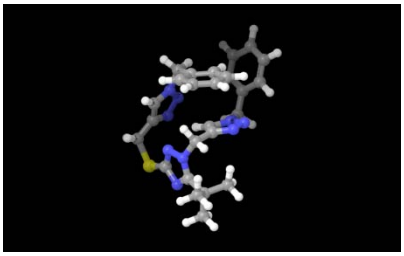
11	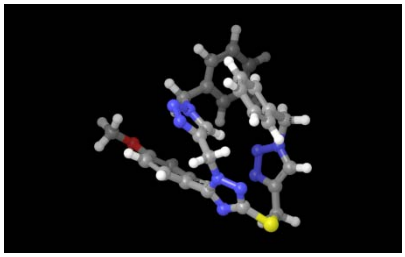		

Table 5.21: *Details of the parameters of DFT calculations.*

Comp. ID	Convergence criterion	No. of iterations.	Time (hours/min)	geometry optimization energy; hartrees
01	3	18	8h 30	-1190.841
02	3	23	2h 42	-1230.146

03	3	21	18h 19	-1348.038
04	2	68	112h 17	-1780.678
05	3	23	58h 2	-1898.561
06	3	28	68h 8	-2431.913
07	3	11	22h 22	-2086.805
08	3	86	120h 19	-1741.364
09	2	53	85h 30	-1780.673
10	3	34	27h 10	-1898.556
11	3	56	124h 47	-2086.823

The minimum energy structural features obtained for 1,2,3/1,2,4-mixed triazole derivative systems are useful in explaining the nOe contacts observed for t-butyl substituent in them with protons on the other side of the triazole ring (which is discussed in Chapter IV). The optimized structures show that these triazole hybrid systems do not have a linear structure. All the hybrid triazoles, containing at least one 1,4 disubstituted 1,2,3 trazole moiety, show a bent structure similar to a turn in oligopeptides. In such conformations, the protons of tertiary butyl group come closer to protons present in groups away from it by several bonds and develop dipolar interactions resulting in the observed nOes.

Chemical shifts are also computed from these geometry optimized structures of hybrid triazole. These calculations have been performed in the same solvent used for NMR measurements. Correlation graphs of experimental and predicted chemical shifts are shown in Fig. 5.3. These graphs exhibit good linear dependencies between the calculated and experimental NMR chemical shifts for compounds studied. The best correlation is seen for the ^{13}C chemical shifts which might be because ^{13}C chemical shifts are expected to be marginally dependent on the solvent. In case of ^{1}H chemical shifts, the protons, which are located on the periphery of the molecule, show larger solvation effects. [9] Chemical shifts of primary, secondary and tertiary nitrogen atoms (non quaternary nitrogen atoms) also depend on the solvent properties, temperature [10] and concentration.

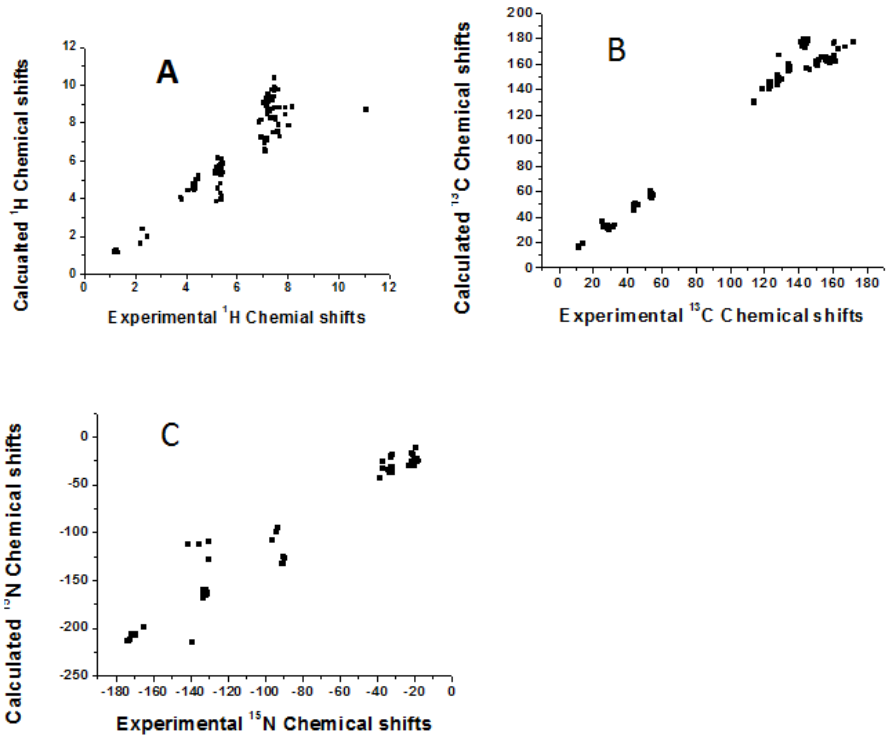

Fig. 5.3: *Graph showing comparison of experimental and theoretical ^{1}H (A), ^{13}C (B) and ^{15}N (C) chemical shifts for hybrid triazole derivatives shown in Scheme 5.5.*

5.7 Conclusions:

In conclusion, a DFT approach at the M06-2X level of theory using the ps 6–31G**++ basis set reliably reproduces the experimental ^{1}H, ^{13}C and ^{15}N NMR chemical shifts trends for triazole derivatives. Data of the compounds studied provide the basis for interpretation of the experimental NMR data of the 1,2,3/1,2,4-triazole hybrid derivatives. The above results indicate that when the 1,2,3-triazole ring is 1,4-disubstituted by the methylene groups, the molecule adopts a bent conformation such that both the substituents orient towards the same face of the 1,2,3-triazole ring.

References:

[1]. A representative example is given in: O. Takahashi, Y. Kohno, M. Nishio, *Chem. Rev.* **2010**, 110, 6049.

[2]. Ersin I., Muharrem Dinçer, Öner Ekici, Alaaddin Cukurovali *Spectrochimica Acta Part A: Molecular and Biomolecular Spectroscopy* **2013,** 101, 218.

[3]. Zhang Y., Z.J. Guo, X.Z. You, *J. Am. Chem. Soc.* **2001**, 123, 9378.,

[4]. Jaguar, version 9.9, *Schrödinger, LLC, New York, NY*, **2012**.

[5]. Parr, R. G.; Yang, W. Density Functional Theory of Atoms and Molecular Orbital Theory; Oxford University Press: New York, **1989**.

[6]. Ersin I., Muharrem Dincer, Oner Ekici, Alaaddin Cukurovali *Spectrochimica Acta Part A: Molecular and Biomolecular Spectroscopy,* **2013**, 101, 218.

[7]. Yixiang C. and Michael D. B. The Journal of Chemical Physics **2005**, 122, 224116.

[8]. David J. Giresen and Nicholas Z. *Phys. Ches. Chem. Chem. Phys*, **2002**, 4, 5498.

[9]. Fogarasi, G.; Zhou, X.; Taylor, P. W.; Pulay, P. *J. Am. Chem. Soc.* **1992,** *114*, 8191.

[10]. *CRC Handbook of Chemistry and Physics;* Weast, R. C., Ed.; 60th edition; CRC Press: Boca Raton, FL, **1979**. Dielectric constants for 20 deg. C was used.

[11]. Water's probe radius is set to 1.40 to reproduce solvation energies properly. All other probe radii are calculated from $r^3 = (3m\Delta)/(4\pi\rho)$ (10^{24} A^3/cm^3), where *r* is the solvent probe radius in Angstroms, *m* is the molecular mass obtained by dividing the molecular weight given in ref. [7] in grams per mole by 6.02 x 10^{23}, Δ is the packing density, and ρ is the density in g/cm^3 at 20 deg. C obtained from ref. [7]. Finding the actual Δ would require a detailed knowledge of the structure of the liquid. All Δ values for these liquids are assumed to be 0.5. (For FCC lattices, Δ is 0.7405, and for BCC lattices, Δ is 0.6802.)

[11]. Barfield M, Fagerness P. *J. Am. Chem. Soc.* **1997**; 119: 8699.

[12]. Levy G. C., Lichter RL. *Nitrogen-15 Nuclear Magnetic Resonance Spectroscopy*. Wiley: New York, **1979**; 32.